USGS-OFR-97-132

U.S. DEPARTMENT OF THE INTERIOR
U.S. GEOLOGICAL SURVEY

STACKED WIDE-ANGLE RECORDINGS OF AIR-GUN SIGNALS FROM THE 1994 LOS ANGELES REGION SEISMIC EXPERIMENT (LARSE), CALIFORNIA

By

Thomas M. Brocher[1], Susan L. Bilek[2], Robert W. Clayton[3], Gary S. Fuis[1], and David A. Okaya[4]

Open-File Report 97-132

[1]345 Middlefield Road, M/S 977, Menlo Park, CA 94025
[2]Earth Sciences Dept., University of California Santa Cruz, Santa Cruz, CA 95064
[3]Seismological Laboratory, Caltech, Pasadena, CA 91125
[4]Dept. Earth Sciences, University of Southern California, Los Angeles, CA 90089-0740

Menlo Park, California
1997

ABSTRACT

This report describes the processing and preliminary interpretation of the largest subset of deep-crustal wide-angle seismic data acquired during the 1994 Los Angeles Regional Seismic Experiment (LARSE). LARSE obtained three wide-angle onshore-offshore seismic profiles that were up to 250 km long using an 138 liter (8400 in^3) air gun array continuously recorded by an array of 174 Reftek recorders deployed along three onshore profiles. Repeated passes of each air gun line were made to improve the quality of the wide-angle onshore-offshore data in this highly urbanized area.

We first describe the steps we used to merge and stack the seismic data from the repeated passes for each onshore-offshore line, and we compare the unstacked and stacked data. We then illustrate many of these stacked recordings made in an inline and fan geometry with respect to the air gun lines, showing that although air gun Line 3 provided few useful inline recordings, it did provide a large number of useful recordings made in a fan geometry with respect to the air gun line. We then present wide-angle records obtained using two sonobuoys launched during the acquisition of air gun Lines 3 and 3R.

We lastly present general observations based on these stacked onshore-offshore data. Amplitudes of wide-angle reflections from the top of the upper mantle (PmP arrivals) recorded by LARSE are 2 to 5 times higher than those of direct P (Pg) arrivals in the distance range of 60 to 130 km, and thus in this distance-range strong ground motions may be related to the crustal and Moho structure. As a result of the LARSE geometry, midpoints for these large-amplitude PmP arrivals lie in a belt several tens of kilometers wide, parallel to and roughly centered on the Los Angeles basin, and underlying all of the urbanized Los Angeles region.

TABLE OF CONTENTS

FIGURES

TABLE OF CONTENTS

TABLE OF CONTENTS

TABLE OF CONTENTS

TABLES

INTRODUCTION

A major component of the 1994 Los Angeles Regional Seismic Experiment (LARSE) was the acquisition of three 220- to 250-km-long onshore-offshore lines (Lines 1 to 3; Figure 1) using an 138 liter (8400 in^3) air gun source and an array of 174 Reftek recorders deployed at 2-km intervals along the landward projections of these lines (Fuis et al., 1996; Okaya et al., 1996). The three onshore-offshore lines were: (1) Line 1 trending N-S from the center of San Clemente Island through Seal Beach to the Mojave Desert, (2) Line 2 trending N-S along the western shores of San Clemente and Catalina Islands through Santa Monica and the 1994 Northridge earthquake epicenter, and (3) Line 3 trending NE-SW from northwest of San Nicolas Island through the center of Los Angeles basin (Figure 1). The goals of this onshore-offshore profiling were summarized by Fuis et al. (1996) and Okaya et al. (1996). Although stacking high-fold common-midpoint seismic reflection data is commonly used for improving data quality, this approach has seldom been used in wide-angle profiling (Brocher and Moses, 1993). The anticipation of high cultural noise levels within the Los Angeles basin, however, lead us to attempt stacking multi-fold wide-angle data to improve its quality. To build the fold of the wide-angle data, we repeated large segments (referred to hereafter as passes) of the air gun Lines 1 and 2 up to 5 times (Figures 2a and 2b), and Line 3 once. As part of this plan, all 174 Refteks continuously recorded all 19,650 air gun shots along these lines (Okaya et al., 1996). Here we describe the stacking of the wide-angle seismic data for each onshore-offshore line and present general observations based on these stacked data.

DATA PROCESSING

The goal of the processing was to combine and stack the data recorded by each Reftek receiver along repeated air gun passes into a single stacked common-receiver gather for the line. A schematic diagram showing the six basic steps in the processing sequence used for the merging and stacking of the wide-angle data is shown in Figure 3. Appendix 1 details the steps taken in ProMAX Version 5.1 to produce stacked common-receiver gathers. (In Appendix 1 we have copied, for the sake of concreteness, a flow used to process Line 1 data.) The starting place for our processing was the Product 2 tapes described by Okaya et al. (1996), which are SEG-Y tapes containing common-receiver gathers for all 174 Refteks for individual air gun passes (e.g., one tape contained all Reftek gathers for air gun Line 3; another tape contained all Reftek gathers for the repeat pass, air gun Line 3R). The data on these tapes have been reduced at 6 km/s.

The identification of air gun shots to be merged and stacked for each pass of the air gun lines represented the single most important step of the entire processing flow. To select air gun

shots for stacking, we visually inspected the merged data from the repeated air gun passes using higher-quality data from a relatively quiet Reftek station, allowing exceptionally noisy data to be identified and kept from further processing. This selection process was repeated for each of Lines 1-3. During this process we found unexpectedly that data recorded during turns of the *Ewing* yielded data significantly out-of-phase (by a quarter-wavelet or more) with data obtained from air gun shots along the intended ship track. Thus, all data recorded during turns of the *Ewing* were excluded from stacking; fortunately, this constituted a small (a few percent) fraction of the total number of air gun shots available for stacking.

In Table 1 we list the cumulate air gun shot numbers (as defined by Okaya et al. (1996)) used for stacking, these represent air gun shots fired when the *Ewing* was on its intended ship track. For Air Gun Line 1, we selected for stacking all or parts of all six air gun passes except for Line 01R (Figure 2a), which yielded exceptionally noisy data due to windy conditions on land. The first 39 shots of Line 01, shot with a repetition rate of 60-sconds, were used to extend the shot line closer to the coast. Although all five passes for Line 2 were stacked (Figure 2b), the southern half of the stacked gathers for Line 2 consist solely of shots from Line 02 and 02R. Because Line 02R was shot with a 90-second air gun repetition rate and Line 02 was shot with a 20-second repetition the southern half of Line 2 essentially consists of traces from Line 02. Both passes for Line 3 (03 and 03R) were shot with the same 20-second repetition rate, therefore the stacked gathers for air gun Line 3 represents the average of the two passes (Brocher et al., 1995).

After identifying the traces to be stacked, the Product 2 tapes of Okaya et al. (1996) were read into the ProMAX system using the *SEGY TAPE IN* flow (Appendix 1). Only the air gun shots to be merged and stacked were read from tape in the *SEG-Y Input* module, using the channel parameter to select the cumulate shot number. Thus, data input and trace selection were performed simultaneously. Further processing was then performed using three flows: *removeturns*, *mergedatasets*, and *bintest*.

To merge data from repeated air gun passes using ProMAX Version 5.1 it is necessary to sort the data by range; this sorting was performed in the *removeturns* flow (Appendix 1). In this flow, the field file identification number (FFID) is used to select the common-receiver gather number for processing. The data were merged using the *mergedatasets* flow. Multiple disk reads and writes were required by the *Merge Sorted Datasets* module, which reads one file from disk outside the module and reads the other disk file from within the module. Once all the data for an air gun line are merged, they can be binned into range bins of any length in the flow *bintest*. Our choice of a 50-m bin length reflects the nominal 50-m air gun shot spacing along the LARSE lines (Brocher et al., 1995), and the need to make bins short enough to insure accurate phase correlation for traces within the bin. Calculation and application of a minor static shift (50 msec or less) in the *Event Alignment in Window*, *Header Statics*, and *Apply Fractional Static* modules were intended

to correct the data for small deviations of the *Ewing* from its intended track, but these corrections were generally insignificant. After correction for these static shifts the data were stacked in the *Ensemble Stack/Combine* module and then written to disk. After repeating these steps for all gathers, we wrote the stacked common-receiver gathers to SEG-Y tapes. Each stacked gather was written separately to exabyte tape, such that each has a 3200-byte and a 400-byte header, and a variable number of traces.

The format of the output tapes, containing stacked common-receiver gathers in SEG-Y format, closely resembles that of the input Product 2 tapes described by Okaya et al. (1996), with the following exceptions. We wrote out only 12 seconds of data to tape, with a sample rate of 10 milliseconds, resulting in 1201 samples per trace. The start times of these data, reduced at 6 km/s, is -5 seconds (Okaya et al., 1996), thus the full time range on our resulting stacked data is -5 to 7 seconds. The user defined SEG-Y trace headers described by Okaya et al. (1996) were not retained. Finally, as an unintended result of our processing flow the trace numbers on the stacked gathers are those of the largest cumulate shot number within each 50-m range bin. As a result the trace numbers (channel numbers) are not in sequential order but do correspond to the cumulate shot numbers as defined by Okaya et al. (1996).

Merging data by range works well for receivers inline with respect to an air gun line. When a receiver is in an oblique geometry to the air gun line, however, merging data by range combines traces having identical source-receiver ranges but having widely separated source locations; this stacking more likely degrades rather than enhances signals. As a consequence, we recommend that only the unstacked data be analyzed for the island stations (gathers 1-4). Similarly, near-shore portions of data recorded at coastal stations along Land Line 1 (gathers 5-23) and along Land Line 3 (gathers 134-165) from shots along air gun Line 2 are also suspect. Finally, data recorded at stations along Land Line 2 from shots along air gun Line 3 combine many shots at the eastern end of the line into 50-m-wide bins due to the oblique geometry of these lines.

Figures 4a and 4b present a comparison between the unmerged data from air gun Lines 03 and 03R recorded at receiver 047 (deployed along LARSE land Line 1), Figure 4c presents the merged data for this receiver for these two passes, and Figure 4d presents the resulting stacked data. Figure 4c illustrates the high coherence of the merged traces, with relatively minor time misalignments between traces. Figures 4a to 4d illustrate the stacking process for the highest-quality data with signal-to-noise (S/N) ratios greater than one. Figures 5a to 5d present a similar comparison between unmerged, merged, and stacked data for the same air gun passes recorded by receiver 157 (deployed along land Line 3), illustrating the stacking process for data having a S/N of one or less. Comparison of Figures 4b and 4d and Figures 5a and 5d illustrates that the S/N levels of the stacked data are not significantly higher than for portions of the unstacked data. For these two gathers, however, the individual air gun pass yielding data having the highest S/N ratio differ

(Line 3 for one, Line 3R for the other), suggesting that the stack provides the best overall display of the data. The unstacked data shown in Figures 4a to 4c and 5a to 5c have not undergone trace bias removal, which is performed prior to stack, resulting in the improved appearance of the stacks. This improvement is particularly noticeable for Figure 5d when compared to the merged data in Figure 5c.

The stacked wide-angle data provide several advantages over the unstacked data: (1) they suppress some incoherent noise, (2) they compress the data volume by up to a factor of 2.5, (3) and they present data for the entire length of the air gun line (most repeats of the lines did not transit the entire line length (Figures 2a and 2b)). Although stacking itself results in rather modest improvement of S/N levels because of the low-fold of the wide-angle data, a significant improvement to the final record quality resulted simply from careful selection of the passes having the highest S/N levels: for Line 1, the best data were provided by the last of six air gun passes, demonstrating the value of repeating the air gun passes.

DESCRIPTION OF THE WIDE-ANGLE DATA

Figure 6 presents a line-drawing showing a schematic interpretation of the stacked wide-angle data, showing the typical appearance of crustal refractions (Pg), the refraction from the upper mantle (Pn), and reflections from the Moho (PmP). Figures 7 to 146 are plots providing examples of the better quality stacked wide-angle data (Quality A and B in Table 2, see below) showing Pg, Pn, and PmP arrivals out to source-receiver ranges up to 250 km. These plots show data recorded in a fan and inline geometry with respect to the air gun lines. Note in Figures 7 to 146 the large static time shifts of arrivals that are associated with large variations in the bathymetry of the seafloor and the thickness of offshore basin sediments. Combined, these variations produce static shifts in the arrival times up to 0.75 s.

Table 2 lists the offset ranges recorded for all the Reftek receivers for Lines 1 to 3. A subjective ranking of the quality of the stacked data from A to F (where A is highest) is also provided in Table 2, to allow a quick if crude guide to the receivers where higher quality data were recorded. We ranked the data prior to bandpass filtering and trace mixing, which helped to further enhance the data quality. Many receivers (gathers) consistently provided higher quality data for all three air gun lines. These receivers included: 1-4, 36-50, 60-70, 89-92, 111-119, 128-133, 155, 157, and 168, which are all located at or close to bedrock outcrops in relatively uninhabited regions. Refteks along the more urbanized corridor used for land Line 3 provided relatively little useful data. Strong, impulsive arrivals (rank A) were observed on approximately 19% of the gathers for all three air gun lines. Somewhat emergent arrivals (rank B) were observed, on about 11% of the gathers. Emergent arrivals (rank C) were seen on about 14% of the gathers. Faint to

very faint arrivals (rank D) were seen on about 21% of the gathers, and arrivals were not observed on approximately 26% of the gathers (rank F). An additional 10% of the Refteks failed to record any data as indicated in Table 2.

Plots showing recordings made using two sonobuoys deployed along air gun Lines 3 and 3R are presented in Figures 147 to 150. The locations and other relevant information about these two sonobuoys are given in Figure 1 and Table 3. The sonobuoy data were recorded on auxiliary channel 174 of the multichannel seismic (MCS) tapes for the FFID numbers shown on Table 3. Figure 147 shows the record obtained from sonobuoy 1 along line 3. Figures 148 to 150 show the records obtained from sonobuoy 2 along lines 3R, TR2, and 2. The sonobuoy recordings made during Lines TR2 and 2 essentially duplicate the ocean-bottom seismometer (OBS) recording of Line 2 made by the OBS deployed at the intersection of Lines 2 and 3 (Figure 1, ten Brink et al., 1996). The sonobuoy recordings along Lines 3 and 3R, however, provide information not duplicated by any other wide-angle recorder.

Sonobuoy 2 transmitted signals for 8 hours during the acquisition of air gun lines 3R, TR2, and 2. We calculate from water wave arrivals that this buoy drifted less than 1 km northward from its initial deployment site. Thus, for each of the three lines, the location of sonobuoy 2 differs, but as a first approximation, its location can be considered as a different fixed point for each air gun line. Except for sonobuoy 1 shown in Figure 147, the sonobuoy data have not been filtered. The data in Figure 147 have been bandpass filtered between 5 and 15 Hz. Approximate ranges shown on these sonobuoy figures were calculated from the direct or reflected water wave arrival, and we assumed direct propagation from source to the sonobuoy.

GENERAL OBSERVATIONS BASED ON THE WIDE-ANGLE DATA

The amplitude of PmP arrivals exceed those of direct P (Pg and Pn) arrivals by factors commonly between 2 and 5 in the offset range between 60 and 130 km. (Figures 7 to 146 have attempted (not always successfully) to preserve the relative amplitude content of the different crustal and mantle arrivals.) This observation is true for all three lines and for recordings made in inline and fan geometries relative to the air gun lines. Detailed views of a high-quality gather in Figures 151 and 152 show the larger amplitudes associated with PmP arrivals compared to Pg arrivals in this distance range. Apart from stacking of the air gun shots, no further processing has been performed on this gather. Large-amplitude PmP midpoints from LARSE lie in a belt several tens of km wide, approximately centered on the Los Angeles basin (Figure 153). The shape of the outer boundary of observed PmP midpoints (Figure 153) probably results from the geometry of LARSE and we lack control on whether this boundary extends outward from that shown. Note

that this region of large-amplitude PmP midpoints relative to Pg and Pn underlies all of the urbanized Los Angeles region.

Mori and Helmberger (1996) noted enhanced SmS amplitudes in southern California based on broad-band recordings of Landers aftershocks. They noted SmS/Sg amplitude ratios of 2 to 5 in the distance range of 80 to 105 km, consistent in the Mojave desert with a crustal thickness of about 28 km. We note similar enhancement of PmP/Pg amplitude ratios at 60 to 130 km ranges; the smaller (60-km) near offset likely results from a thinner (22-25 km) crust along the coast of the Los Angeles region (ten Brink et al., 1995). We believe that the enhanced (post-critically reflected) SmS (based on our observations of PmP) at 60 km is responsible for a 25% enhancement of earthquake magnitudes noted at 60 km in southern California (Hutton and Boore, 1987).

Data recorded from shots along air gun Line 2 located to the south of the Catalina Ridge generally show much lower S/N ratios than do data recorded from shots located to the north of the Catalina Ridge (Figures 43 to 89). Although the larger S/N ratios may, in part, reflect the lower-fold of the wide-angle data for shots located to the south of Catalina Ridge (Figure 2b), ten Brink et al. (1995) made the same observation on unstacked OBS data along air gun Line 2. These new observations support ten Brink et al.'s (1995) hypothesis that a barrier to the northward propagation of seismic waves extending to depths of at least 8 km may exist at Catalina Ridge.

The inline wide-angle data recorded along land Line 3 provided few useful wide-angle recordings (Okaya et al., 1996). Recorders deployed along land Line 3 also provided relatively few high-quality recordings of air gun lines 1 and 2. Recordings of air gun Line 3 made in a fan geometry, however, provided many high-quality gathers (Figures 90 to 142). These recordings provide a range of raypath azimuths that can be used to determine whether the Pn velocity has an azimuthal variation. PmP midpoints between shots along air gun Line 3 and recorders along Line 1 lie beneath Santa Monica and Los Angeles. Thus these fan data provide direct sampling of the crust beneath urbanized areas of Los Angeles.

The ranking of data quality of the gathers in Table 2 indicates that the highest quality data were acquired at or near basement outcrop in relatively uninhabited regions. Although useful wide-angle data were also acquired near the coast and at the edges of the basins, Table 2 indicates that the stations located within the centers of populated Cenozoic basins failed to provide useful wide-angle data, even after stacking of the data recorded during repeated air gun passes.

ACKNOWLEDGMENTS

This work was supported by the National Earthquake Hazards Reduction Program, the National Science Foundation, and the Southern California Earthquake Center. Many individuals on the *Ewing* and onshore, and acknowledged in previous Open-File Reports, helped to acquire the wide-angle data. We thank IRIS PASSCAL for the use of the Refteks and their field support during LARSE. Fiona McBride, University of Texas El Paso, stripped the sonobuoy data for Lines 3 and 3R from the multichannel reflection data tapes. We thank Jim Mori and Dave Boore for helpful discussions of PmP amplitudes. Rufus Catchings made many constructive comments in a review of an earlier draft of this manuscript.

REFERENCES CITED

Brocher, T.M., and M.J. Moses, Onshore-offshore wide-angle seismic recordings of the San Francisco Bay Area Seismic Imaging eXperiment (BASIX): The five-day recorder data: *U. S. Geological Survey Open-file Report 93-276*, 89 pp., 1993.

Brocher, T., R. Clayton, K. Klitgord, R. Bohannon, R. Sliter, J. McRaney, J. Gardner, and J. Keene, Multichannel seismic-reflection profiling on the R/V *Maurice Ewing* during the Los Angeles Region Seismic Experiment (LARSE), California: *U.S. Geological Survey Open File Report 95-228,* 73 pp., 1995.

Fuis, G.S., D.A. Okaya, R.W. Clayton, W.J. Lutter, T. Ryberg, T.M. Brocher, T. Henyey, M. Benthien, P.M. Davis, J. Mori, R.D. Catchings, U.S. ten Brink, M.D. Kohler, K.D. Klitgord, and R.G. Bohannon, Images of crust beneath Southern California will aid study of earthquakes and their effects: *EOS, Trans. Amer. Geophys. Un., v. 77*, p. 173, 176, 1996.

Hutton, L.K., and D.M. Boore, The M_L scale in southern California: *Bull. Seism. Soc. Am., v. 77,* p. 2074-2094, 1987.

Mori, J., and D. Helmberger, Large-amplitude Moho reflections from Landers aftershocks, southern California: *Bull. Seism. Soc. Am., v. 86*, p. 1845-1852, 1996.

Okaya, D.A., J. Bhowmic, G.S. Fuis, J.M. Murphy, M.C. Robertson, A. Chakraborty, M.L. Benthien, K. Hafner, and J.J. Norris, Report for air-gun data acquired at onshore stations during the 1994 Los Angeles Region Seismic Experiment (LARSE), California: *U.S. Geological Survey Open File Report 96-297*, 224 p., 1996.

ten Brink, U.S., R. Drury, D. Okaya, R. Bohannon, T.M. Brocher, and G. Fuis, Crustal structure of the inner California Borderland - Preliminary results: *EOS, Trans. Amer. Geophys. Un., v. 76,* Supplement, F348, 1995.

ten Brink, U.S., R.M. Drury, G.K. Miller, T. Brocher, and D. Okaya, Los Angeles Region Seismic Experiment (LARSE), California off-shore Seismic Refraction data: *U.S. Geological Survey Open-File Report* 96-27, 29 pp., 1996.

Table 1. Cumulate Air Gun Shot Numbers (Channels) Stacked

Line 1		Line 2		Line 3	
Pass	Shot Number	Pass	Shot Number	Pass	Shot Number
01/1	1-39	02/9	11084-14086	03/6	5800-8166
01X/3	2964-3811	02R/10	14203-14922	03R/7	8248-10658
01Y/4	3968-4635	02X/11	14923-16177		
01A/15	9595-20717	02Y/12	16317-17737		
01B/16	20822-22128	02Z/13	17738-18499		

Table 2. Offset Ranges Recorded During LARSE Lines 1 to 3

LARSE Air Gun Line 1

Gather No. (FFID)	Data Range (km)	
	Islands	
001	012.5-085.4*	B
002	016.1-075.9*	B
003	007.4-040.0	A
004	007.4-040.0	A
	Land Line 1	
005	--	
006	013.4-090.6	C
007	014.4-059.1*	D
008	022.8-095.2*	C
009	018.0-095.2	C
010	--	
011	--	
012	024.3-101.4	D
013	026.5-103.7	F
014	028.1-105.3	F
015	095.4-161.3	F
016	--	
017	034.4-111.5	D
018	037.3-114.5	D
019	038.4-115.5	C
020	040.0-117.0	B
021	042.7-119.8	B
022	043.5-120.5	D
023	063.6-122.7*	F
024	--	
025	050.3-127.5	F
026	069.8-129.0*	F
027	054.6-131.7	F
028	056.5-133.6	F
029	058.4-135.6	F
030	078.3-137.5*	F
031	087.2-117.8*	
032	064.1-141.3	C
033	--	
034	084.1-143.2*	C
035	068.0-145.3	C
036	087.8-147.0*	A
037	072.2-149.4	A
038	073.8-151.1	B
039	076.0-153.2	A
040	096.2-155.4*	C
041	080.4-157.6	A
042	099.9-159.1*	A
043	084.2-161.4	B
044	085.9-163.1	A
045	087.9-165.1	B
046	090.4-167.6	A
047	092.2-169.4	A
048	094.1-171.2	A
049	095.1-173.0	A
050	098.0-175.2	C
051	100.2-177.5	F
052	102.6-179.8	D
053	104.3-181.5	D
054	106.4-183.6	F
055	108.2-185.4	D
056	110.1-187.3	D
057	112.3-189.5	C
058	114.4-191.6	D
059	116.0-193.2	F
060	118.1-195.3	B
061	120.3-197.4	C
062	123.2-200.5	B
063	124.3-178.3*	B
064	126.3-203.5	A
065	128.4-205.6	B
066	--	
067	132.2-209.4	C
068	135.6-212.8	B
069	138.1-215.3	C
070	139.9-217.1	C
071	142.1-160.2*	D
072	144.1-221.2	D
073	146.1-223.2	D
074	148.3-225.4	D
075	150.5-195.1*	D
076	152.2-229.3	D
077	154.1-231.2	B
078	156.6-233.8	D
079	158.1-202.7*	D
080	160.2-237.4	D
081	162.0-239.1	C
082	164.1-241.2	C
083	165.9-242.9	F
084	167.7-244.8	D
085	170.0-247.0	F
086	172.0-249.0	F
	Land Line 2	
087	061.6-064.2*	F
088	060.6-120.8	A
089	062.7-123.0	B
090	064.5-096.6*	A
091	064.6-126.2	A
092	066.9-128.7	B
093	067.9-103.0*	F
094	069.6-132.0	D
095	071.2-133.9	F
096	072.7-135.7	F
097	074.2-137.7	F
098	076.5-140.2	D
099	078.5-142.6	D
100	080.1-114.3	F
101	082.1-146.6	D
102	--	
103	085.2-150.1	D
104	087.2-152.4	D
105	089.0-154.3	D
106	090.3-155.8	D
107	092.9-158.6	C
108	095.4-161.3	D
109	098.2-164.5	D
110	099.5-165.9	D
111	102.2-168.5	B
112	119.3-171.2*	C
113	106.6-173.7	B
114	108.2-175.8	C
115	111.5-179.0*	B
116	112.6-180.3	C
117	114.2-182.6	B
118	117.6-185.8	D
119	119.7-187.9	C
120	121.6-189.8	D
121	--	
122	127.5-196.0	D
123	129.1-197.9	F
124	131.8-200.7	F
125	134.1-203.1	D
126	136.7-205.7	D
127	--	
128	141.2-210.7	C
129	143.6-213.0	C
130	145.9-215.4	C
131	148.0-217.7	D
132	150.0-219.9	C
133	137.6-190.5*	B
	Land Line 3	
134	030.7-095.1	F
135	029.7-095.7	F
136	028.5-096.4	F
137	028.3-097.3	F
138	028.0-097.8	F
139	028.0-098.6	D
140	027.5-099.7	F
141	027.5-069.4*	F
142	027.7-101.9	F
143	028.5-071.8*	F

Table 2. Offset Ranges Recorded During LARSE Lines 1 to 3

144	031.4-104.3	D
145	032.0-105.0	F
146	028.9-105.8	F
147	030.8-107.8	F
148	031.6-108.9	F
149	032.9-110.2	D
150	034.5-111.7	D
151	036.2-113.3	F
152	037.7-114.5	F
153	045.6-116.5*	F
154	041.5-117.9	D
155	043.5-119.6	B
156	--	
157	047.4-122.8	B
158	--	
159	051.9-126.5	F
160	053.3-127.4	C
161	--	
162	057.8-099.1*	F
163	060.2-133.1	D
164	062.0-134.5	D
165	--	
166	066.6-138.4	F
167	069.0-140.3	D
168	071.3-142.4	B
169	074.4-144.7	C
170	077.3-147.3	D
171	079.3-149.0	D
172	--	
173	083.0-152.0	F
174	085.7-154.4	F

A = Strong Arrivals
B = Moderate Arrivals
C = Fair Arrivals
D = Faint Arrivals
F = No Arrivals Seen
-- = No Data

*Means the full offset range was not recorded by this receiver.

LARSE Air Gun Line 2

Gather No. (FFID)	Data Range (km)	
	Islands	
001	022.9-126.1	A
002	010.4-110.9	A
003	032.9-083.9	A
004	011.5-090.9	B
	Land Line 1	
005	049.3-134.3	D
006	049.6-137.0	F
007	050.2-138.0	F
008	050.2-141.5	D
009	050.2-141.5	F
010	--	
011	--	
012	050.0-147.6	F
013	051.6-150.0	D
014	051.6-151.5	F
015	047.3-199.3	F
016	--	
017	051.3-157.5	F
018	052.7-160.6	D
019	053.2-161.6	D
020	053.0-163.0	C
021	052.7-165.6	D
022	052.7-166.3	F
023	054.0-168.5	D
024	--	
025	057.5-173.5	F
026	058.8-175.0	F
027	059.3-177.7	F
028	060.7-179.6	F
029	062.1-181.6	F
030	063.8-147.1*	F
031	084.7-086.4*	F
032	067.9-187.6	C
033	--	
034	--	
035	070.7-191.6	C
036	072.4-193.3	B
037	072.4-195.6	B
038	074.2-197.3	A
039	075.2-199.4	A
040	--	
041	077.6-203.7	B
042	078.6-205.2	B
043	081.4-207.6	A
044	083.4-209.4	A
045	085.5-211.4	A
046	088.4-214.1	A
047	090.8-215.9	A
048	092.2-217.8	A
049	093.5-219.6	B
050	094.4-221.6	C
051	095.9-223.8	F
052	097.8-226.2	F
053	099.3-227.9	D
054	100.8-230.0	C
055	102.4-231.8	C
056	104.7-185.2*	C
057	106.5-235.9	C
058	108.1-238.0	C
059	109.5-239.6	F
060	111.2-241.7	A
061	113.4-243.9	B
062	115.6-246.8	A
063	116.3-247.8	A
064	118.5-249.9	A
065	119.9-251.9	B
066	--	
067	124.0-255.9	B
068	127.5-259.3	C
069	129.4-261.7	B
070	131.7-263.6	C
071	133.3-265.8	D
072	135.3-267.8	C
073	136.6-269.7	F
074	138.8-271.9	D
075	140.7-274.1	D
076	142.0-275.8	C
077	144.0-277.7	B
078	146.5-280.2	C
079	--	
080	150.3-283.9	D
081	152.3-285.7	D
082	154.6-287.8	D
083	156.5-289.5	D
084	158.3-291.5	D
085	161.2-293.8	F
086	162.8-295.8	F
	Land Line 2	
087	--	
088	005.8-157.8	A
089	007.8-159.9	A
090	009.9-021.4*	A
091	011.4-163.4	A
092	013.9-165.9	A
093	--	
094	017.3-169.3	B

Table 2. Offset Ranges Recorded During LARSE Lines 1 to 3

095	019.2-171.2	D
096	021.1-173.1	F
097	023.1-175.1	F
098	025.8-177.8	C
099	028.2-180.2	C
100	029.9-181.9	F
101	032.2-184.2	B
102	--	
103	035.7-187.8	C
104	038.3-190.3	D
105	040.2-192.2	C
106	041.8-193.8	D
107	044.4-196.5	C
108	047.3-199.3	D
109	050.6-202.6	C
110	052.0-204.0	D
111	054.5-206.5	B
112	057.2-209.2	D
113	060.1-212.0	A
114	062.3-214.3	C
115	065.4-217.4	A
116	066.8-218.8	A
117	069.6-221.4	A
118	072.3-224.3	B
119	074.4-226.4	A
120	076.2-228.2	C
121	--	
122	082.4-234.4	D
123	084.5-236.5	D
124	087.3-239.3	C
125	089.6-241.6	B
126	092.2-244.2	A
127	--	
128	097.4-249.4	A
129	099.6-251.6	A
130	102.1-254.1	A
131	104.5-256.5	A
132	106.6-258.6	A
133	076.9-228.9	A

Land Line 3

134	020.0-136.2	D
135	022.3-137.2	D
136	025.6-138.6	F
137	027.8-140.1	F
138	029.5-140.9	F
139	031.2-141.9	F
140	034.2-143.5	F
141	036.2-145.0	F
142	038.3-146.4	F
143	041.0-130.1*	F
144	042.7-149.4	F
145	045.3-150.5	F
146	048.2-151.6	F
147	049.9-153.8	F
148	052.6-155.1	F
149	054.5-156.6	D
150	056.5-158.3	D
151	059.4-160.1	F
152	062.0-161.5	F
153	064.0-163.5	F
154	066.3-165.1	D
155	068.7-167.0	C
156	--	
157	073.2-170.4	B
158	--	
159	078.5-174.3	F
160	080.6-175.3	B
161	--	
162	085.1-089.6*	F
163	087.9-181.2	D
164	090.0-182.7	F
165	--	
166	094.7-186.7	F
167	097.5-188.6	F
168	099.5-190.7	A
169	103.2-193.1	C
170	106.0-195.7	F
171	108.3-197.4	F
172	--	
173	112.2-200.4	F
174	115.0-202.8	F

A = Strong Arrivals
B = Moderate Arrivals
C = Fair Arrivals
D = Faint Arrivals
F = No Arrivals Seen
-- = No Data

*Means the full offset range was not recorded by this receiver.

LARSE Air Gun Line 3

Gather No. (FFID)	Data Range (km)	
	Island	
001	100.9-135.8	A
002	083.7-119.3	A
003	059.4-131.2	A
004	038.4-108.7	A
	Land Line 1	
005	037.4-092.3*	F
006	037.5-154.7	
007	038.0-155.6	D
008	037.8-156.8	D
009	037.8-156.8	
010	--	
011	--	
012	038.5-159.2	F
013	040.5-161.6	D
014	040.8-162.1	F
015	065.6-152.6*	F
016	--	
017	042.4-164.4	F
018	044.6-166.7	F
019	045.5-167.6	D
020	045.8-167.9	A
021	046.6-168.5	A
022	046.9-168.8	F
023	048.8-170.5	D
024	--	
025	053.4-174.9	F
026	054.8-176.3	F
027	056.3-177.3	F
028	057.8-178.6	F
029	059.8-180.5	D
030	061.8-133.4*	
031	070.2-114.2*	D
032	066.2-186.6	D
033	--	
034	--	
035	069.6-189.6	D
036	071.5-191.3	A
037	072.5-191.7	A
038	074.4-193.5	A
039	075.9-194.6	A
040	--	
041	079.2-197.1	A
042	080.5-198.2	A
043	083.3-200.9	A

Table 2. Offset Ranges Recorded During LARSE Lines 1 to 3

044	085.3-203.0	A
045	087.5-205.2	A
046	090.5-208.1	A
047	092.8-210.4	A
048	094.4-211.8	A
049	096.0-213.1	A
050	097.3-213.9	A
051	099.2-215.4	F
052	101.4-217.2	
053	103.0-218.6	D
054	104.8-220.1	C
055	106.6-221.7	B
056	108.8-224.0	C
057	110.8-225.6	C
058	112.6-227.1	C
059	114.1-228.5	F
060	116.1-230.1	B
061	118.3-232.2	A
062	120.9-234.2	A
063	121.7-234.9	A
064	123.9-237.0	A
065	125.6-238.3	A
066	--	
067	129.7-242.3	A
068	133.2-245.6	A
069	135.4-247.3	A
070	137.6-249.7	B
071	139.4-251.1	B
072	141.5-253.1	C
073	143.0-254.1	F
074	145.3-256.3	C
075	147.3-258.0	C
076	148.8-259.1	B
077	150.8-261.2	A
078	153.3-263.5	C
079	159.8-192.0*	C
080	157.1-267.3	C
081	159.1-269.2	C
082	161.4-271.6	C
083	163.2-273.5	C
084	165.1-275.2	D
085	167.8-278.2	F
086	169.6-279.6	F

Land Line 2

087	--	
088	025.9-123.7	A
089	028.2-124.3	A
090	030.2-125.4	A
091	030.9-127.4	A
092	033.4-128.7	A
093	034.8-130.2	
094	036.6-130.9	B
095	038.4-132.1	D
096	040.2-133.5	D
097	042.1-135.1	F
098	044.6-136.8	D
099	046.9-138.6	D
100	048.6-139.7	F
101	050.9-141.2	D
102	--	
103	054.3-143.8	D
104	056.7-145.9	D
105	058.6-147.3	C
106	060.1-148.7	D
107	062.8-150.4	A
108	065.6-152.6	A
109	068.8-155.4	A
110	070.2-156.5	B
111	072.8-157.7	A
112	075.5-159.8	C
113	078.0-163.1	C
114	080.1-165.4	C
115	083.4-087.7*	A
116	084.7-168.6	A
117	087.1-172.0	A
118	090.2-173.2	C
119	092.3-174.6	B
120	094.1-175.8	D
121	--	
122	100.4-180.8	D
123	102.4-183.0	F
124	105.2-185.2	D
125	107.5-187.0	B
126	110.1-189.1	B
127	--	
128	115.2-194.0	A
129	117.5-195.5	A
130	119.9-197.6	A
131	122.2-199.9	B
132	124.4-201.8	A
133	094.9-111.0*	A

Land Line 3

134	007.7-129.3	A
135	010.1-131.7	B
136	013.5-135.1	F
137	016.1-137.8	F
138	017.9-139.6	F
139	019.7-141.4	F
140	023.0-144.6	D
141	025.2-147.0	F
142	027.6-149.3	D
143	030.2-152.0	F
144	032.4-154.2	F
145	034.9-156.7	F
146	037.8-159.5	F
147	040.0-161.8	F
148	042.7-164.5	F
149	044.8-166.5	D
150	047.0-168.8	D
151	050.0-171.8	F
152	052.7-174.4	D
153	055.0-176.8	D
154	057.4-179.2	D
155	059.9-181.8	C
156	--	
157	064.7-186.5	A
158	--	
159	070.2-192.0	F
160	072.2-193.9	D
161	--	
162	077.0-198.8	F
163	079.8-201.6	D
164	081.9-203.7	D
165	--	
166	086.8-208.7	F
167	089.6-211.4	F
168	091.8-213.6	B
169	095.4-217.2	D
170	098.4-220.2	F
171	100.7-222.5	F
172	--	
173	104.6-226.4	F
174	107.5-229.3	F

A = Strong Arrivals
B = Moderate Arrivals
C = Fair Arrivals
D = Faint Arrivals
F = No Arrivals Seen
-- = No Data

*Means the full offset range was not recorded by this receiver.

Table 3. Sonobuoy Locations and Parameters

Sono-buoy No.	Line No	Launch Time and Location: UTC Day:HrMn	Lat. (N) Deg. Min.	Long. (W) Deg. Min.	MCS File FFID No.	Water Temp. (°C)	Drift (knots)
01	03	289:0100	33 44.7679	118 46.9194	650	18.7	
		(Tapes LA23-25A*)			1509		
02	03R	290:0046	33 48.0328	118 36.2865	2276	18.1	0.5
		(Tapes LA35-36*)			2551		
	TR2	(Tape LA38*)				141	
					295		
	2	(Tapes LA39-40*)			354		
					601		

*Tape numbers as defined by Brocher et al. (1995).

APPENDIX 1: PROMAX PROCESSING SEQUENCE

INPUT DATA and SELECT AIR GUN SHOTS

Flow *SEGY TAPE IN*

SEG-Y Input	
Type of Storage	Tape
Input MULTIPLE files from tapes?	Yes
Multiple file SELECTION	Input All
IBM Standard Label?	No
Store reel header in processing history?	Yes
Display ensemble information	No
Number of errors in a row before ABORTing job?	5
Input AUXILIARY traces?	No
Input data's SAMPLE RATE	0.0
Maximum time to get	12000.0
Get CHANNEL NUMBER from trace headers	Yes
Input trace FORMAT	Get from header
Is this stacked data?	No
MAXIMUM traces per ensemble	120
Primary SORT header word (domain of data)?	SHOT
Input PRIMARY selection choice	FFID
Specify PRIMARY input list	134-174/
Input SECONDARY selection choice	Channel
Specify CHANNEL input list	20822-22128/
Use the coordinate scalar	Yes
Enter PRIMARY tape drive device path name	/dev/rst0
Tape drive/file is on REMOTE machine?	No
Use a tape drive stacker?	No
Remap SEGY header values?	No
Disk Data Output	
Output Dataset Filename	01B/16(134-174)
New, or Existing, File?	New
Record LENGTH to output	12000.0
'Compress' the data?	No
Skip primary disk storage?	Yes
Pre-Geometry Database Initialization	No

SORT and MERGE DATA

Flow *removeturns* (removeturns is repeated 5 times in the flow, once for each of the 5 air gun passes 1/1, 01X/3, 01Y/4, 01A/15, and 01B/16, by changing the dataset names in *Disk Data Input* and *Disk Data Input*)

Disk Data Input	
Number of datasets	1
Trace read option	Sort
Primary header	FFID
Secondary header	None
Sort order	(FFID#, eg. 174)/
Select dataset	01B/16(134-174)

APPENDIX 1: PROMAX PROCESSING SEQUENCE

Inline Sort

Primary sort	FFID
Secondary sort	OFFSET
Primary sort order	Ascending
Secondary sort order	Ascending
Maximum traces per output	3000
Maximum traces in buffer	3000
Buffer type	Disk
Compress data	No
Multiple pass?	No

Disk Data Output

Output dataset filename	*filename, e.g.* 174b
File	New
Length to output	12000 ms
Compress data	No
Skip primary disk storage	Yes
Pre-geometry database initialization?	No

Flow *mergedatasets*

Disk Data Input

Datasets to input	1
Trace read option	Get all
Dataset name	*filename,* e.g. 174, from flow *removeturns*

Merge Sorted Datasets

Input from disk or tape?	Disk
Primary sort order	Ascending
Secondary sort order	Ascending
Dataset to merge with pipe	*filename,* e.g. 174x from *removeturns*
Maximum traces	9000

Disk Data Output

Output dataset filename	*filename,* e.g. 174x0
File	New
Length to output	12000 (ms)
Compress data	No
Skip primary disk storage	Yes
Pre-geometry database initialization?	No

Disk Data Input

Datasets to input	1
Trace read option	Get all
Dataset name	*filename*, e.g. 174y, from flow *removeturns*

Merge Sorted Datasets

Input from disk or tape?	Disk
Primary sort order	Ascending
Secondary sort order	Ascending
Dataset to merge with pipe	*filename* (from previous Disk Data Output, e.g. 174x0)
Maximum traces	9000

Disk Data Output	
Output dataset filename	*filename*, e.g. 174x0y
File	New
Length to output	12000 (ms)
Compress data	No
Skip primary disk storage	Yes
Pre-geometry database initialization?	No
Disk Data Input	
Datasets to input	1
Trace read option	Get all
Dataset name	*filename*, e.g. 174a from flow *removeturns*
Merge Sorted Datasets	
Input from disk or tape?	Disk
Primary sort order	Ascending
Secondary sort order	Ascending
Dataset to merge with pipe	*filename* (from previous Disk Data Output, e.g. 174x0y)
Maximum traces	9000
Disk Data Output	
Output dataset filename	*filename*, e.g. 174x0ya
File	New
Length to output	12000 (ms)
Compress data	No
Skip primary disk storage	Yes
Pre-geometry database initialization?	No
Disk Data Input	
Datasets to input	1
Trace read option	Get all
Dataset name	*filename*, e.g. 174b from flow *removeturns*
Merge Sorted Datasets	
Input from disk or tape?	Disk
Primary sort order	Ascending
Secondary sort order	Ascending
Dataset to merge with pipe	*filename* (from previous Disk Data Output, 174x0ya)
Maximum traces	9000
Disk Data Output	
Output dataset filename	*filename*, e.g. merge174
File	New
Length to output	12000 (ms)
Compress data	No
Skip primary disk storage	Yes
Pre-geometry database initialization?	No

STACK DATA

Flow *bintest*

Disk Data Input	
Datasets to input	1
Trace read option	Get all
Dataset name	*filename* from *mergedatasets*, e.g. merge174

APPENDIX 1: PROMAX PROCESSING SEQUENCE

Trace DC Removal		
Type of central value	Mean	
Trace Binning		
Header to bin	OFFSET	
Binned header	BOFFSET	
Binned format	Integer	
Header bin centers	10000-300000(50)	
Binned entry values	10000-300000(50)	
Event Alignment in Window		
Maximum allowable static shift	50	
Allowable % of hard zeros	50	
Number of traces in window	5	
Method of building model trace	Brute Stack	
Ignore end of ensembles?	Yes	
Seek and report reversed traces?	No	
Accumulate statics in TOT_ALIGN	No	
Get analysis window parms from database?	No	
Primary header word	OFFSET	
Secondary header word	None	
Window analysis parms	10000:4000-8000/	(Beginning offset of the window: time of window (ms))
Header Statics		
Bulk shift static	0.0000	
What about previous statics?	Add to previous	
Apply how many static header entries?	1	
First header word to apply	ALINSTAT	
How to apply statics	Add	
Apply Fractional Static		
Ensemble Stack/Combine		
Type of operation	Stack only	
How are trace headers determined?	Last	
Secondary key bin size	50 (m)	
Maximum traces per ensemble	3000	
Warnings if maximum exceeded?	Yes	
Primary trace order header	FFID	
Secondary trace order header	BOFFSET	
Output trace secondary key order	Ascending	
Disk Data Output		
Output dataset filename	e.g. stack174	
File	New	
Length to output	12000 (ms)	
Compress data	No	
Skip primary disk storage	Yes	
Pre-geometry database initialization?	No	

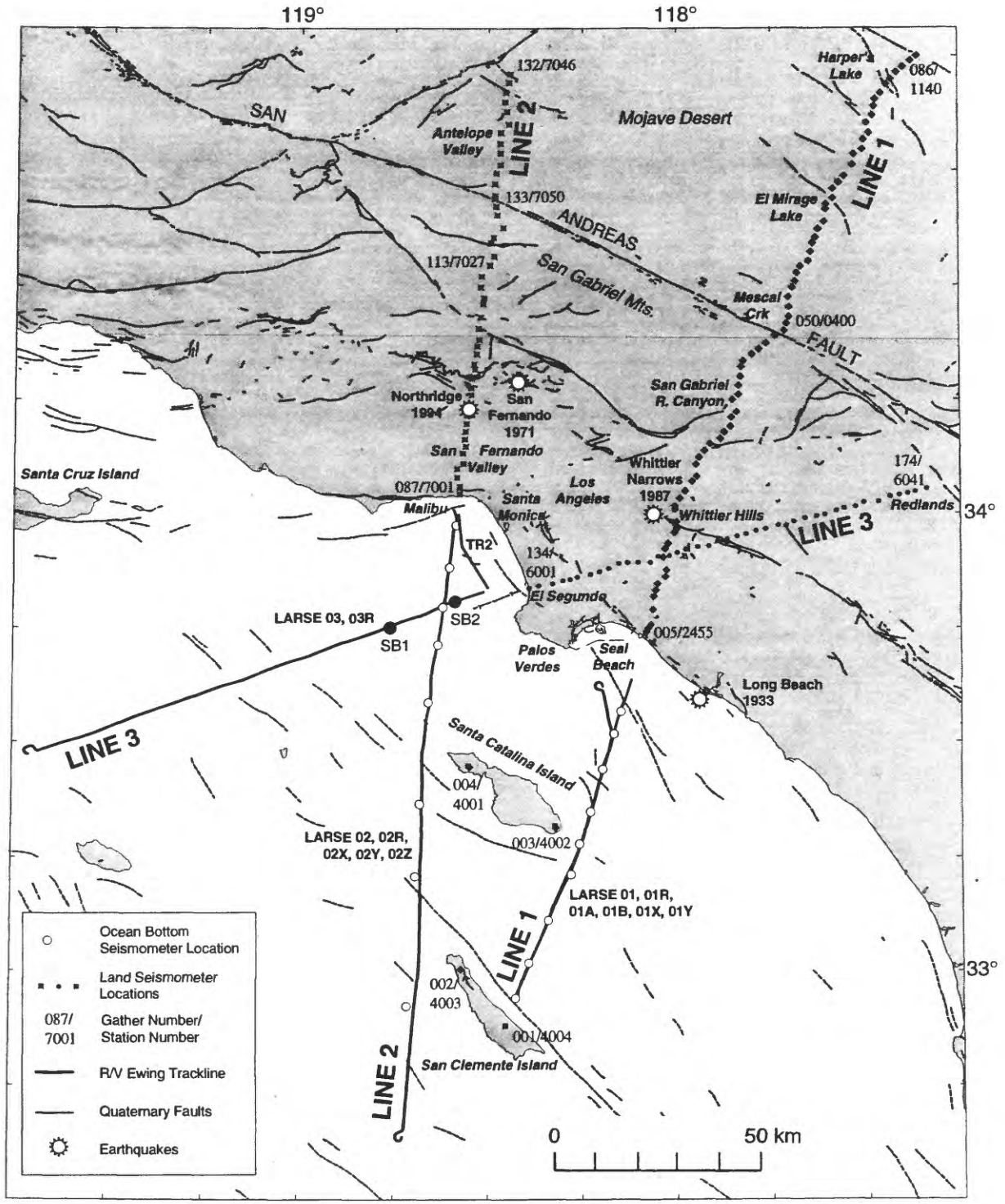

Fig. 1. An overview of the offshore-onshore component of the LARSE experiment showing locations of LARSE lines 1 to 3, modified from Okaya et al. (1996). Locations of stations along the three land arrays are also shown. Receivers are numbered by gather numbers used in this report (1 to 174) and stake numbers used in Okaya et al. (1996). Locations of Sonobuoys 1 and 2 (SB1 and SB2), deployed along Lines 3 and 3R are shown by filled circles.

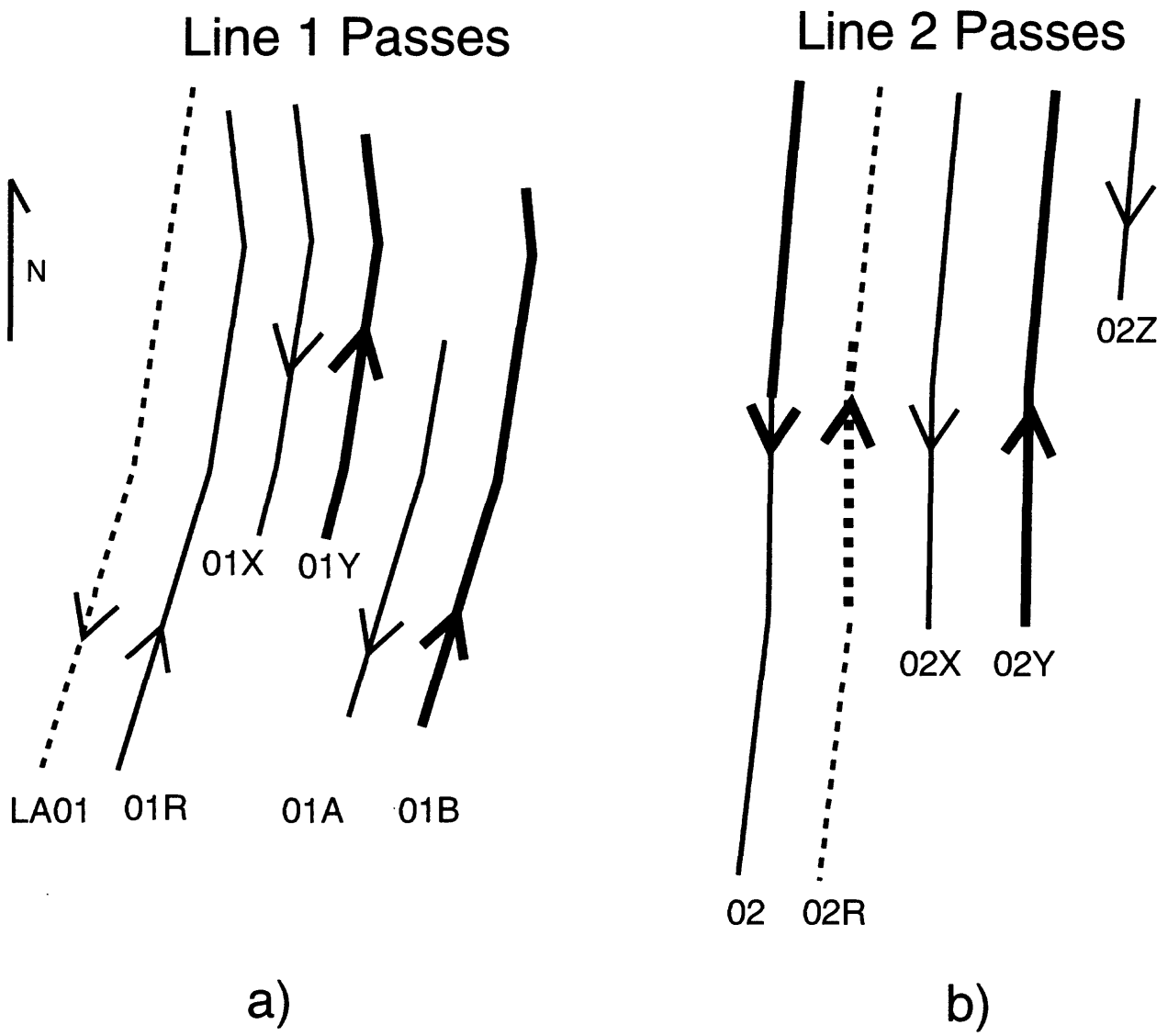

Fig. 2. Schematic trackline plots for LARSE (a) Line 1 and (b) Line 2, showing the individual passes made over the lines. Note that passes were coincident and have been offset from each other in this figure for clarity. Arrow shows direction of *Ewing* track. Except for the pass, LA01, the northern ends for all of the Line 1 passes were kinked to the northwest to avoid the coastal shipping lanes. Heavy lines indicate ship tracks acquired during late night hours (2200 to 0600 L). Passes LA01 and 02R are dashed to indicate the longer (60- and 90-second, respectively) repetition rate leading to a lower-density of air gun shots.

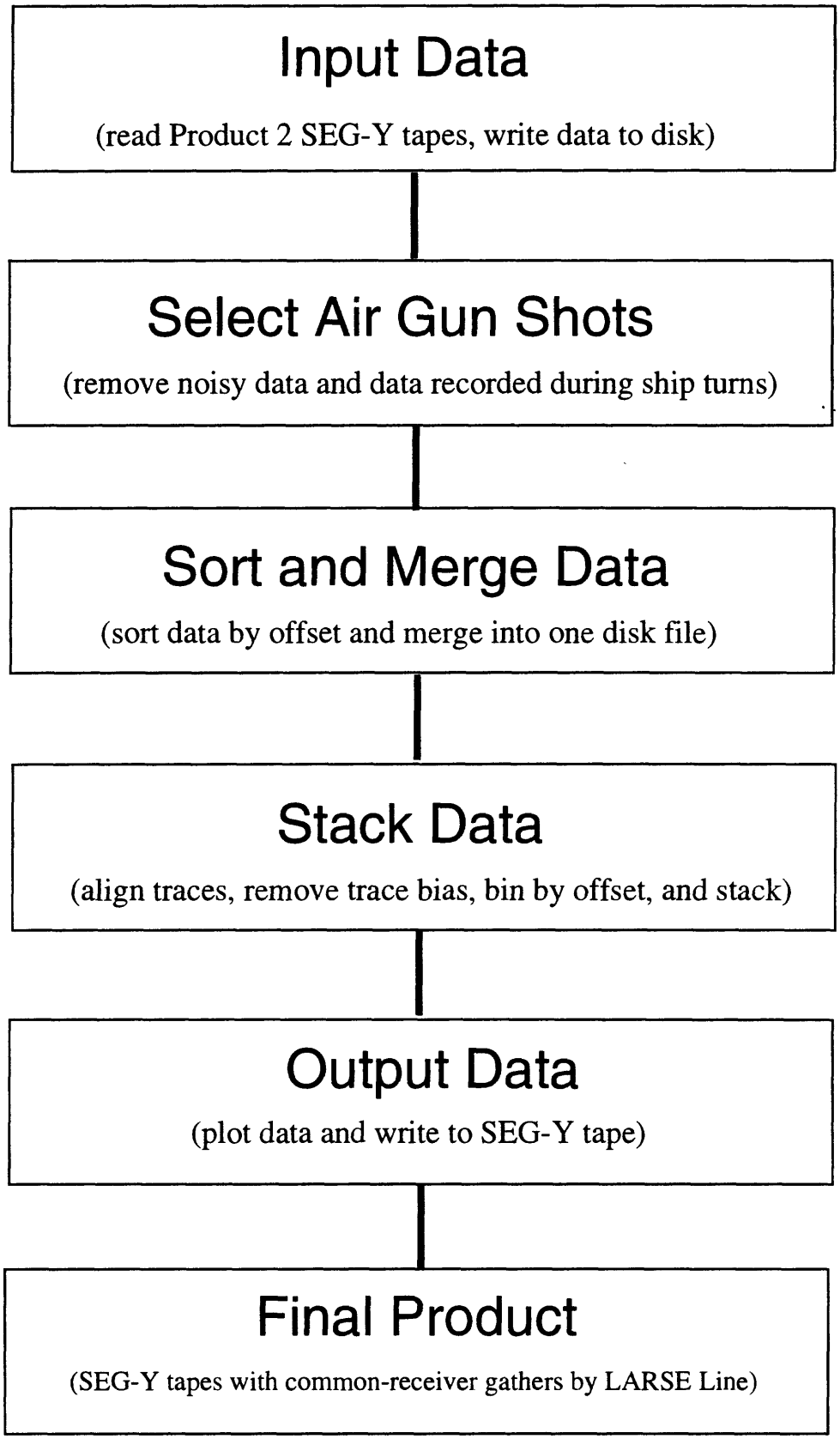

Fig. 3. Schematic diagram showing data processing flow described in detail in Appendix 1.

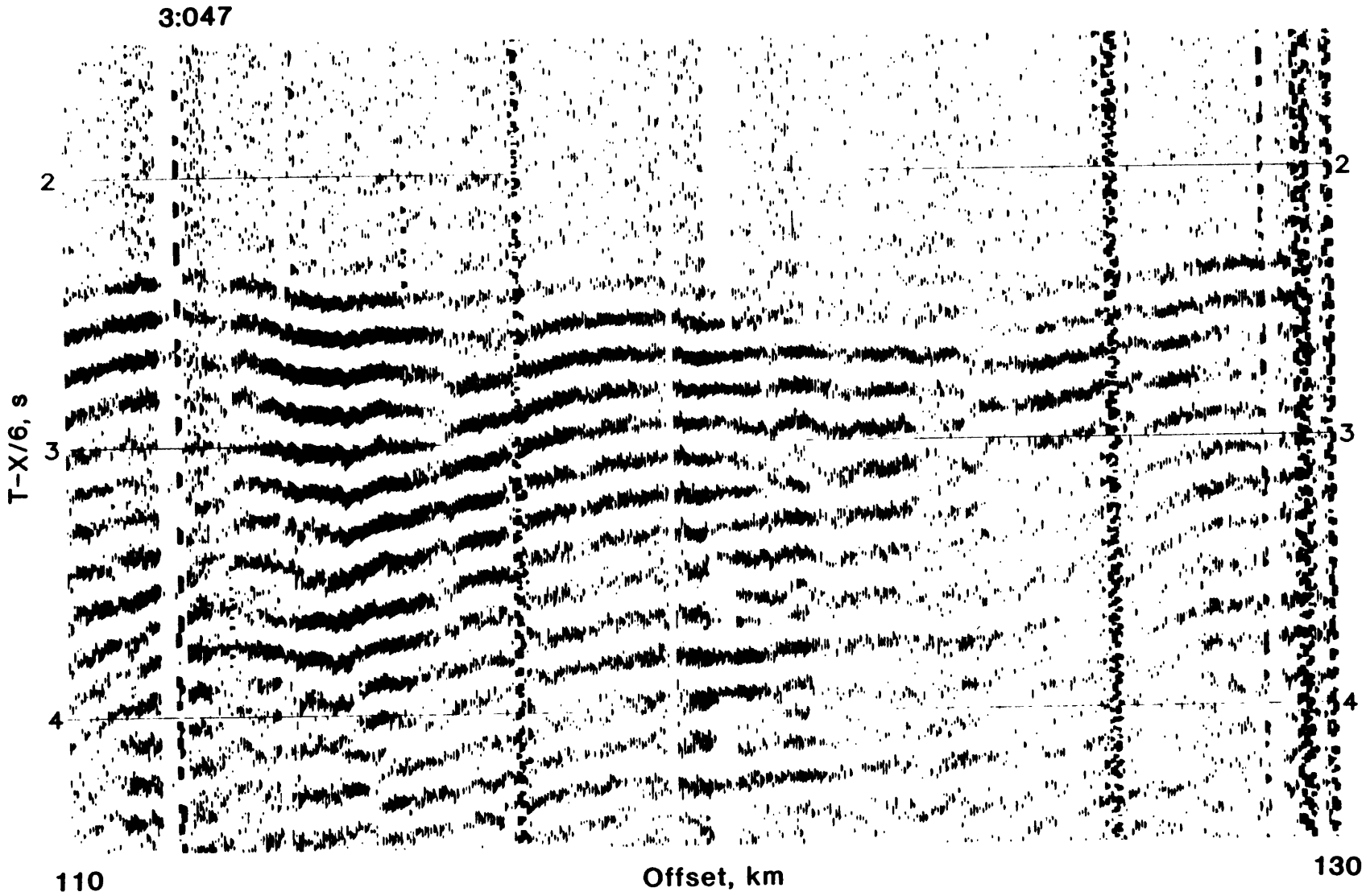

Figure 4a. Portion of common receiver gather 047 for shots along LARSE air gun Line 3, reduced at 6 km/s.

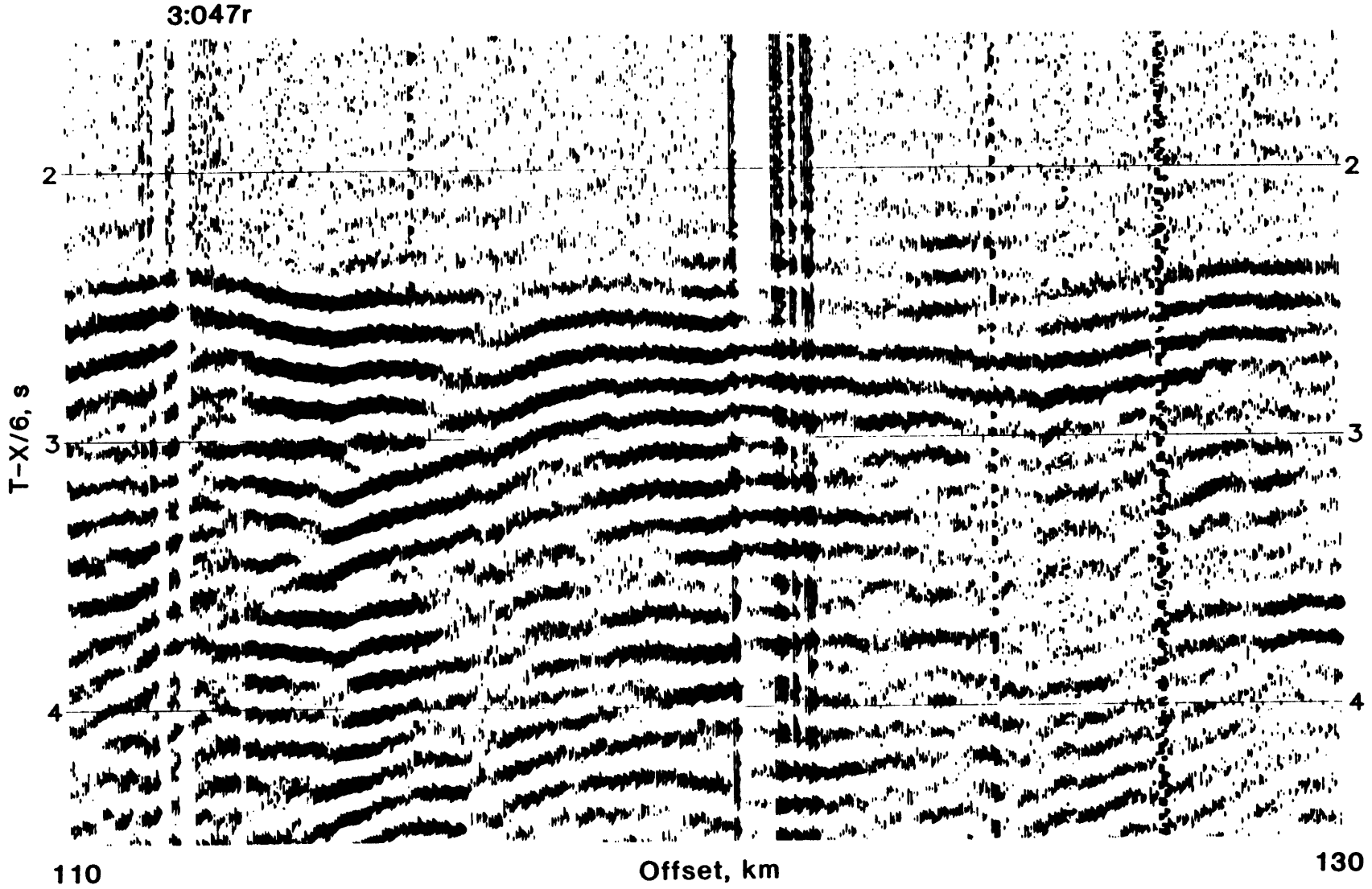

Figure 4b. Portion of common receiver gather 047 for shots along LARSE air gun Line 3R, reduced at 6 km/s.

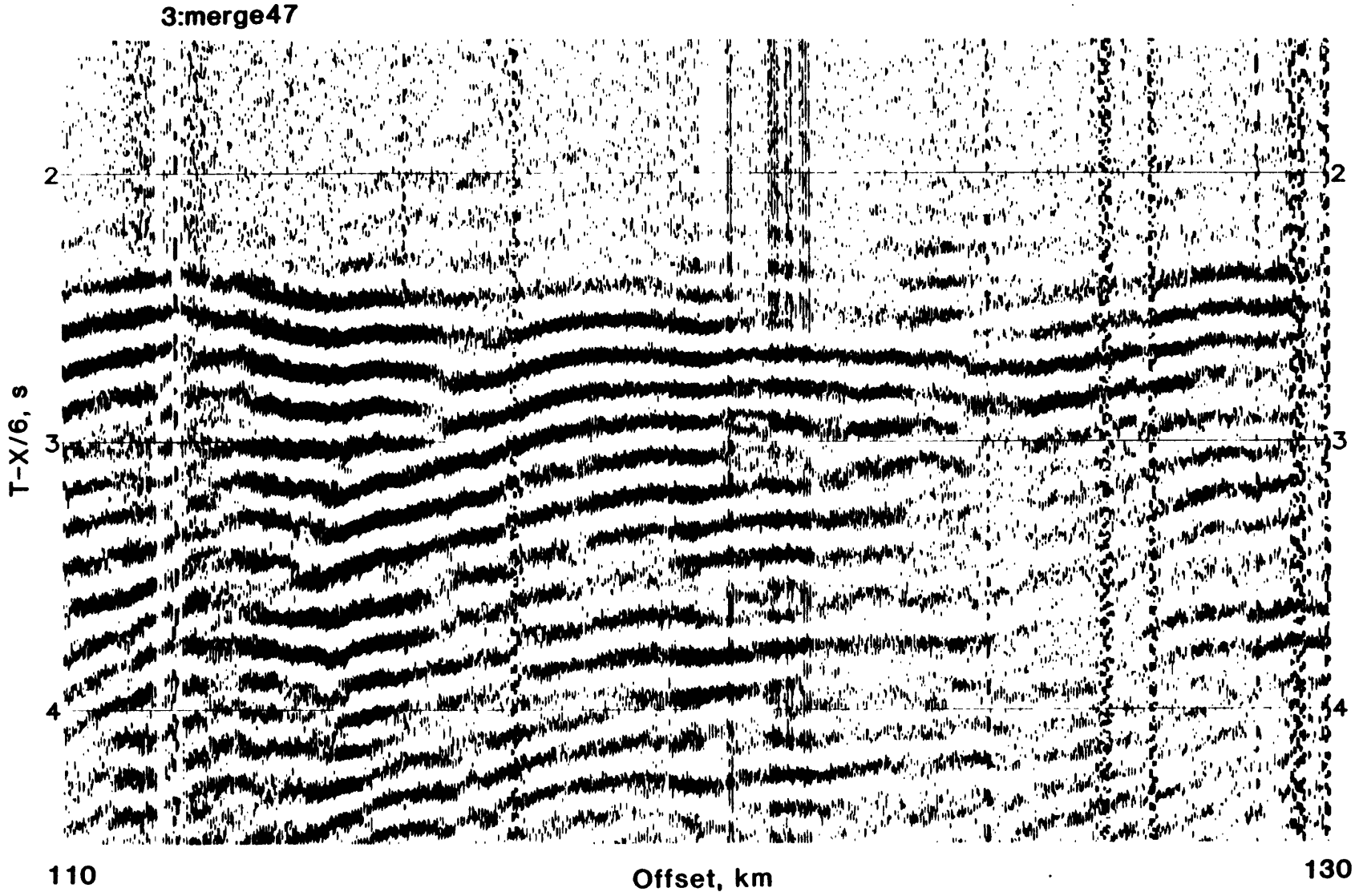

Figure 4c. Portion of merged common receiver gather 047 for shots along LARSE air gun Lines 3 and 3R, reduced at 6 km/s.

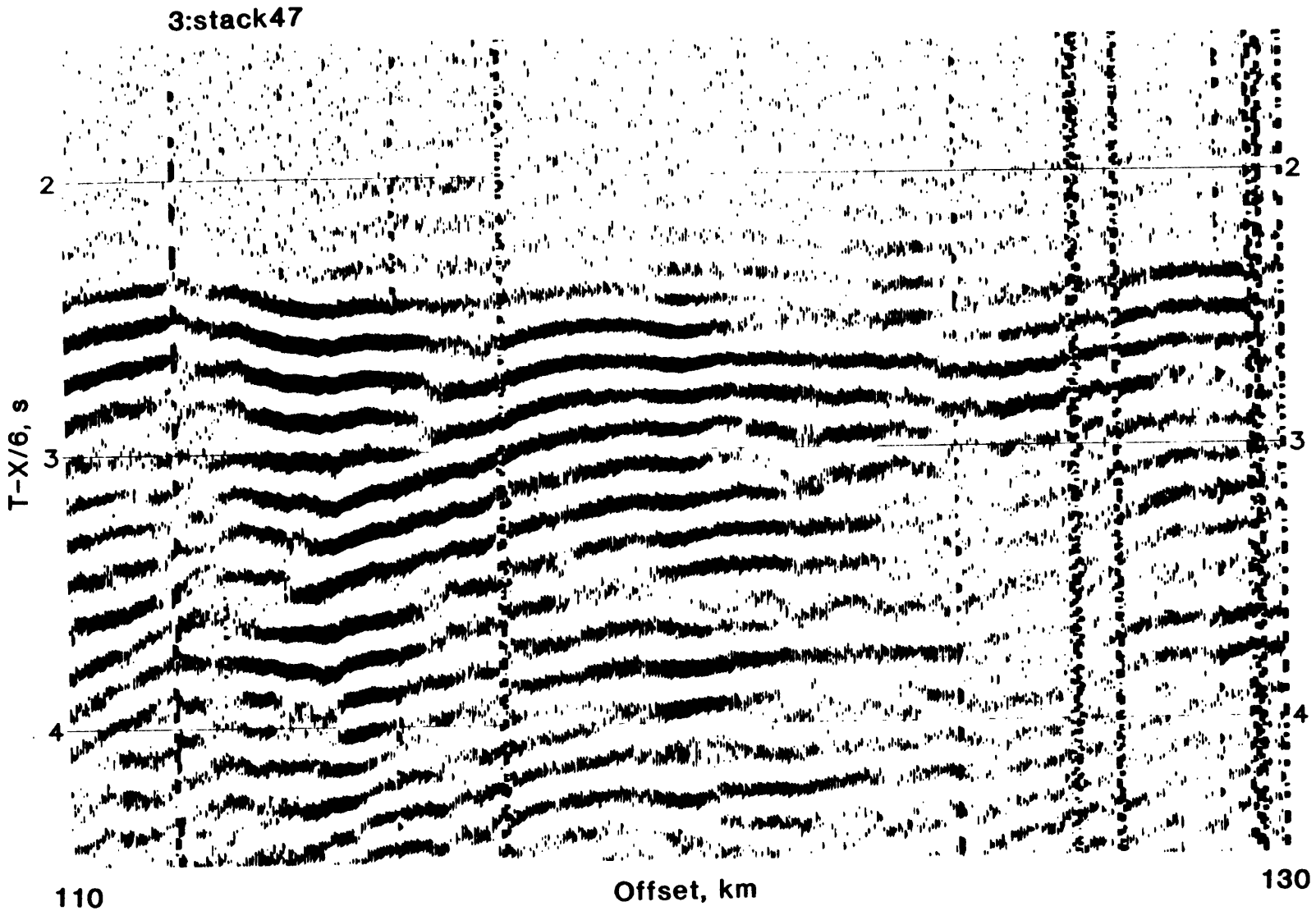

Figure 4d. Portion of stacked common receiver gather 047 for shots along LARSE air gun Lines 3 and 3R, reduced at 6 km/s.

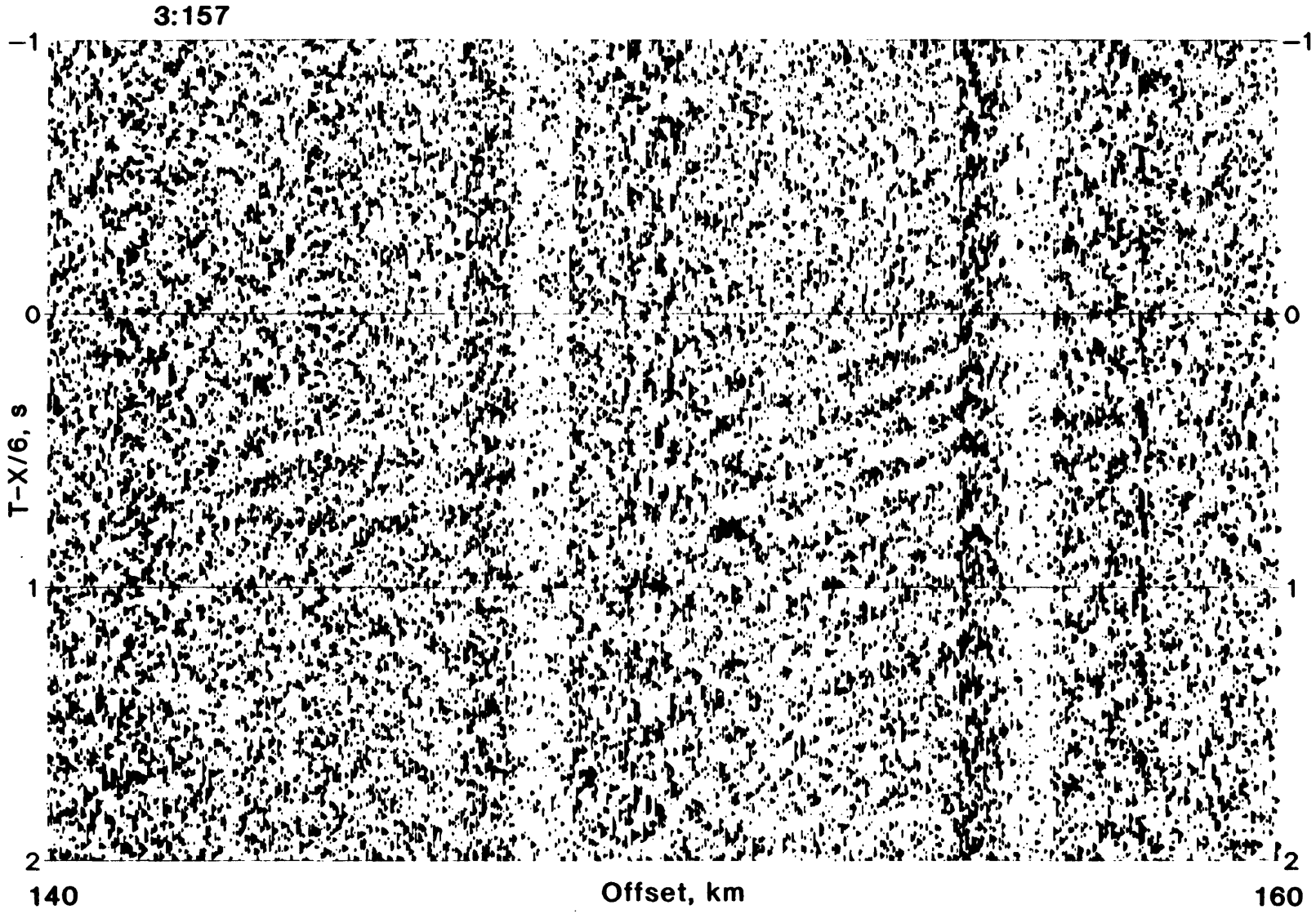

Figure 5a. Portion of common receiver gather 157 for shots along LARSE air gun Line 3, reduced at 6 km/s.

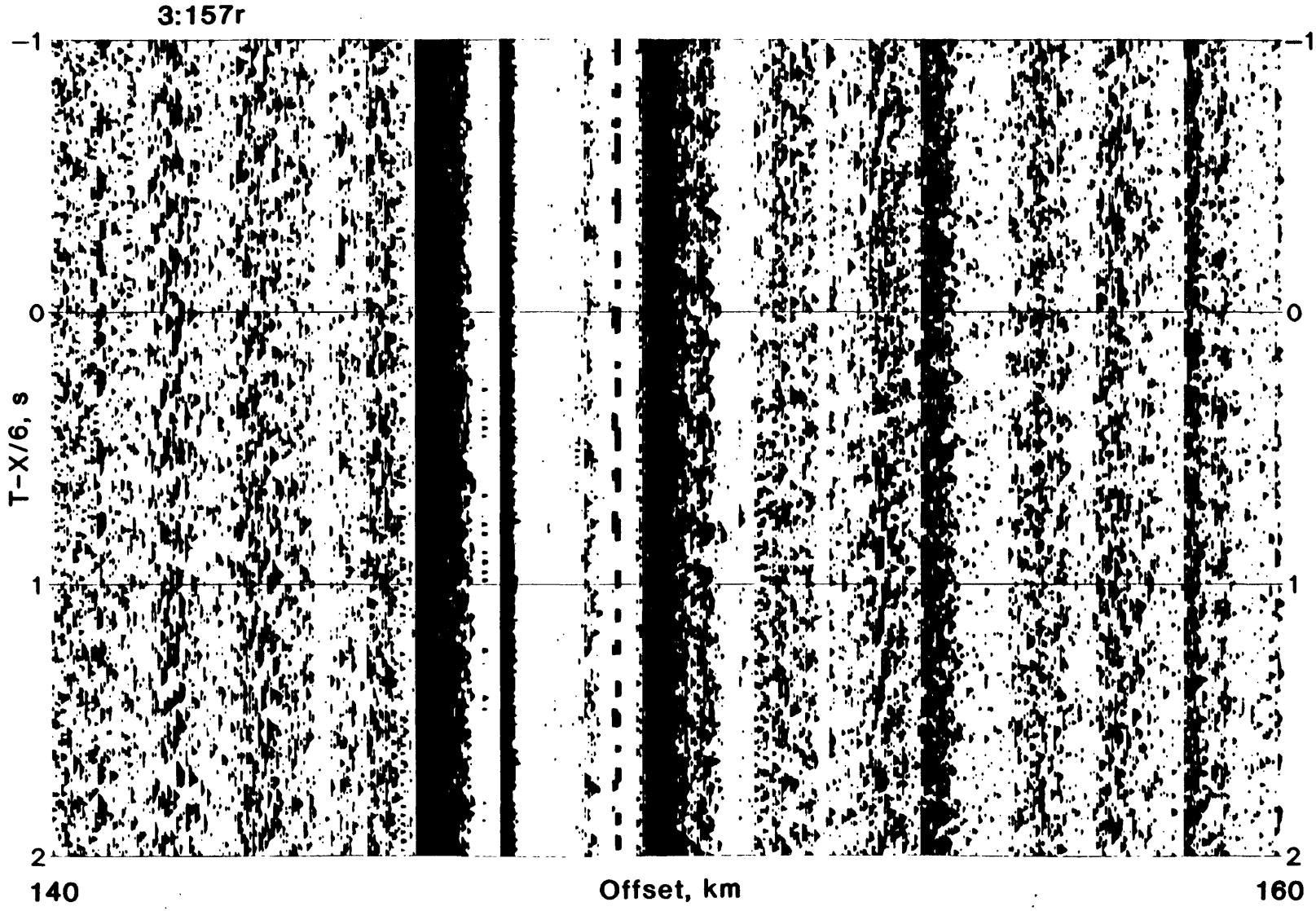

Figure 5b. Portion of common receiver gather 157 for shots along LARSE air gun Line 3R, reduced at 6 km/s.

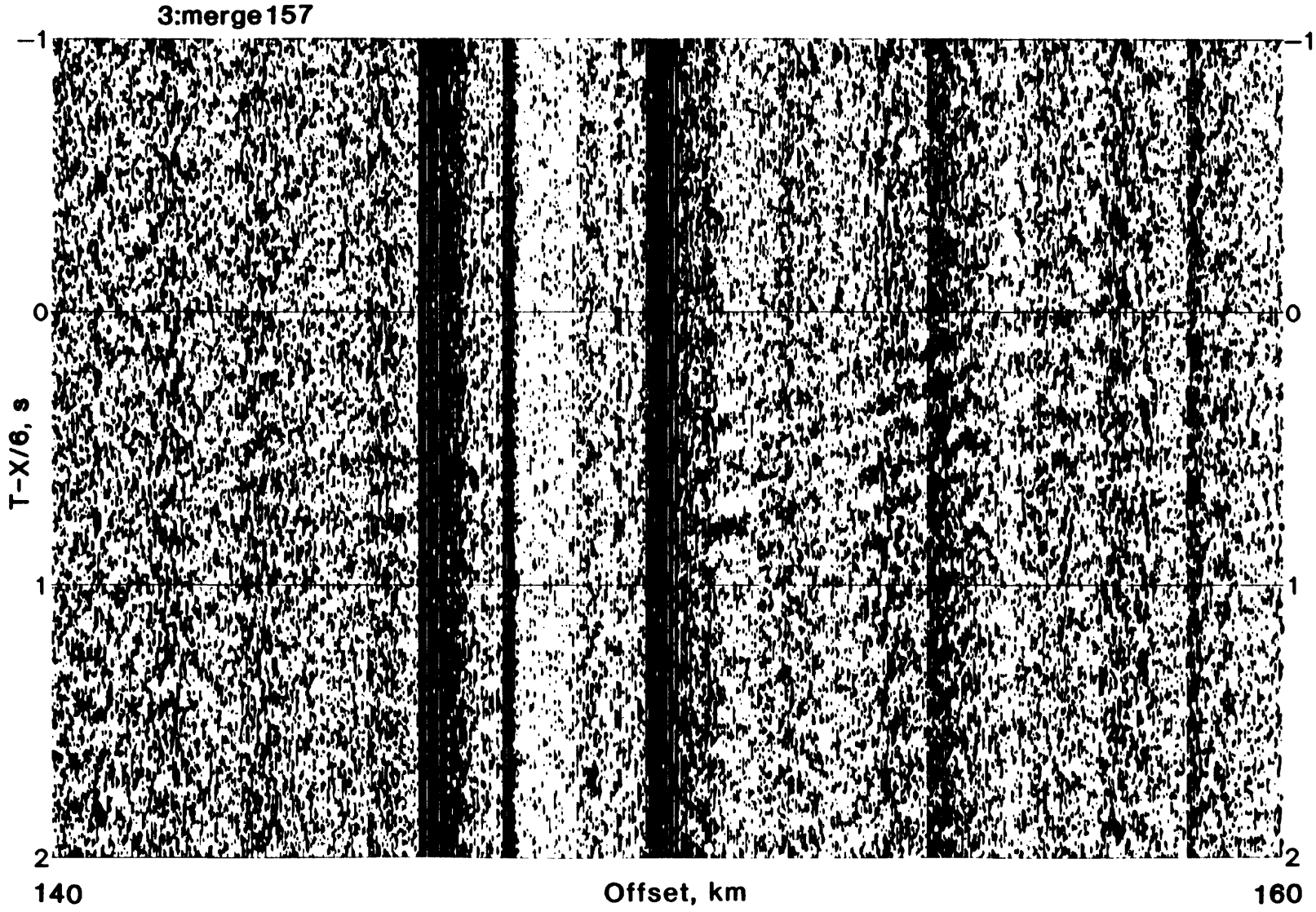

Figure 5c. Portion of merged common receiver gather 157 for shots along LARSE air gun Lines 3 and 3R, reduced at 6 km/s.

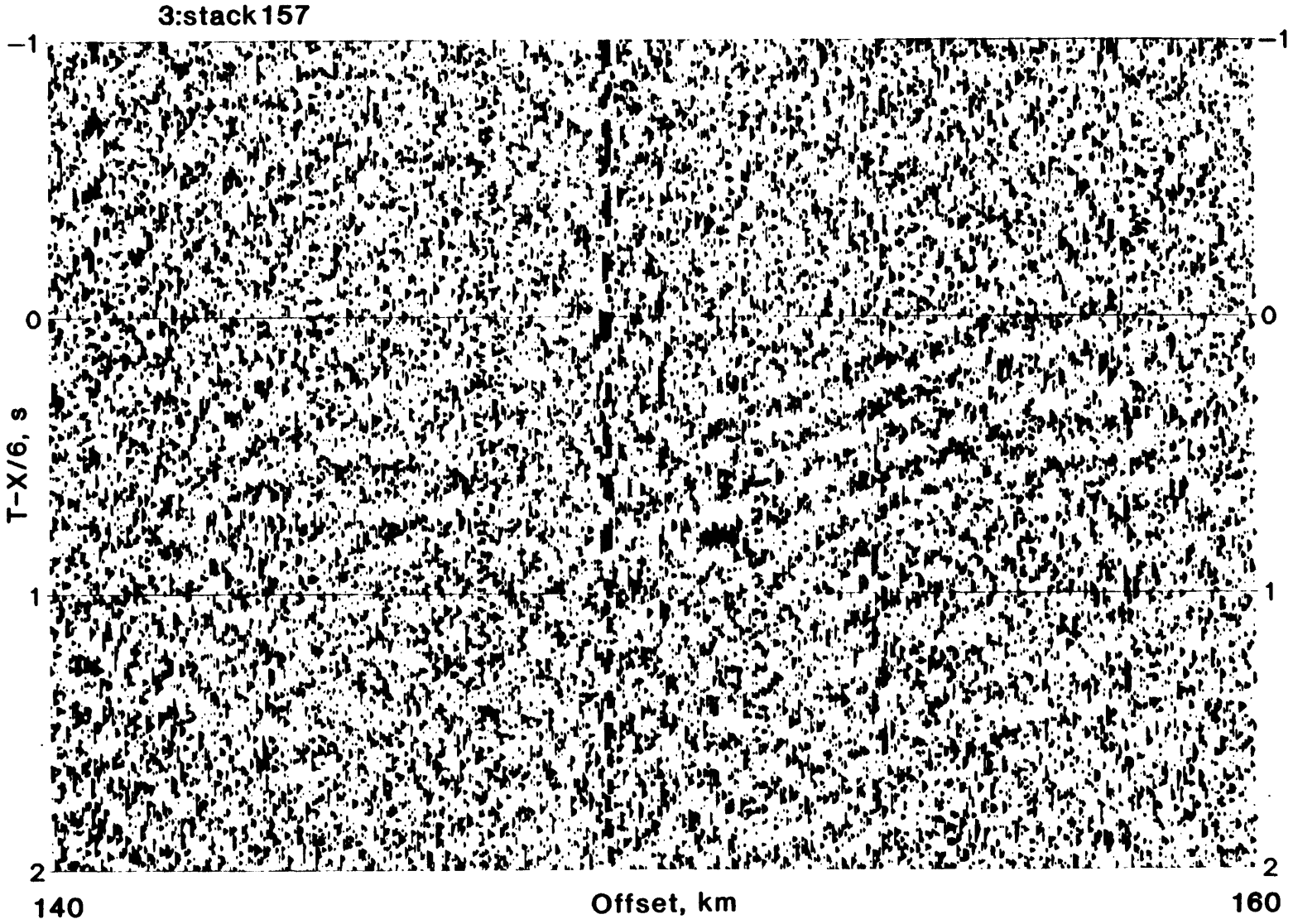

Figure 5d. Portion of stacked common receiver gather 157 for shots along LARSE air gun Lines 3 and 3R, reduced at 6 km/s.

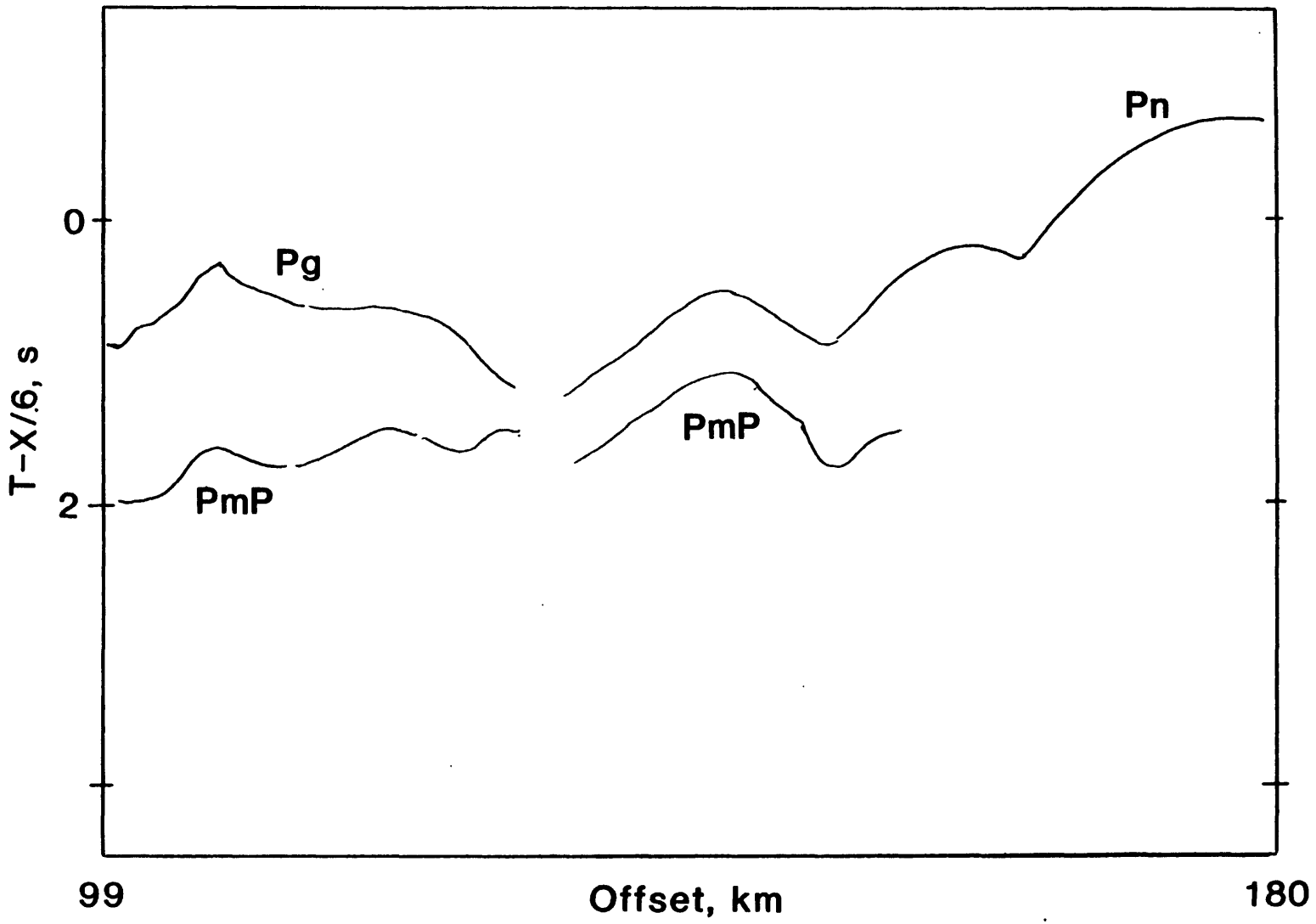

Figure 6. Schematic illustration showing typical arrivals (Pg, Pn, and PmP) observed on LARSE wide-angle common receiver gathers.

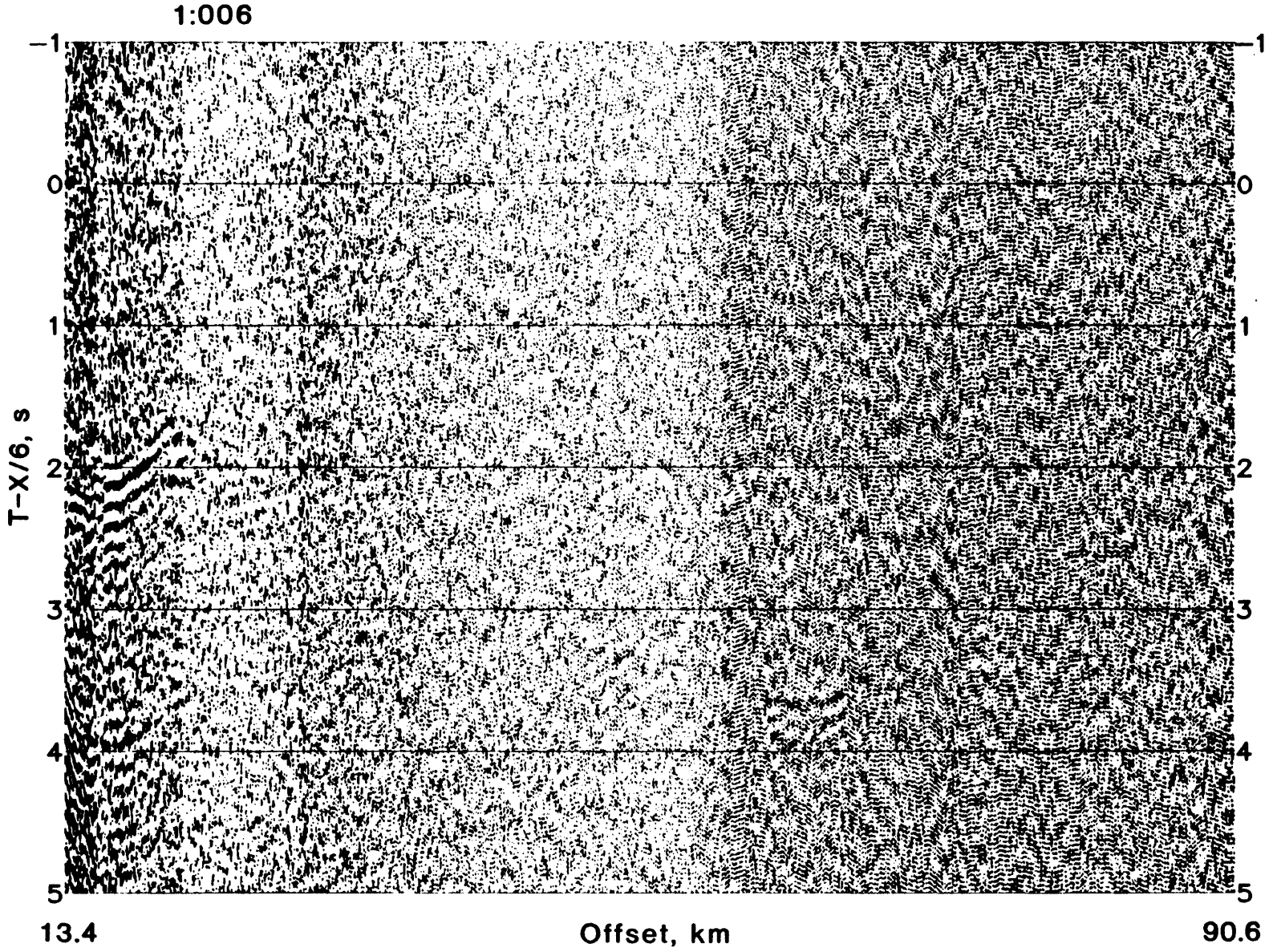

Figure 7. Stacked common receiver gather 006 for shots along LARSE air gun Line 1, reduced at 6 km/s.

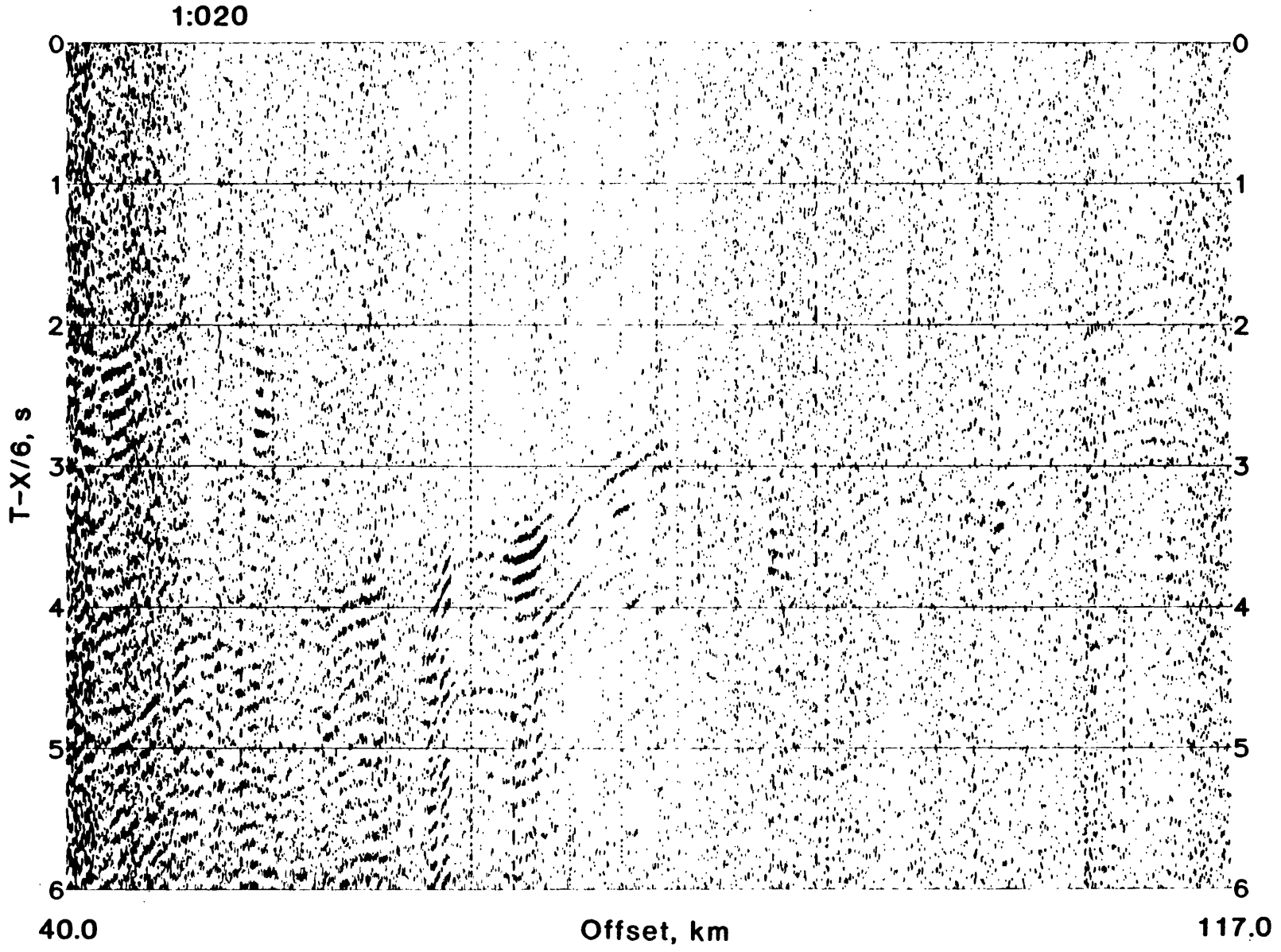

Figure 8. Stacked common receiver gather 020 for shots along LARSE air gun Line 1, reduced at 6 km/s.

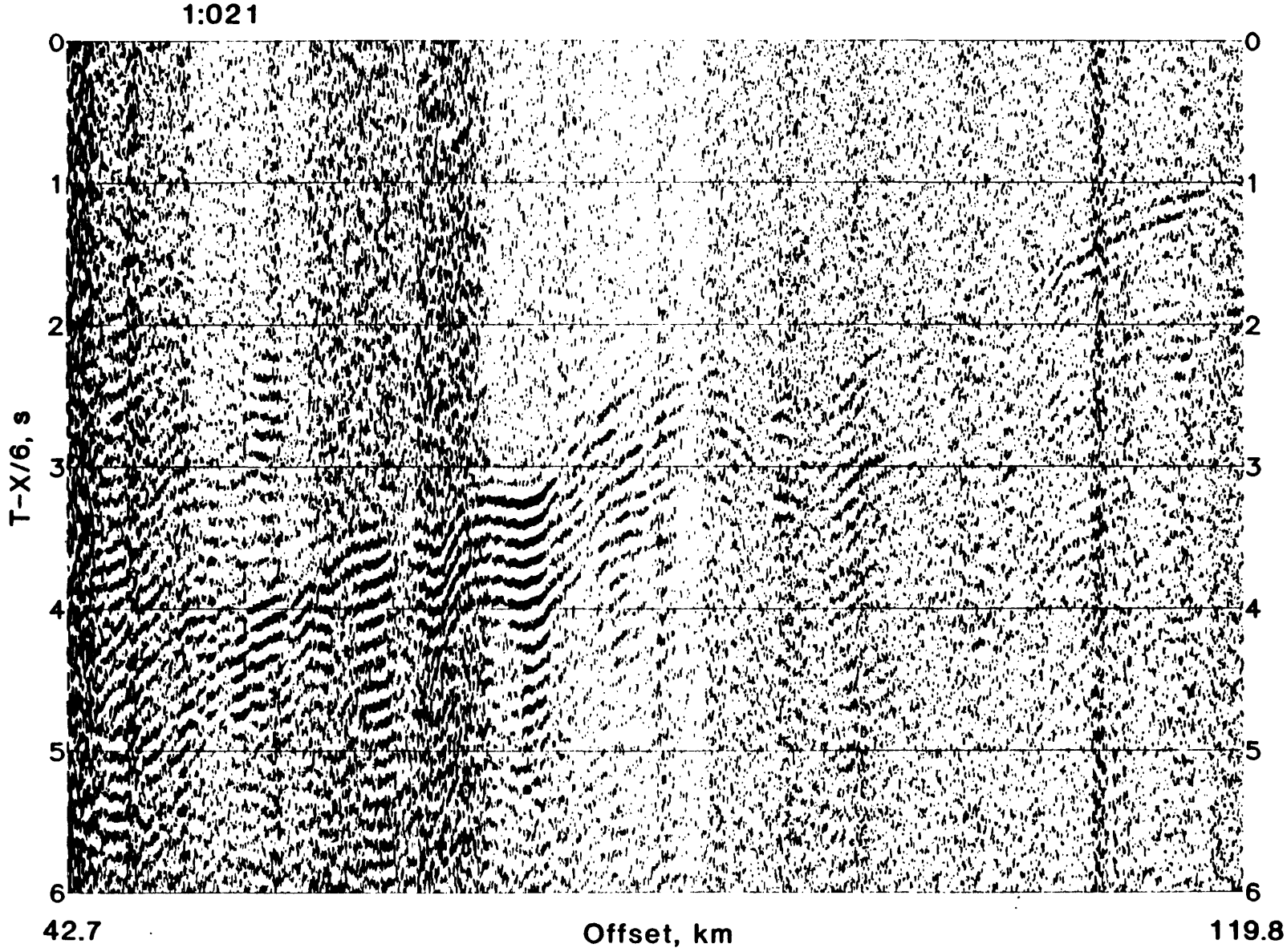

Figure 9. Stacked common receiver gather 021 for shots along LARSE air gun Line 1, reduced at 6 km/s.

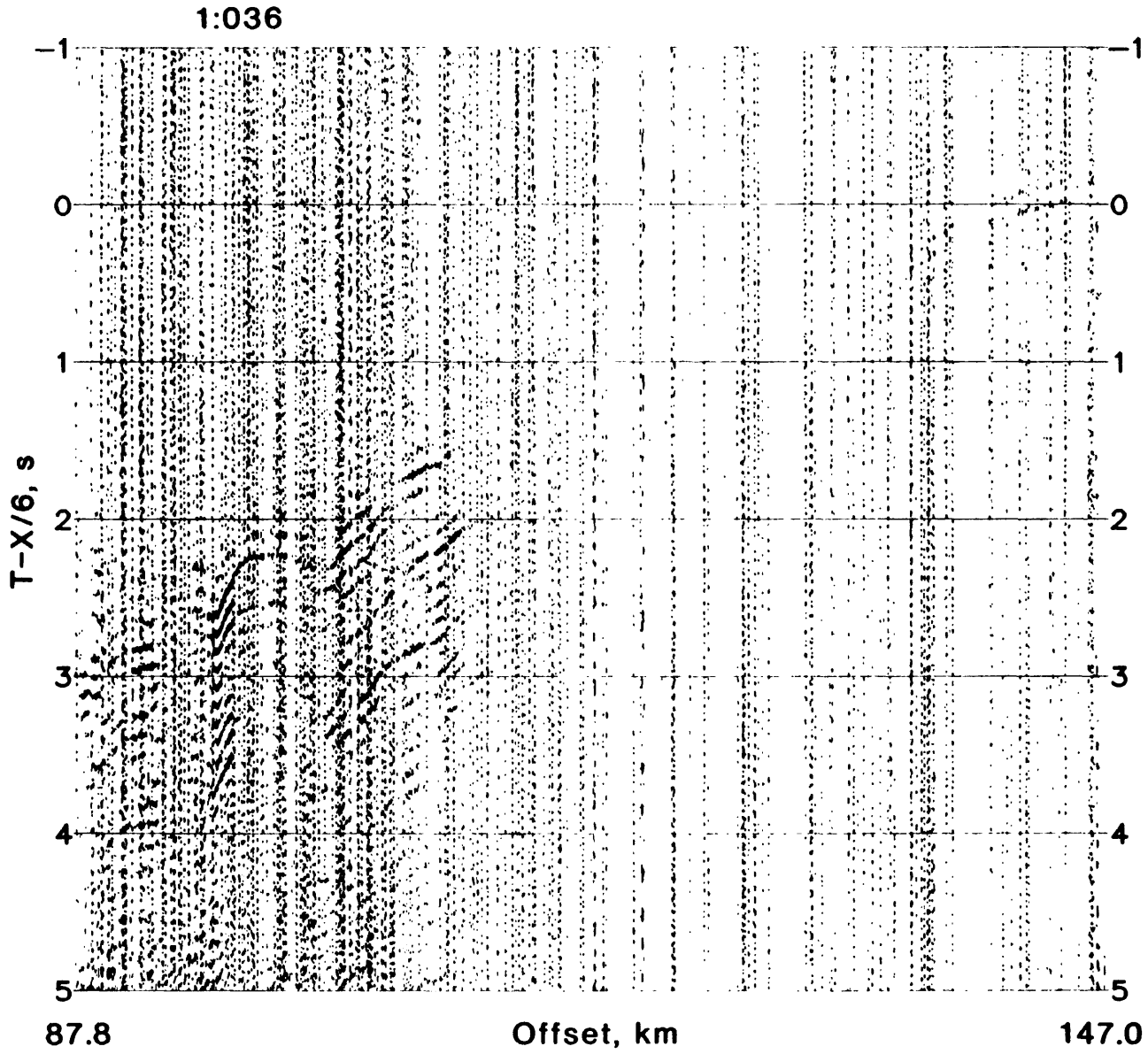

Figure 10. Stacked common receiver gather 036 for shots along LARSE air gun Line 1, reduced at 6 km/s.

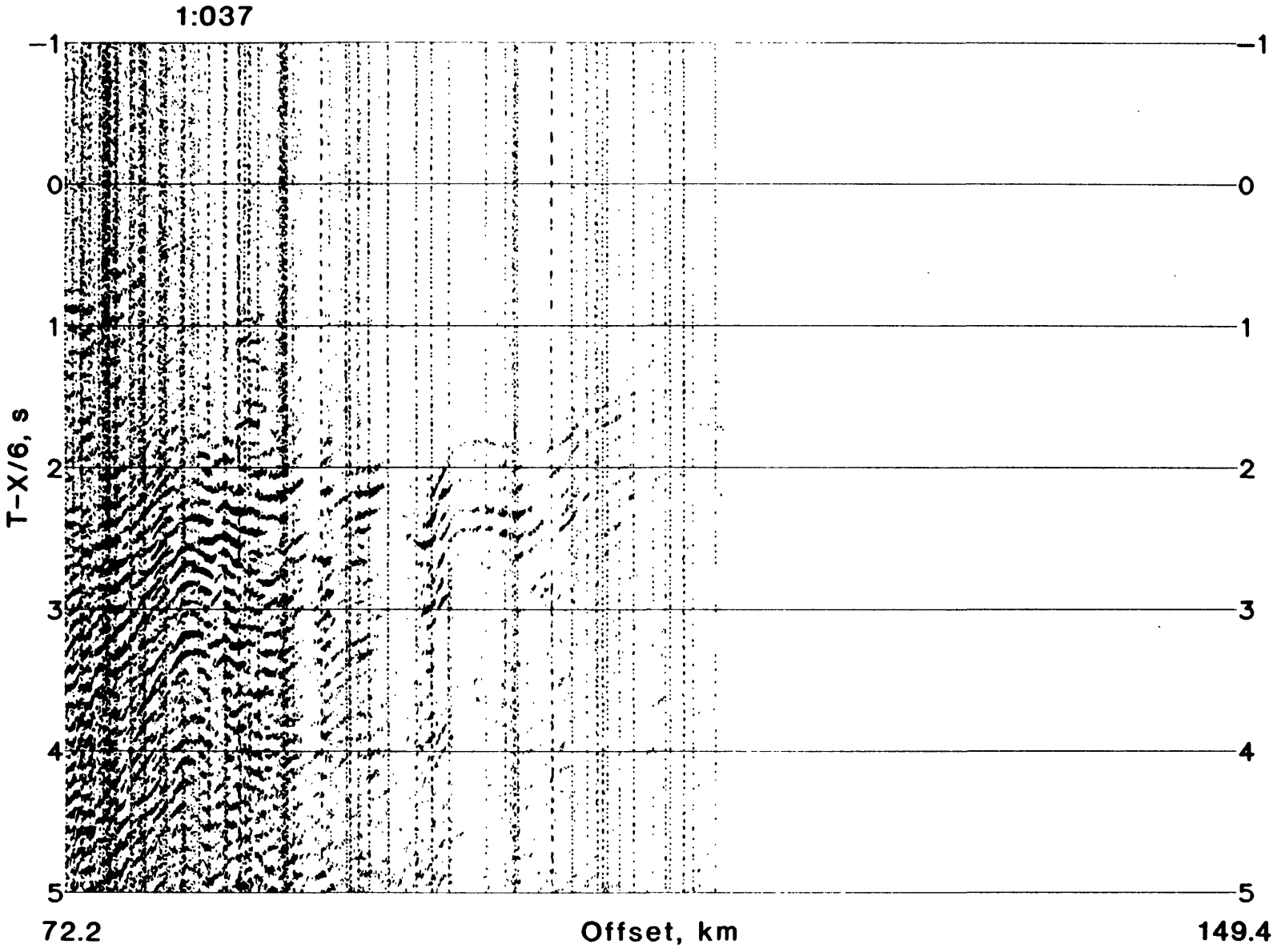

Figure 11. Stacked common receiver gather 037 for shots along LARSE air gun Line 1, reduced at 6 km/s.

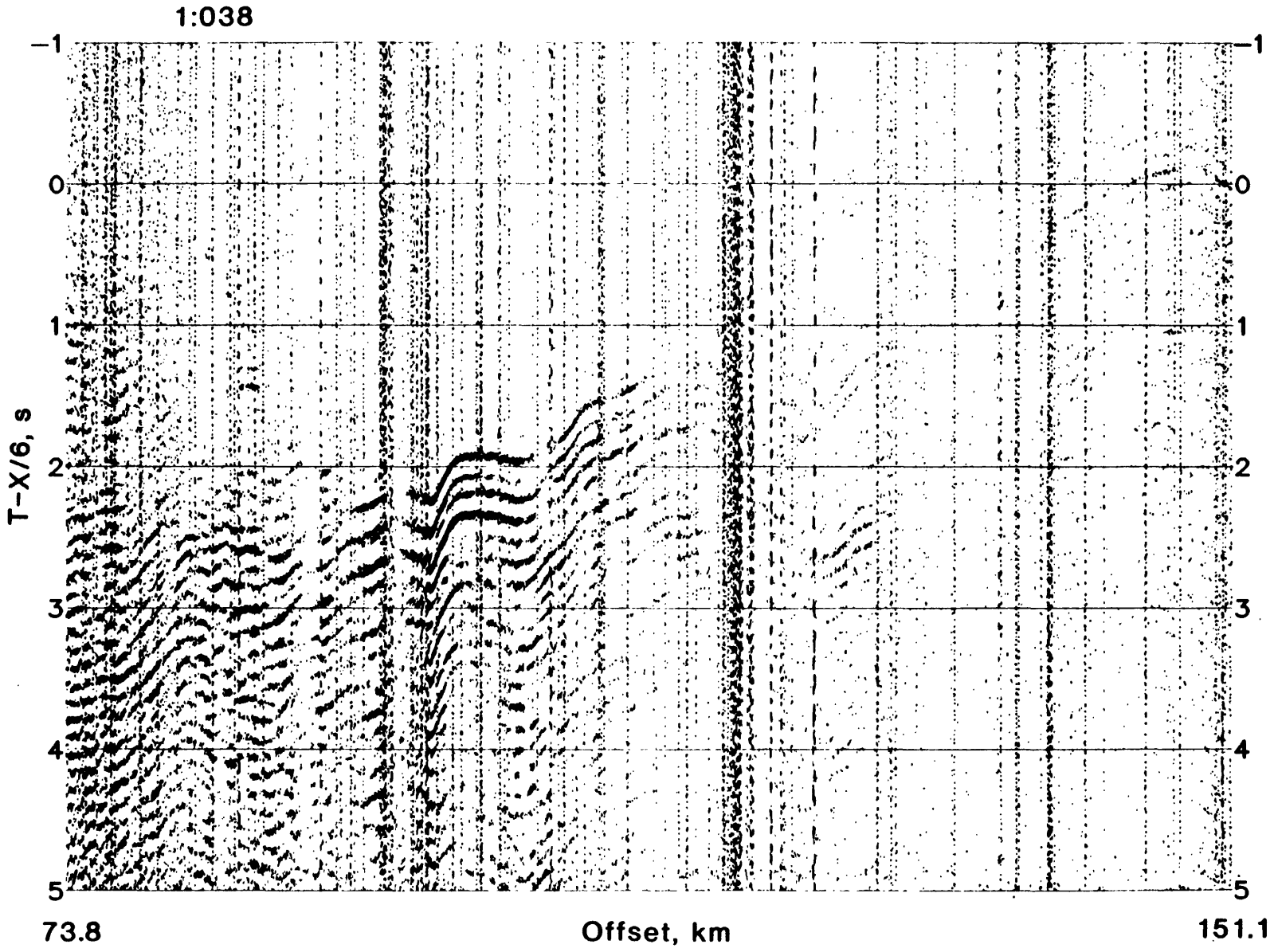

Figure 12. Stacked common receiver gather 038 for shots along LARSE air gun Line 1, reduced at 6 km/s.

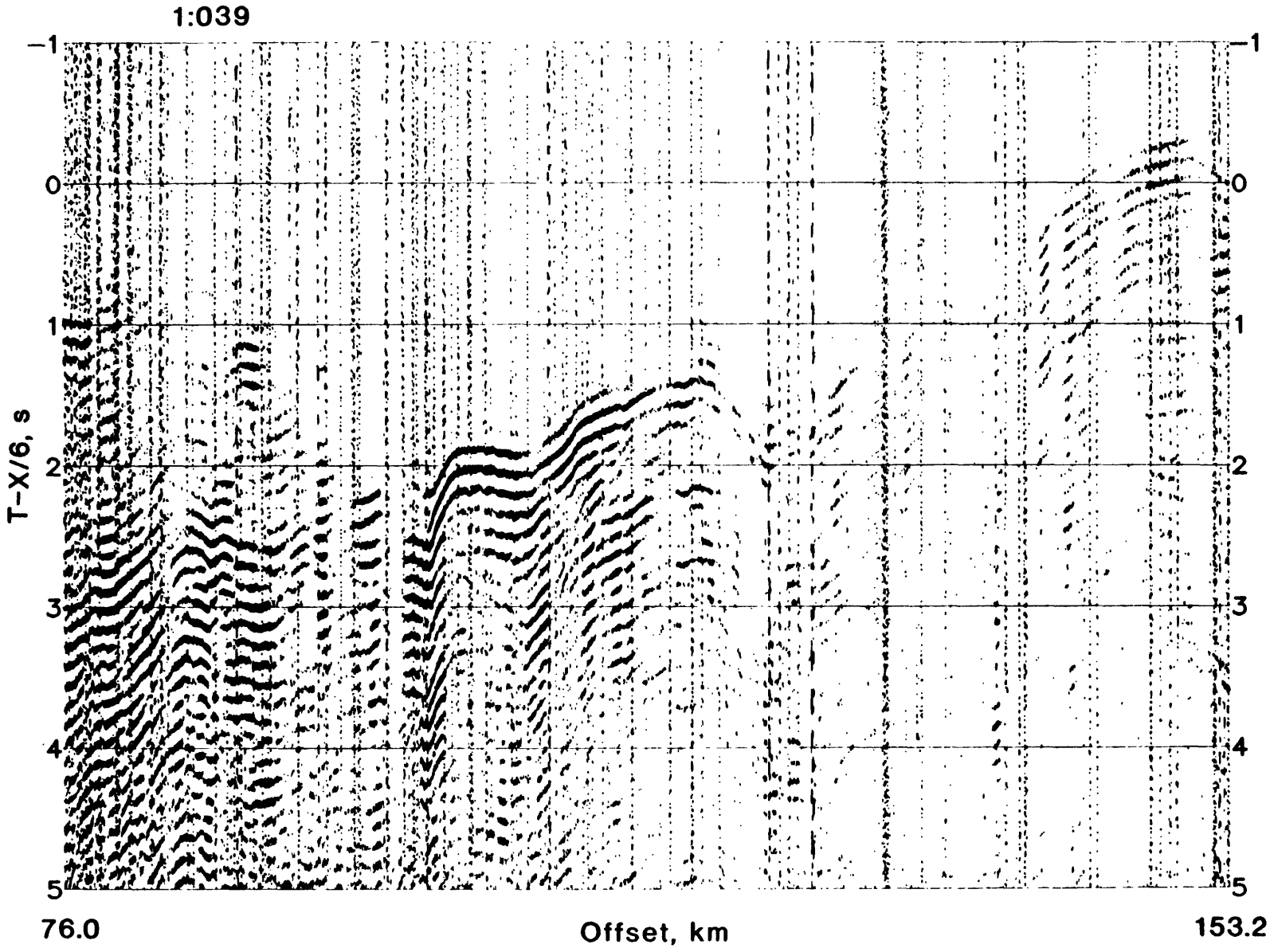

Figure 13. Stacked common receiver gather 039 for shots along LARSE air gun Line 1, reduced at 6 km/s.

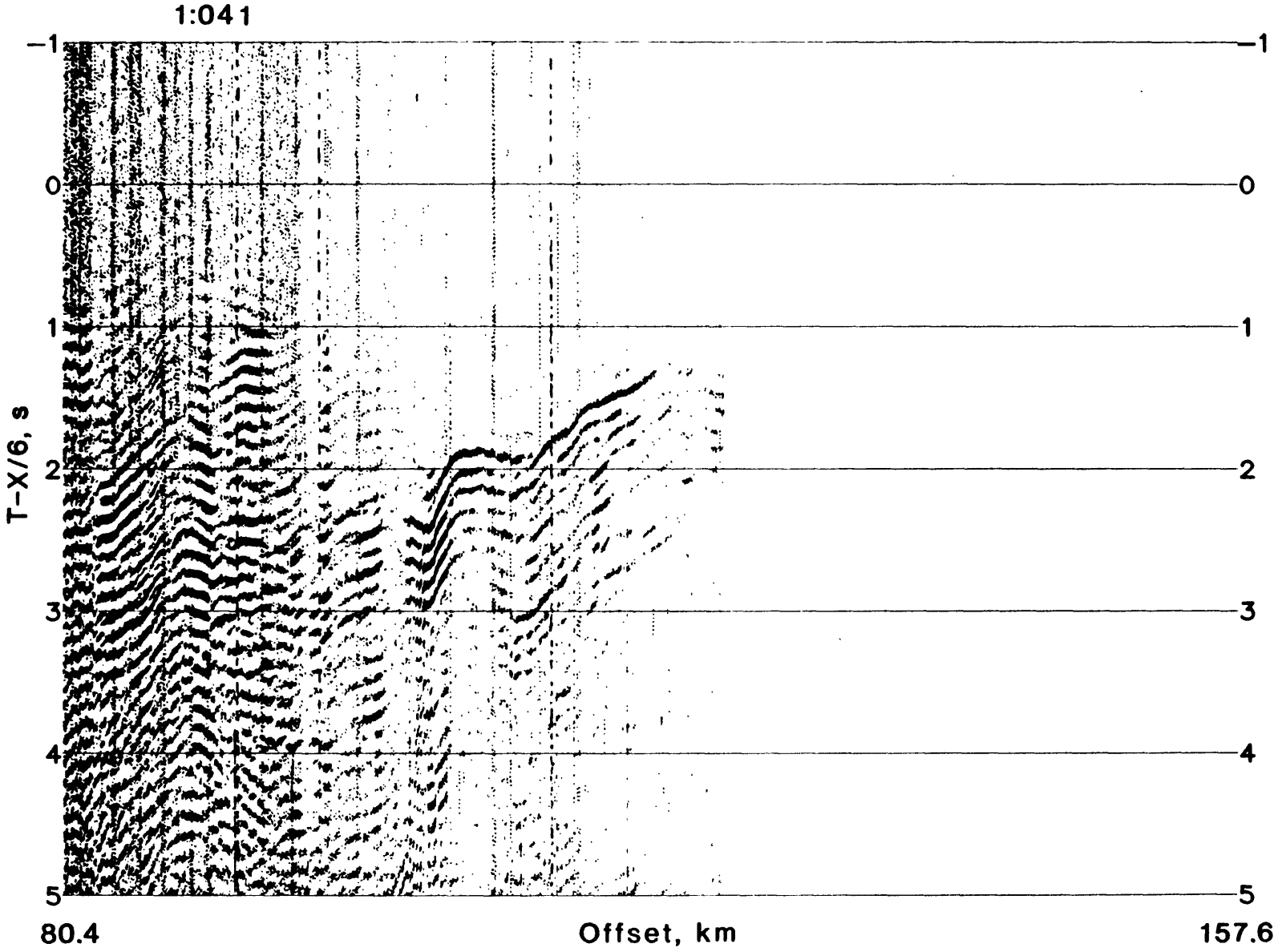

Figure 14. Stacked common receiver gather 041 for shots along LARSE air gun Line 1, reduced at 6 km/s.

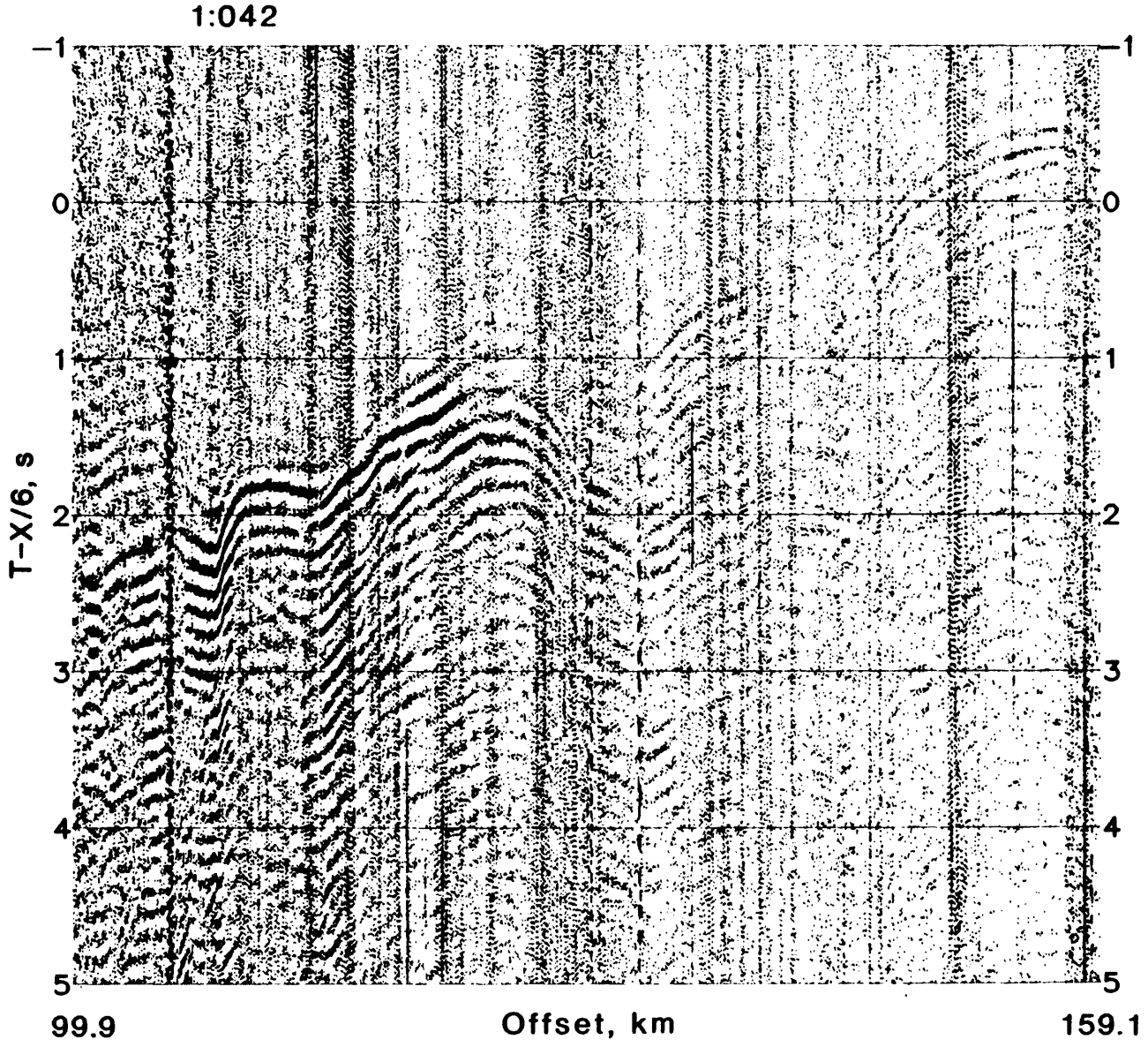

Figure 15. Stacked common receiver gather 042 for shots along LARSE air gun Line 1, reduced at 6 km/s.

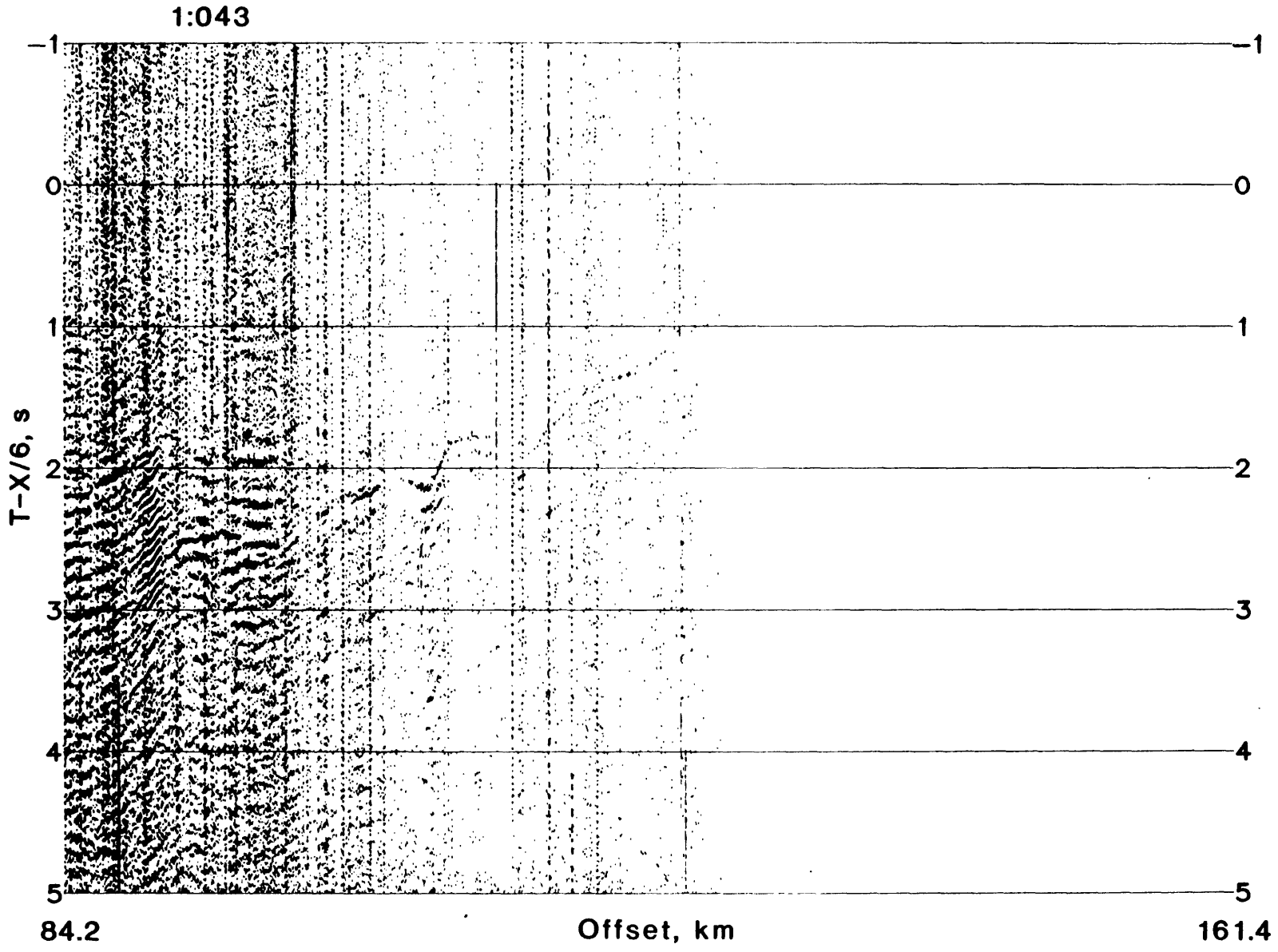

Figure 16. Stacked common receiver gather 043 for shots along LARSE air gun Line 1, reduced at 6 km/s.

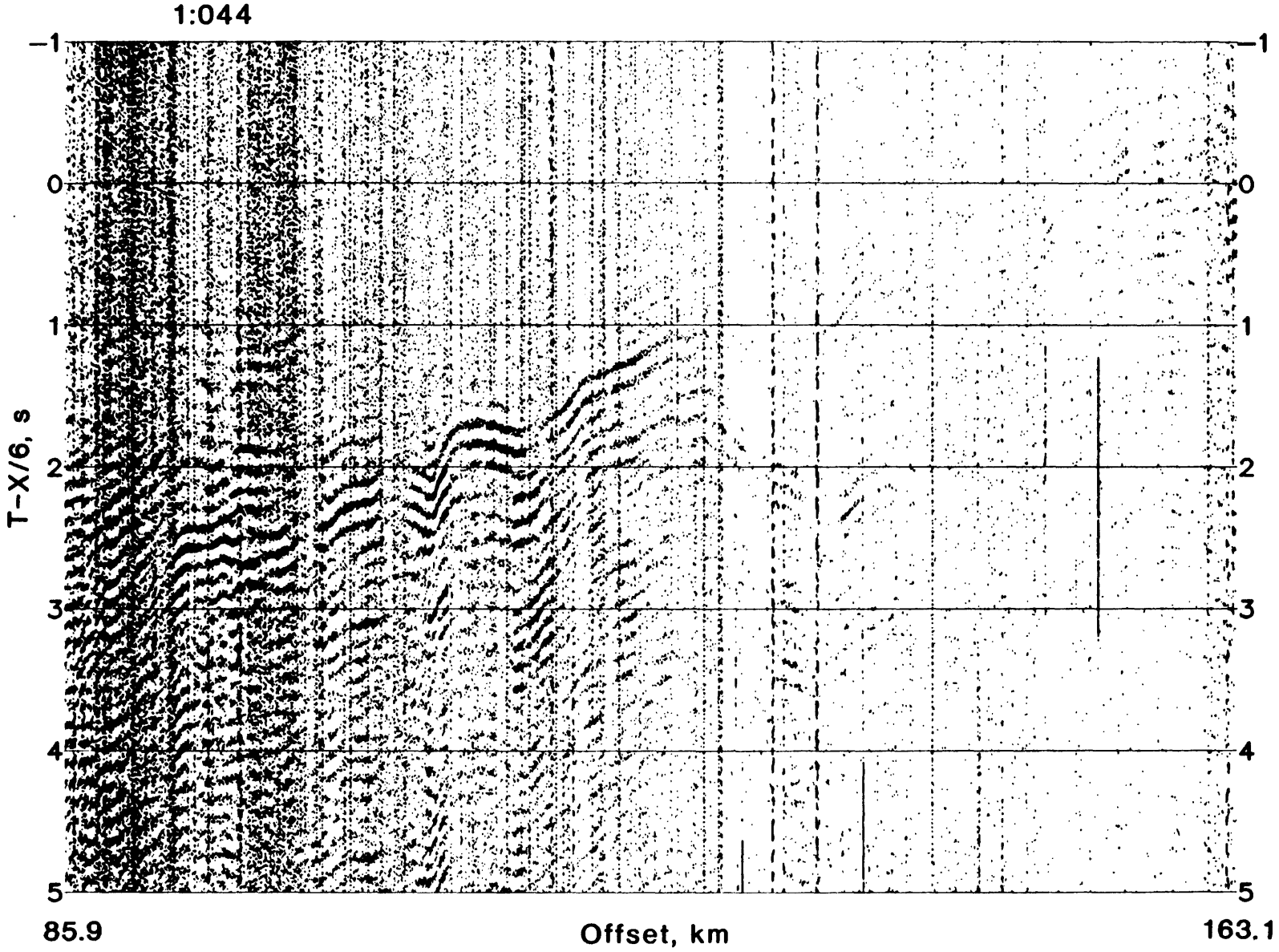

Figure 17. Stacked common receiver gather 044 for shots along LARSE air gun Line 1, reduced at 6 km/s.

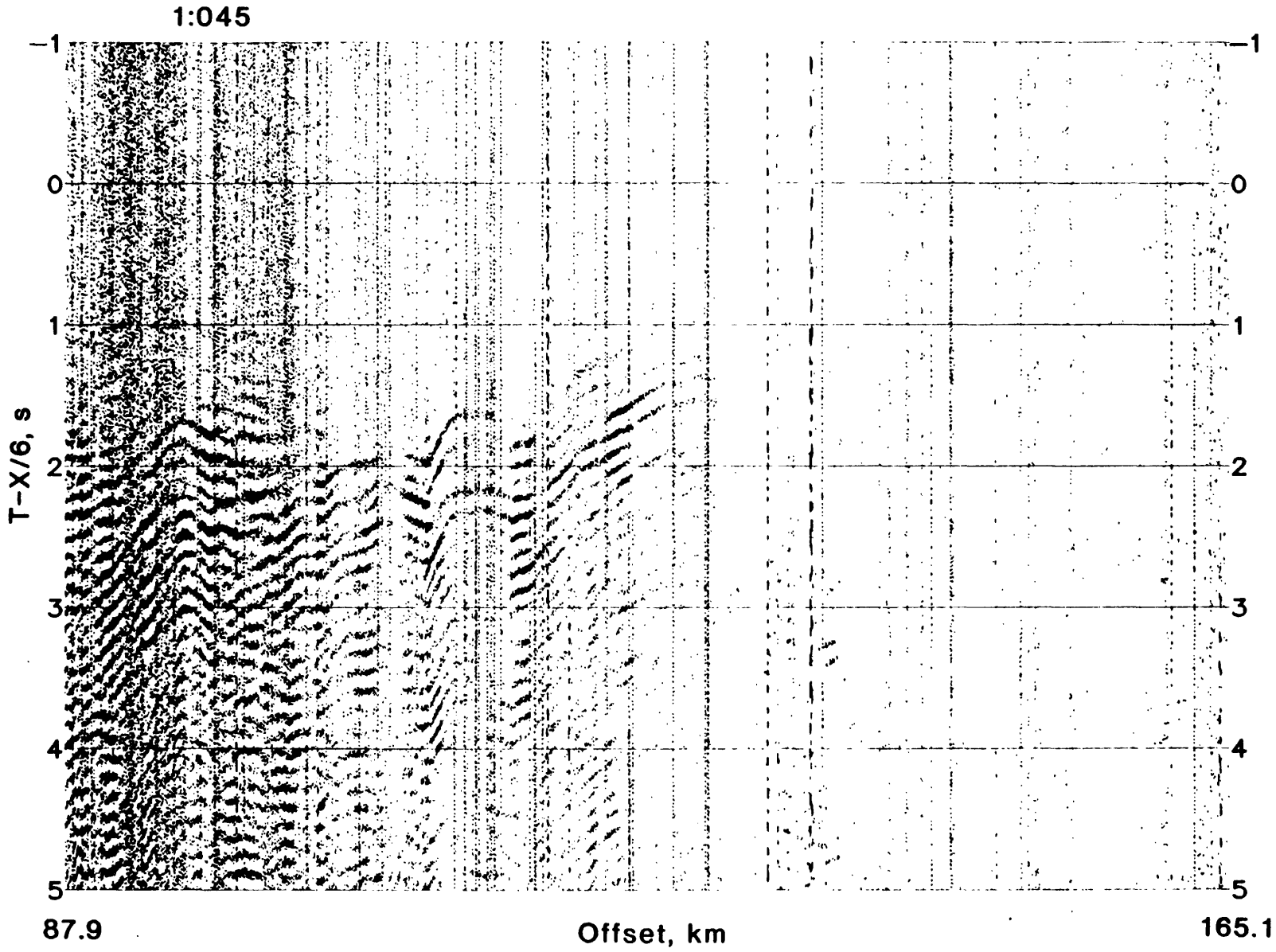

Figure 18. Stacked common receiver gather 045 for shots along LARSE air gun Line 1, reduced at 6 km/s.

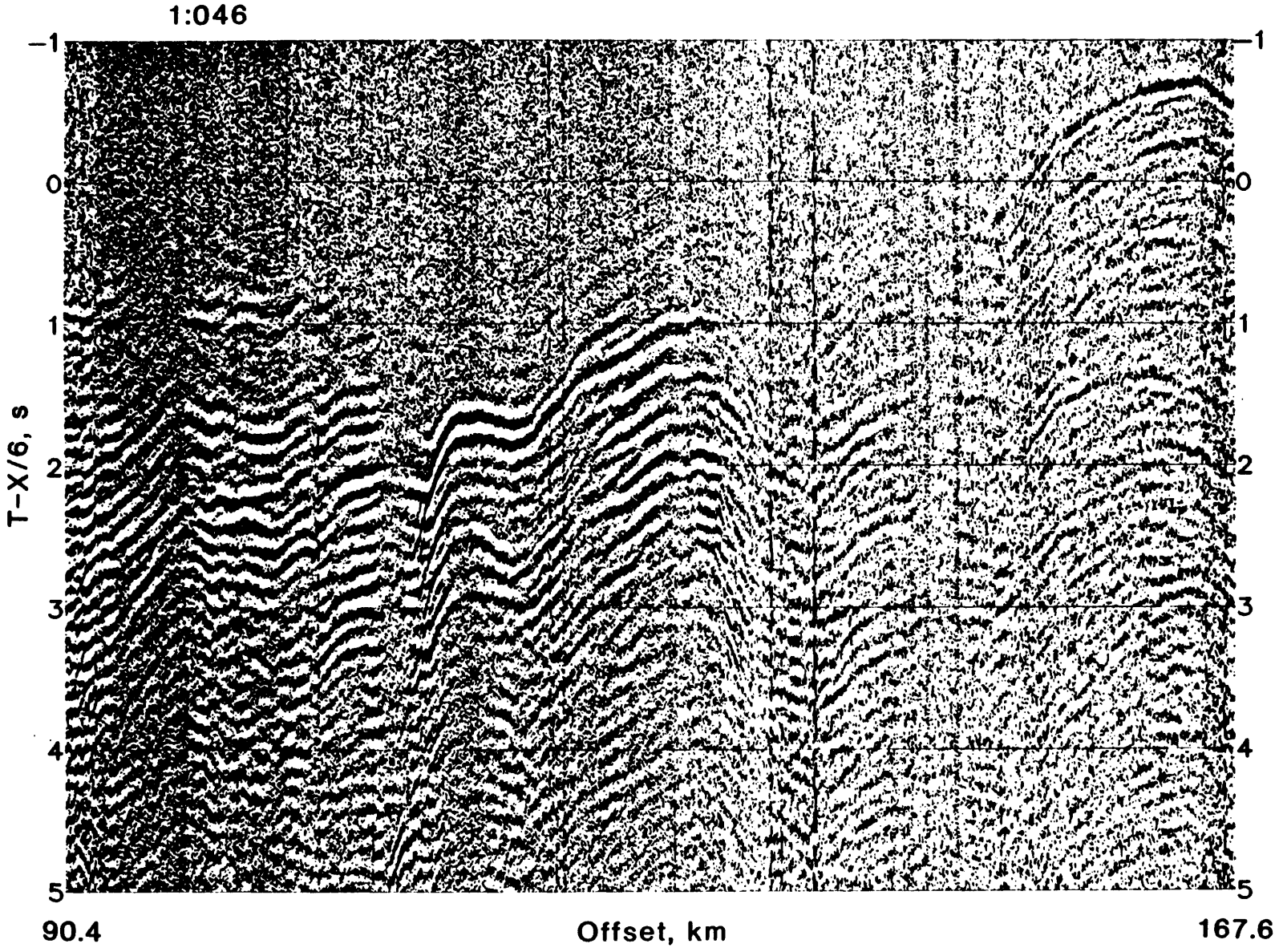

Figure 19. Stacked common receiver gather 046 for shots along LARSE air gun Line 1, reduced at 6 km/s.

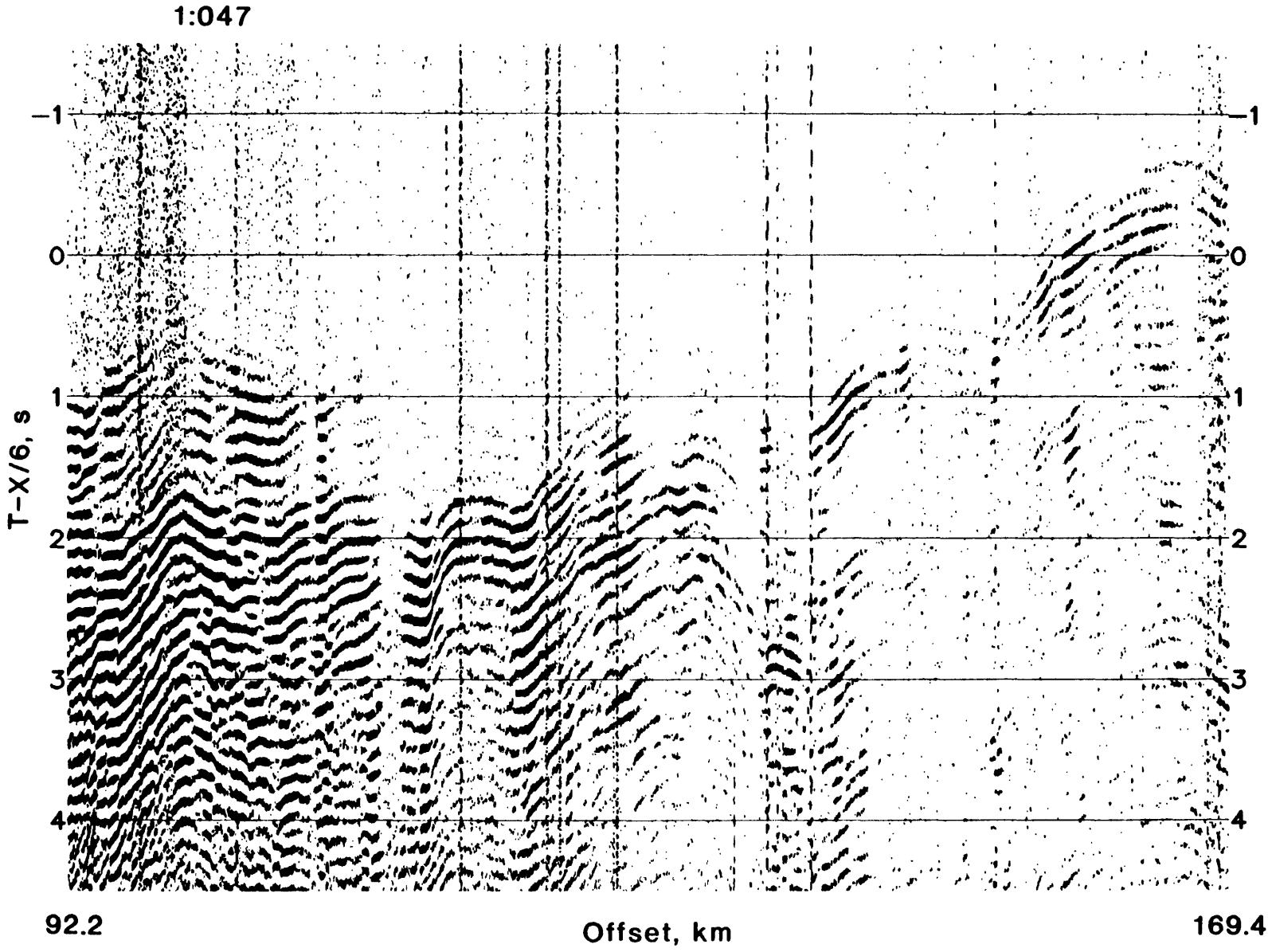

Figure 20. Stacked common receiver gather 047 for shots along LARSE air gun Line 1, reduced at 6 km/s.

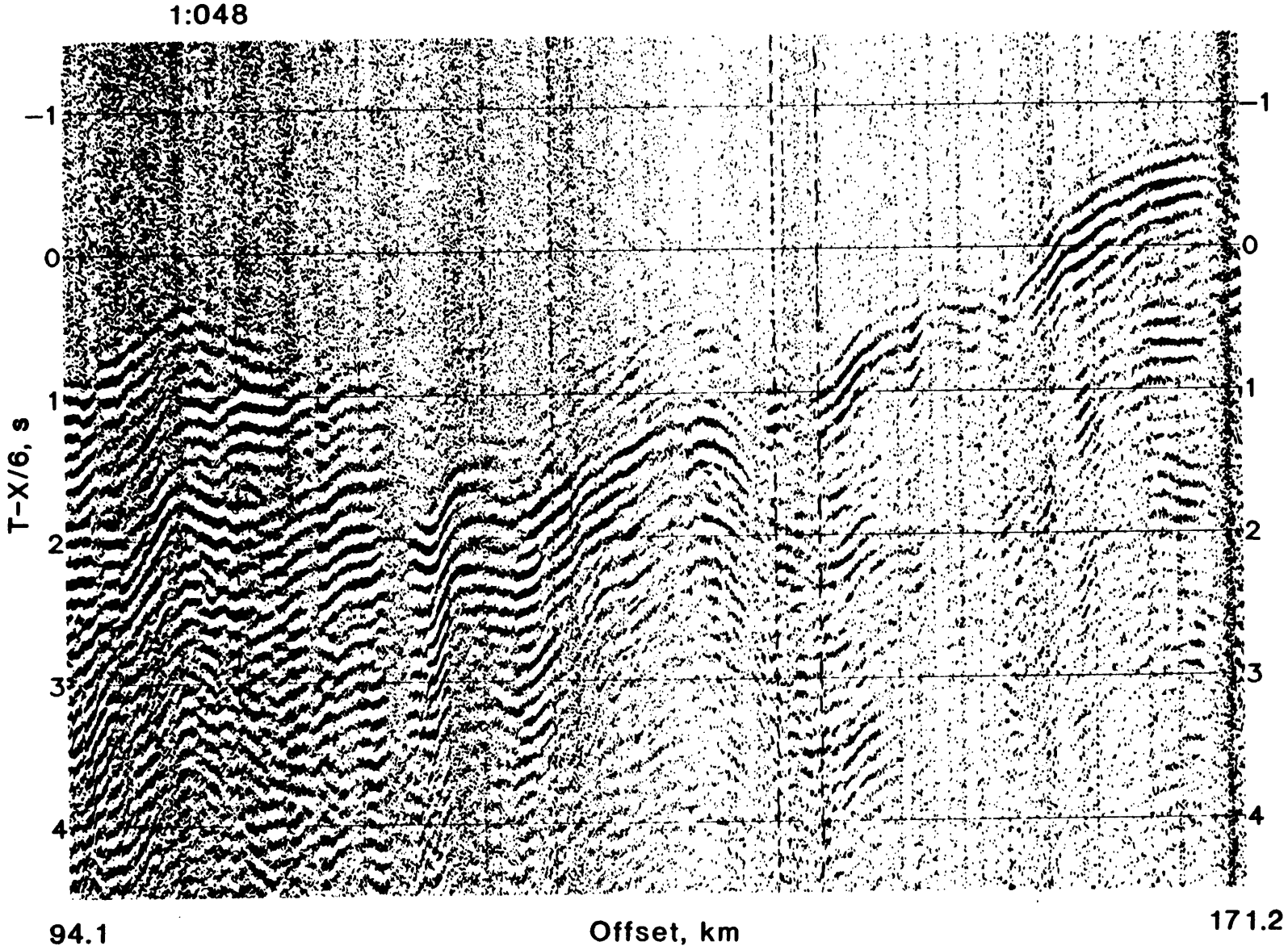

Figure 21. Stacked common receiver gather 048 for shots along LARSE air gun Line 1, reduced at 6 km/s.

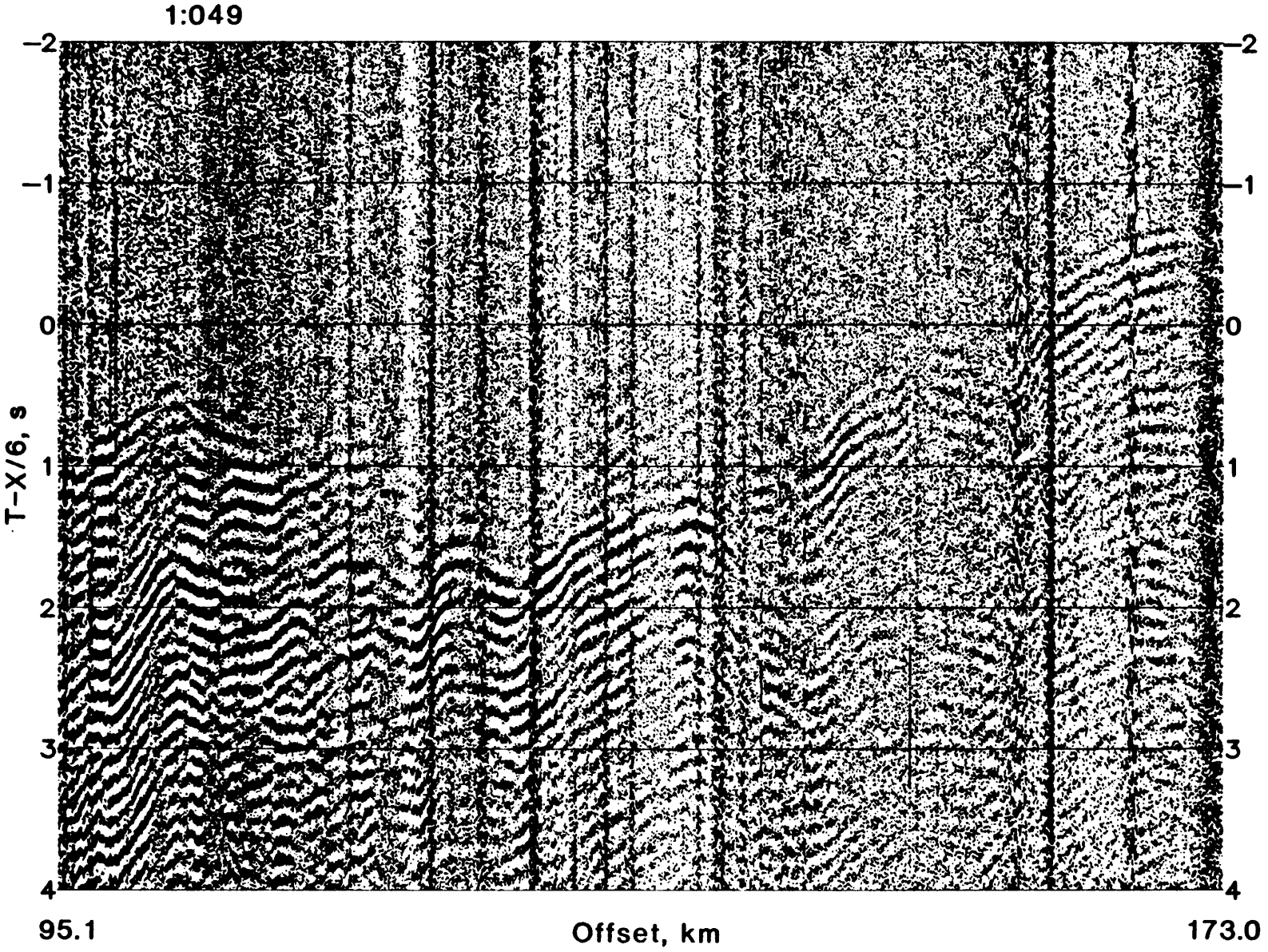

Figure 22. Stacked common receiver gather 049 for shots along LARSE air gun Line 1, reduced at 6 km/s.

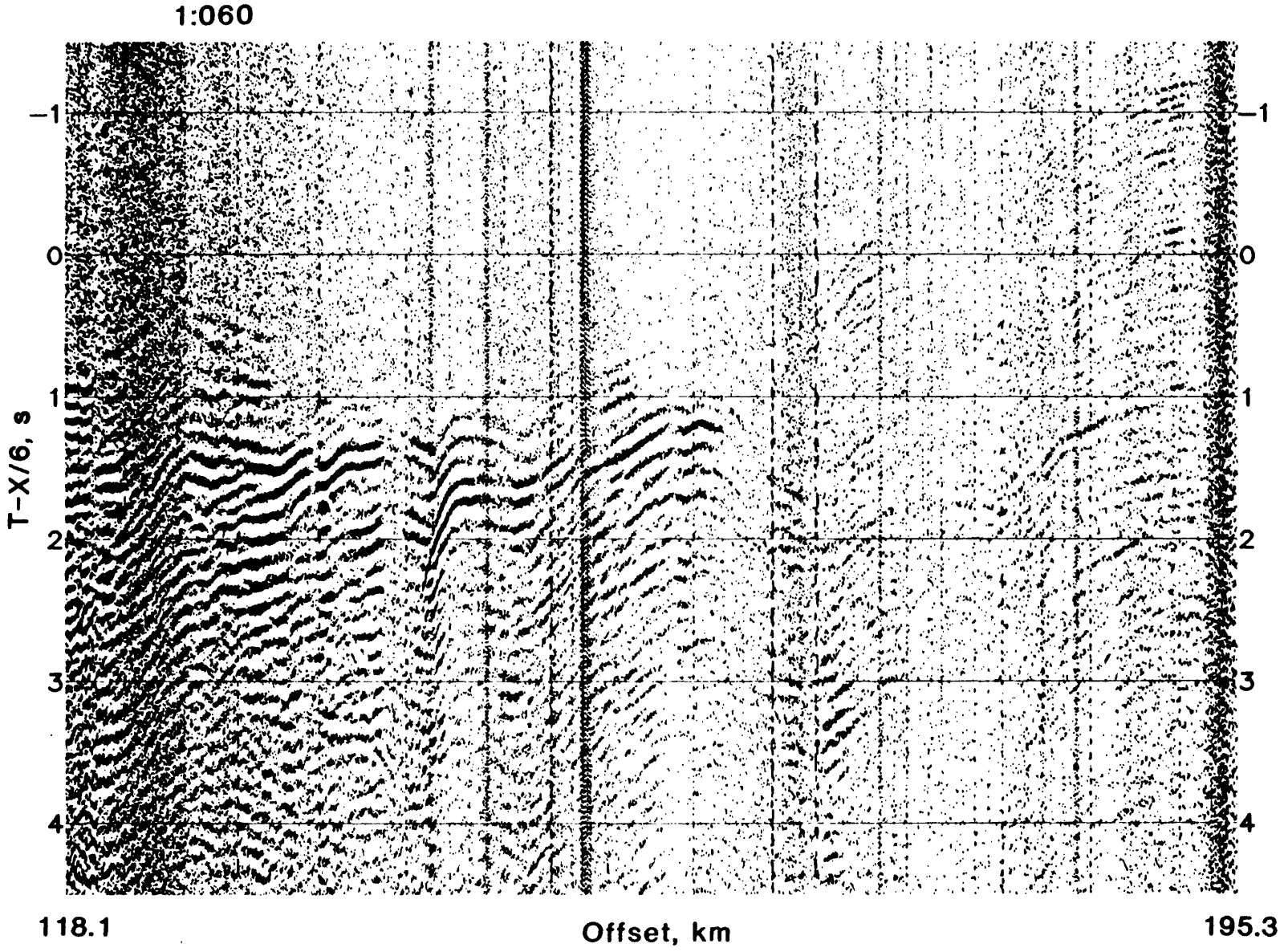

Figure 23. Stacked common receiver gather 060 for shots along LARSE air gun Line 1, reduced at 6 km/s.

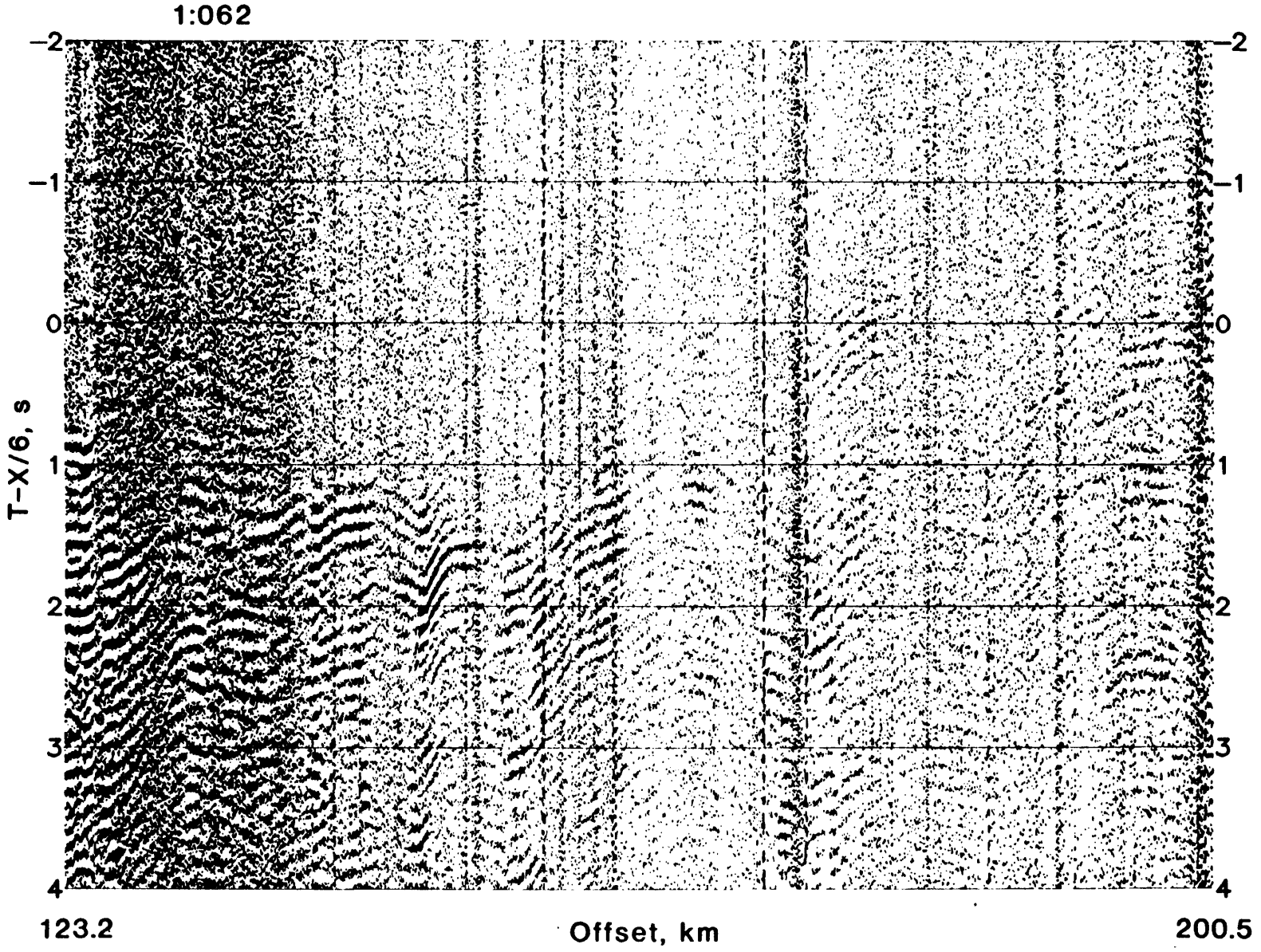

Figure 24. Stacked common receiver gather 062 for shots along LARSE air gun Line 1, reduced at 6 km/s.

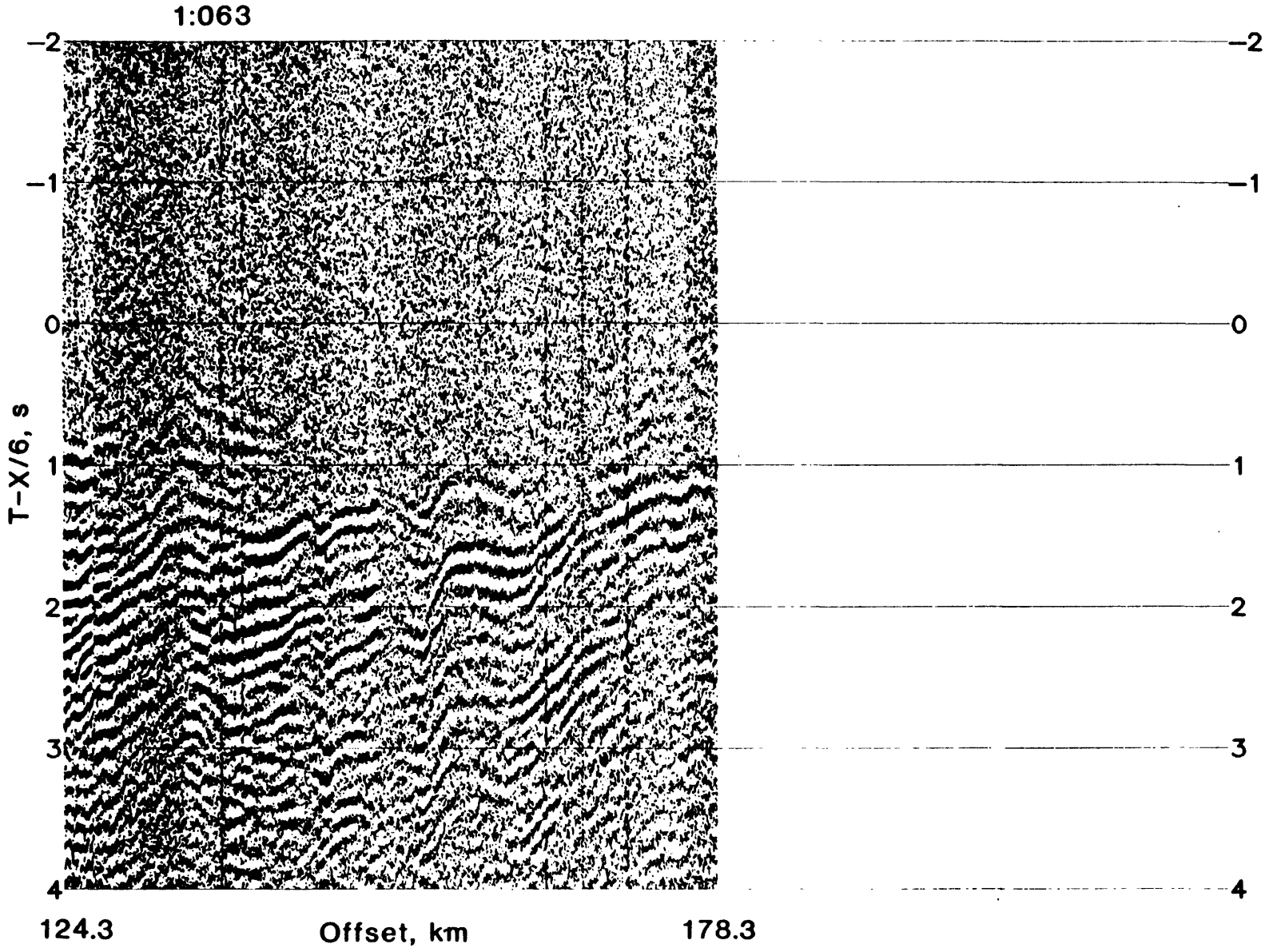

Figure 25. Stacked common receiver gather 063 for shots along LARSE air gun Line 1, reduced at 6 km/s.

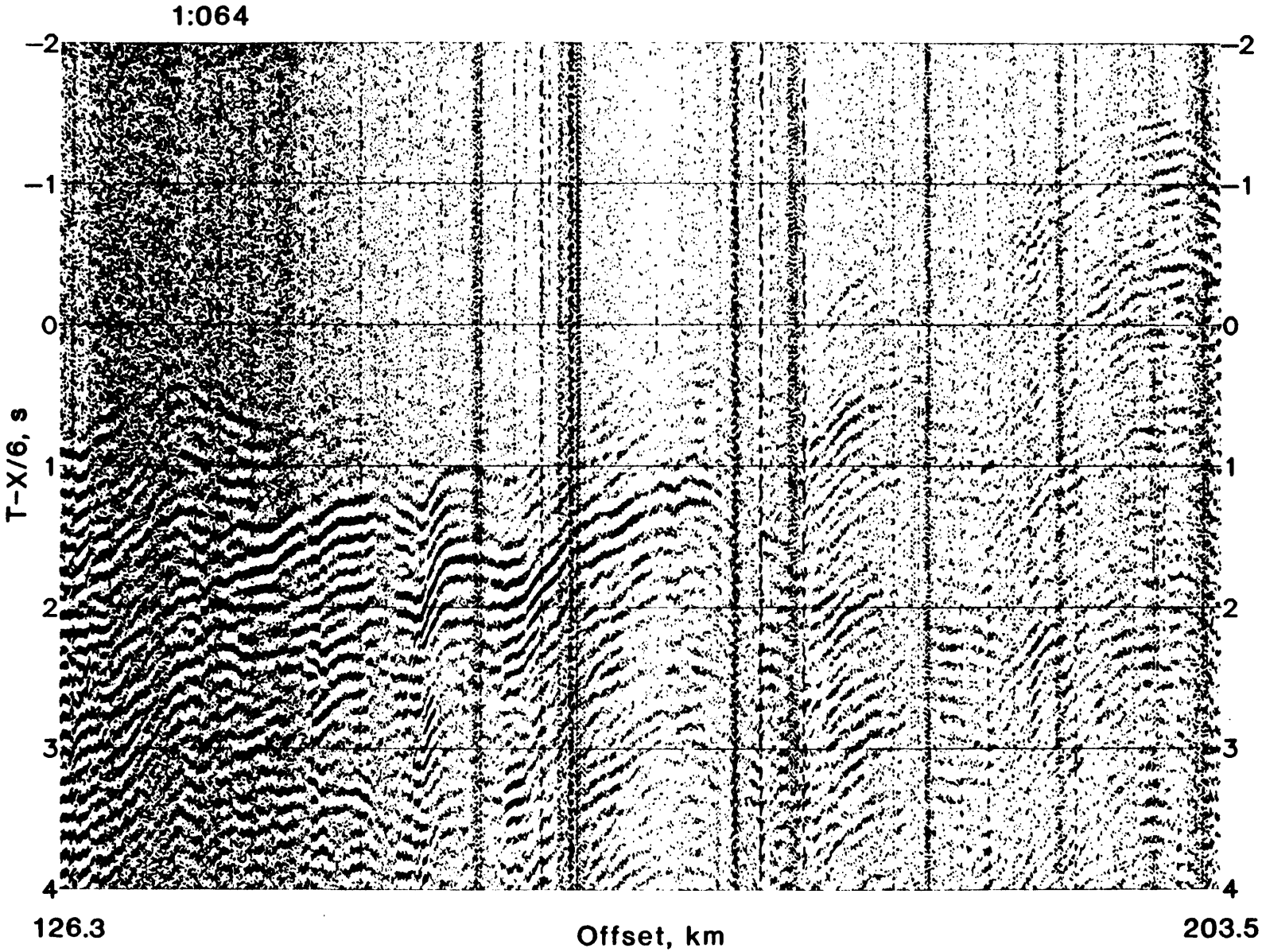

Figure 26. Stacked common receiver gather 064 for shots along LARSE air gun Line 1, reduced at 6 km/s.

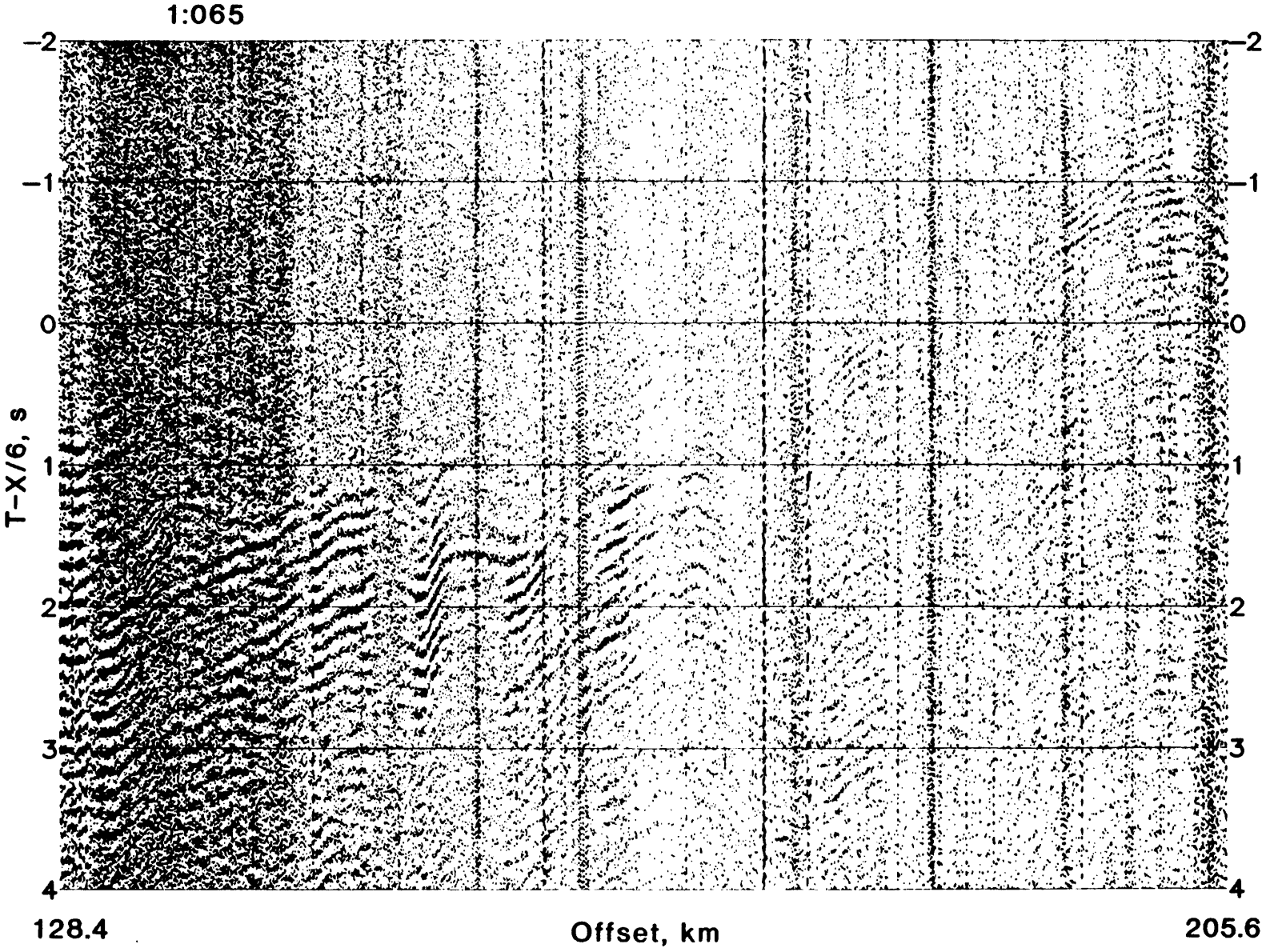

Figure 27. Stacked common receiver gather 065 for shots along LARSE air gun Line 1, reduced at 6 km/s.

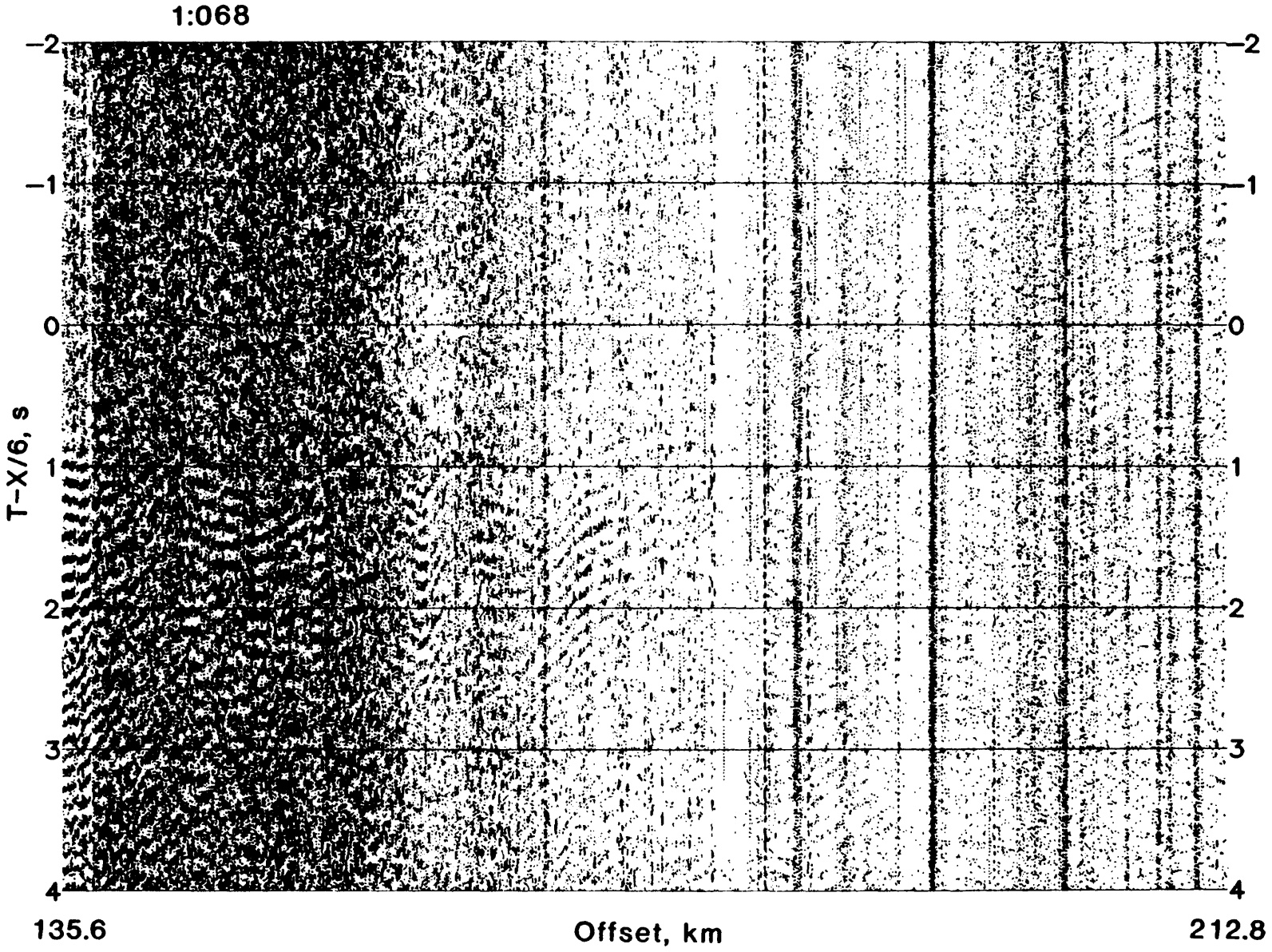

Figure 28. Stacked common receiver gather 068 for shots along LARSE air gun Line 1, reduced at 6 km/s.

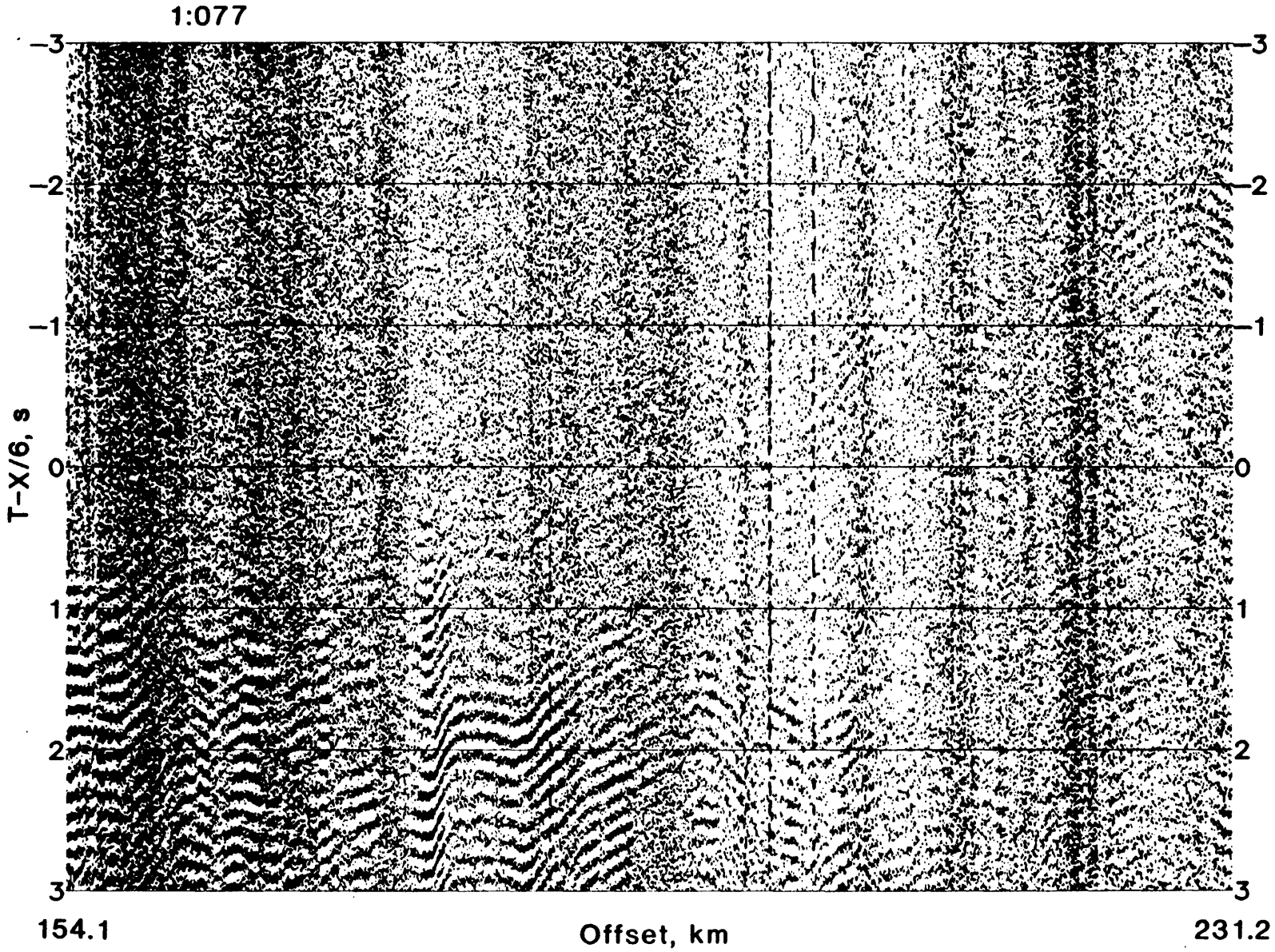

Figure 29. Stacked common receiver gather 077 for shots along LARSE air gun Line 1, reduced at 6 km/s.

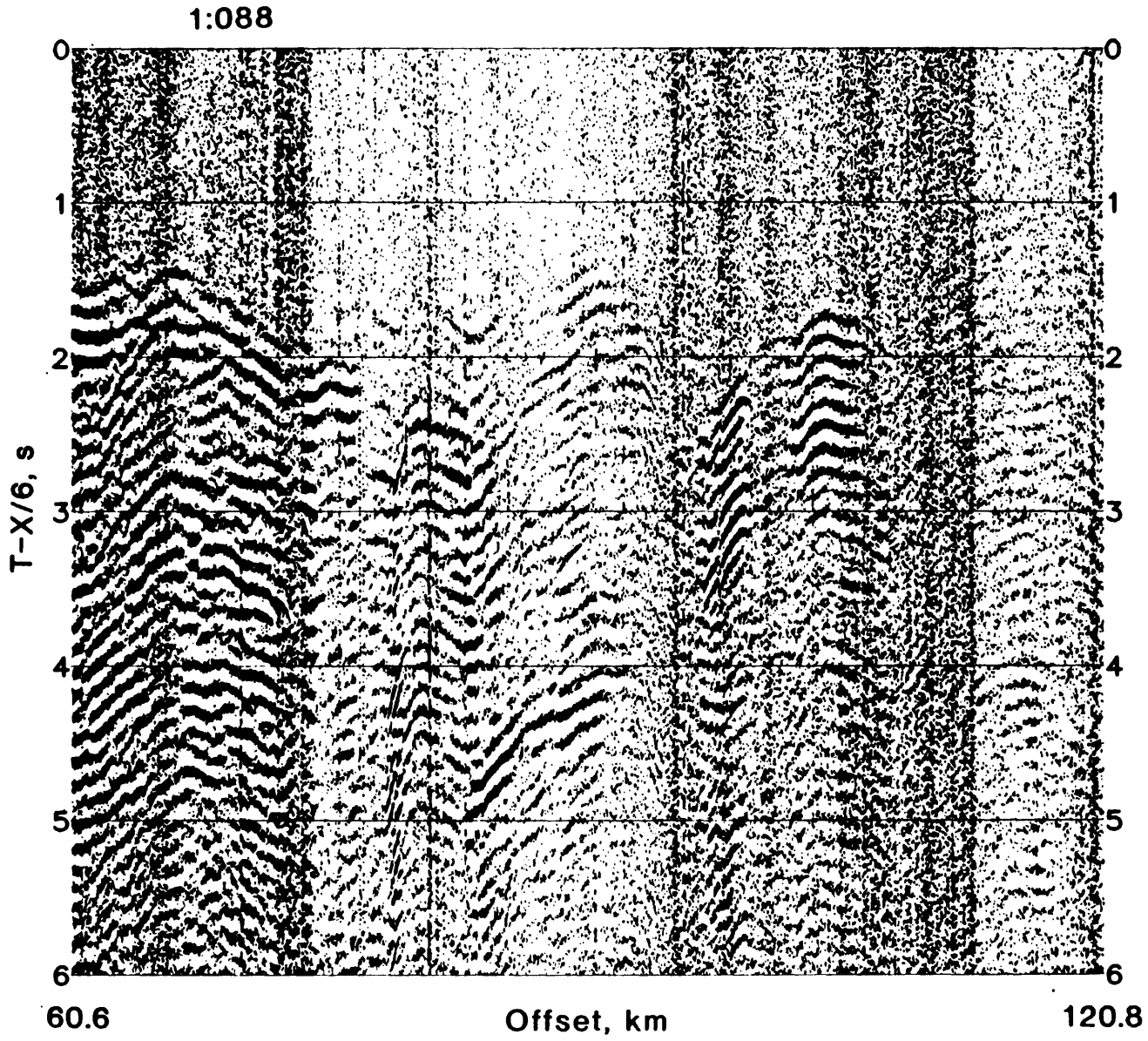

Figure 30. Stacked common receiver gather 088 for shots along LARSE air gun Line 1, reduced at 6 km/s.

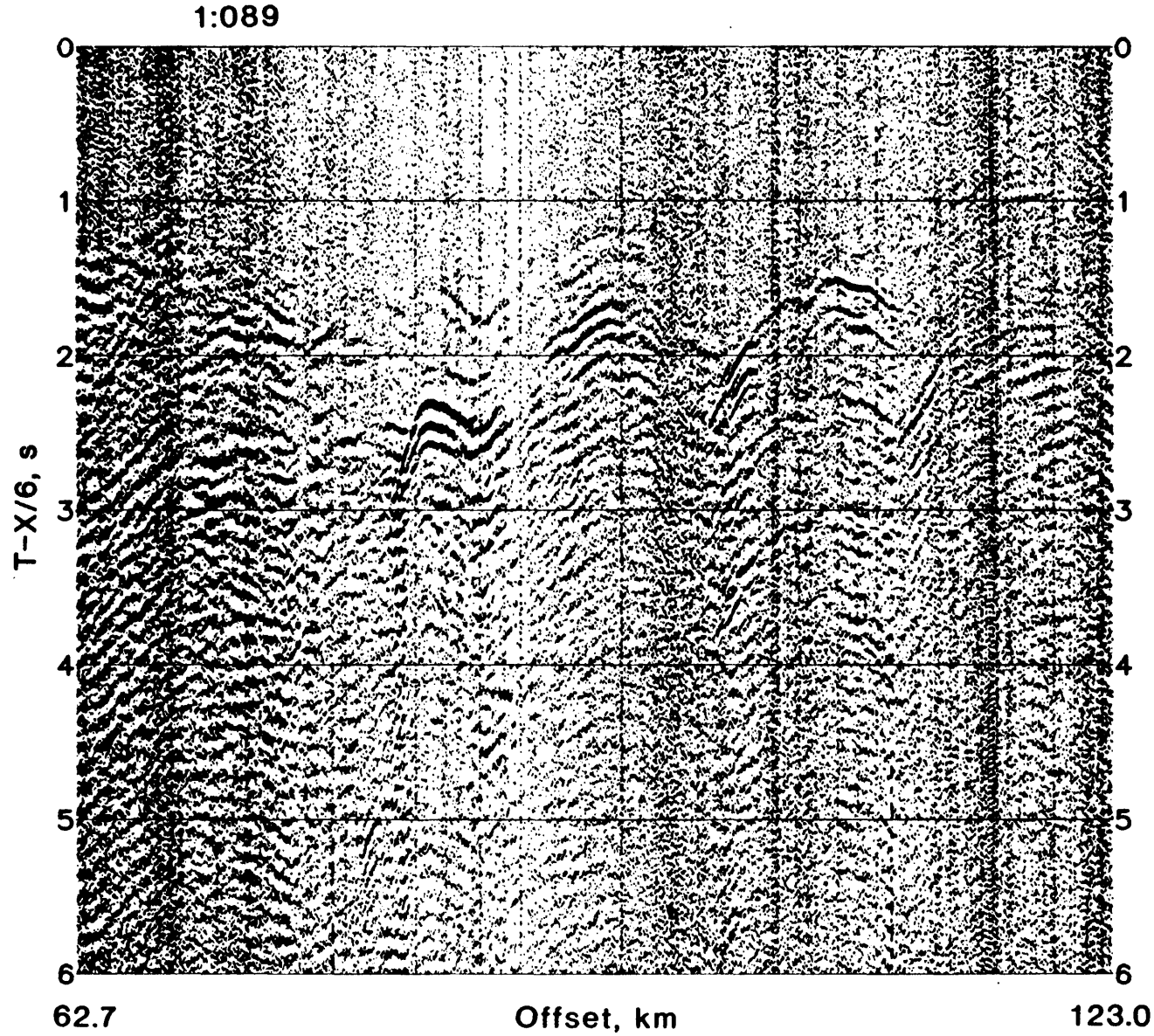

Figure 31. Stacked common receiver gather 089 for shots along LARSE air gun Line 1, reduced at 6 km/s.

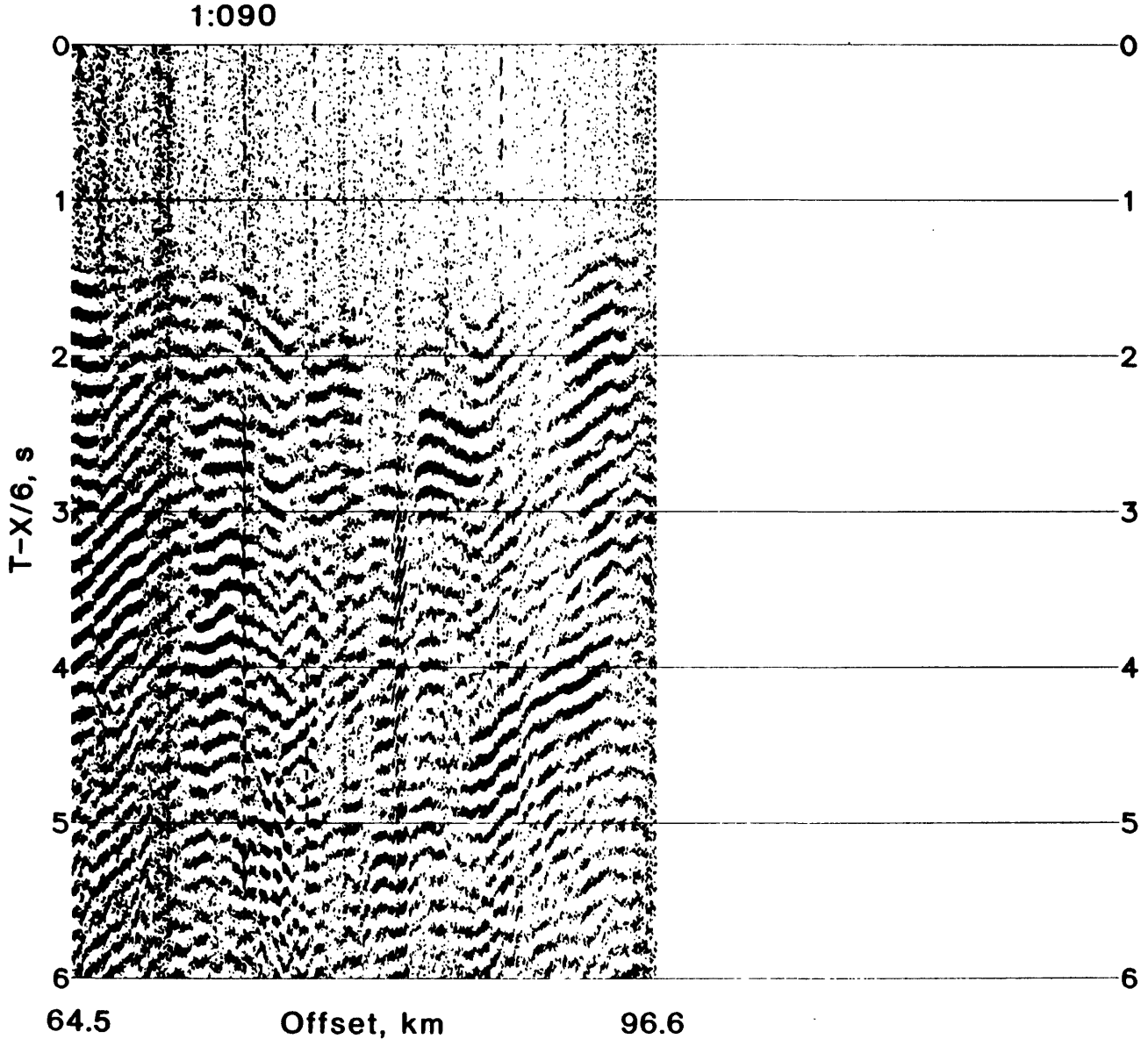

Figure 32. Stacked common receiver gather 090 for shots along LARSE air gun Line 1, reduced at 6 km/s.

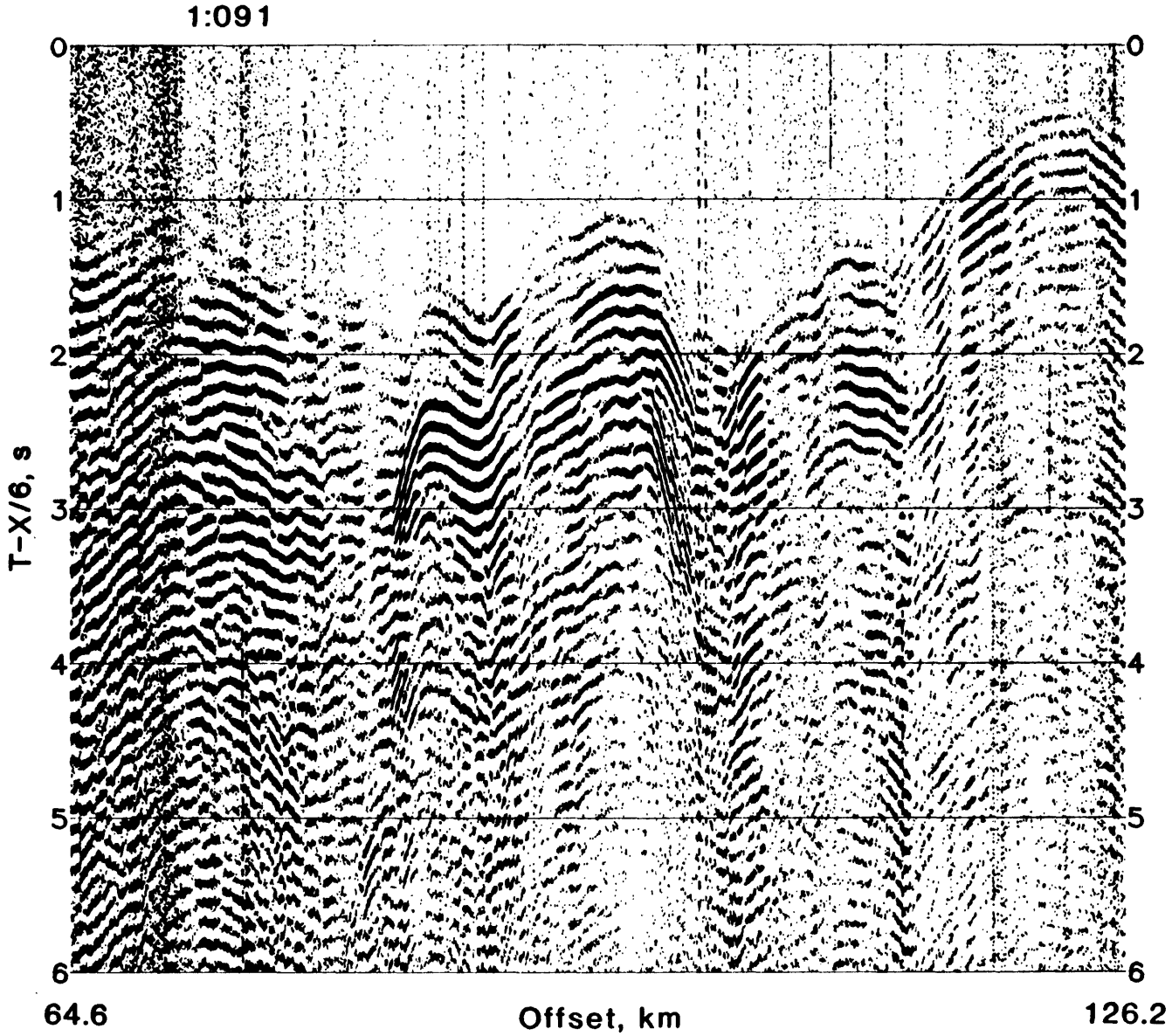

Figure 33. Stacked common receiver gather 091 for shots along LARSE air gun Line 1, reduced at 6 km/s.

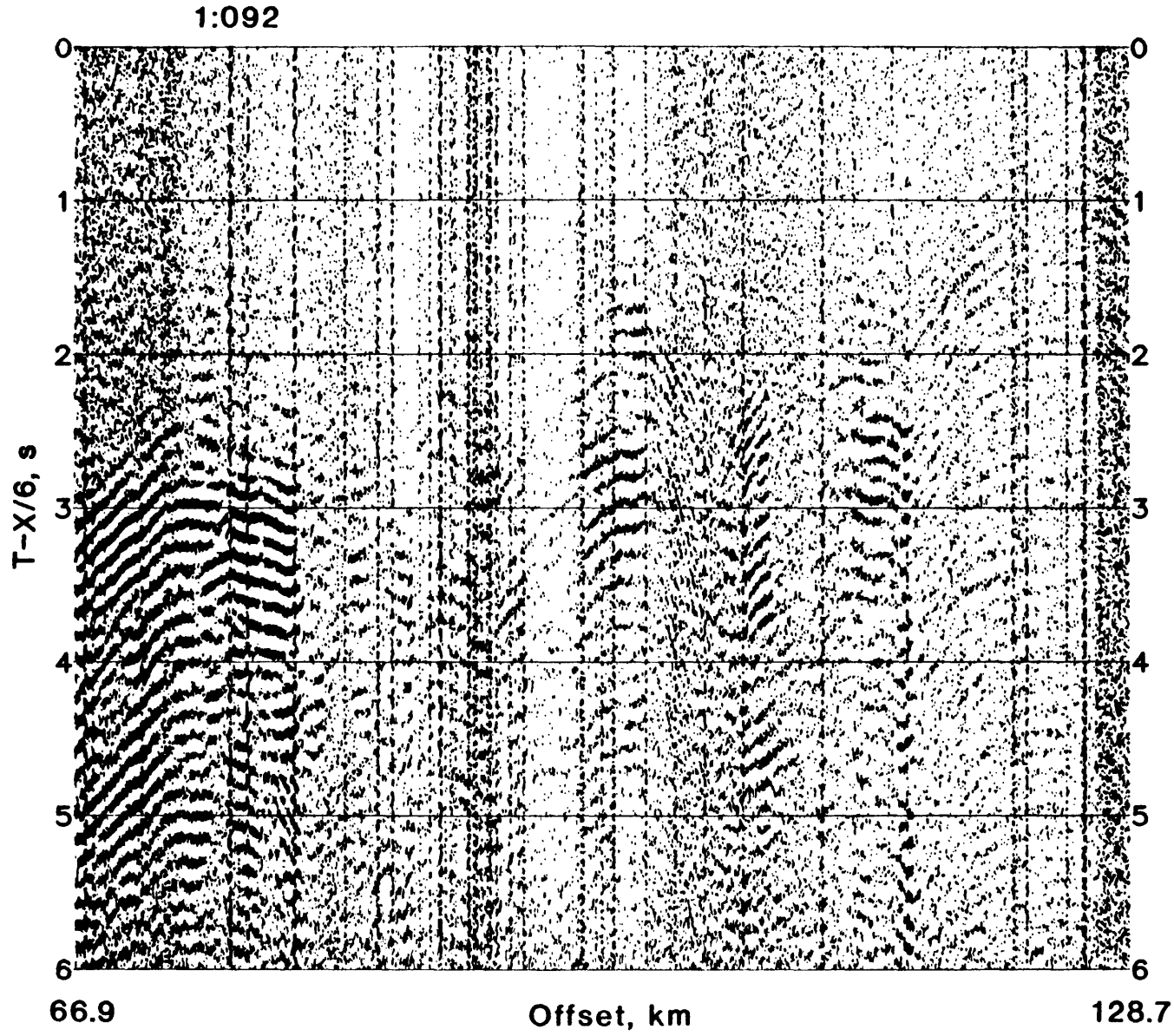

Figure 34. Stacked common receiver gather 092 for shots along LARSE air gun Line 1, reduced at 6 km/s.

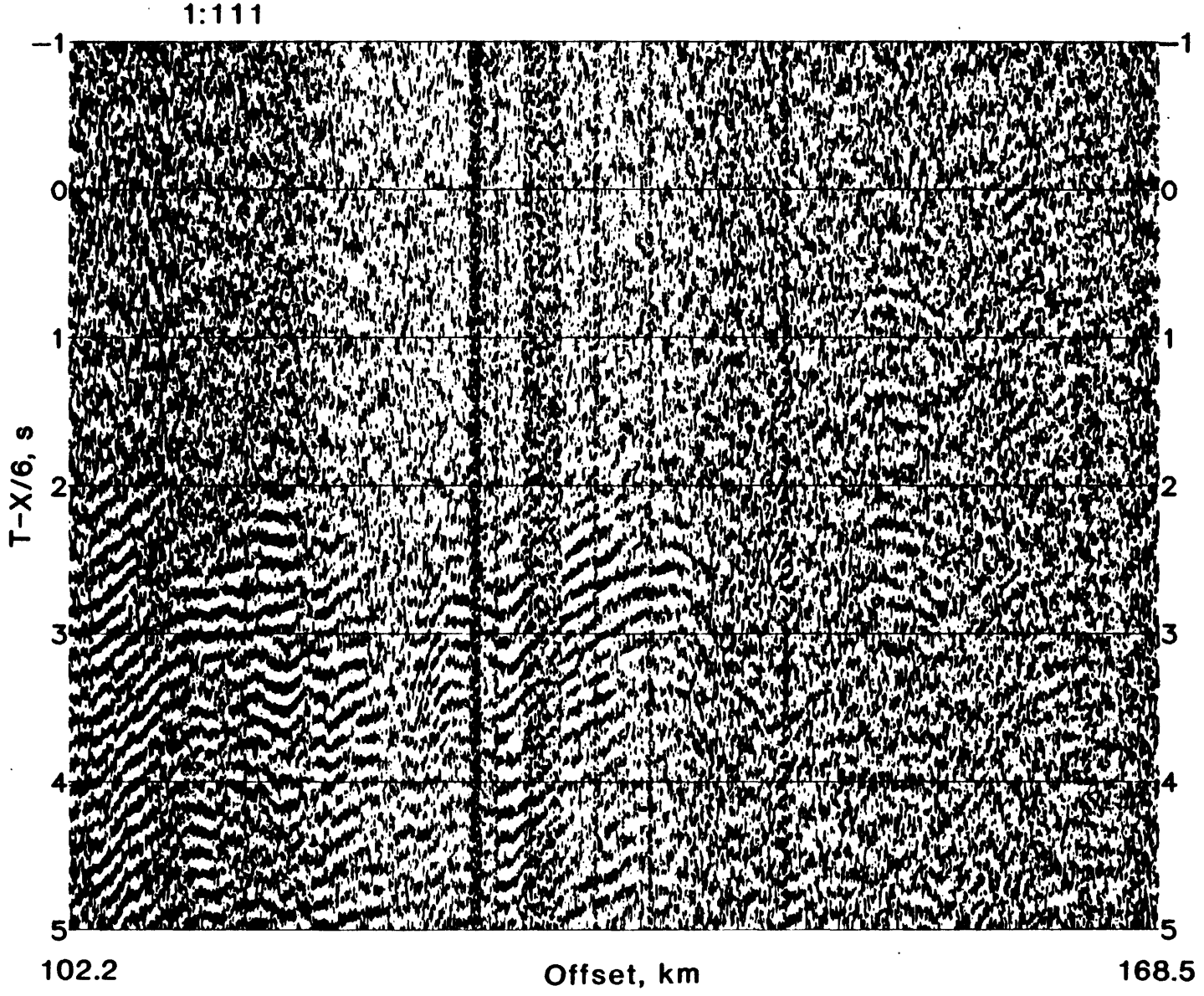

Figure 35. Stacked common receiver gather 111 for shots along LARSE air gun Line 1, reduced at 6 km/s.

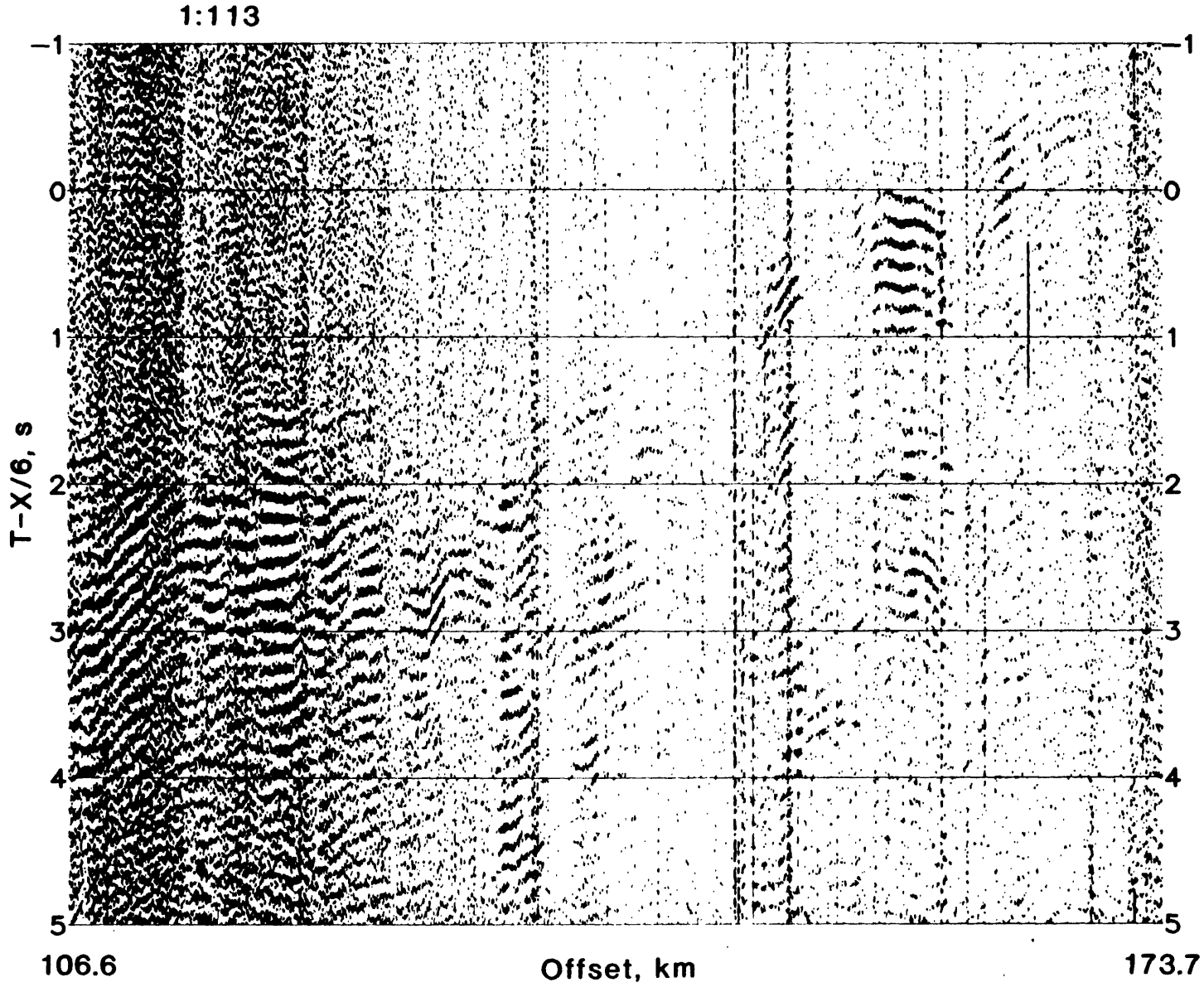

Figure 36. Stacked common receiver gather 113 for shots along LARSE air gun Line 1, reduced at 6 km/s.

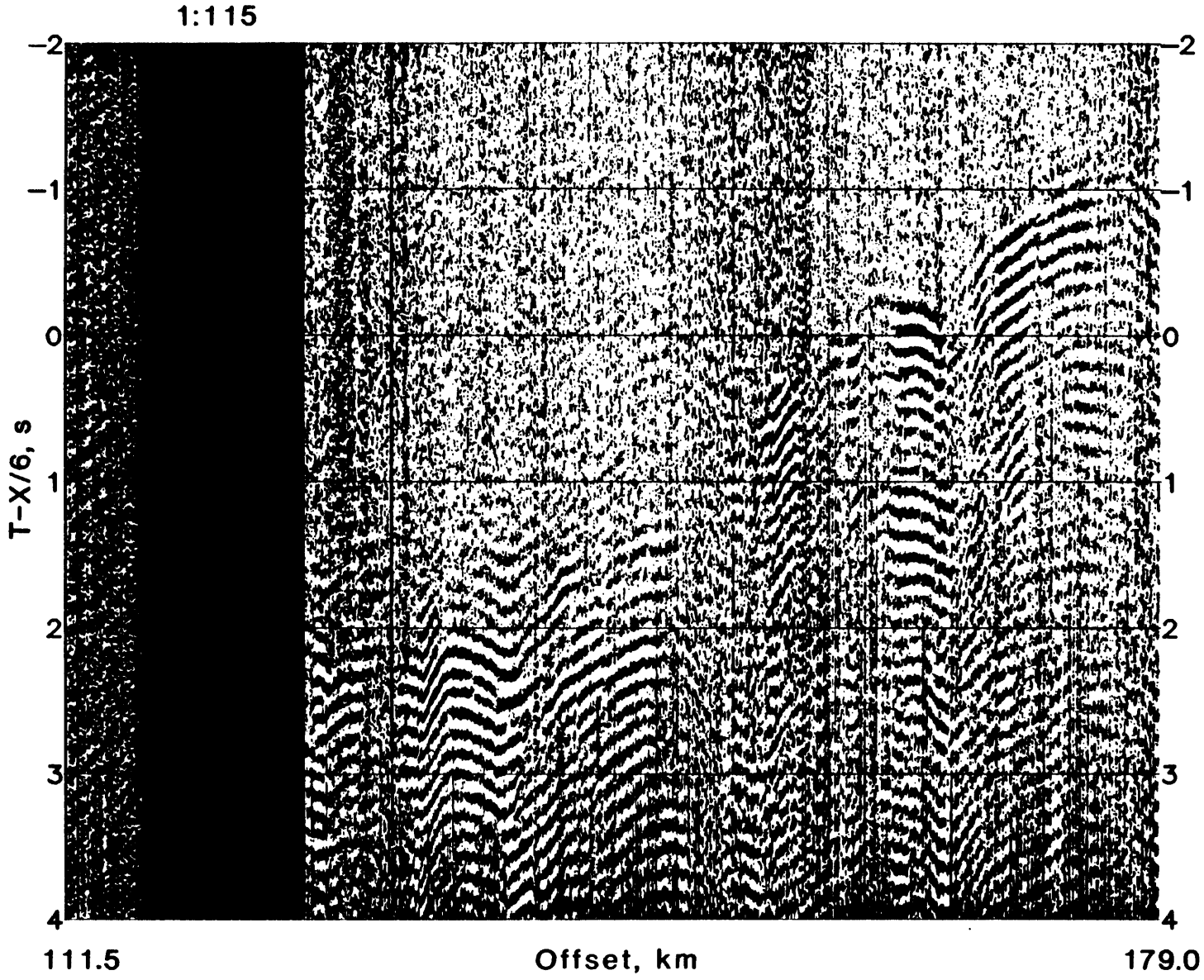

Figure 37. Stacked common receiver gather 115 for shots along LARSE air gun Line 1, reduced at 6 km/s.

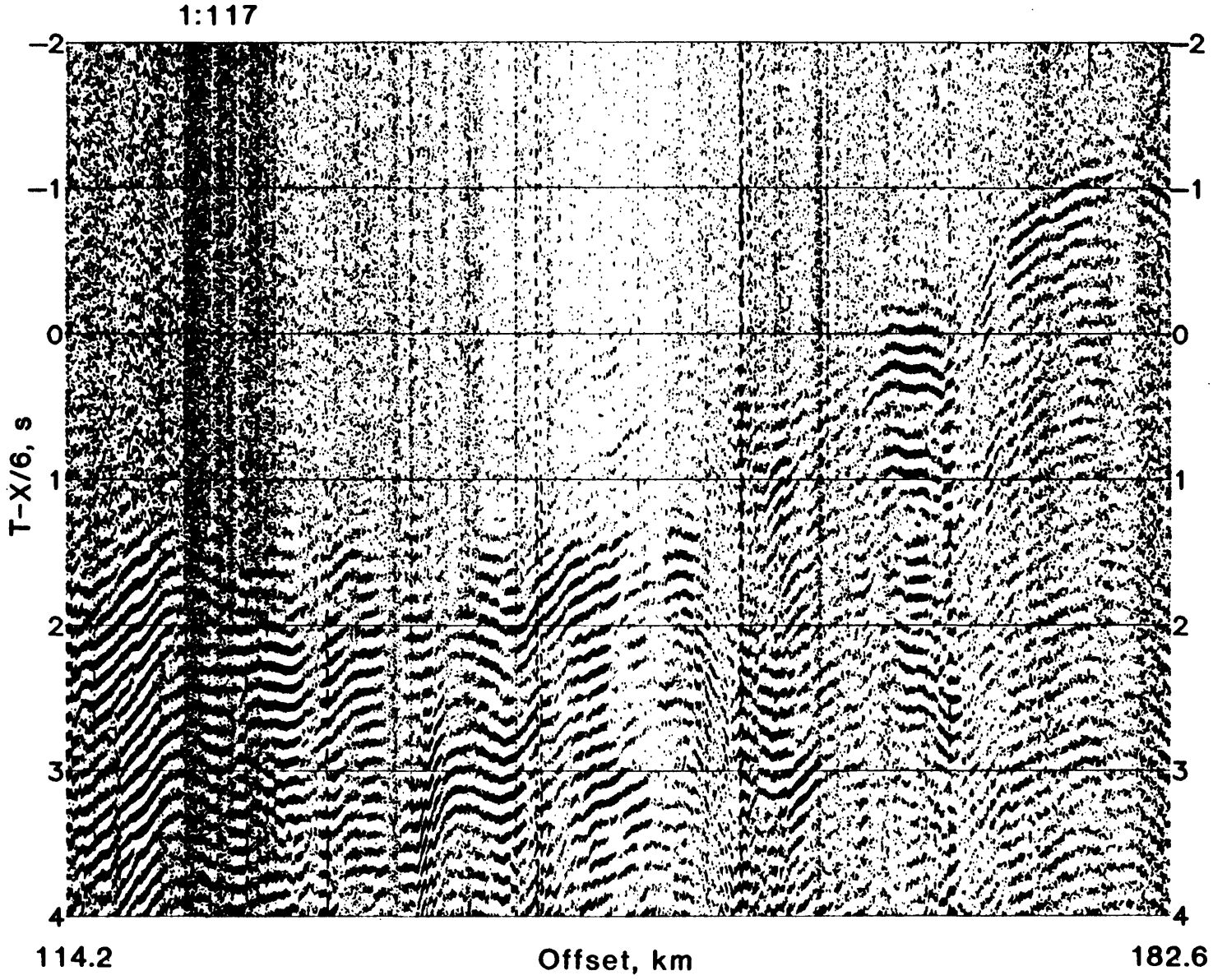

Figure 38. Stacked common receiver gather 117 for shots along LARSE air gun Line 1, reduced at 6 km/s.

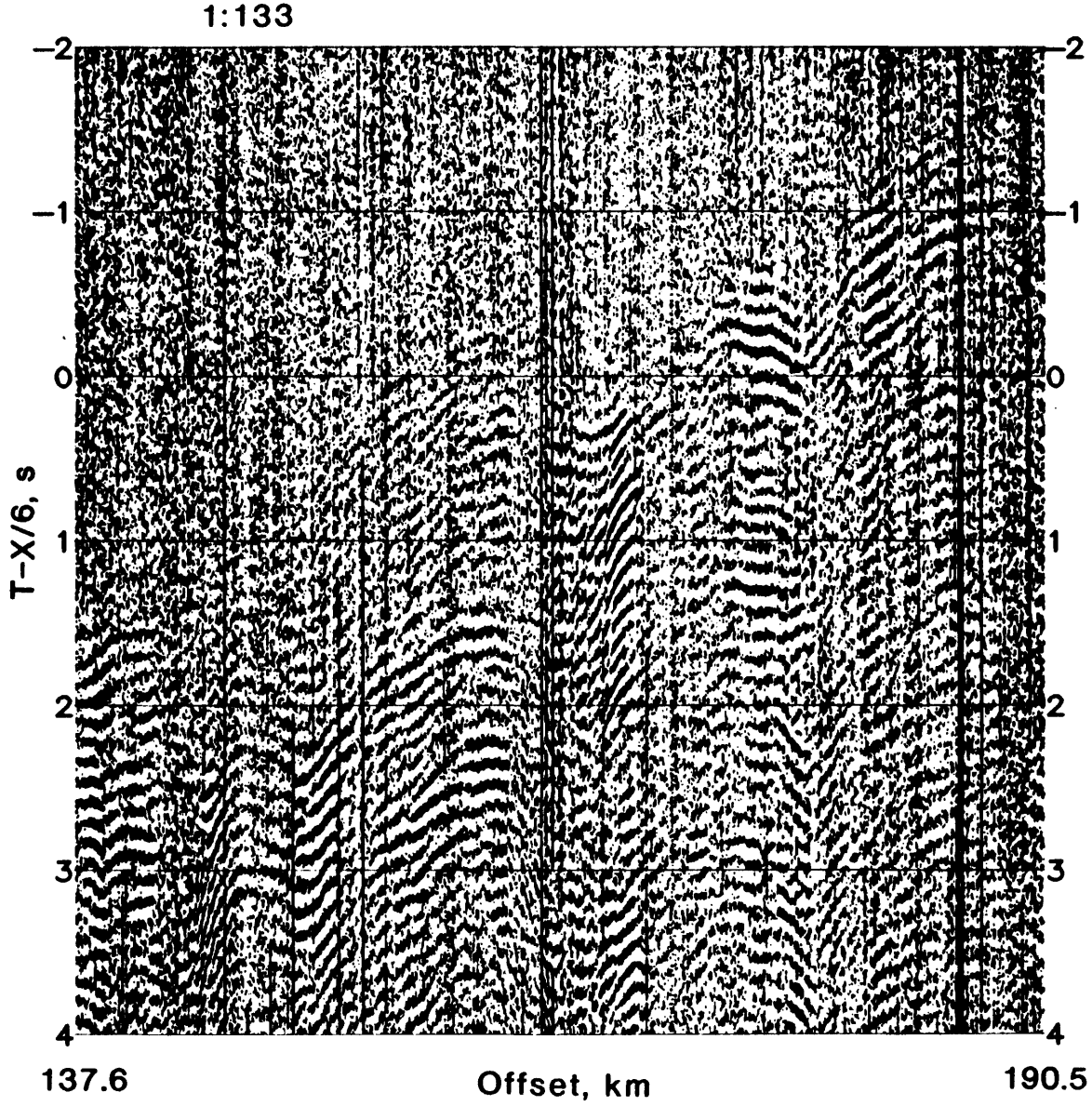

Figure 39. Stacked common receiver gather 133 for shots along LARSE air gun Line 1, reduced at 6 km/s.

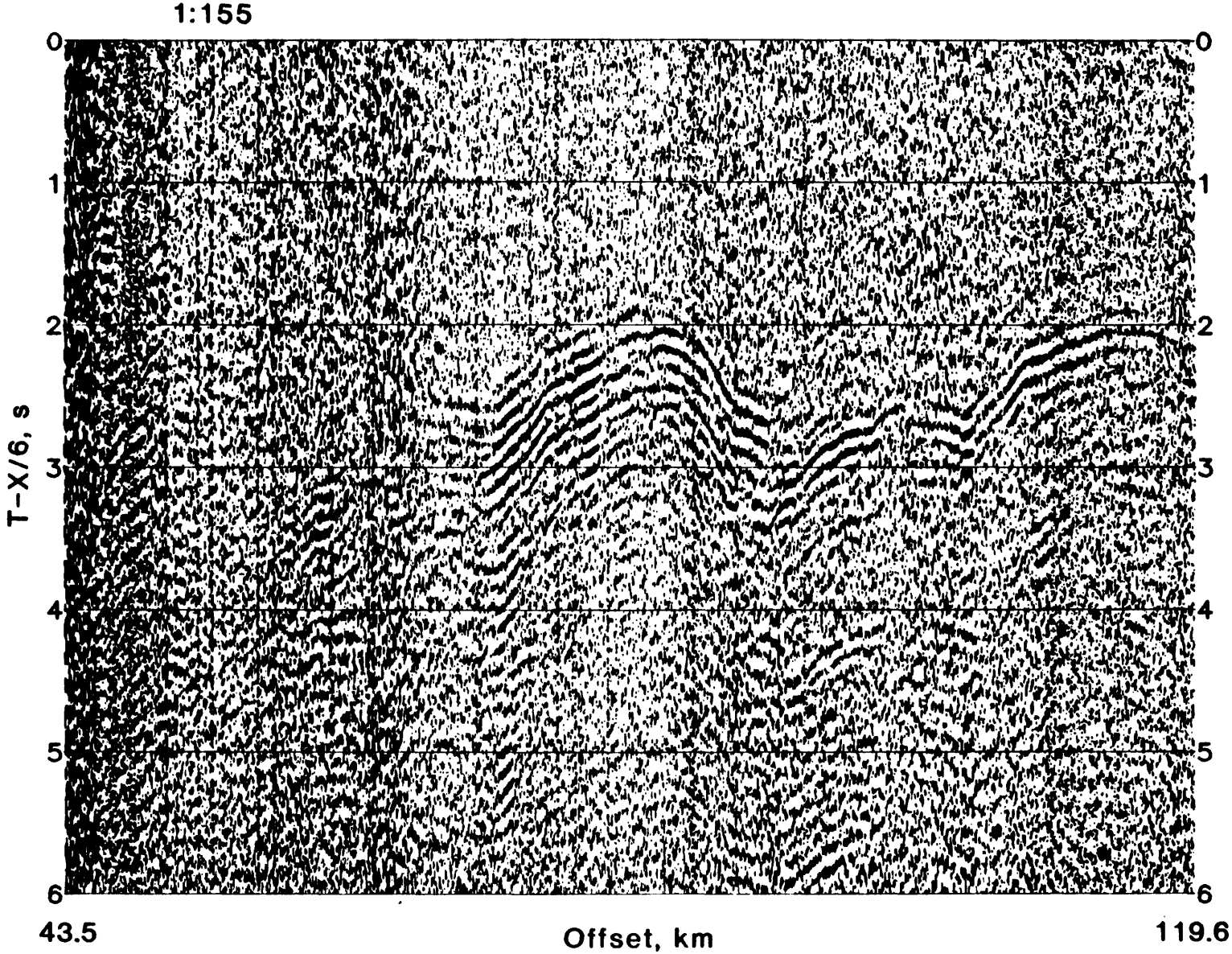

Figure 40. Stacked common receiver gather 155 for shots along LARSE air gun Line 1, reduced at 6 km/s.

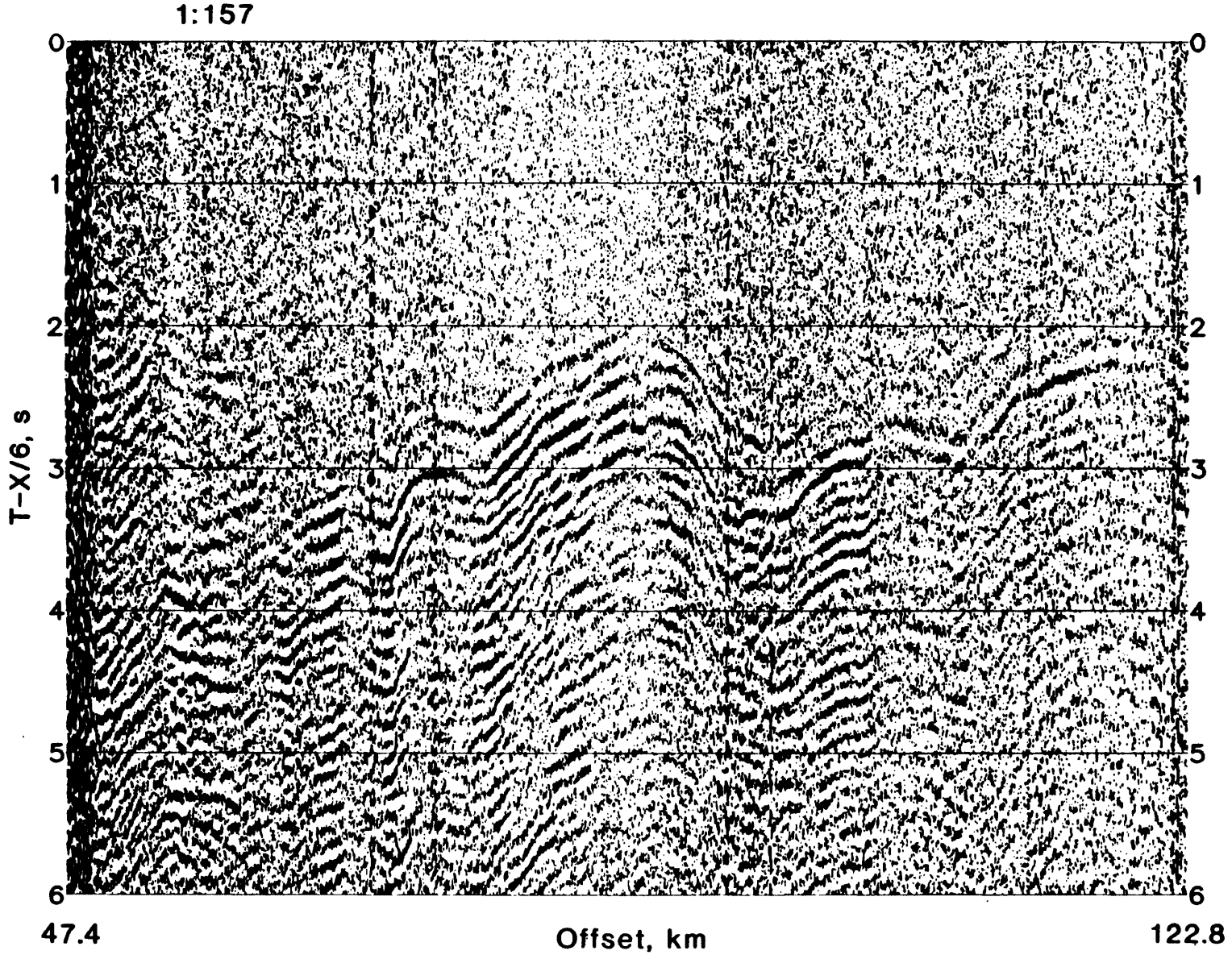

Figure 41. Stacked common receiver gather 157 for shots along LARSE air gun Line 1, reduced at 6 km/s.

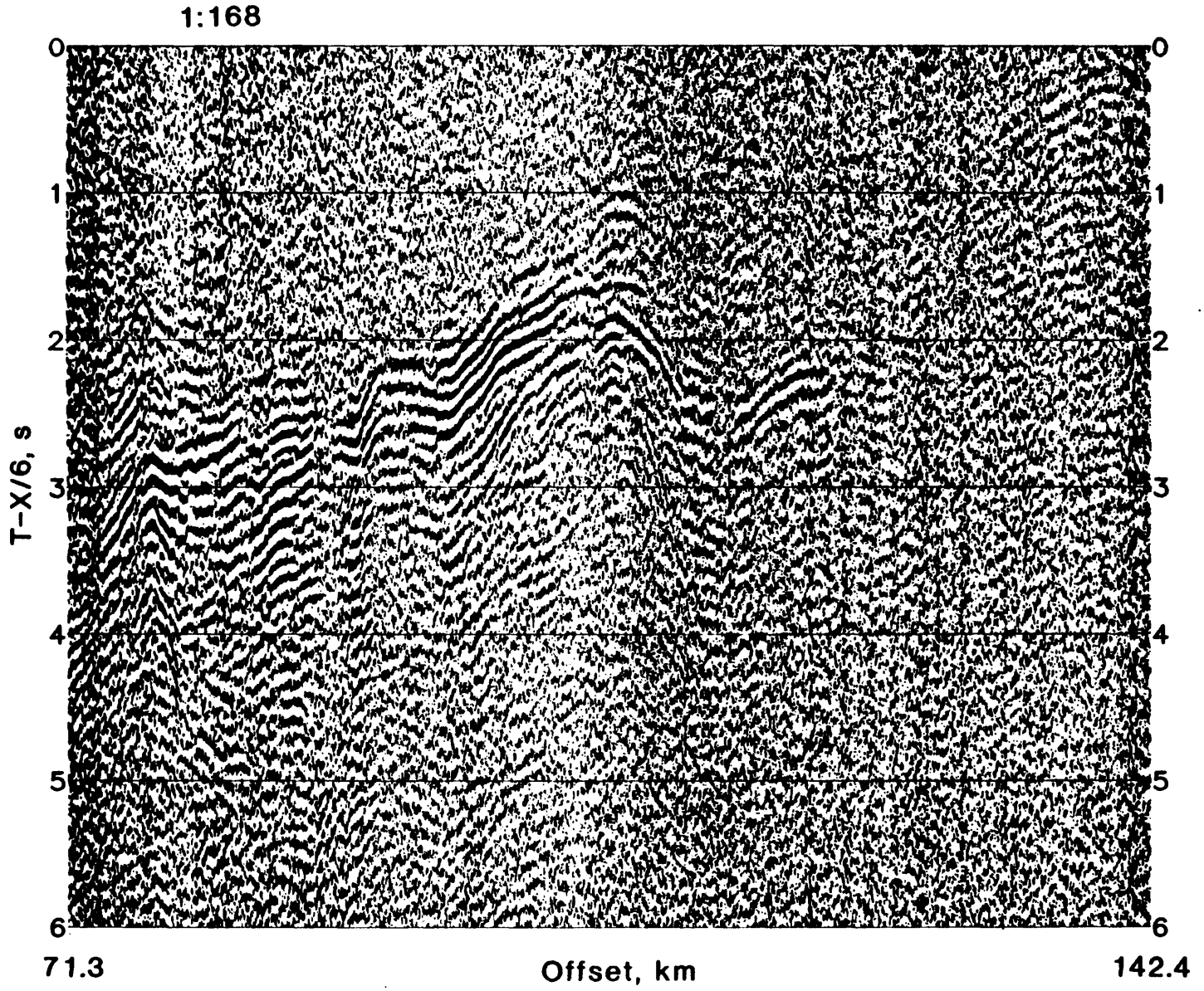

Figure 42. Stacked common receiver gather 168 for shots along LARSE air gun Line 1, reduced at 6 km/s.

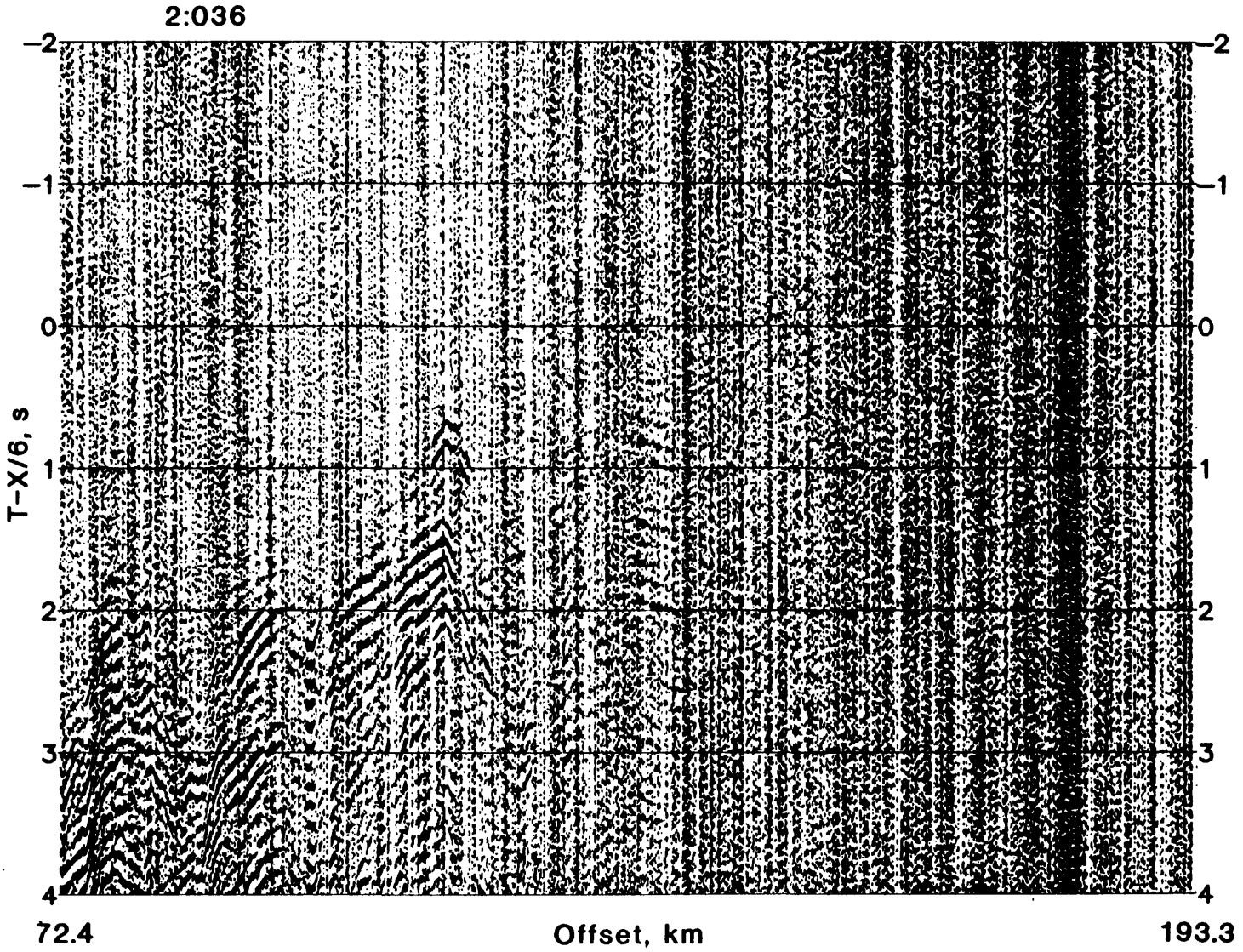

Figure 43. Stacked common receiver gather 036 for shots along LARSE air gun Line 2, reduced at 6 km/s.

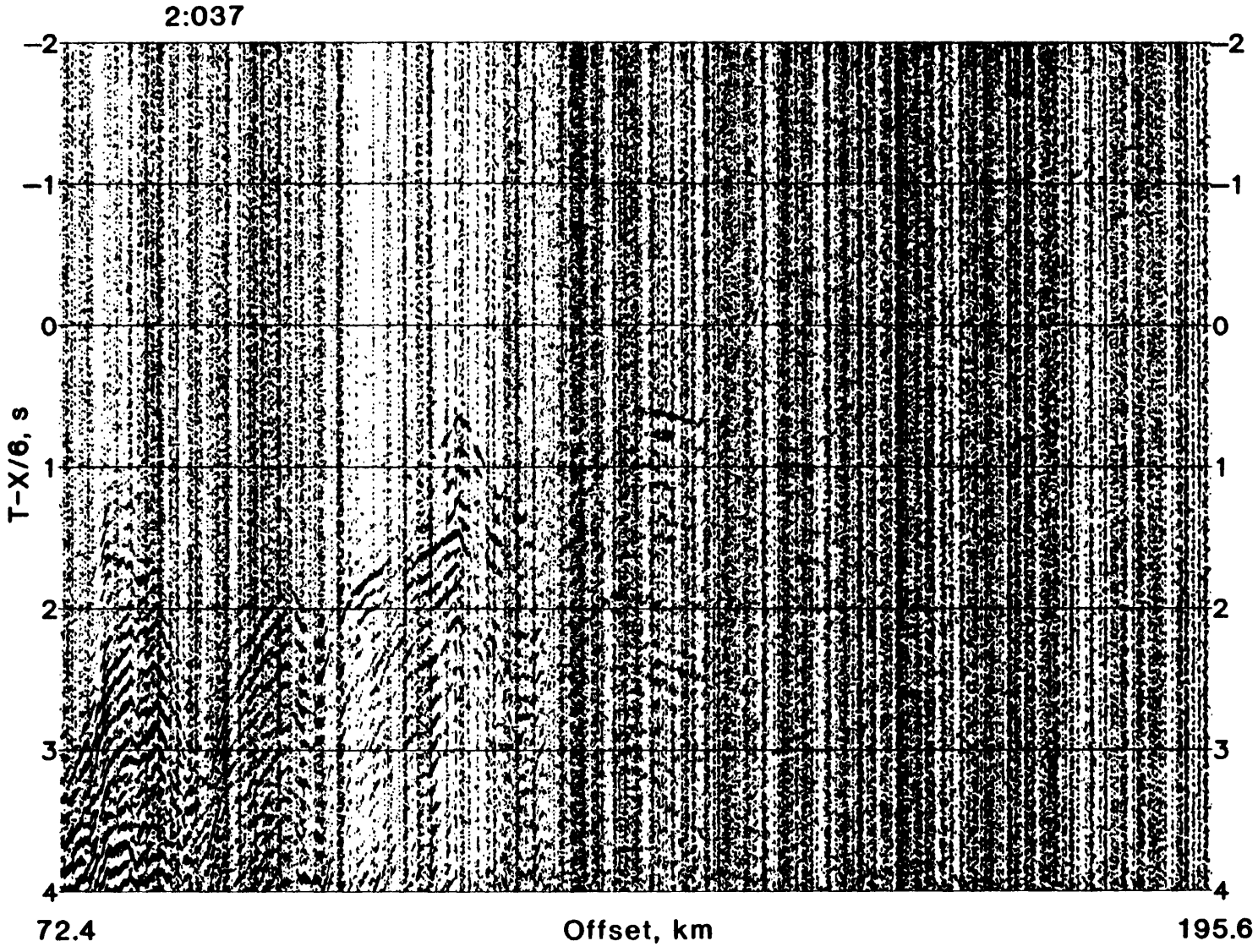

Figure 44. Stacked common receiver gather 037 for shots along LARSE air gun Line 2, reduced at 6 km/s.

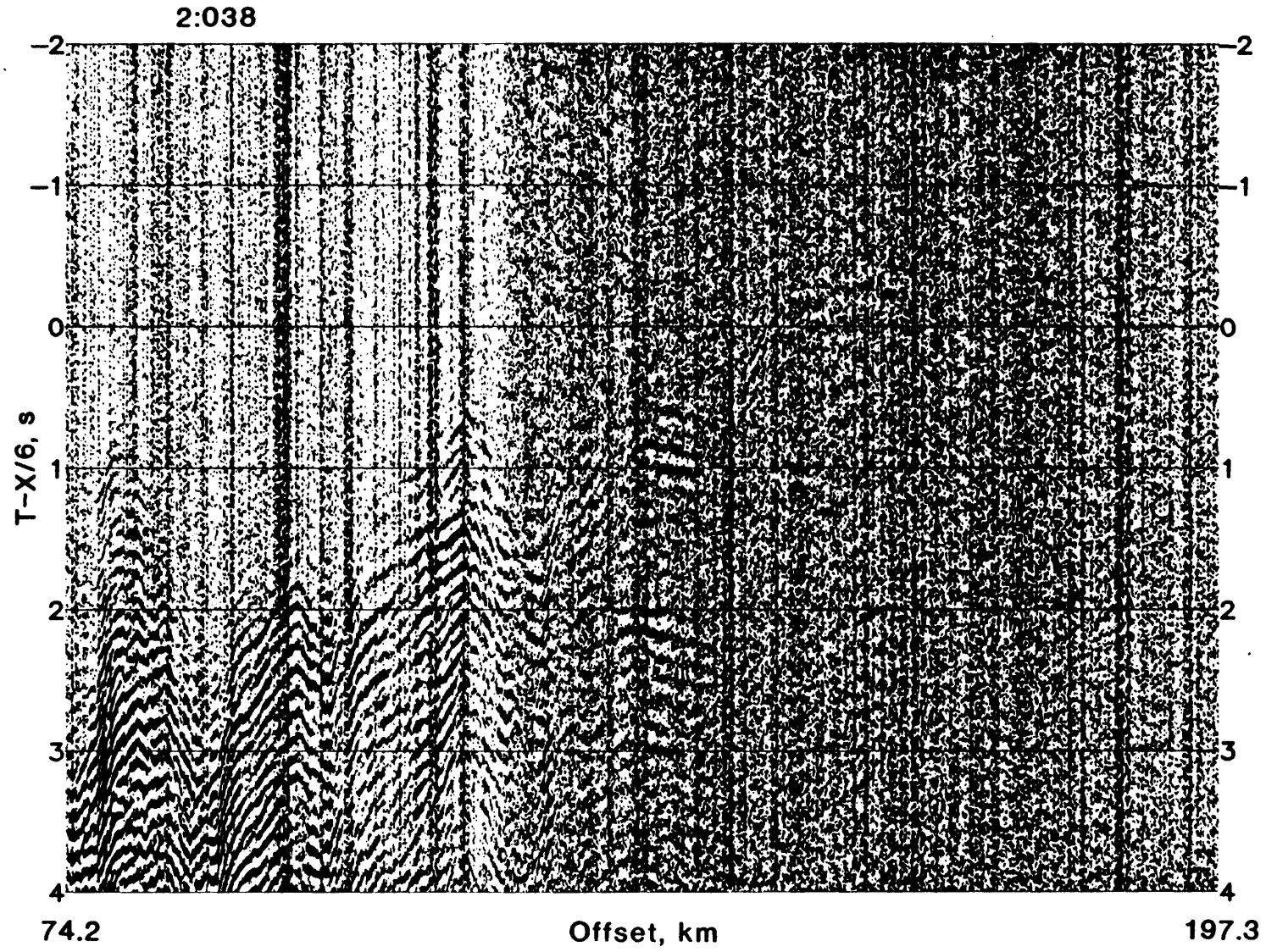

Figure 45. Stacked common receiver gather 038 for shots along LARSE air gun Line 2, reduced at 6 km/s.

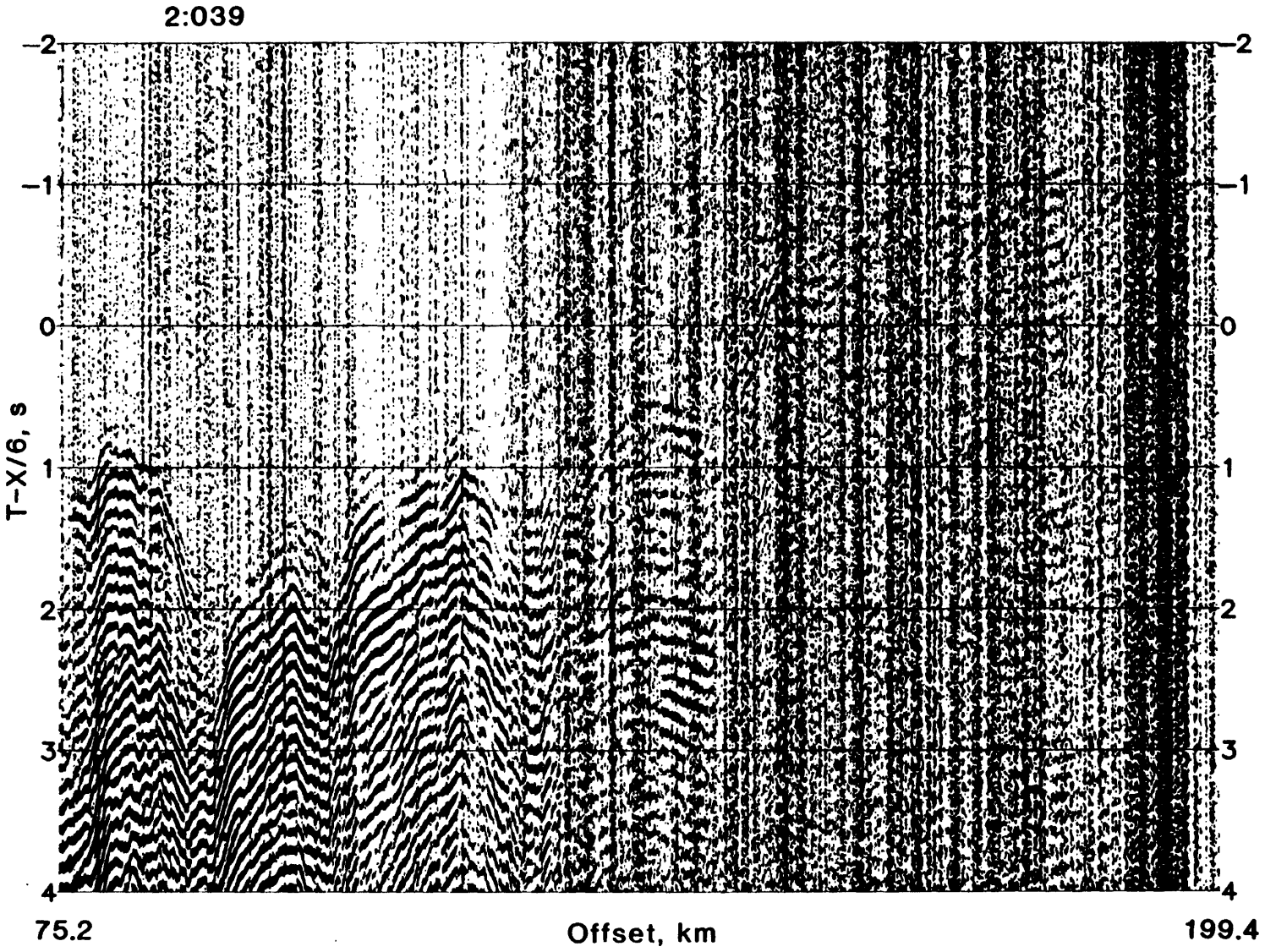

Figure 46. Stacked common receiver gather 039 for shots along LARSE air gun Line 2, reduced at 6 km/s.

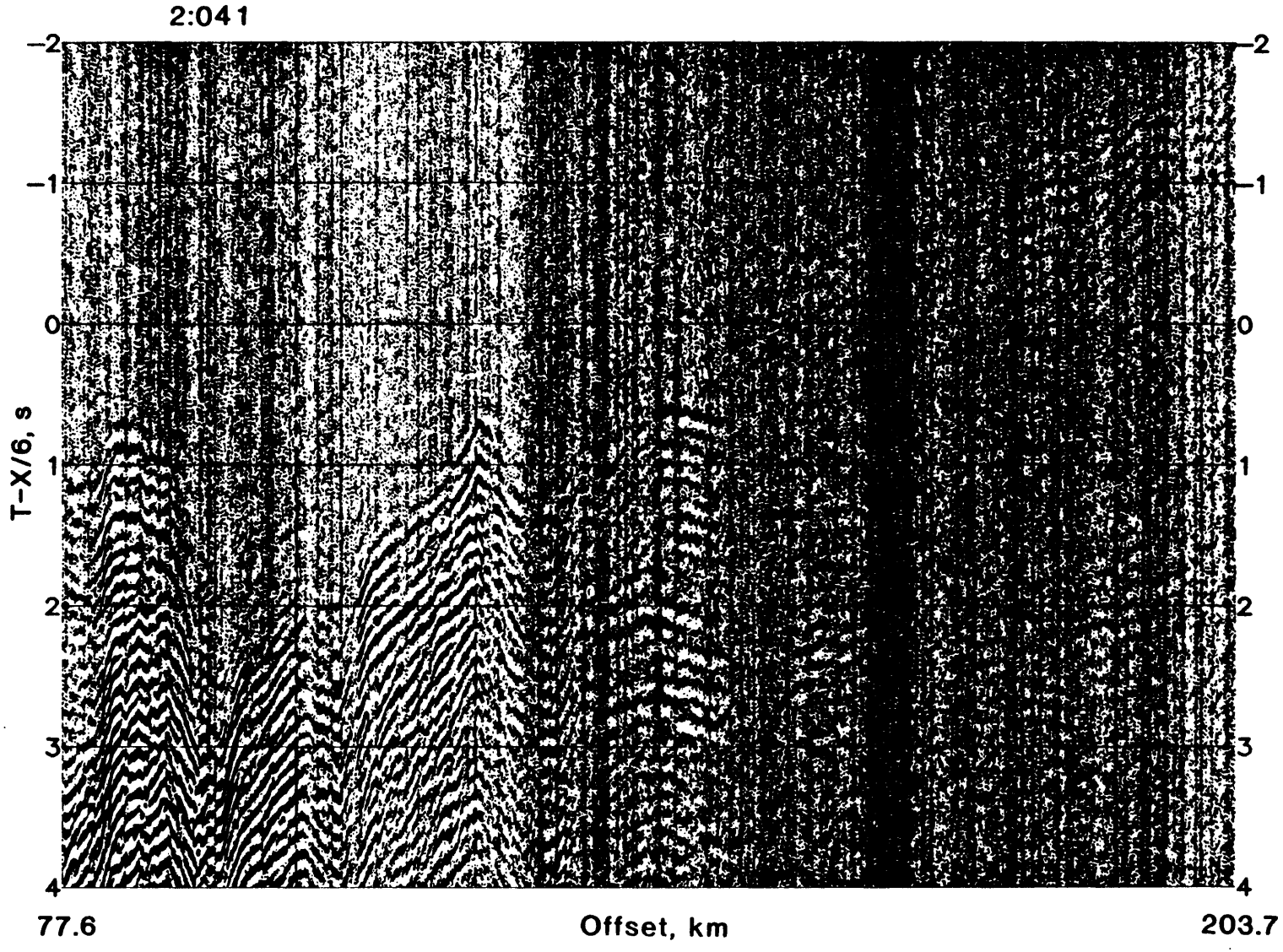

Figure 47. Stacked common receiver gather 041 for shots along LARSE air gun Line 2, reduced at 6 km/s.

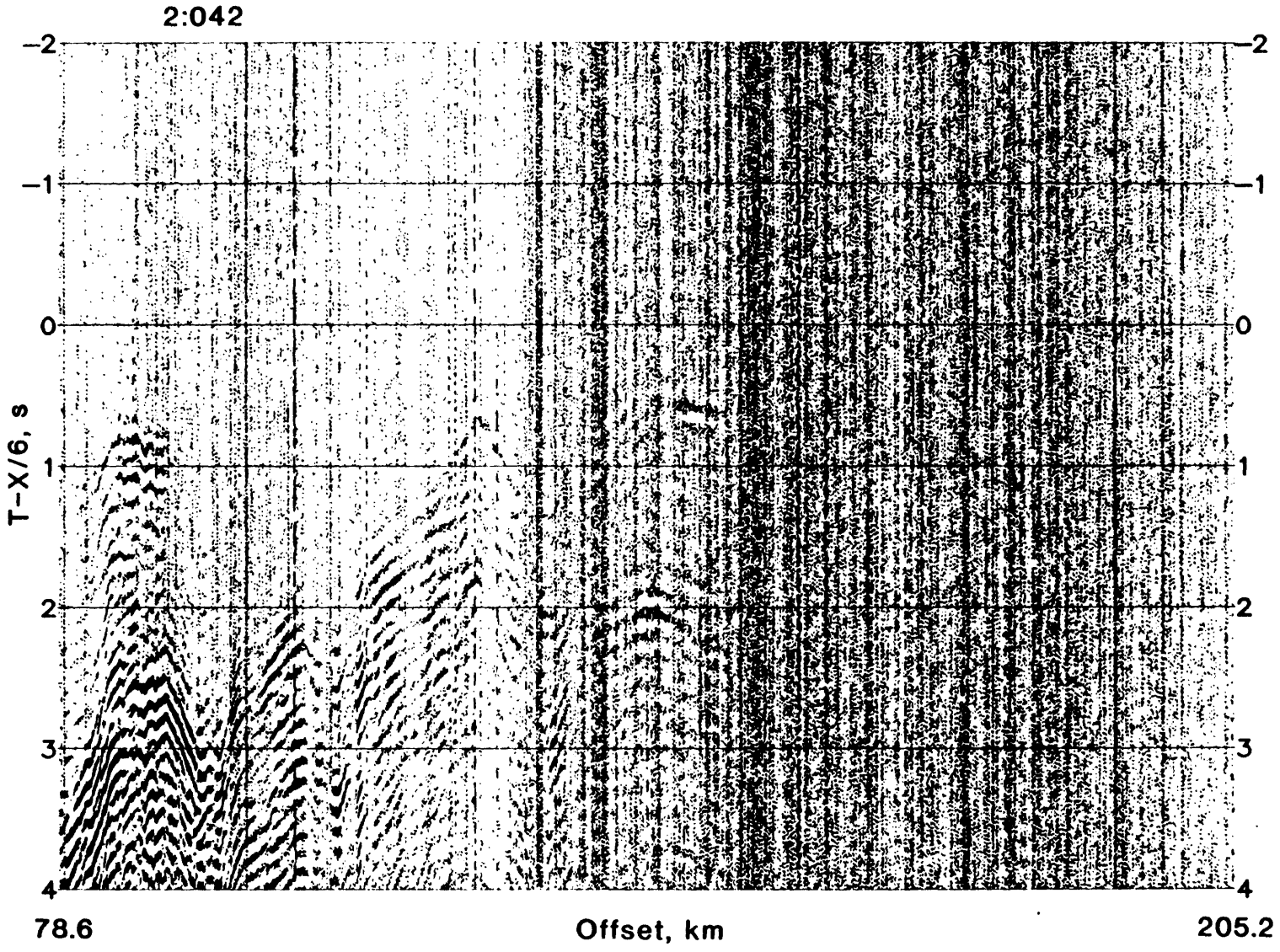

Figure 48. Stacked common receiver gather 042 for shots along LARSE air gun Line 2, reduced at 6 km/s.

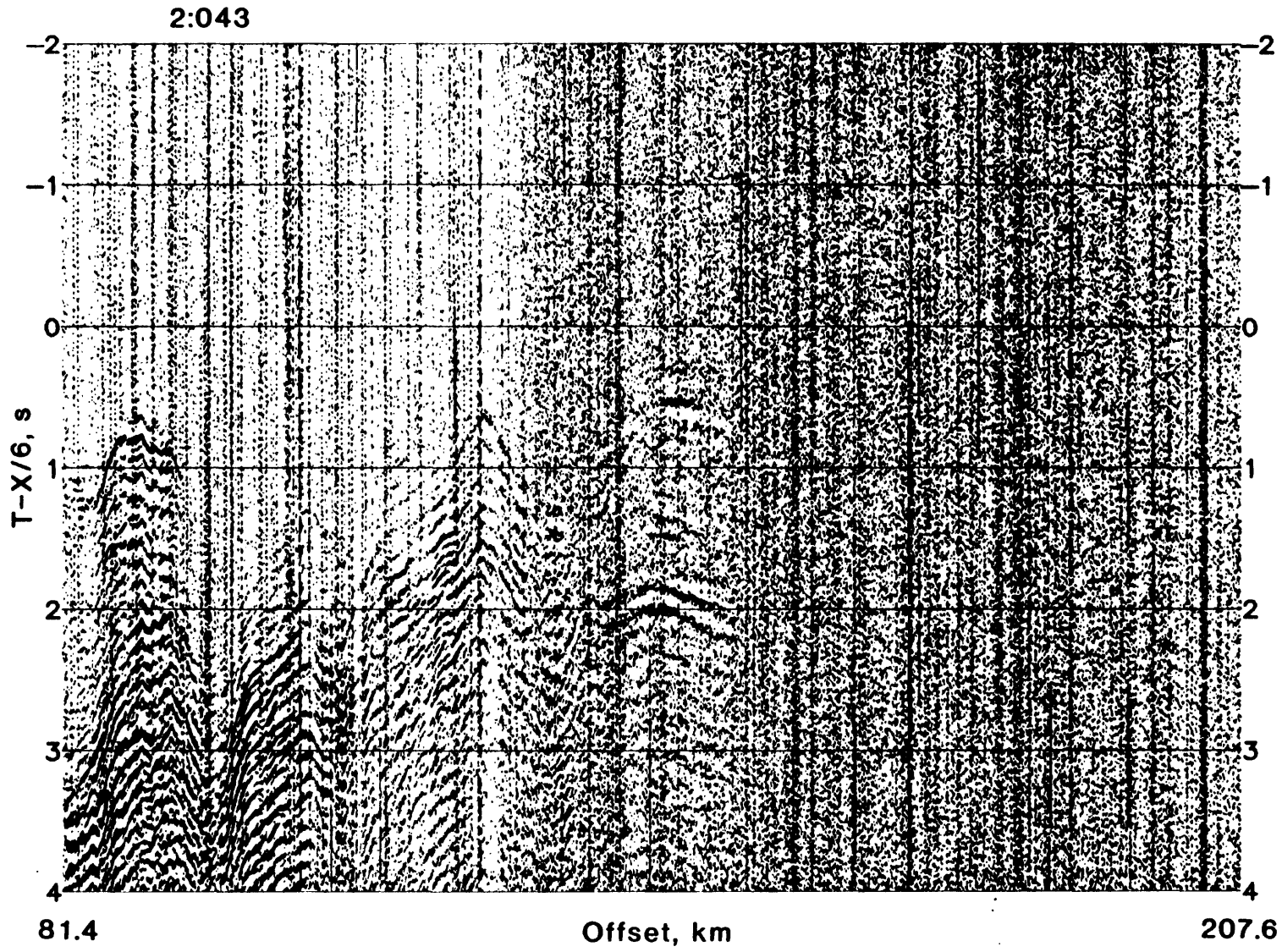

Figure 49. Stacked common receiver gather 043 for shots along LARSE air gun Line 2, reduced at 6 km/s.

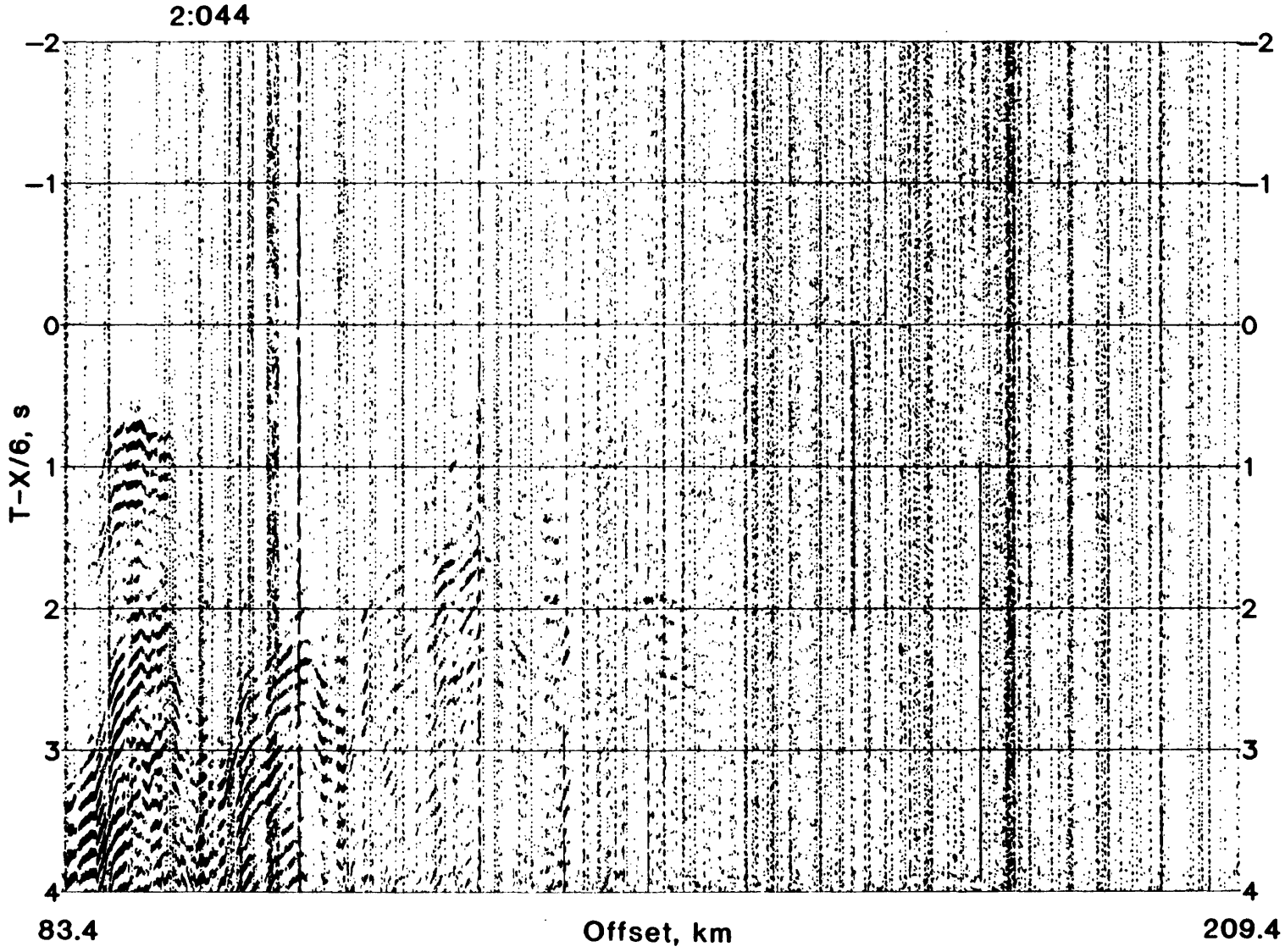

Figure 50. Stacked common receiver gather 044 for shots along LARSE air gun Line 2, reduced at 6 km/s.

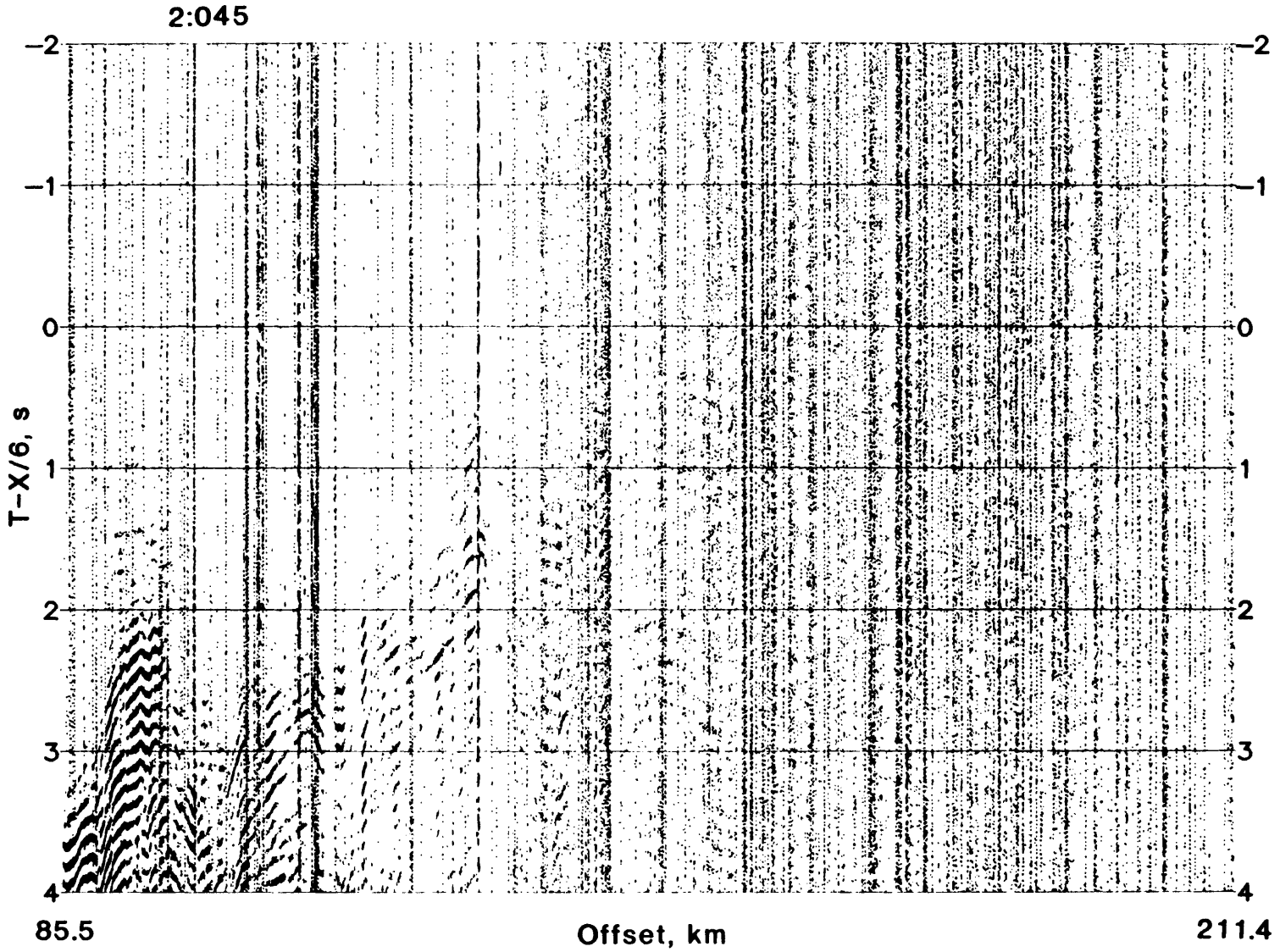

Figure 51. Stacked common receiver gather 045 for shots along LARSE air gun Line 2, reduced at 6 km/s.

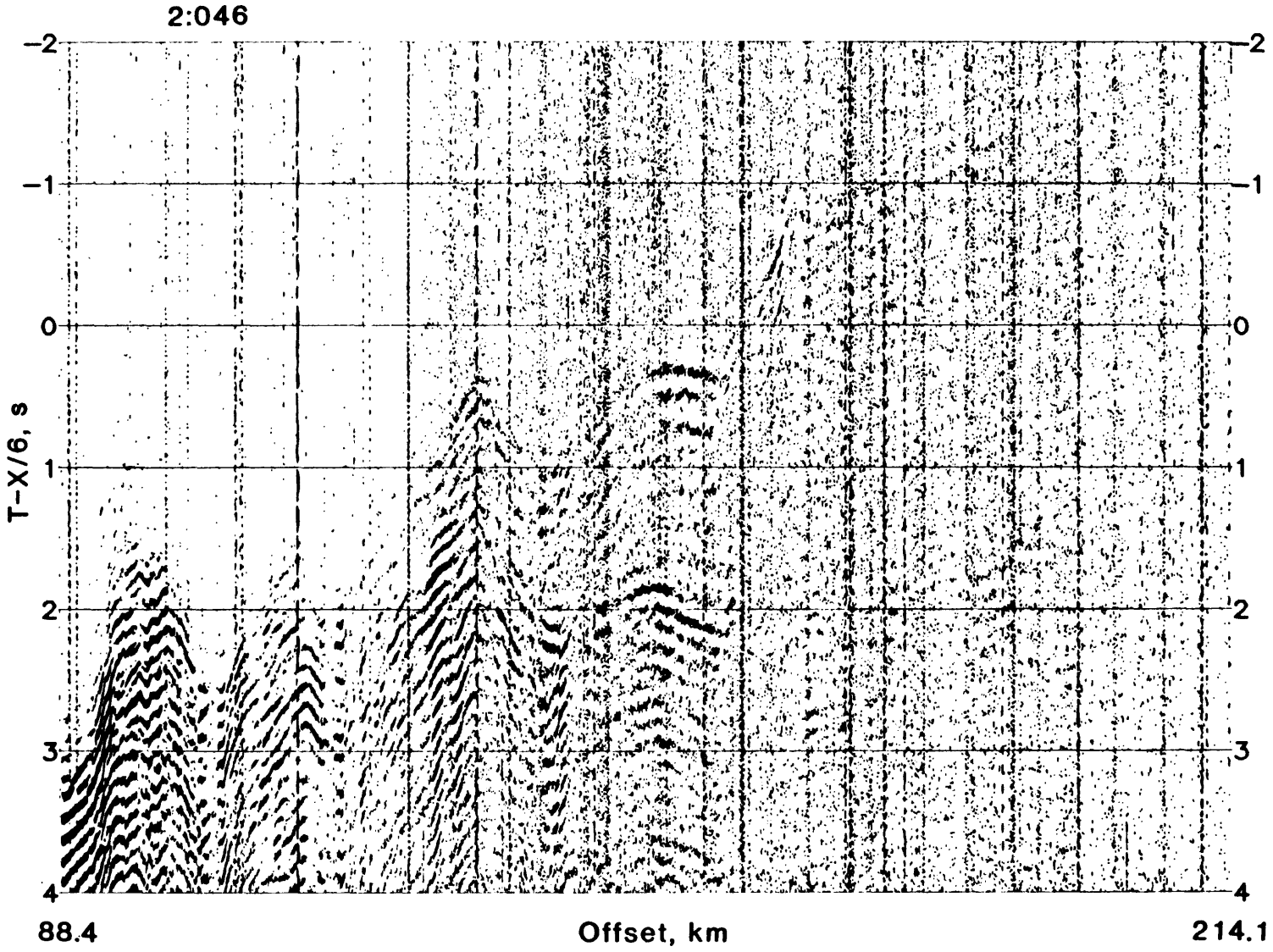

Figure 52. Stacked common receiver gather 046 for shots along LARSE air gun Line 2, reduced at 6 km/s.

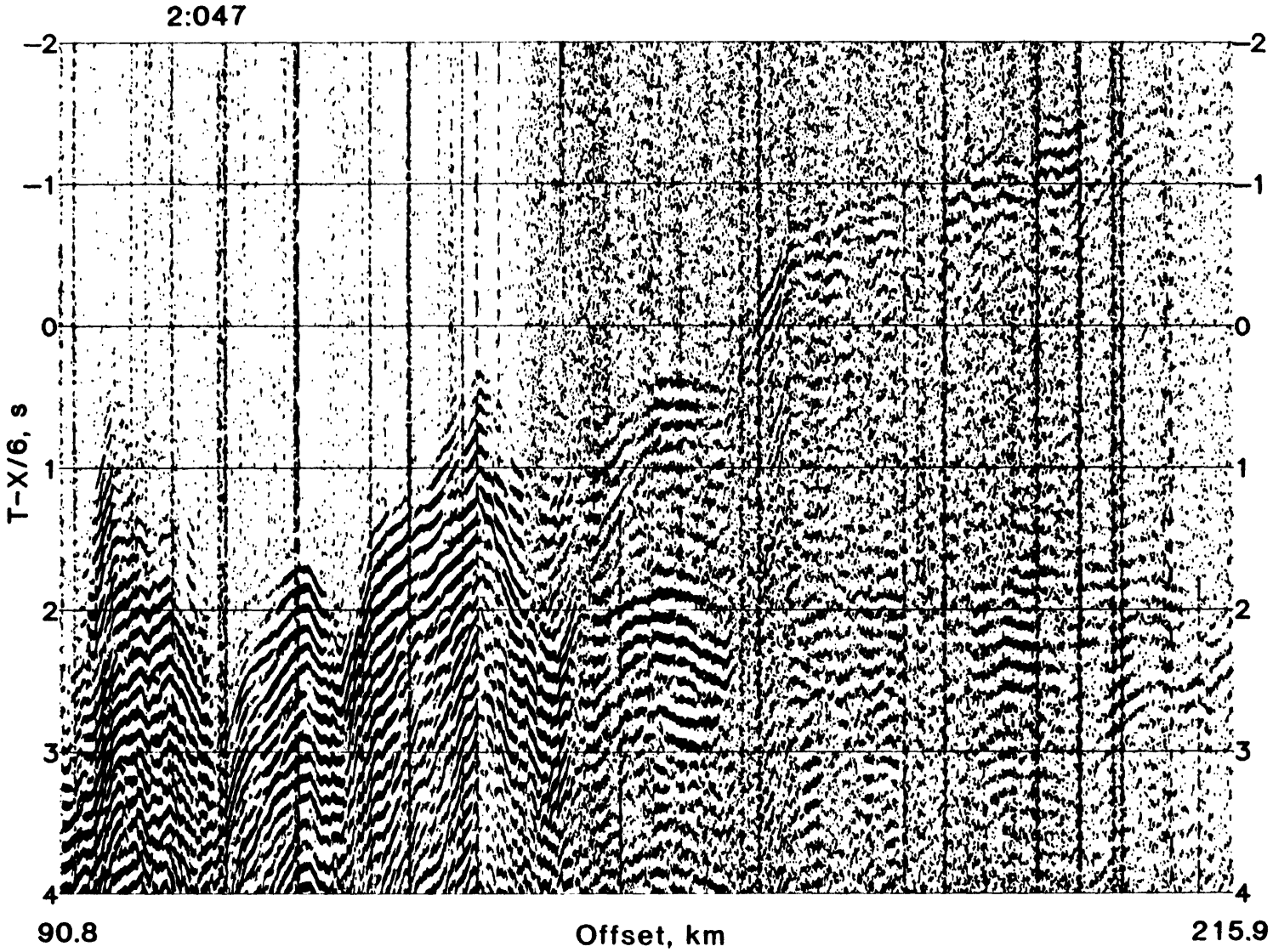

Figure 53. Stacked common receiver gather 047 for shots along LARSE air gun Line 2, reduced at 6 km/s.

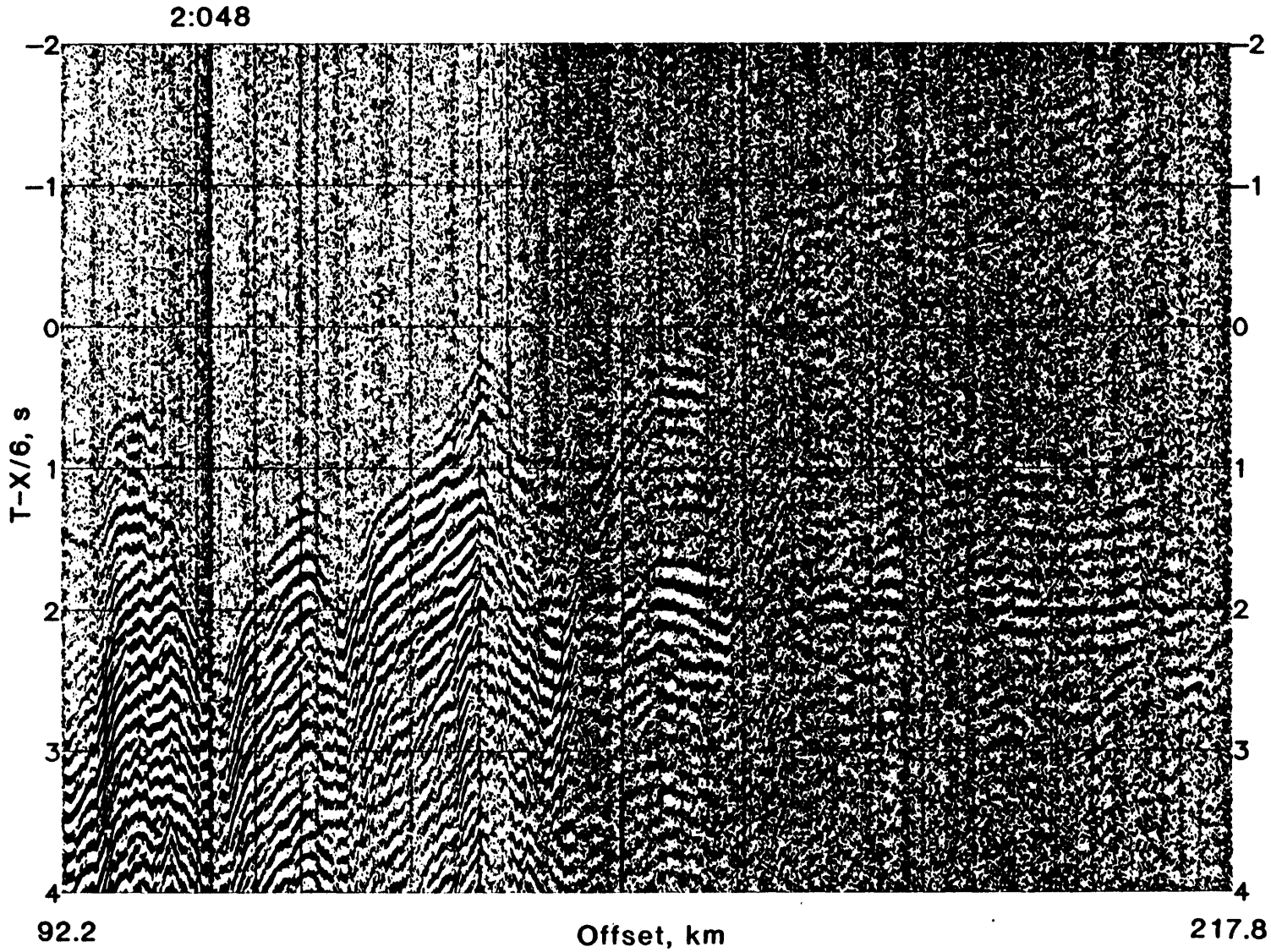

Figure 54. Stacked common receiver gather 048 for shots along LARSE air gun Line 2, reduced at 6 km/s.

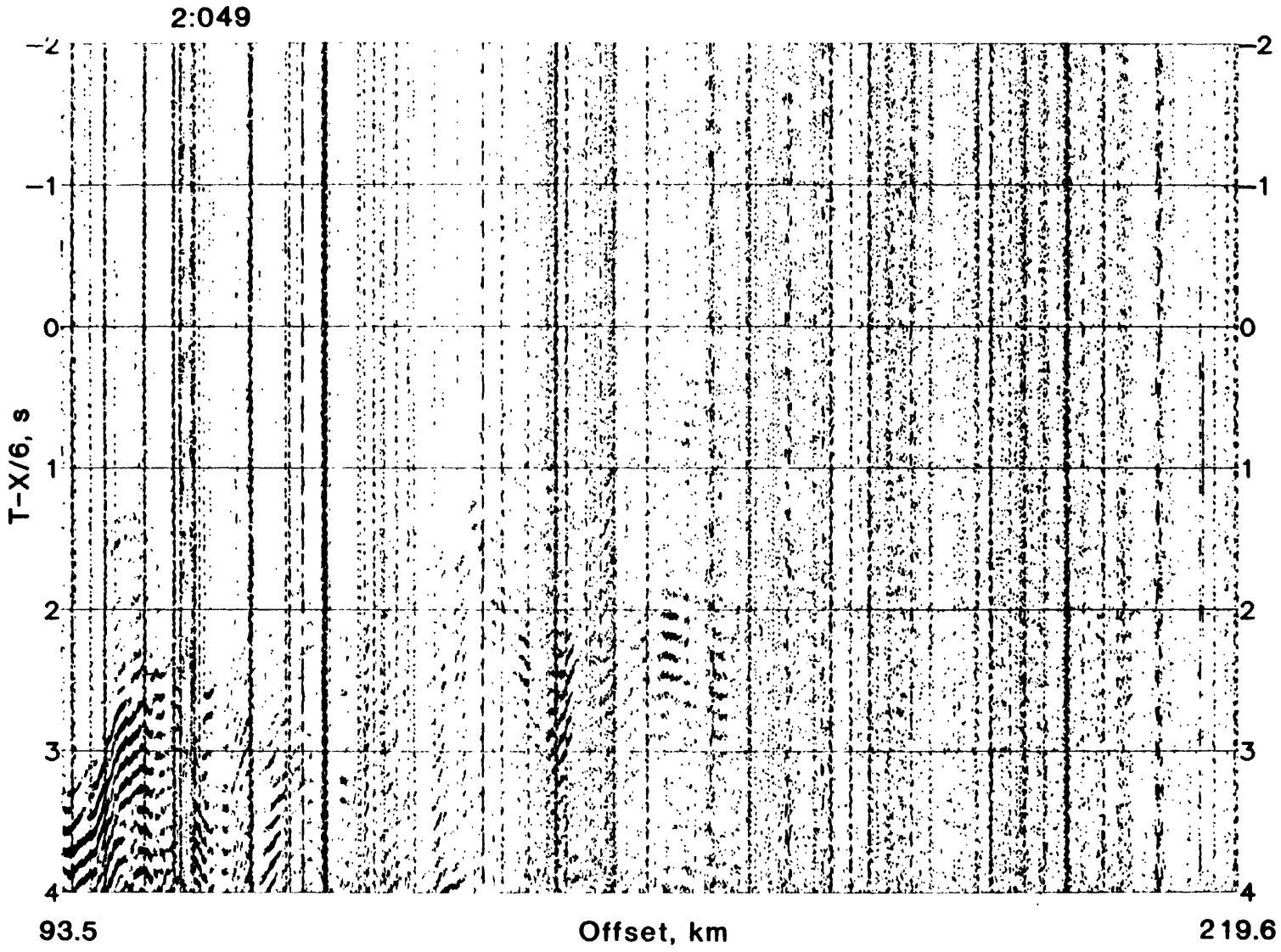

Figure 55. Stacked common receiver gather 049 for shots along LARSE air gun Line 2, reduced at 6 km/s.

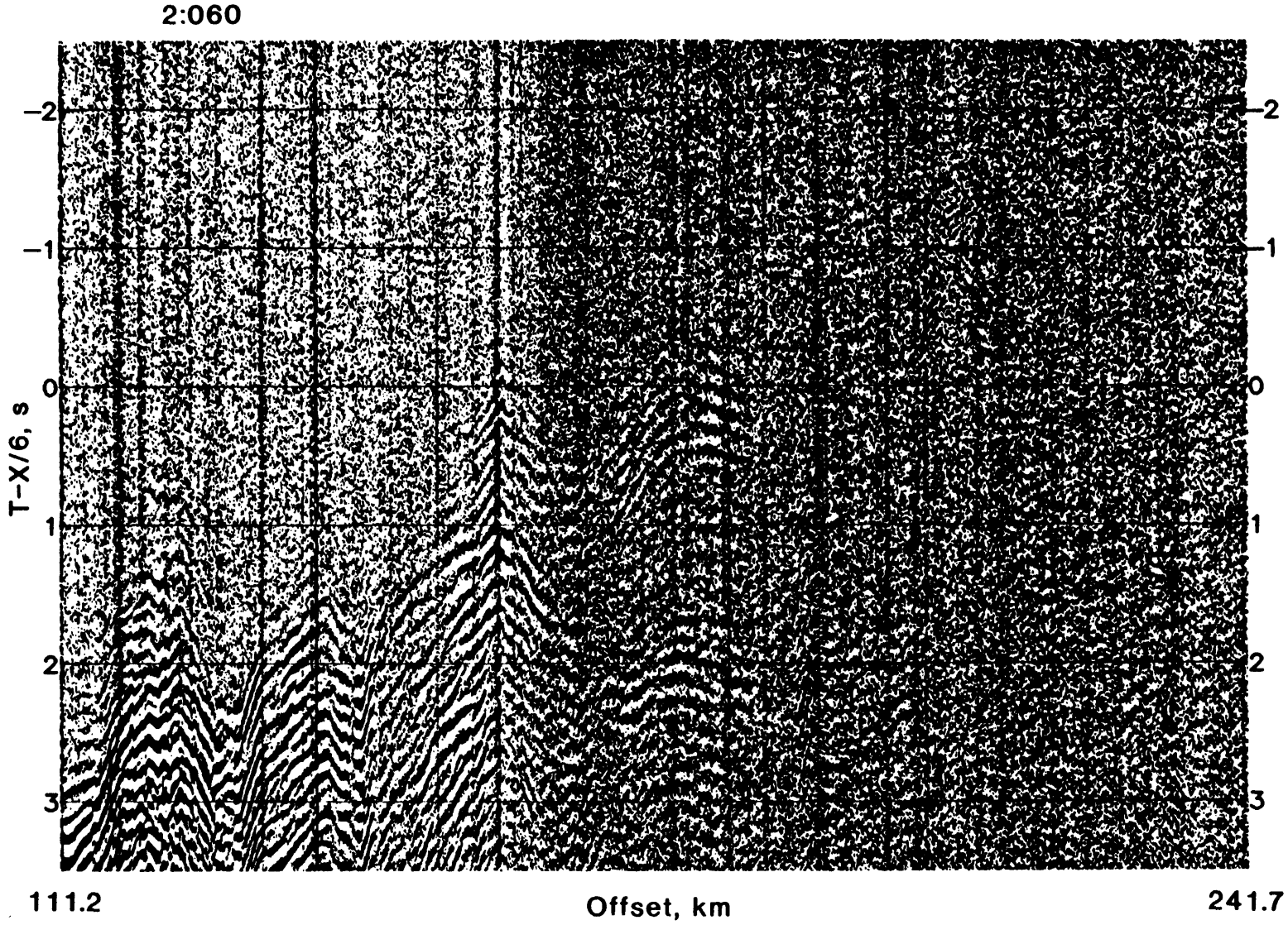

Figure 56. Stacked common receiver gather 060 for shots along LARSE air gun Line 2, reduced at 6 km/s.

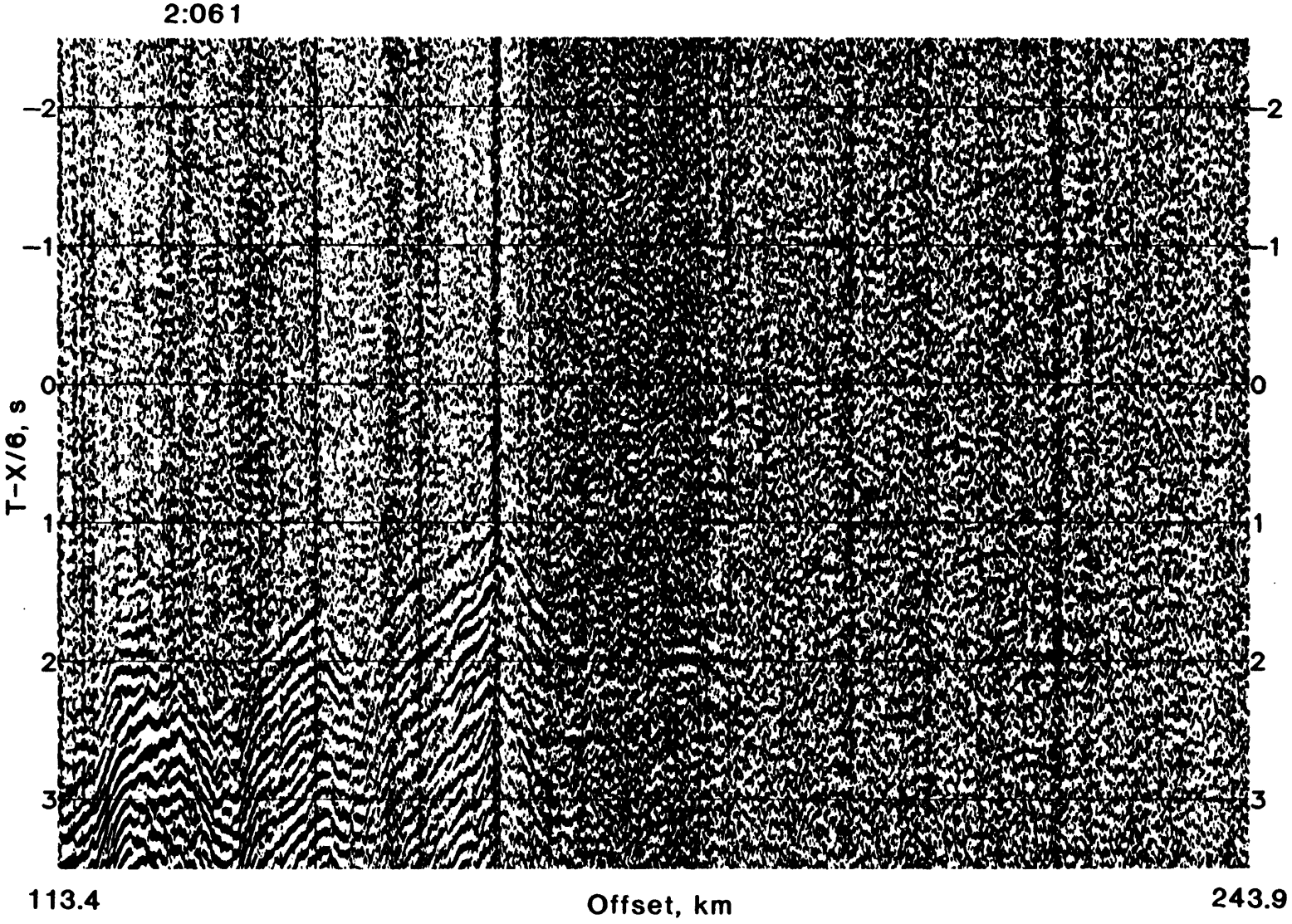

Figure 57. Stacked common receiver gather 061 for shots along LARSE air gun Line 2, reduced at 6 km/s.

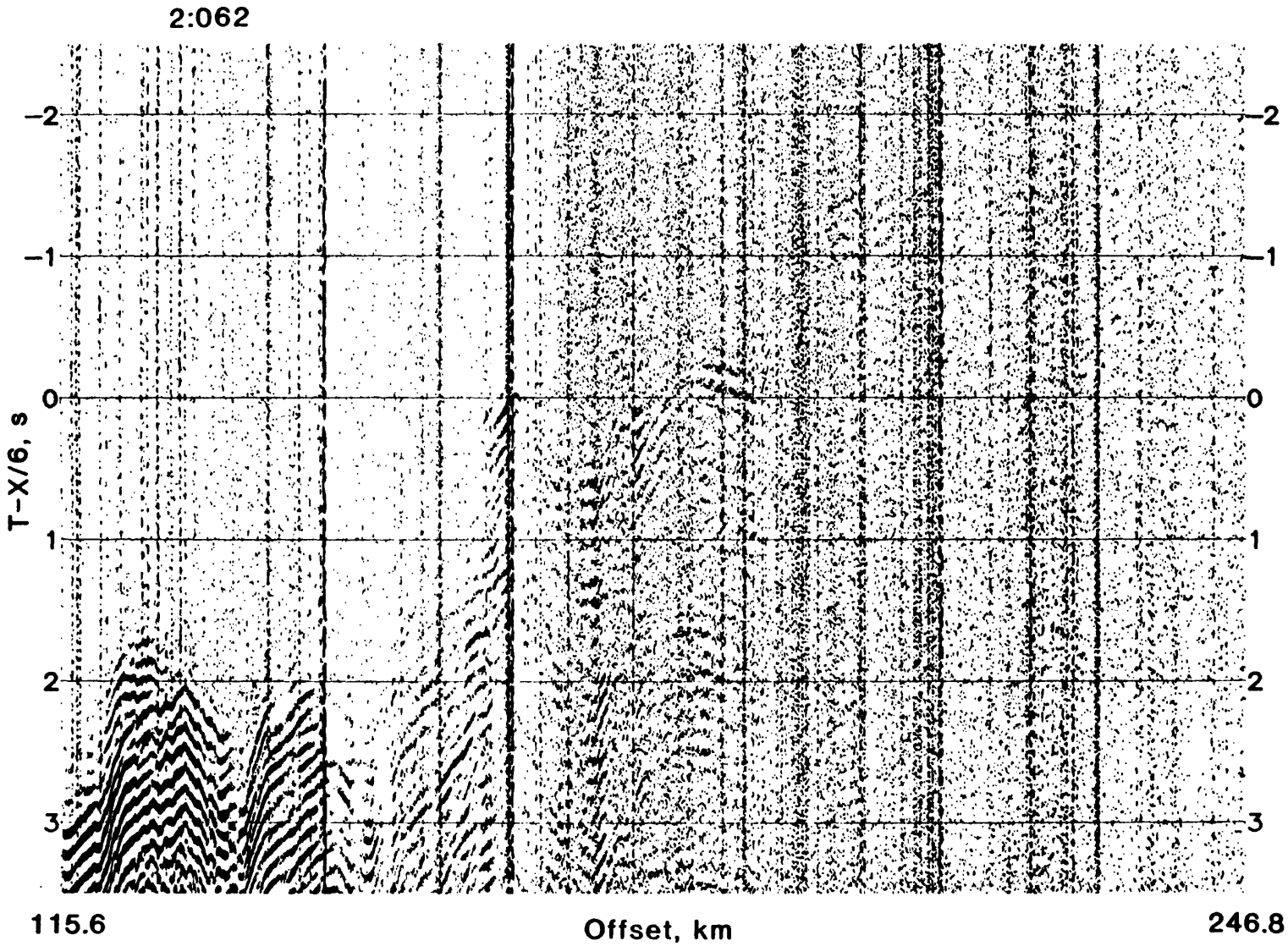

Figure 58. Stacked common receiver gather 062 for shots along LARSE air gun Line 2, reduced at 6 km/s.

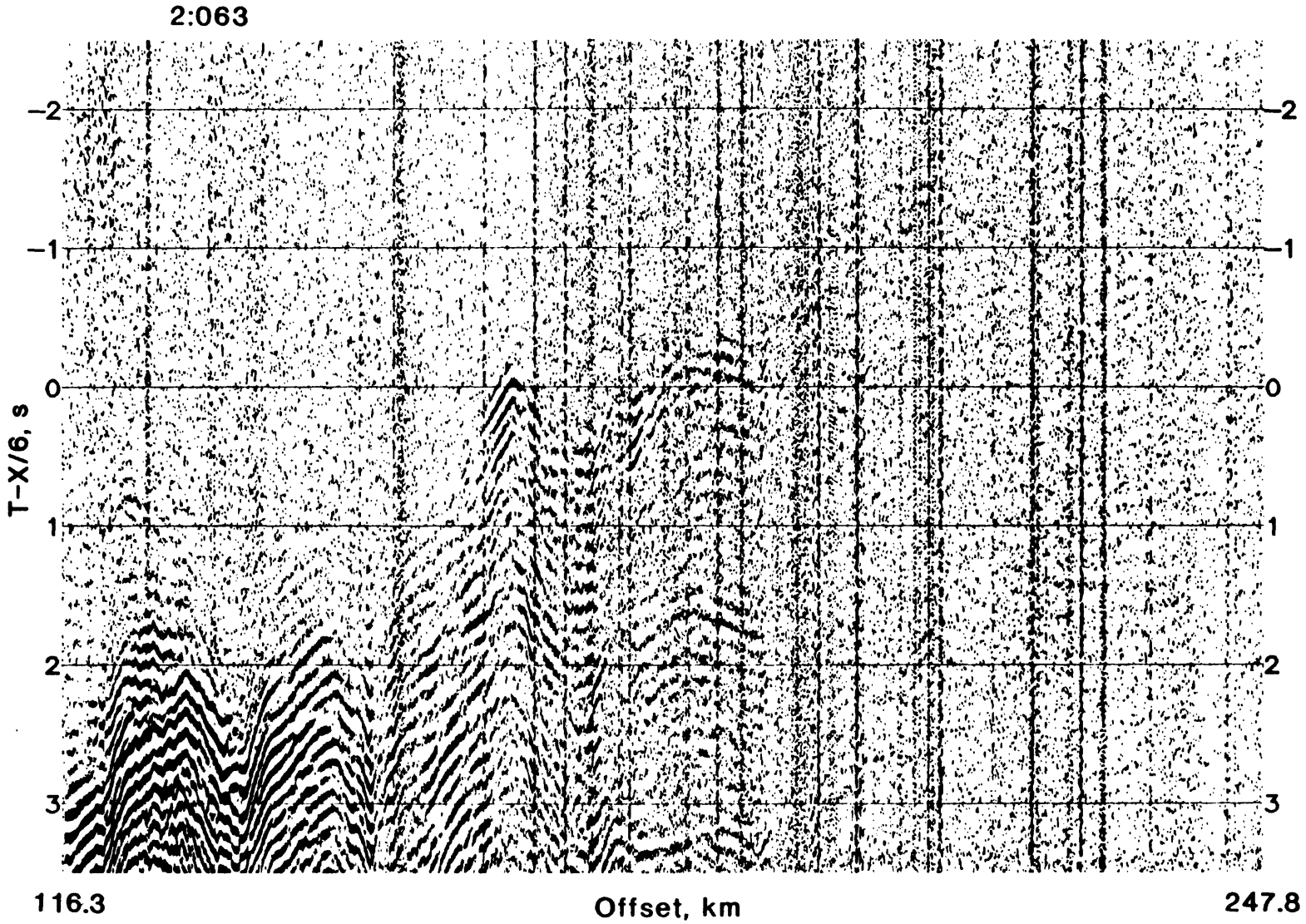

Figure 59. Stacked common receiver gather 063 for shots along LARSE air gun Line 2, reduced at 6 km/s.

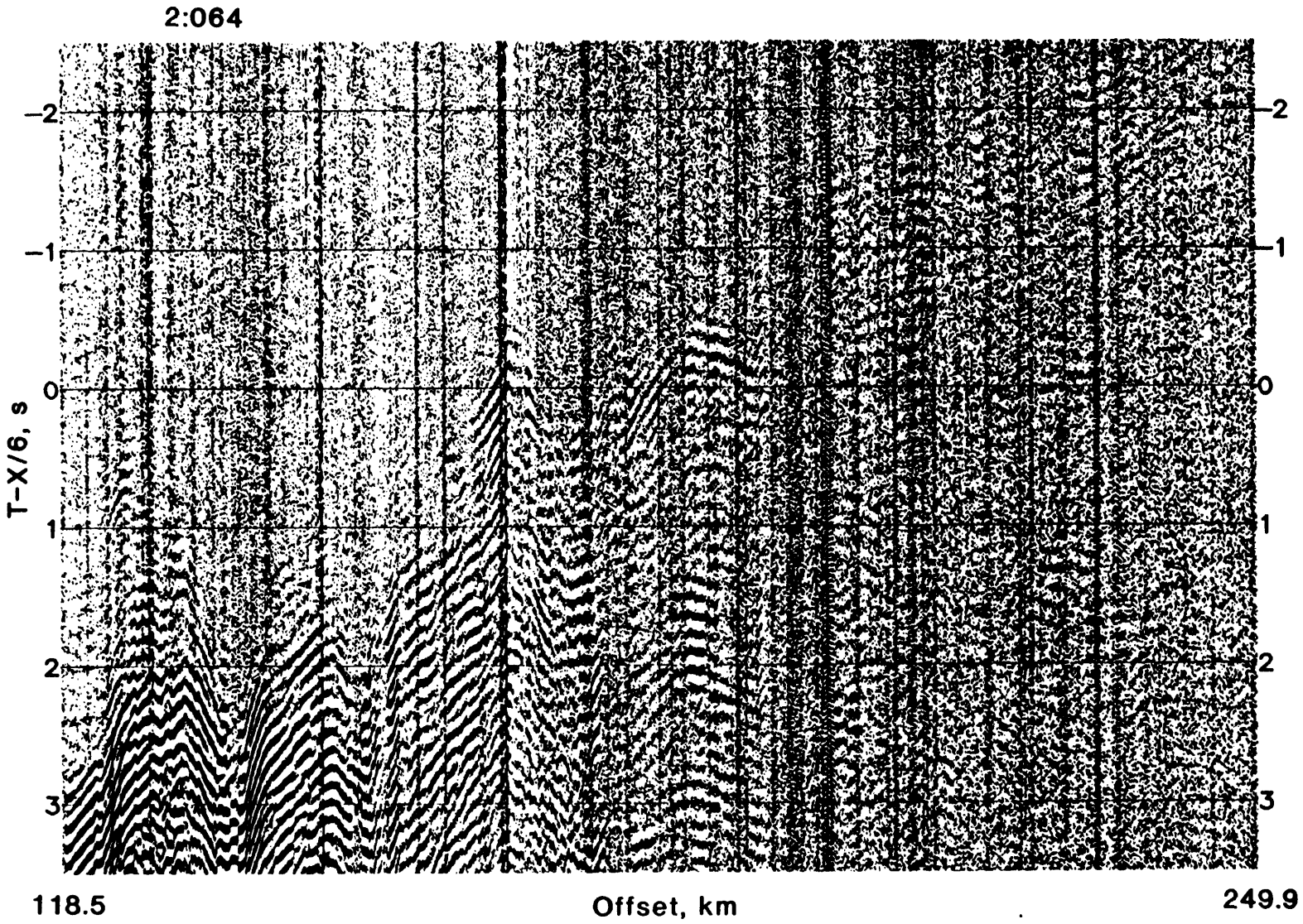

Figure 60. Stacked common receiver gather 064 for shots along LARSE air gun Line 2, reduced at 6 km/s.

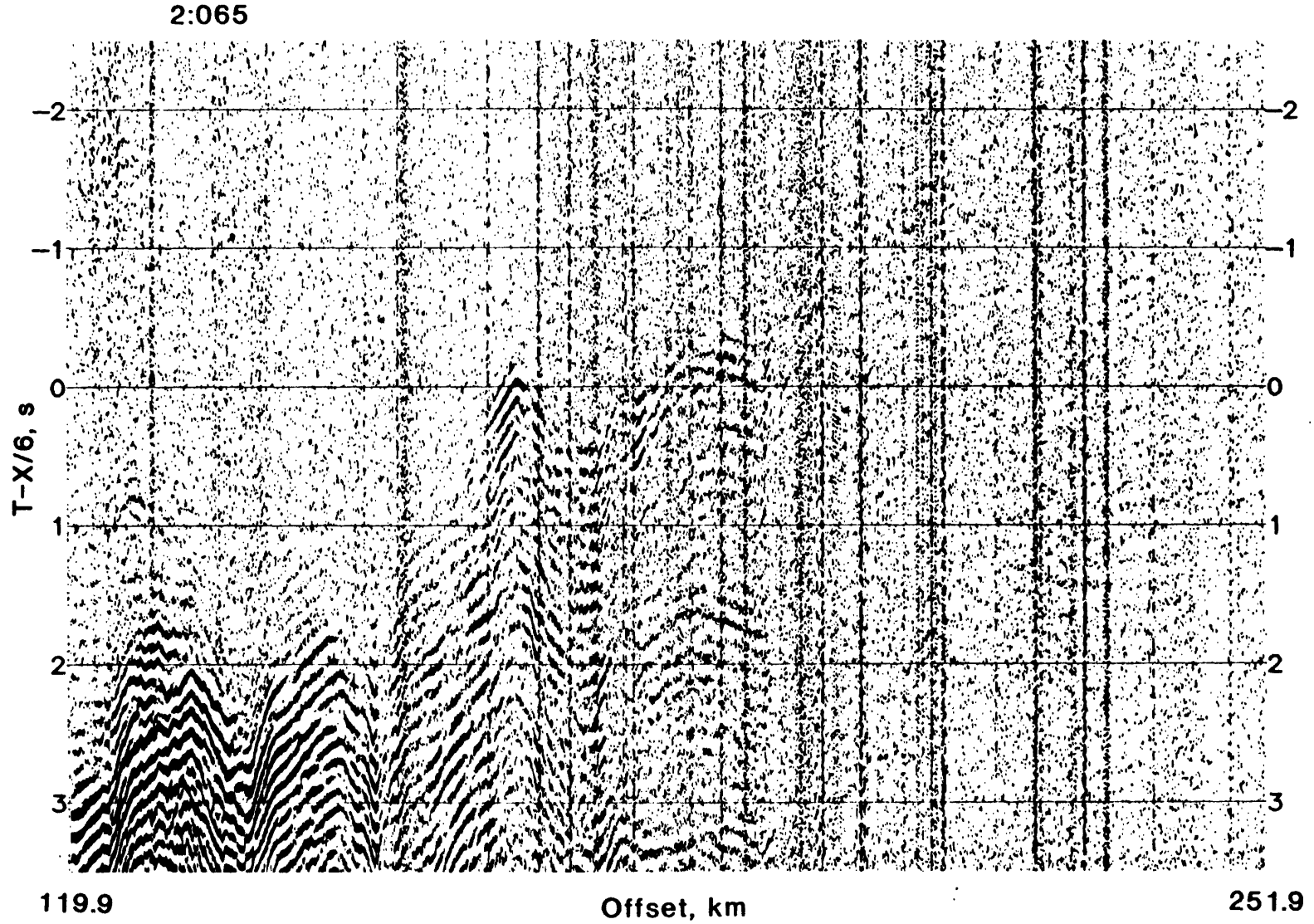

Figure 61. Stacked common receiver gather 065 for shots along LARSE air gun Line 2, reduced at 6 km/s.

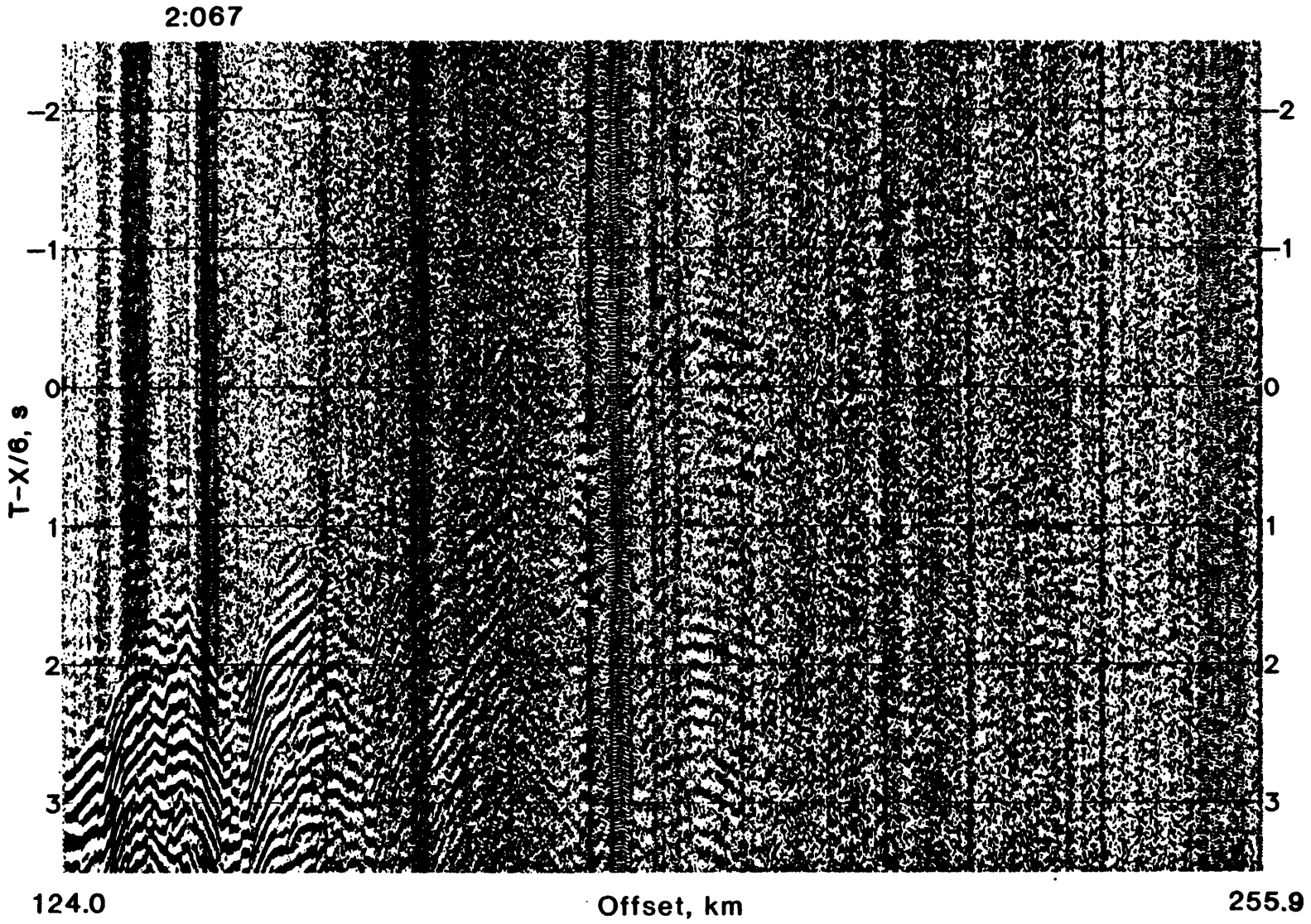

Figure 62. Stacked common receiver gather 067 for shots along LARSE air gun Line 2, reduced at 6 km/s.

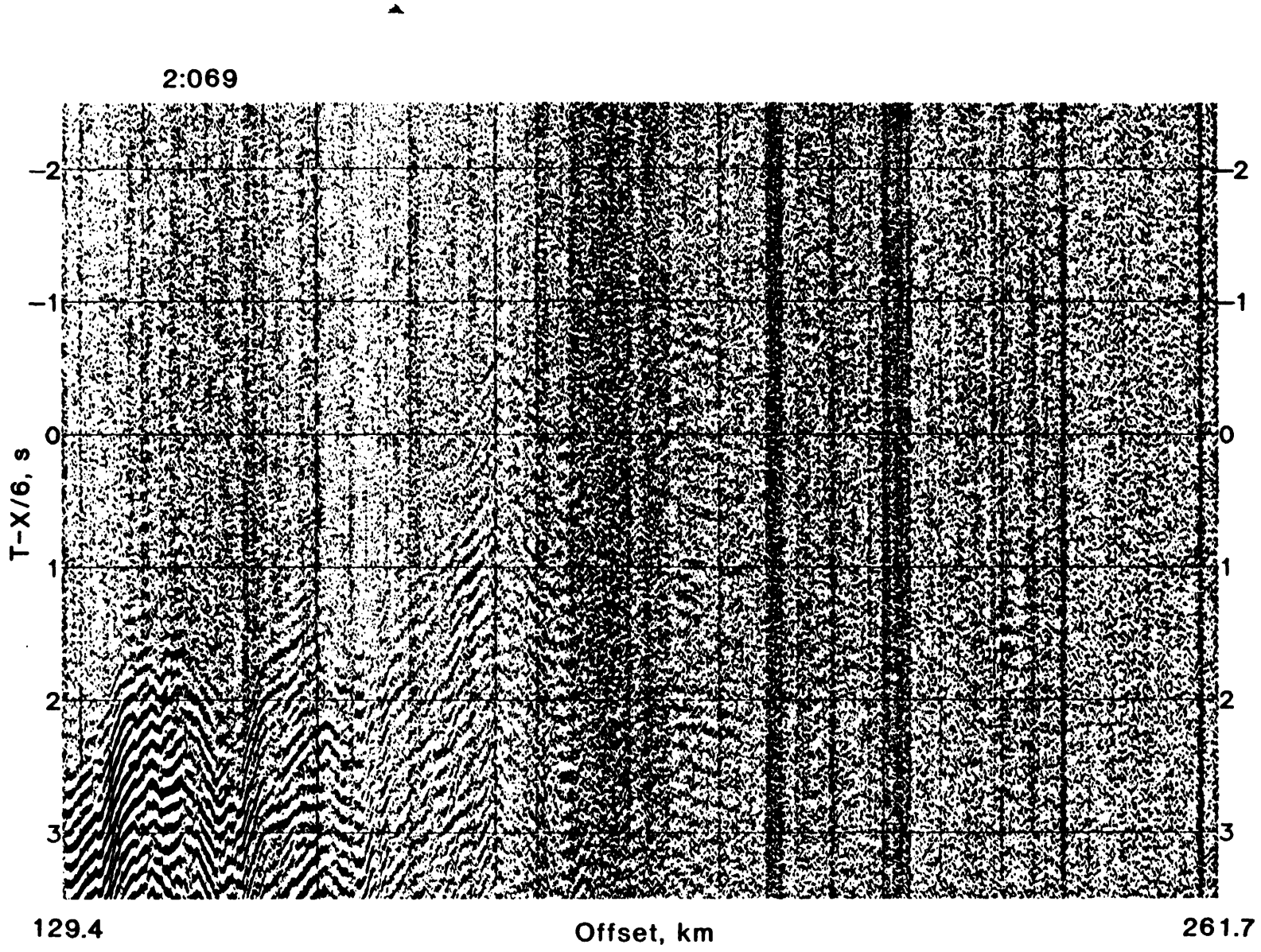

Figure 63. Stacked common receiver gather 069 for shots along LARSE air gun Line 2, reduced at 6 km/s.

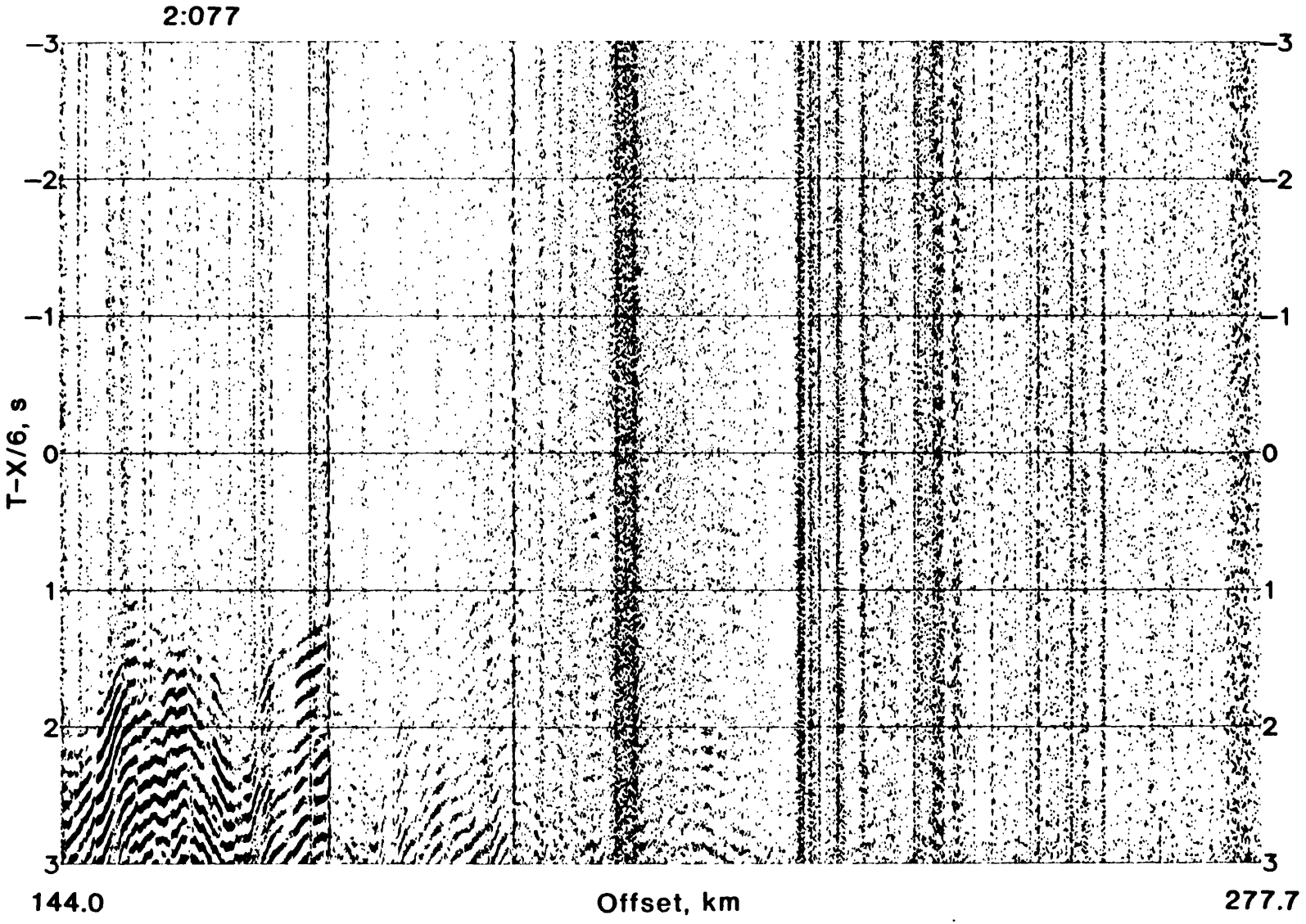

Figure 64. Stacked common receiver gather 077 for shots along LARSE air gun Line 2, reduced at 6 km/s.

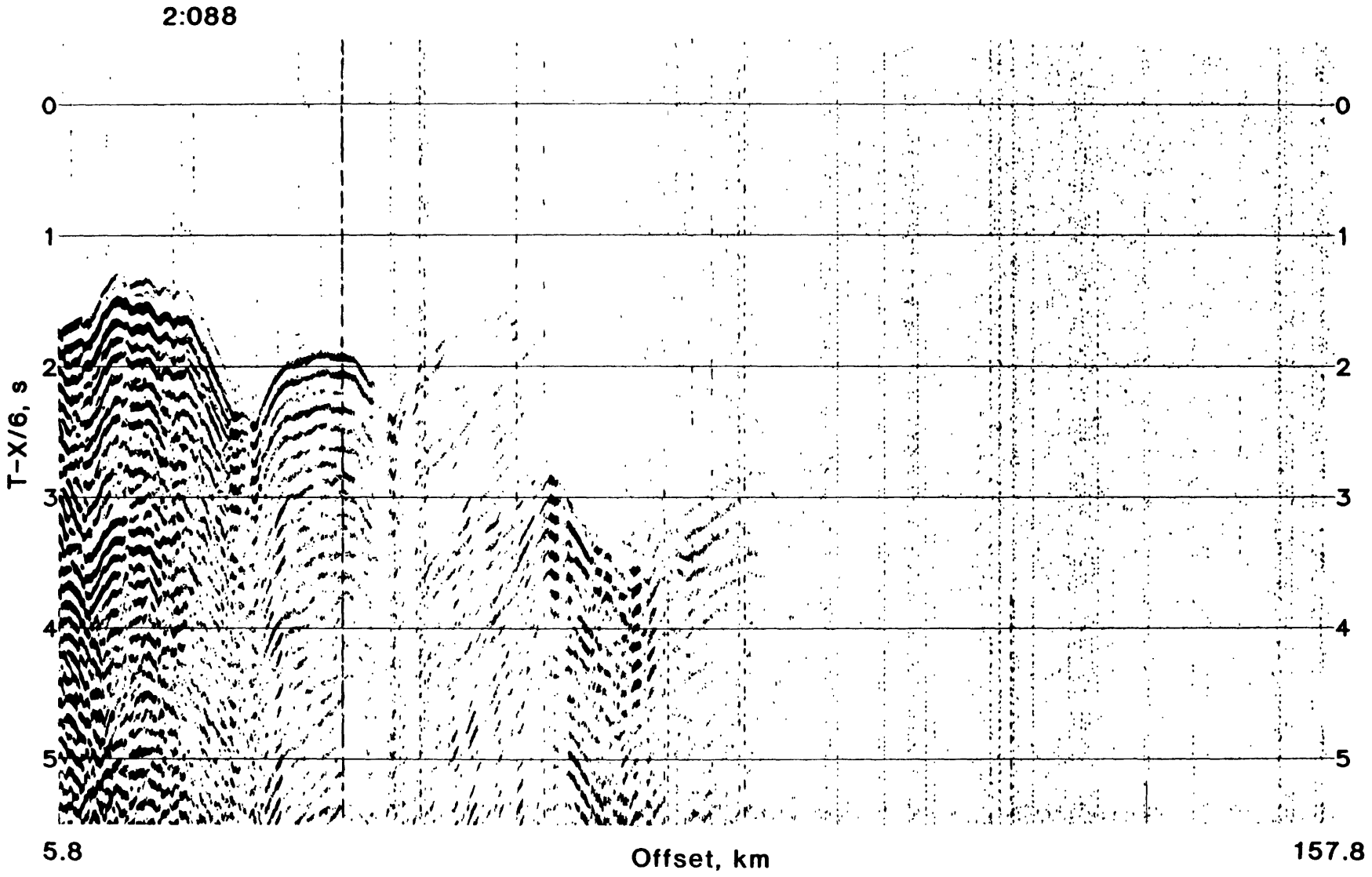

Figure 65. Stacked common receiver gather 088 for shots along LARSE air gun Line 2, reduced at 6 km/s.

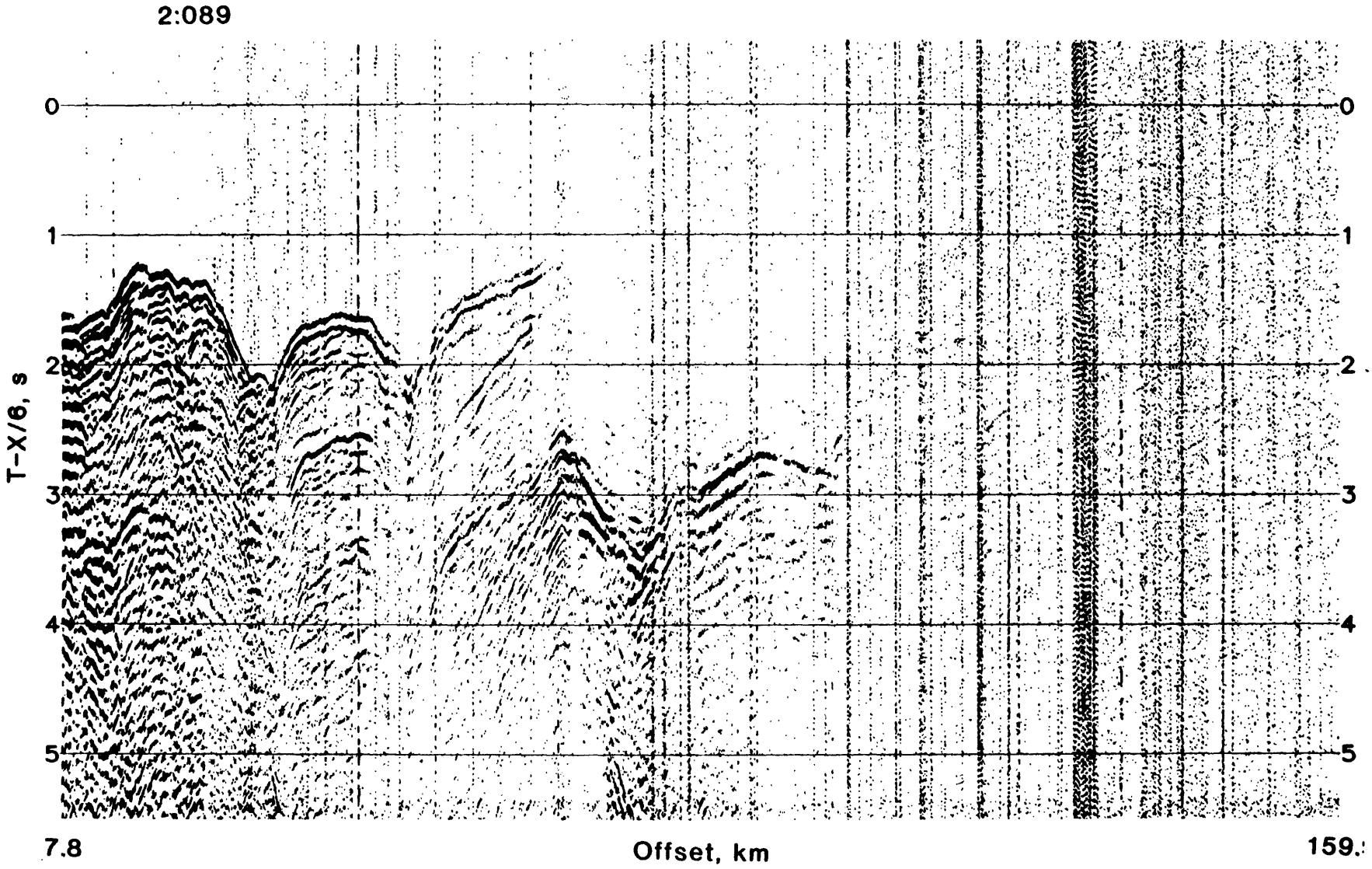

Figure 66. Stacked common receiver gather 089 for shots along LARSE air gun Line 2, reduced at 6 km/s.

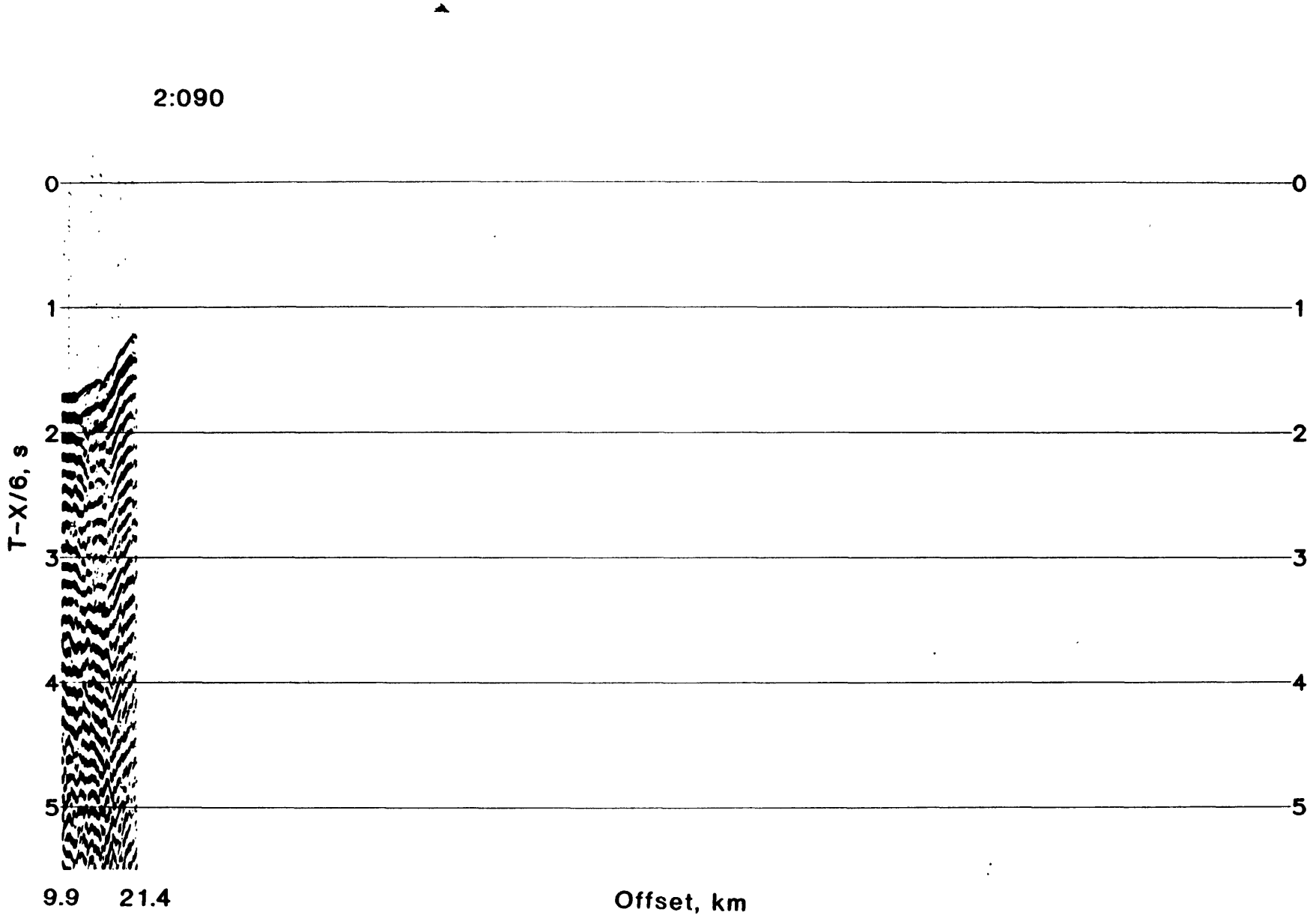

Figure 67. Stacked common receiver gather 090 for shots along LARSE air gun Line 2, reduced at 6 km/s.

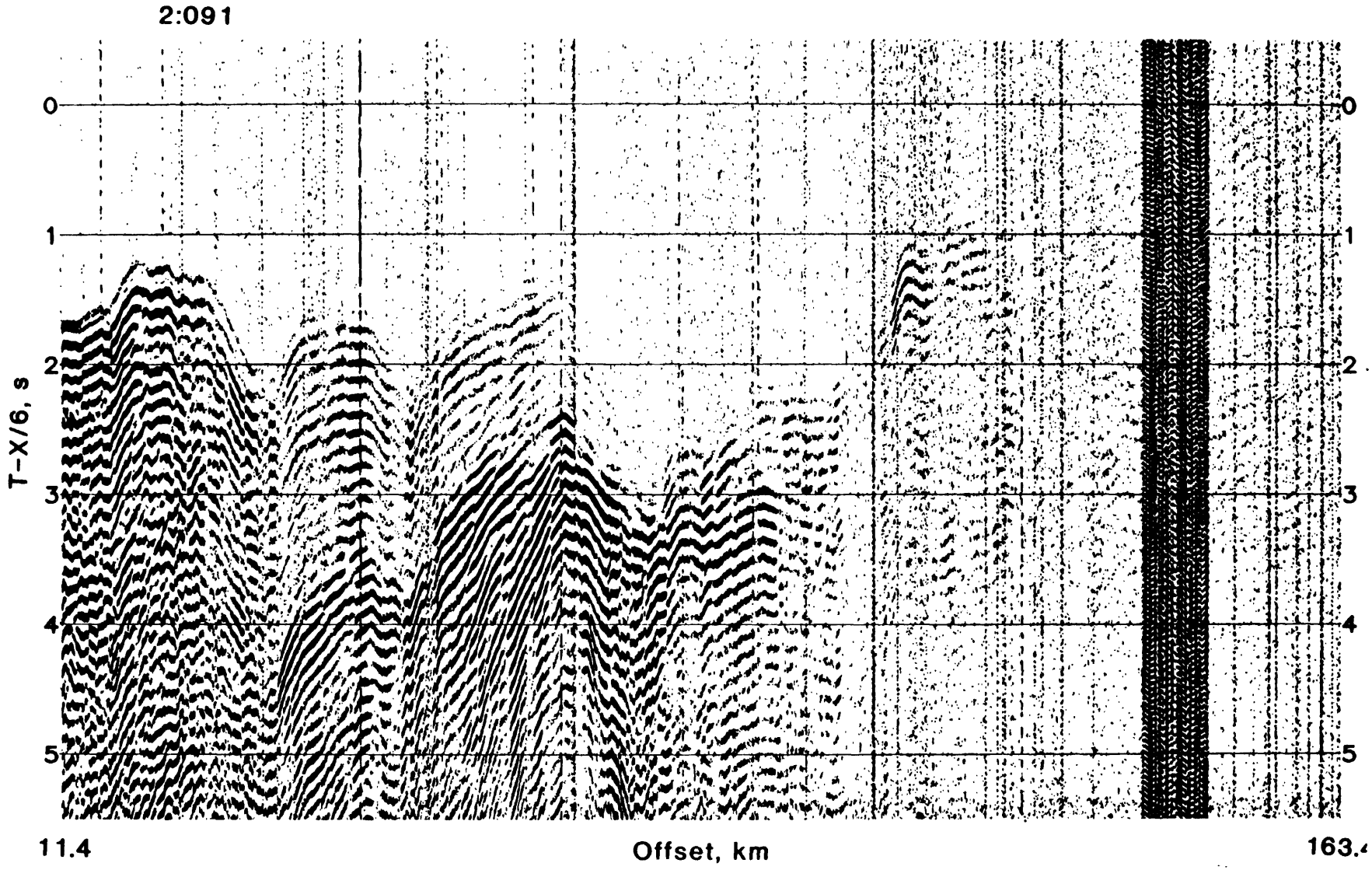

Figure 68. Stacked common receiver gather 091 for shots along LARSE air gun Line 2, reduced at 6 km/s.

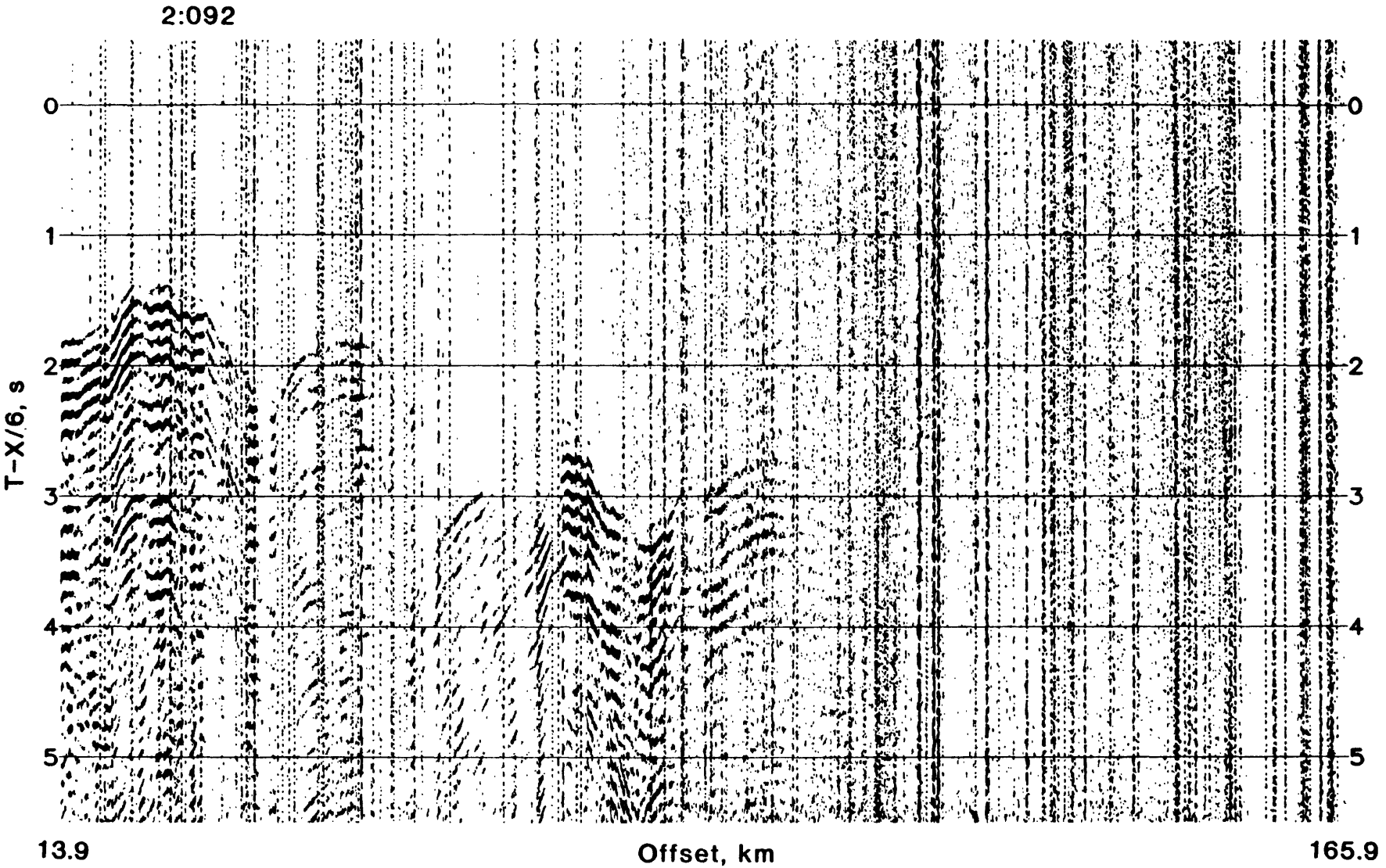

Figure 69. Stacked common receiver gather 092 for shots along LARSE air gun Line 2, reduced at 6 km/s.

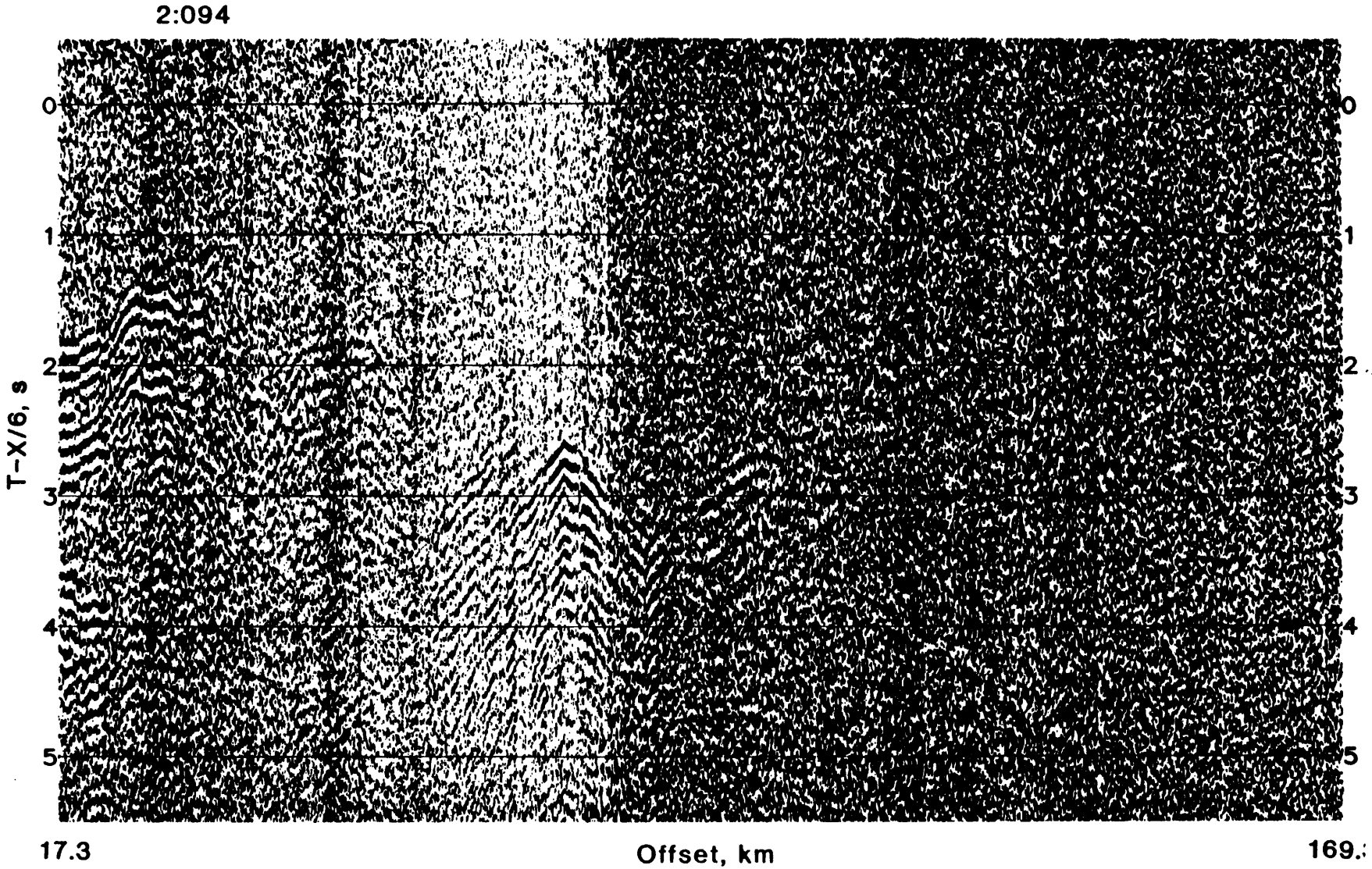

Figure 70. Stacked common receiver gather 094 for shots along LARSE air gun Line 2, reduced at 6 km/s.

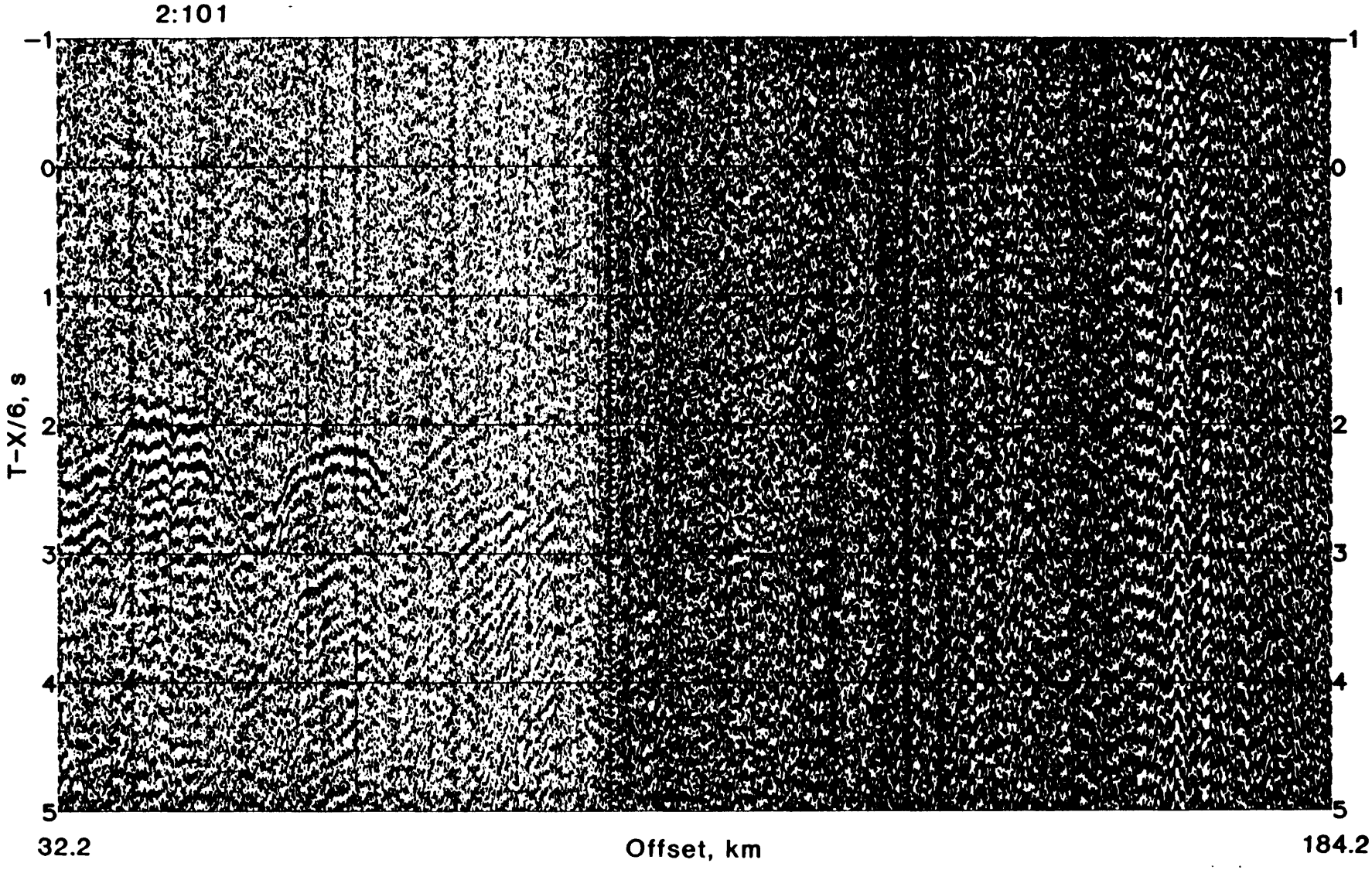

Figure 71. Stacked common receiver gather 101 for shots along LARSE air gun Line 2, reduced at 6 km/s.

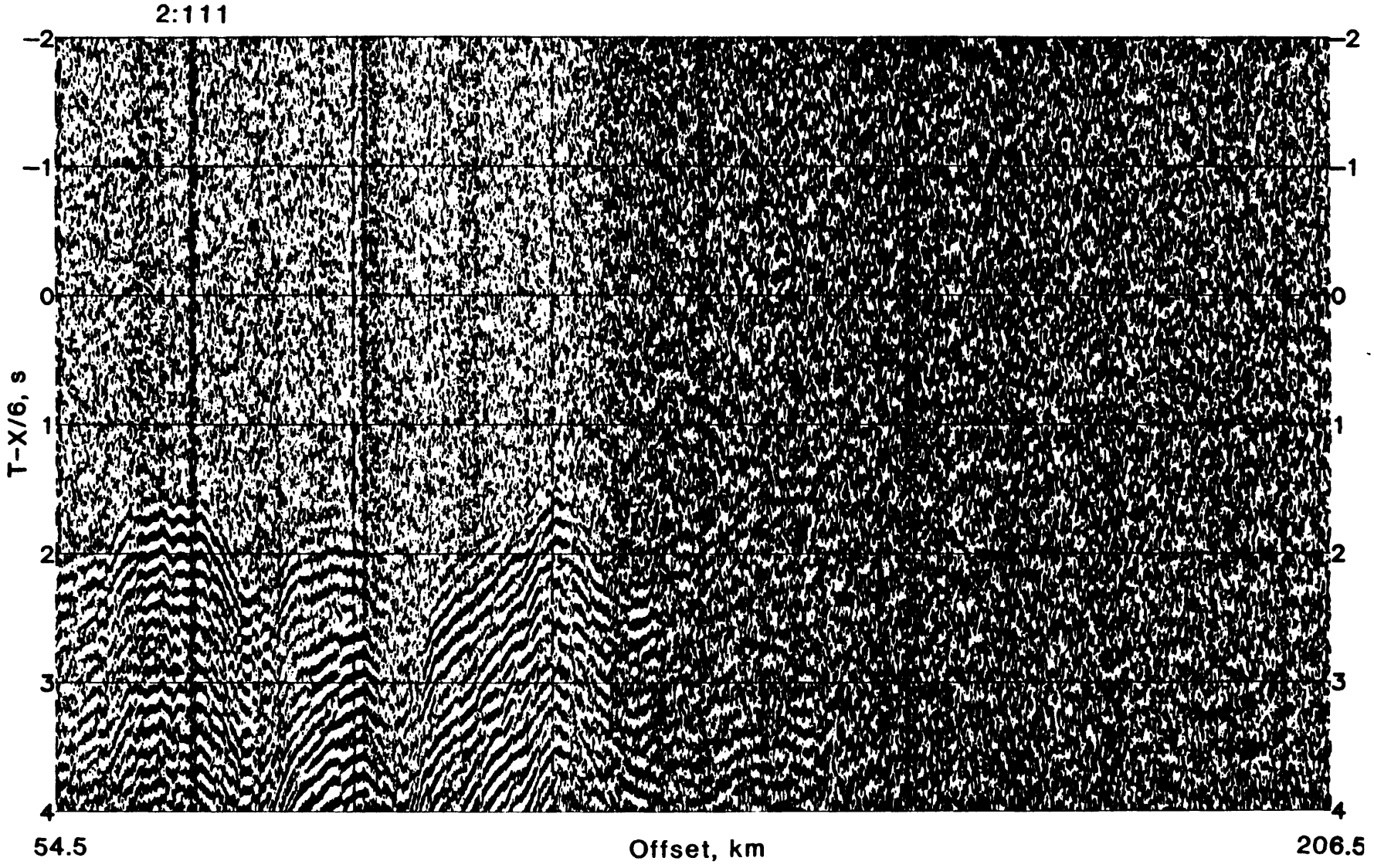

Figure 72. Stacked common receiver gather 111 for shots along LARSE air gun Line 2, reduced at 6 km/s.

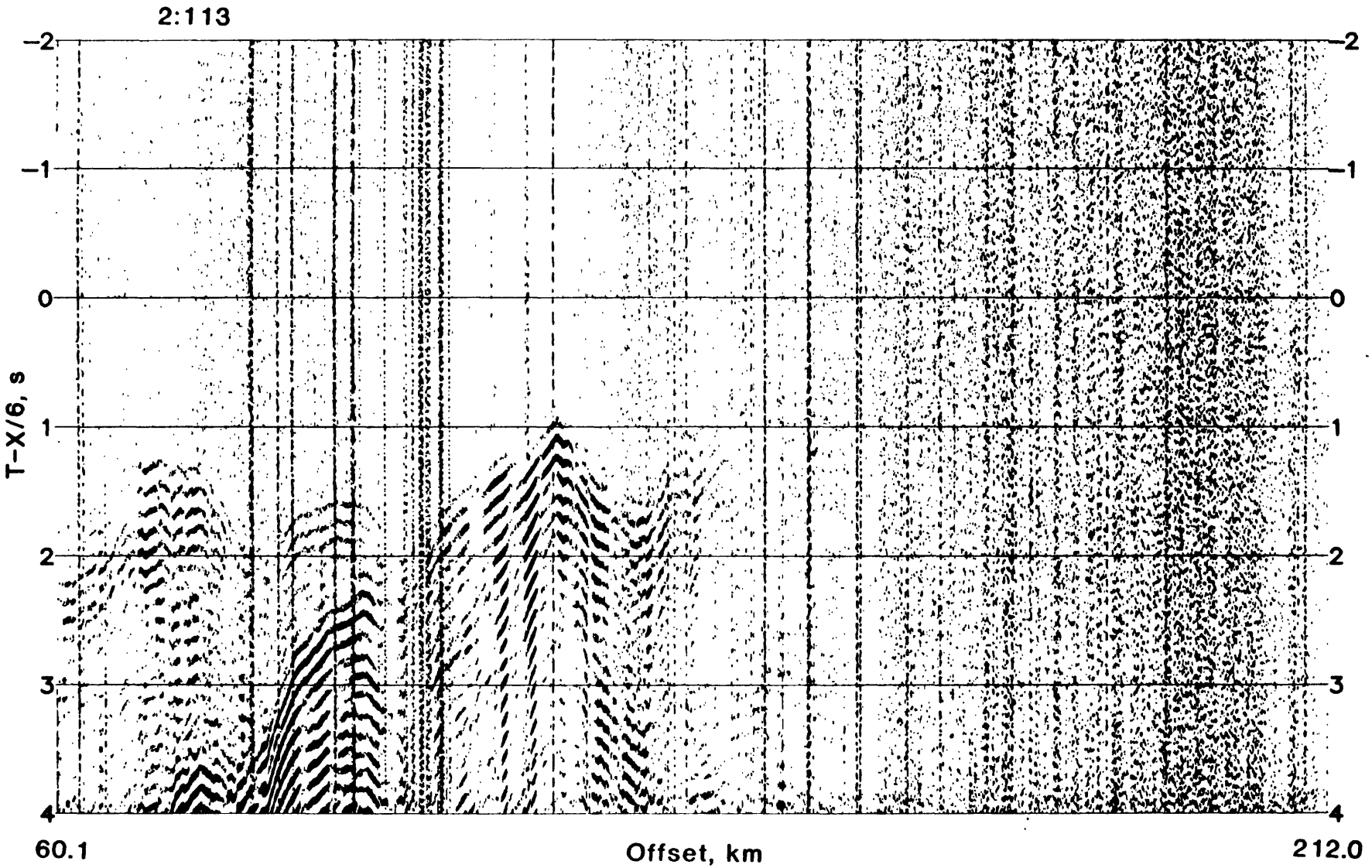

Figure 73. Stacked common receiver gather 113 for shots along LARSE air gun Line 2, reduced at 6 km/s.

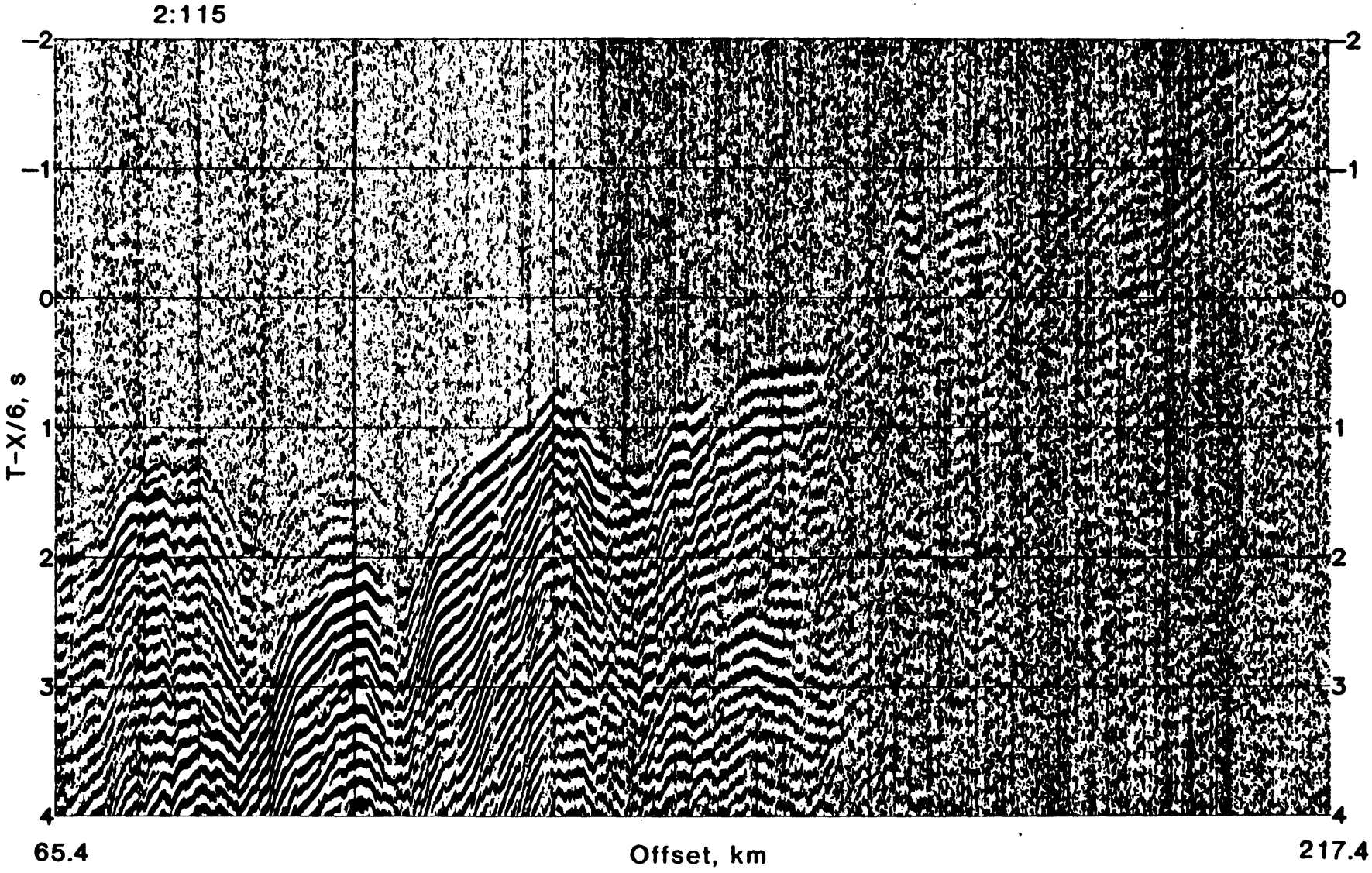

Figure 74. Stacked common receiver gather 115 for shots along LARSE air gun Line 2, reduced at 6 km/s.

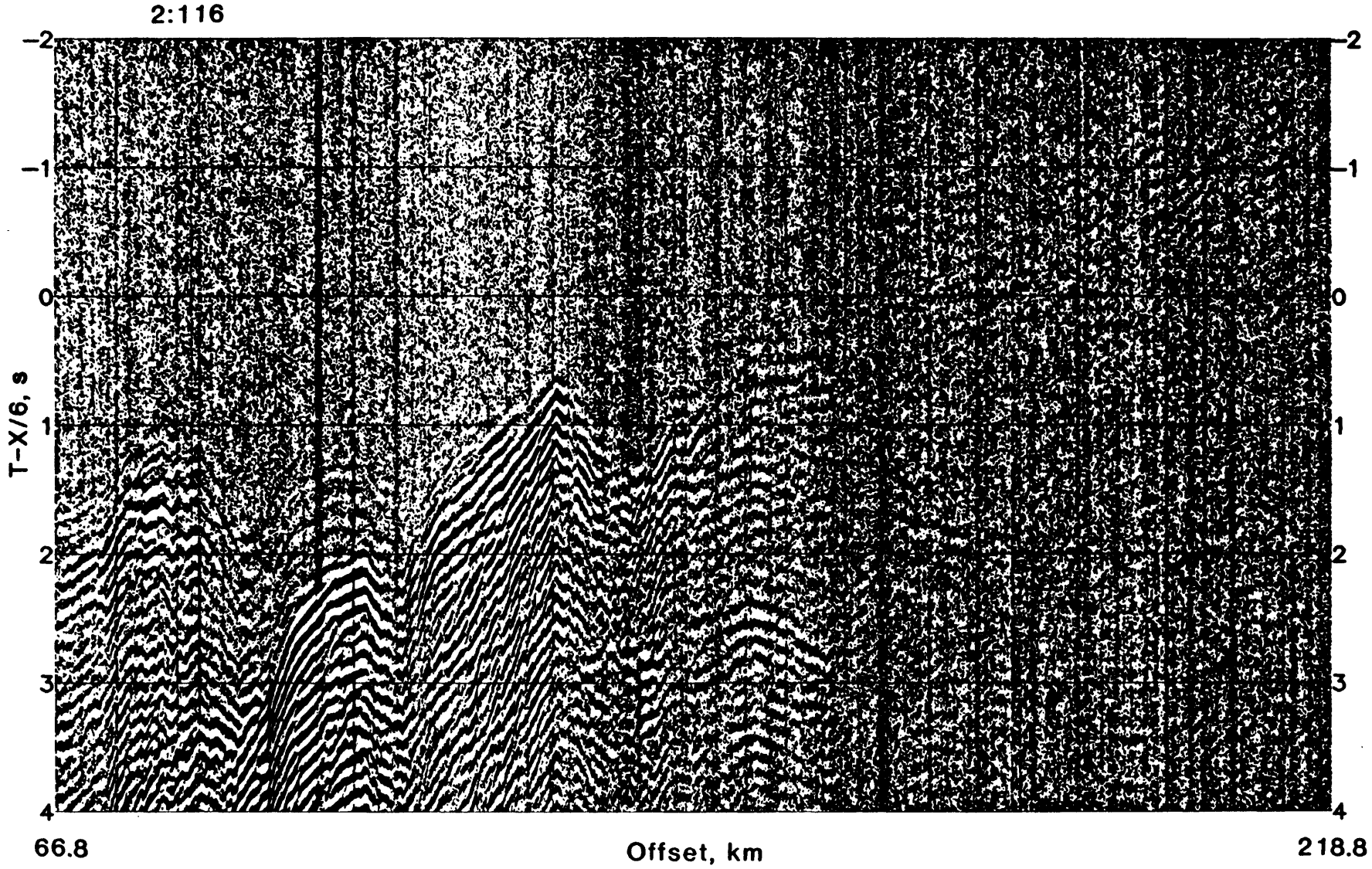

Figure 75. Stacked common receiver gather 116 for shots along LARSE air gun Line 2, reduced at 6 km/s.

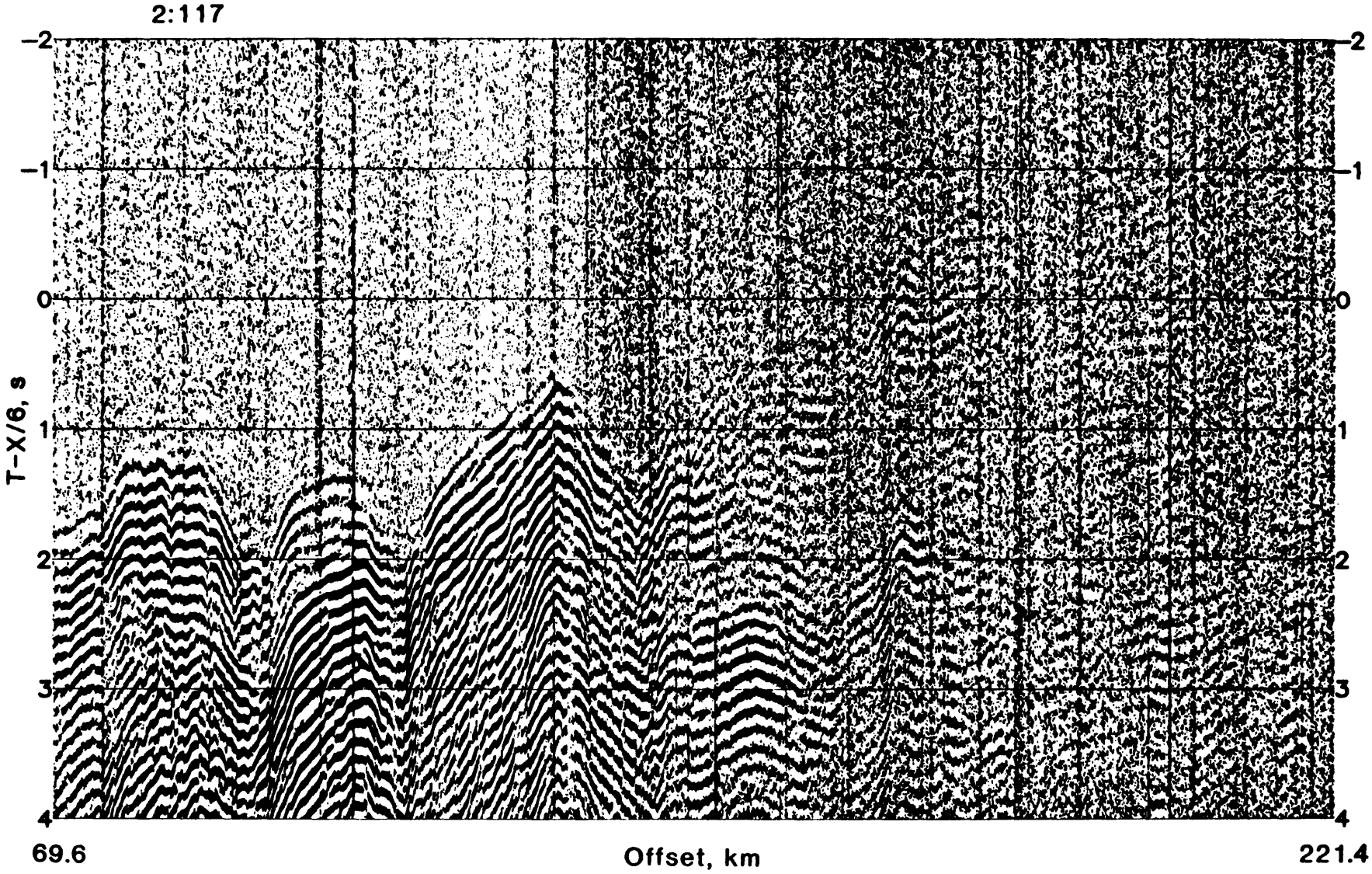

Figure 76. Stacked common receiver gather 117 for shots along LARSE air gun Line 2, reduced at 6 km/s.

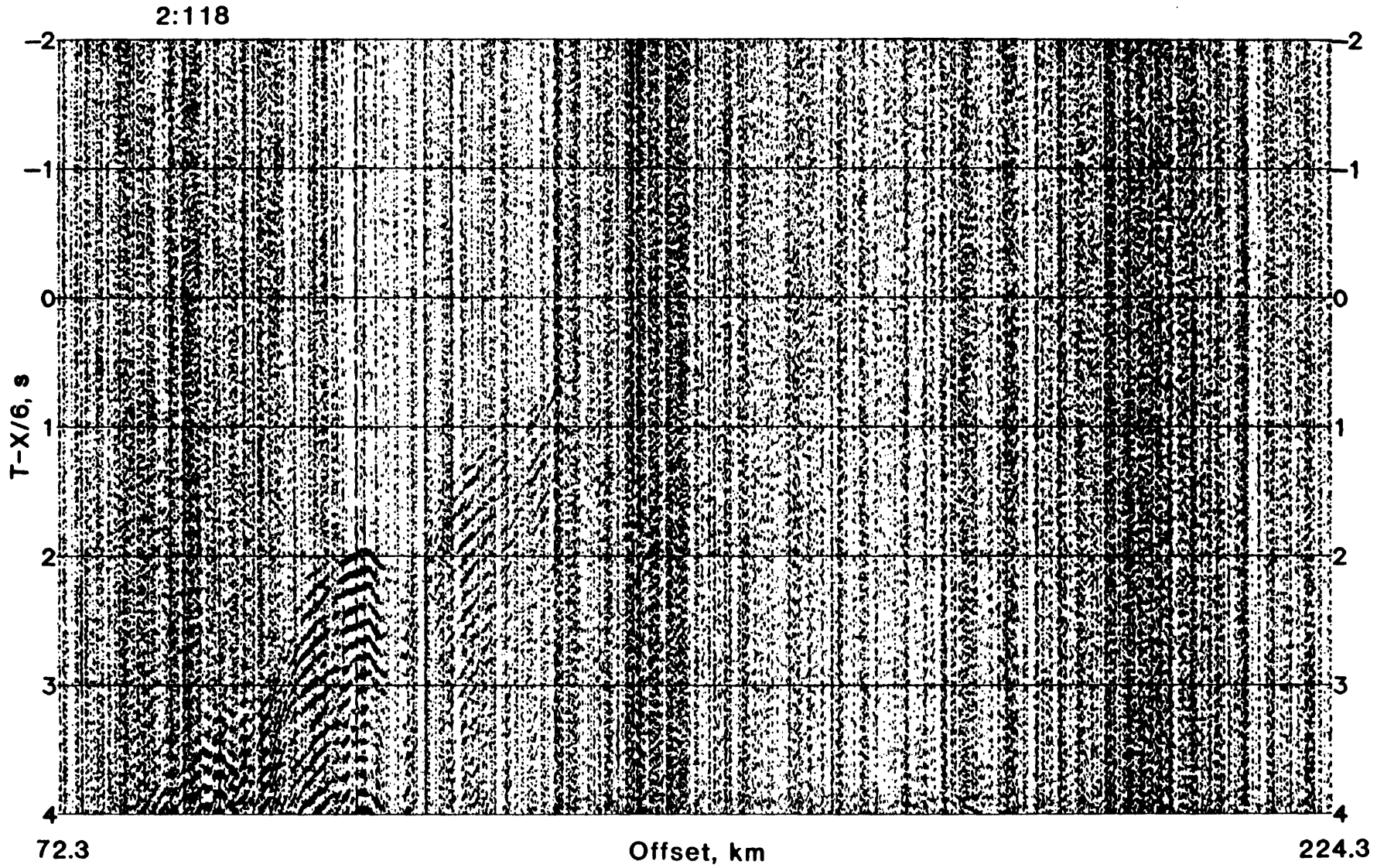

Figure 77. Stacked common receiver gather 118 for shots along LARSE air gun Line 2, reduced at 6 km/s.

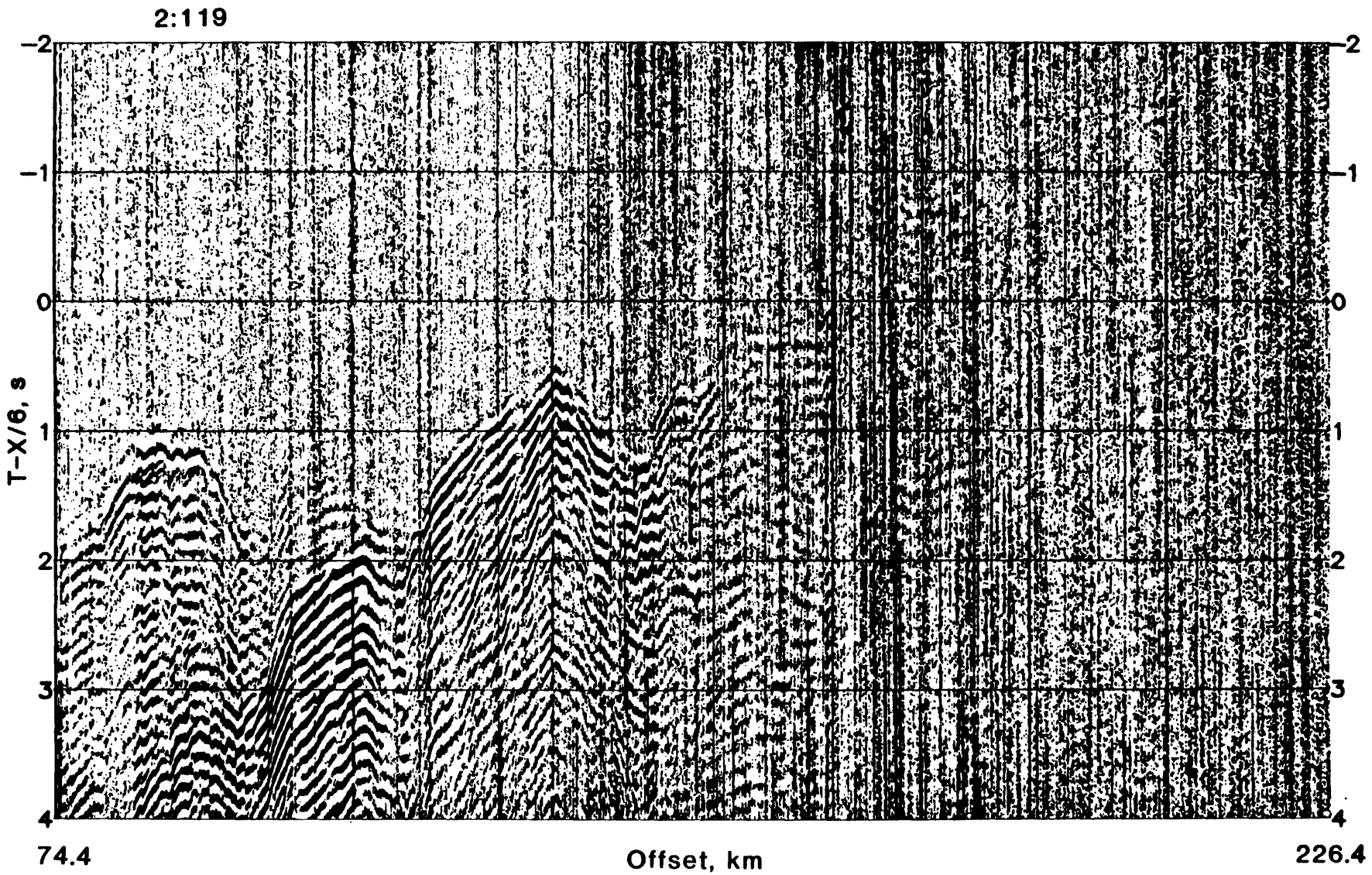

Figure 78. Stacked common receiver gather 119 for shots along LARSE air gun Line 2, reduced at 6 km/s.

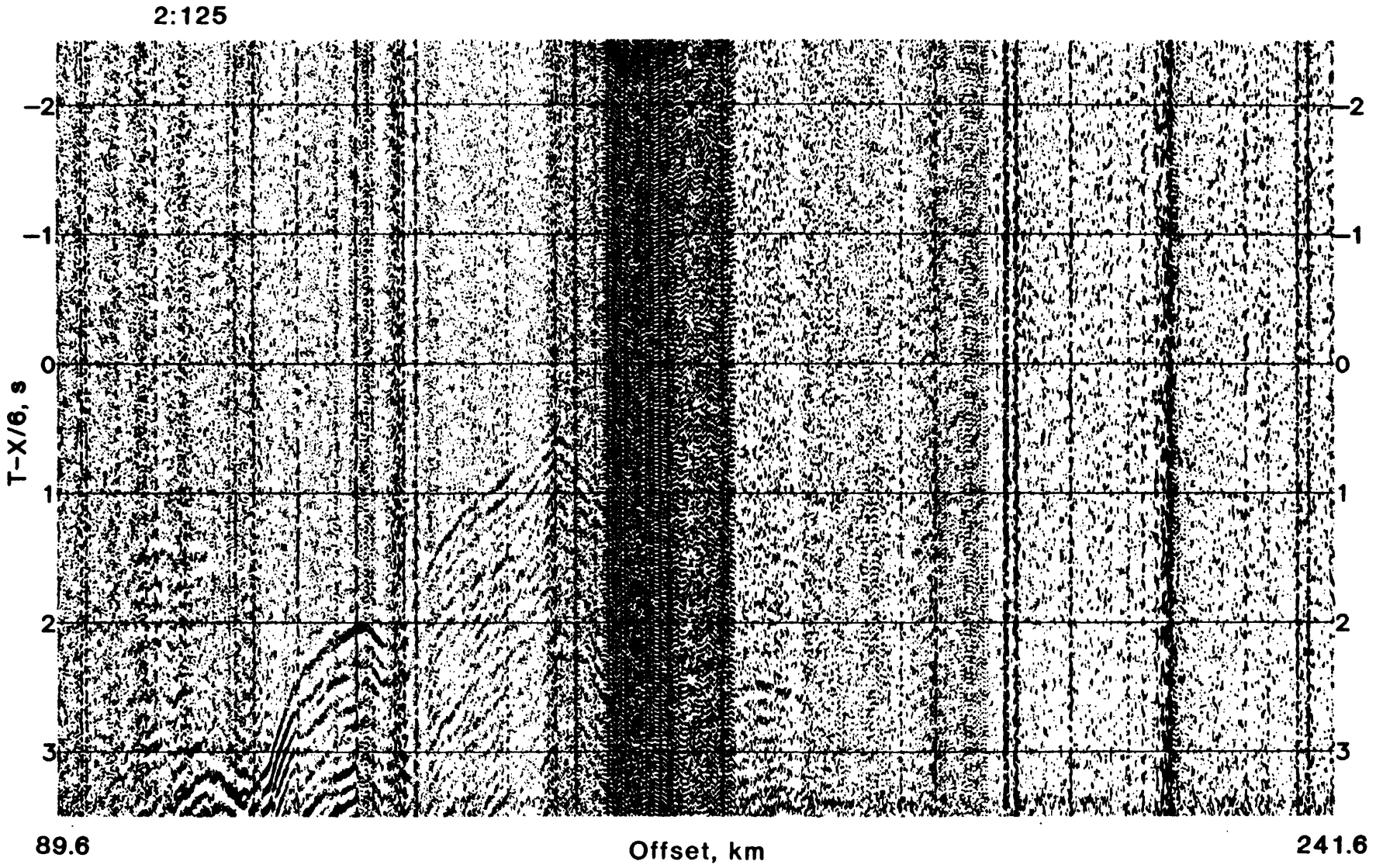

Figure 79. Stacked common receiver gather 125 for shots along LARSE air gun Line 2, reduced at 6 km/s.

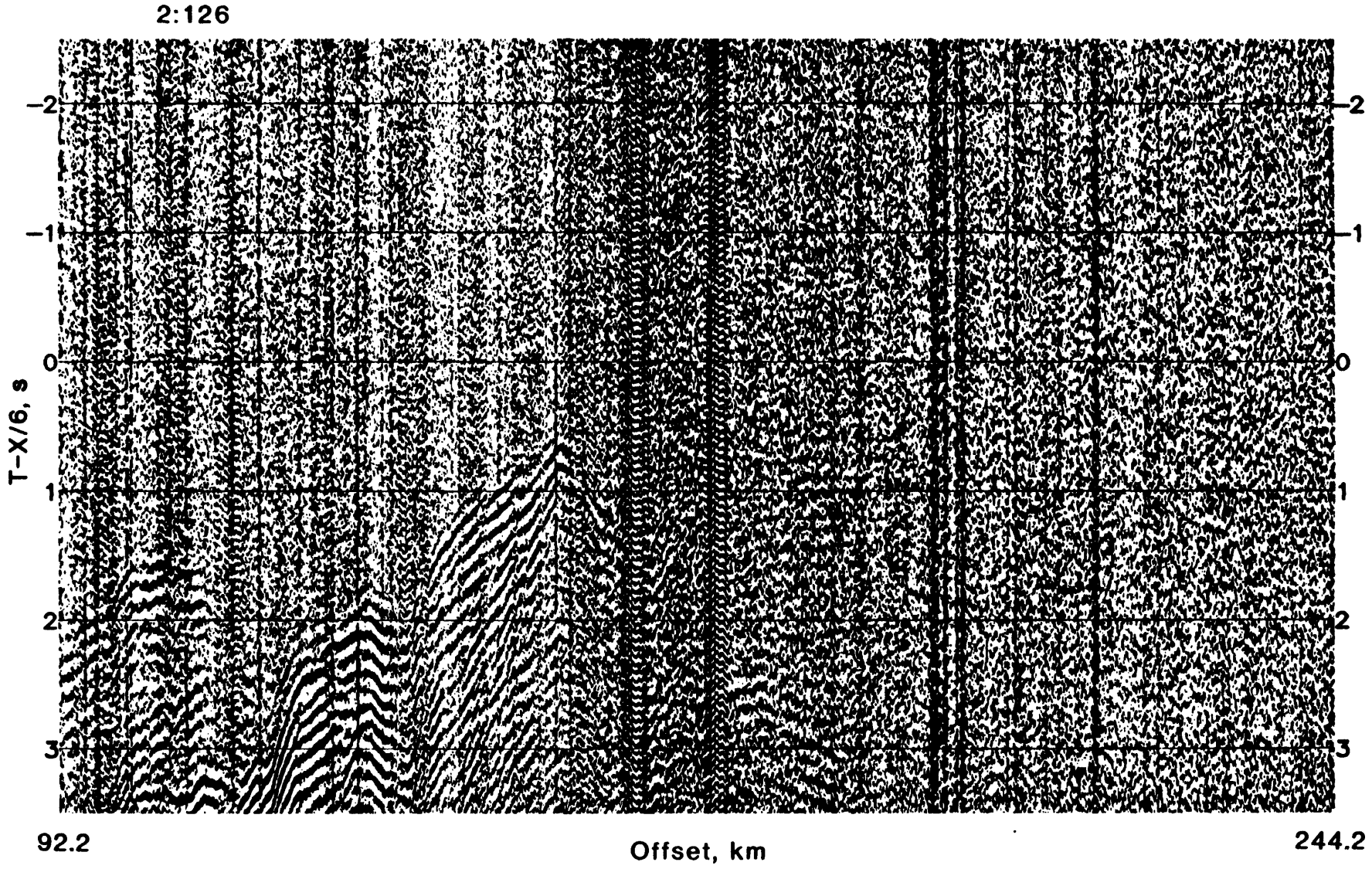

Figure 80. Stacked common receiver gather 126 for shots along LARSE air gun Line 2, reduced at 6 km/s.

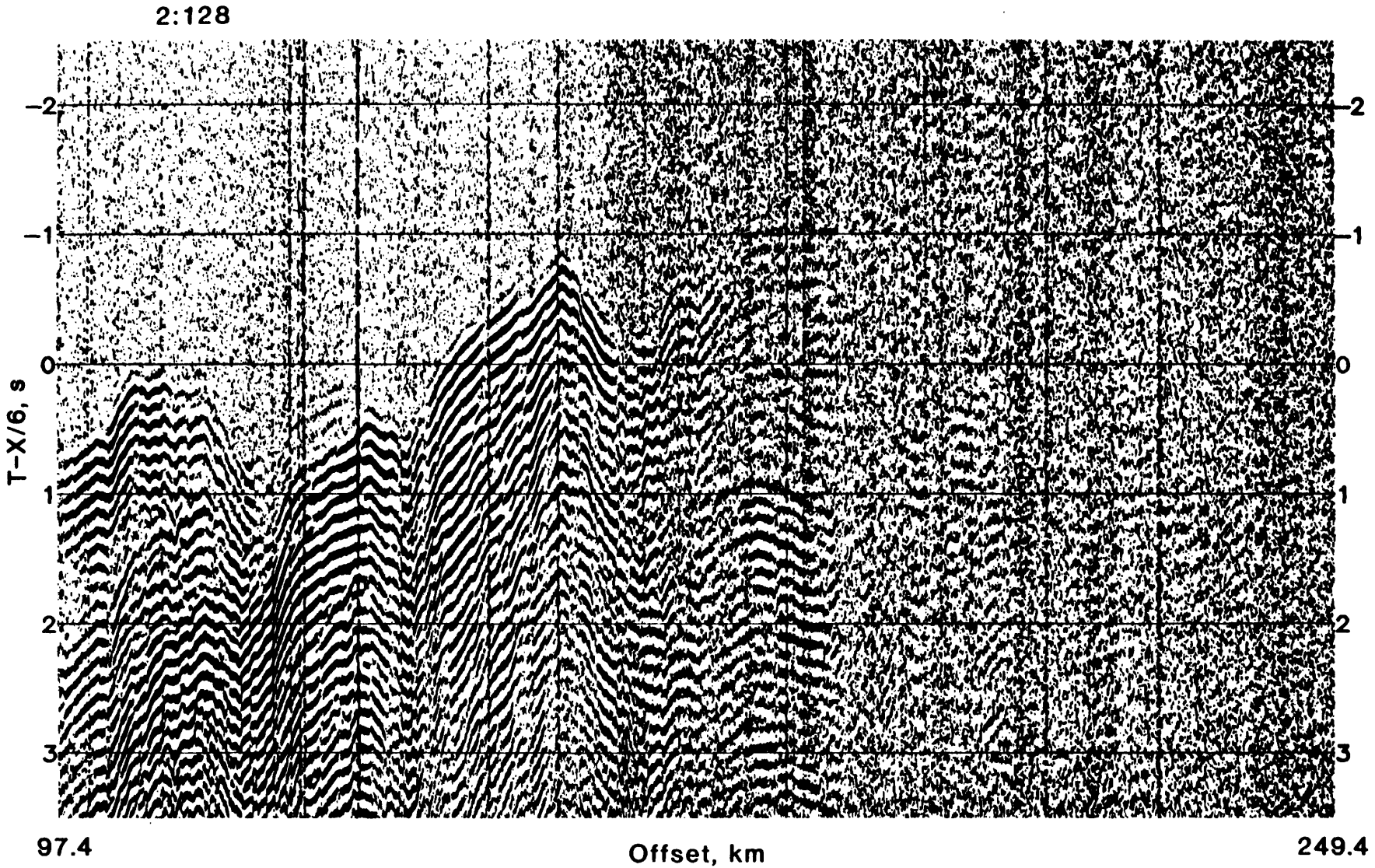

Figure 81. Stacked common receiver gather 128 for shots along LARSE air gun Line 2, reduced at 6 km/s.

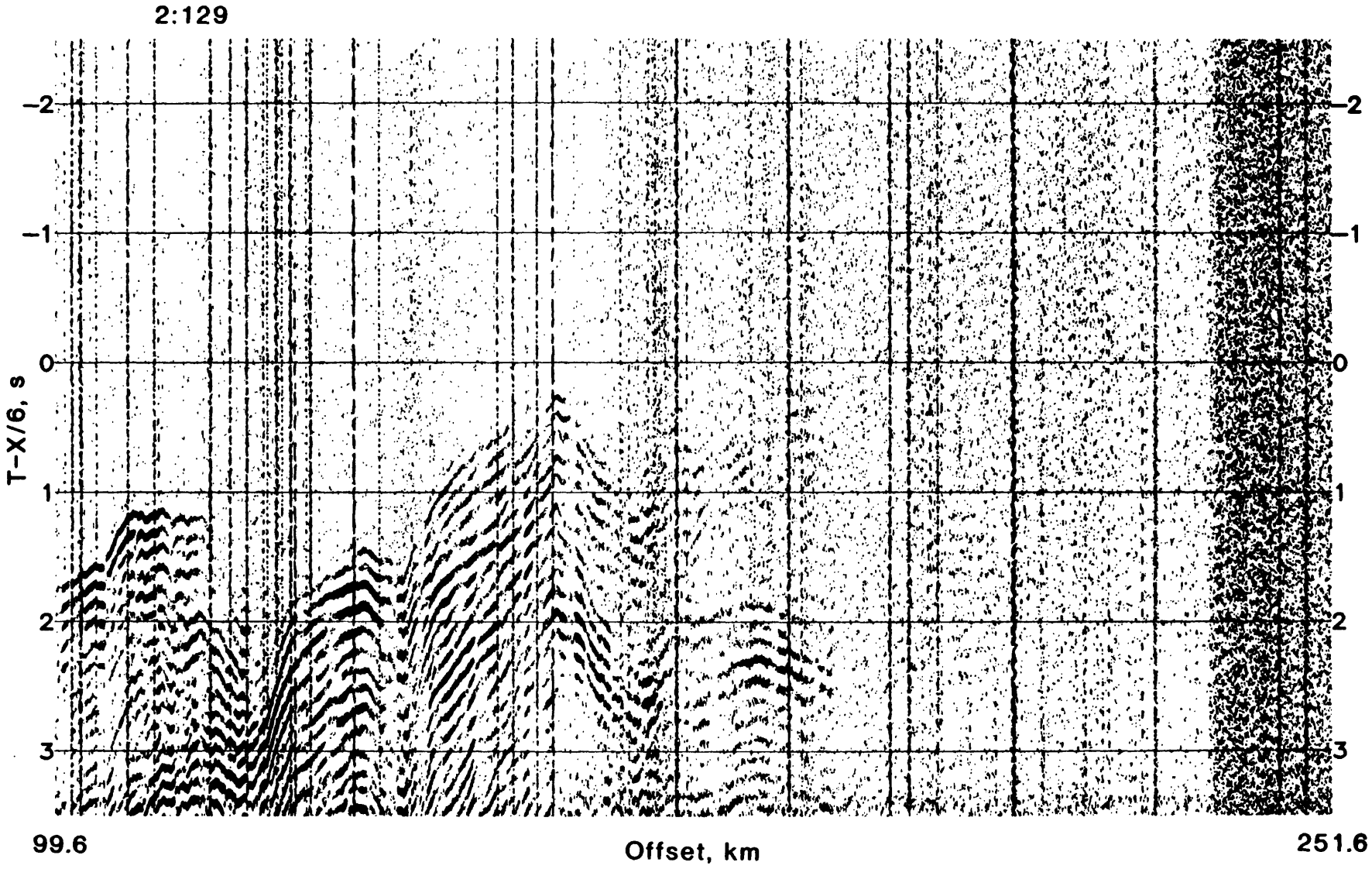

Figure 82. Stacked common receiver gather 129 for shots along LARSE air gun Line 2, reduced at 6 km/s.

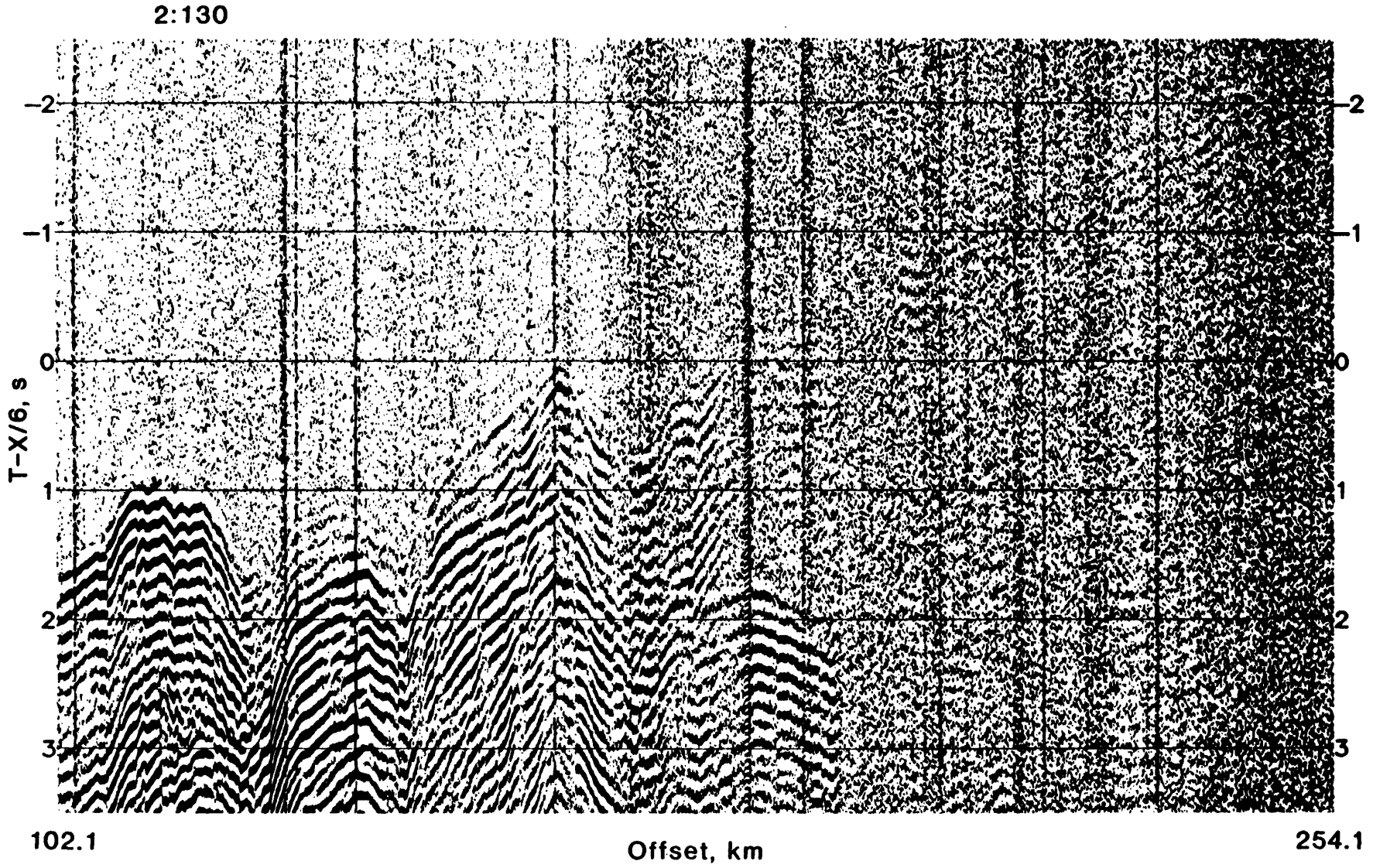

Figure 83. Stacked common receiver gather 130 for shots along LARSE air gun Line 2, reduced at 6 km/s.

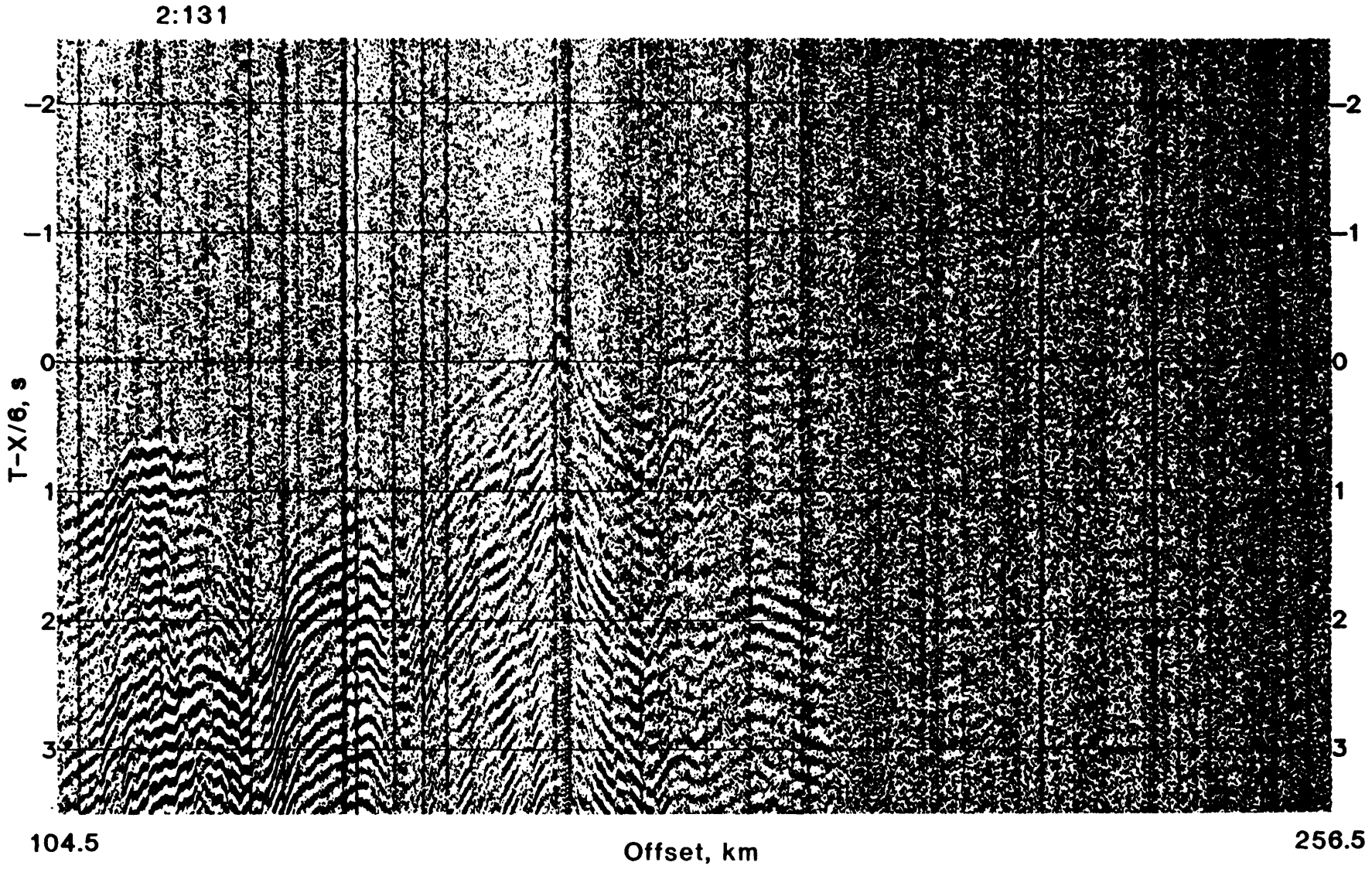

Figure 84. Stacked common receiver gather 131 for shots along LARSE air gun Line 2, reduced at 6 km/s.

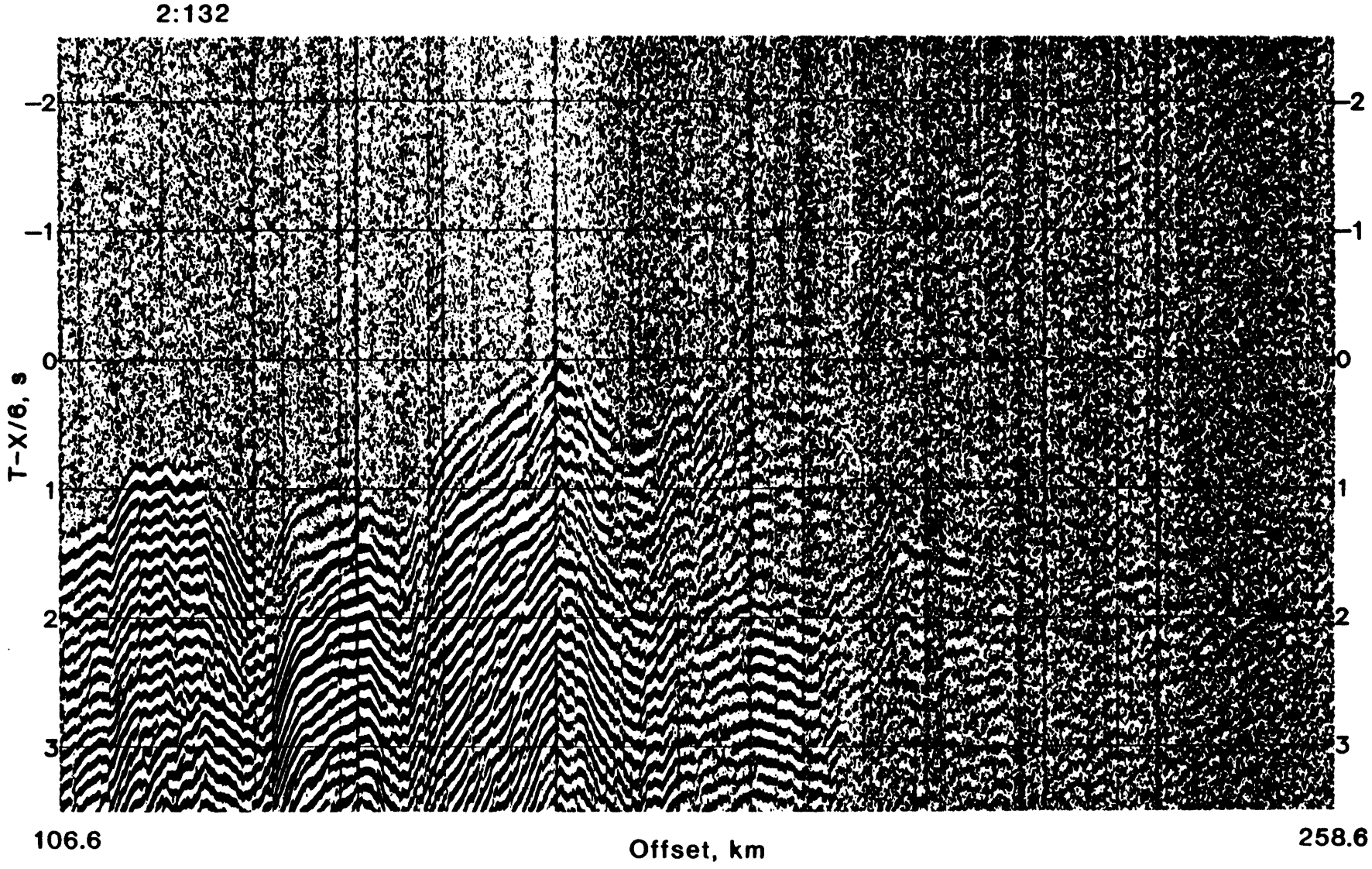

Figure 85. Stacked common receiver gather 132 for shots along LARSE air gun Line 2, reduced at 6 km/s.

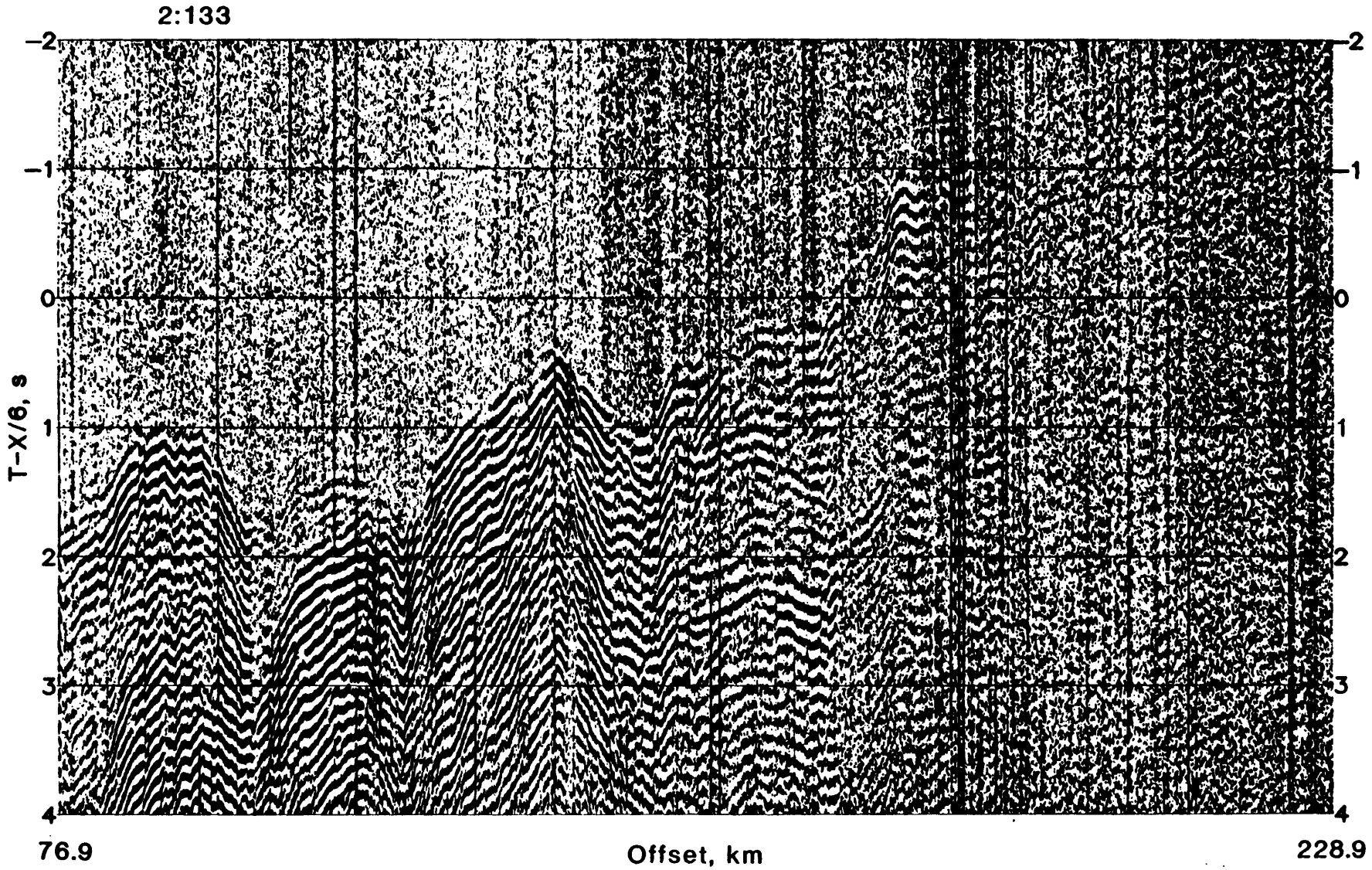

Figure 86. Stacked common receiver gather 133 for shots along LARSE air gun Line 2, reduced at 6 km/s.

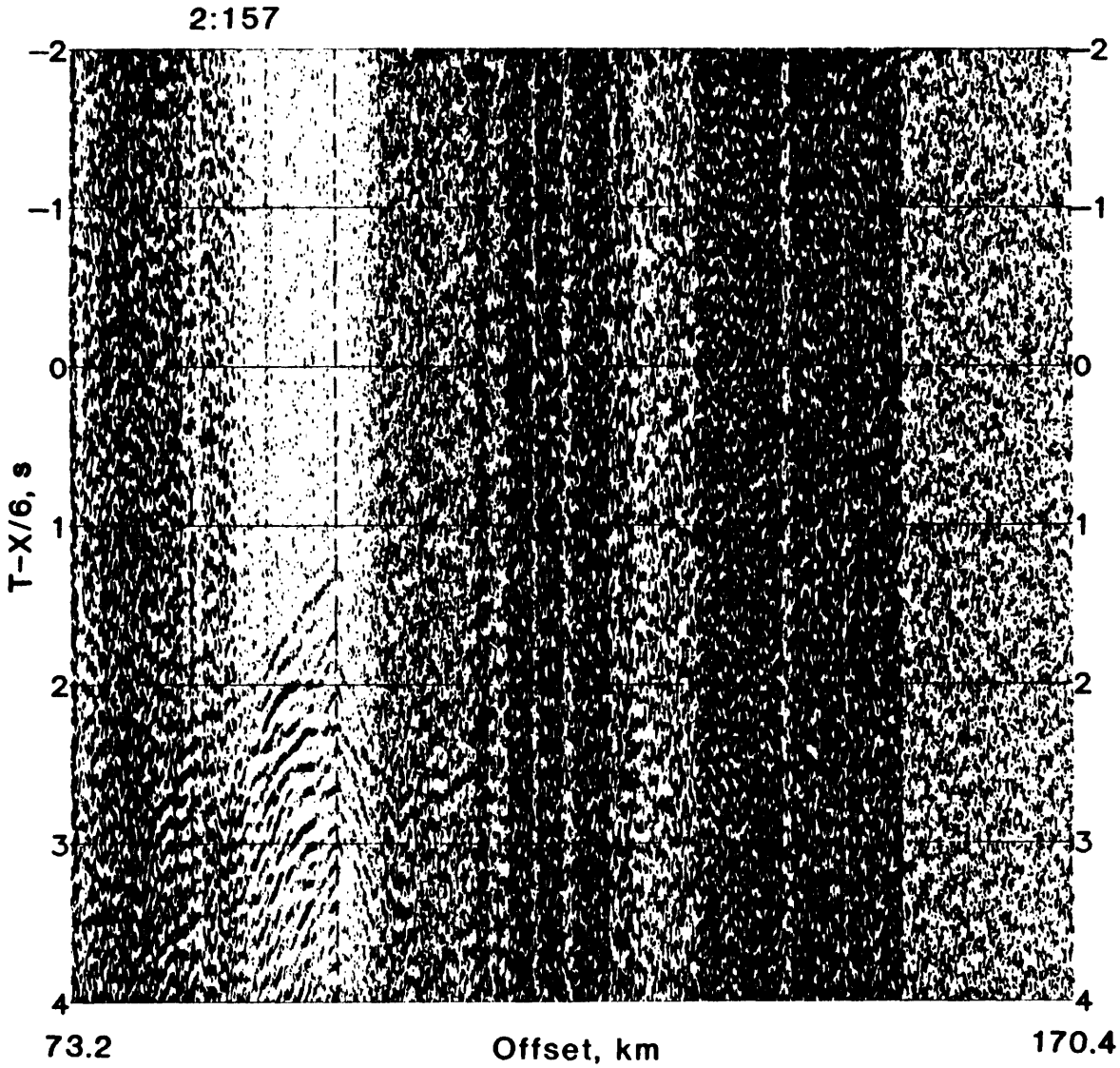

Figure 87. Stacked common receiver gather 157 for shots along LARSE air gun Line 2, reduced at 6 km/s.

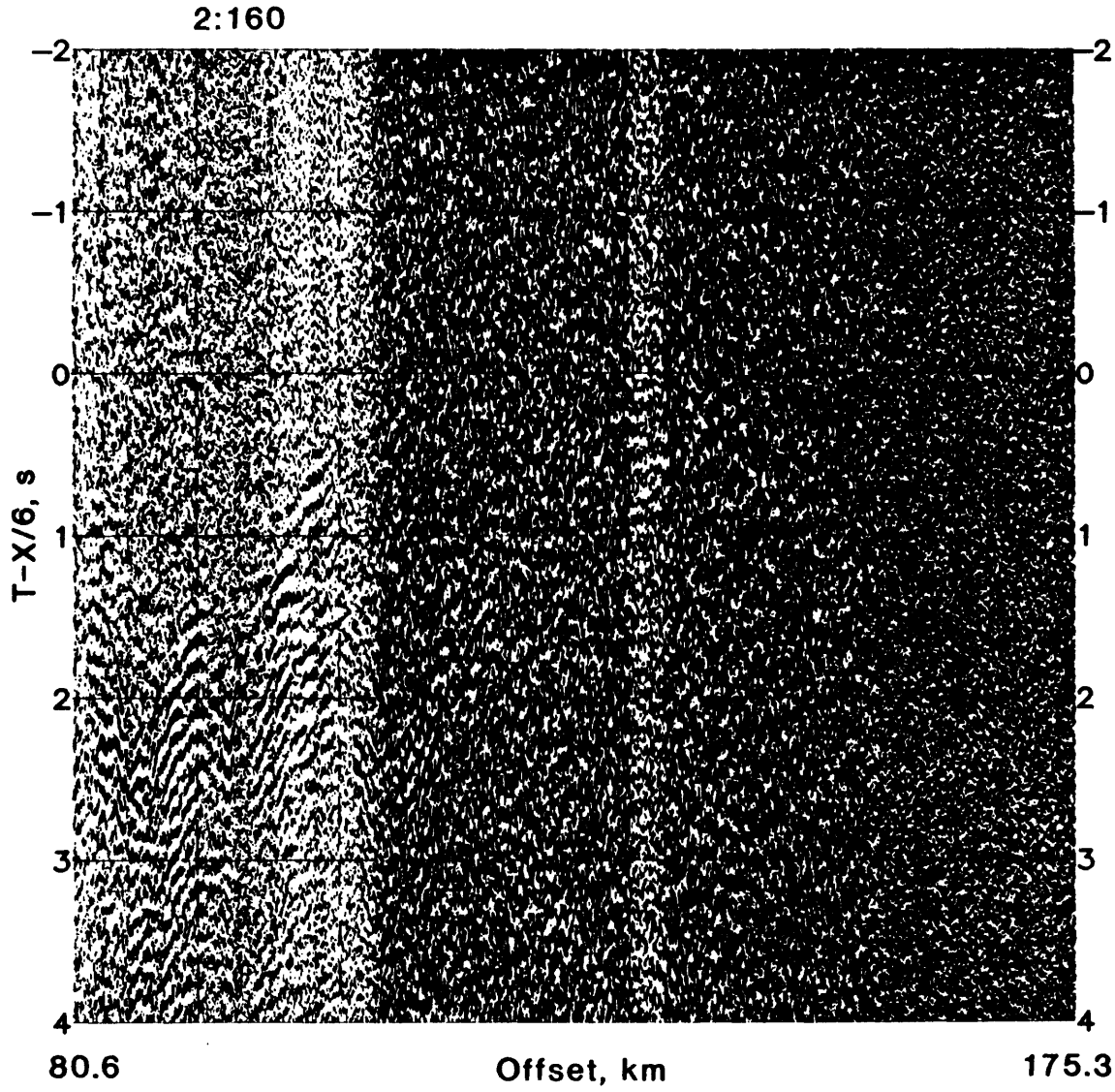

Figure 88. Stacked common receiver gather 160 for shots along LARSE air gun Line 2, reduced at 6 km/s.

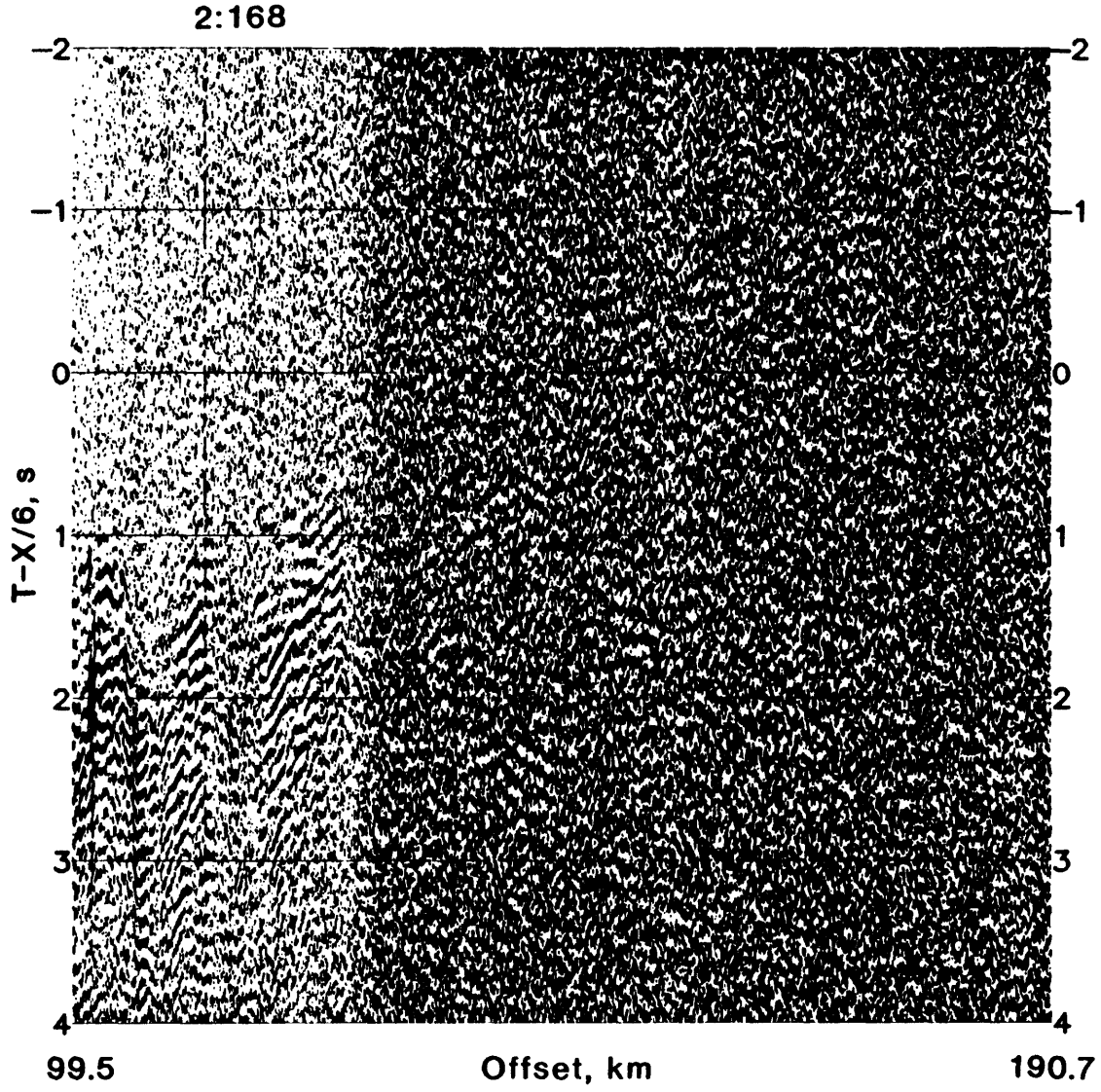

Figure 89. Stacked common receiver gather 168 for shots along LARSE air gun Line 2, reduced at 6 km/s.

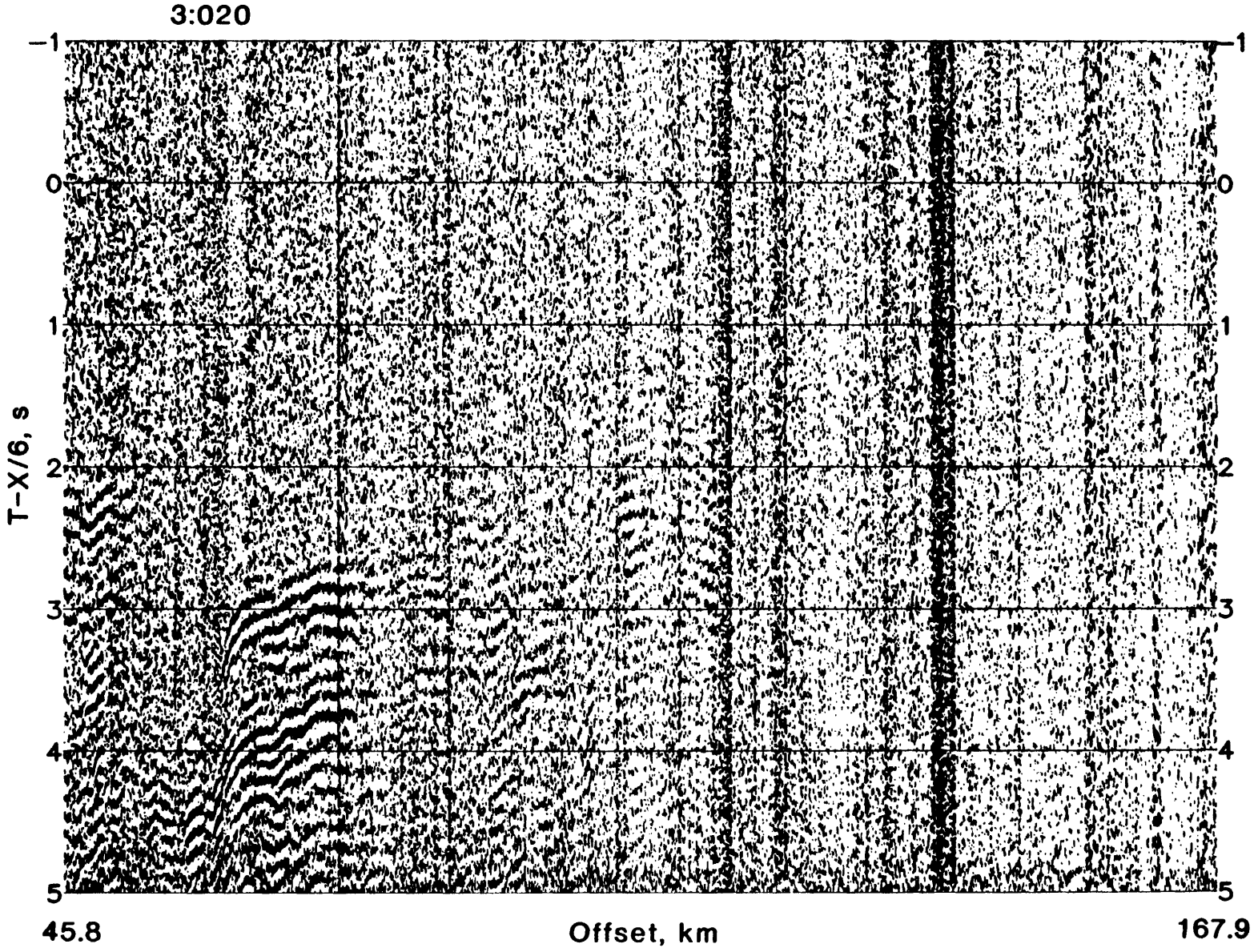

Figure 90. Stacked common receiver gather 020 for shots along LARSE air gun Line 3, reduced at 6 km/s.

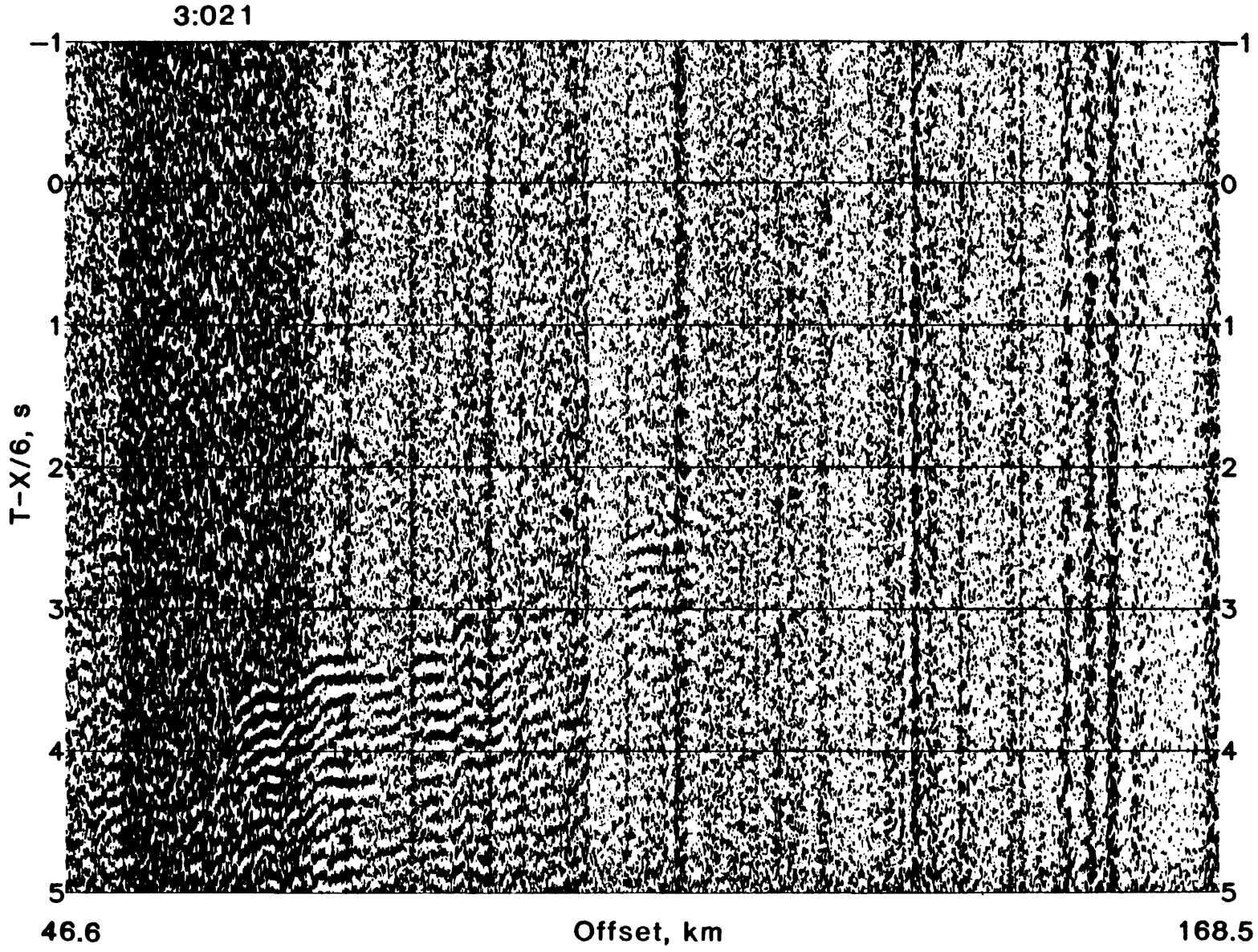

Figure 91. Stacked common receiver gather 021 for shots along LARSE air gun Line 3, reduced at 6 km/s.

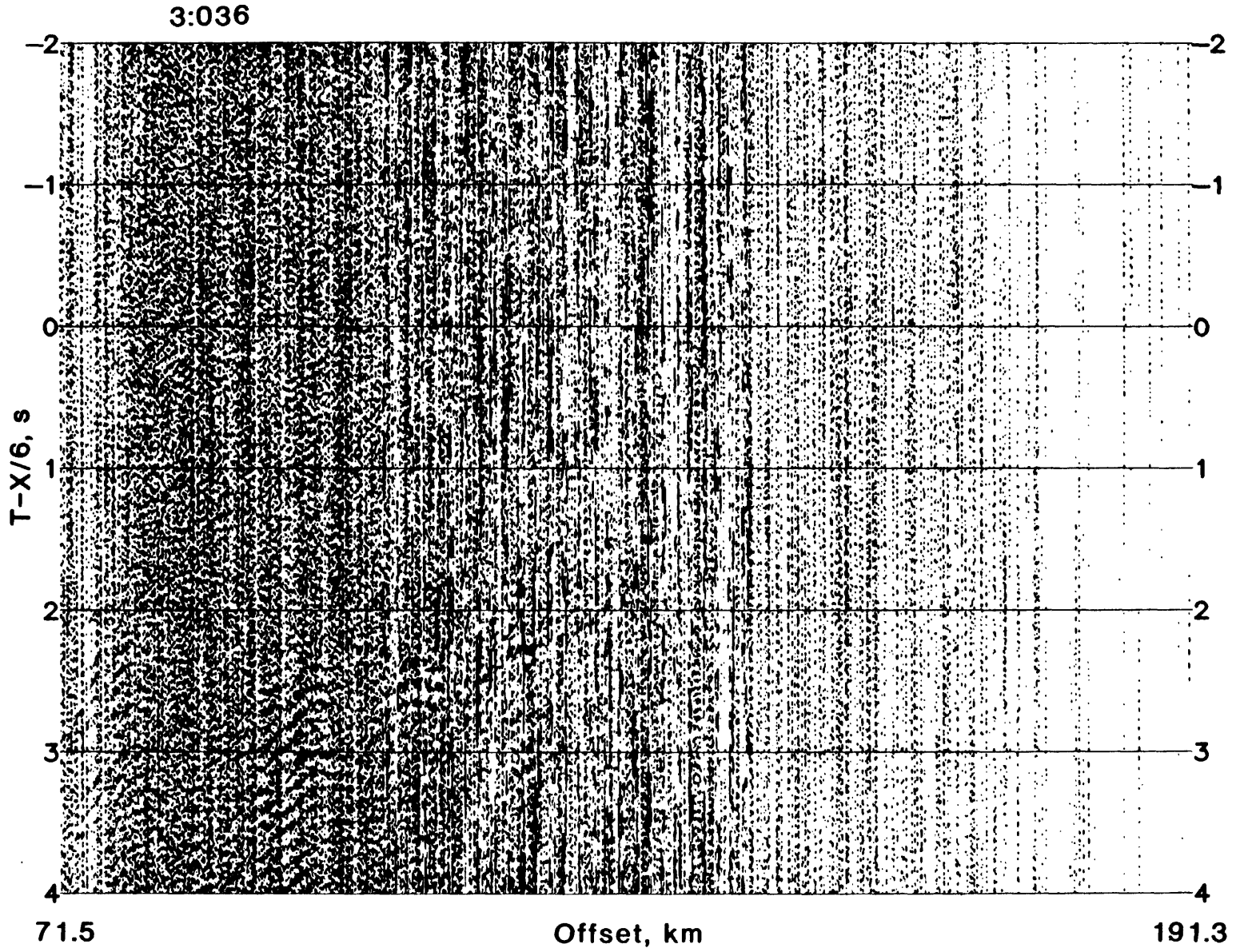

Figure 92. Stacked common receiver gather 036 for shots along LARSE air gun Line 3, reduced at 6 km/s.

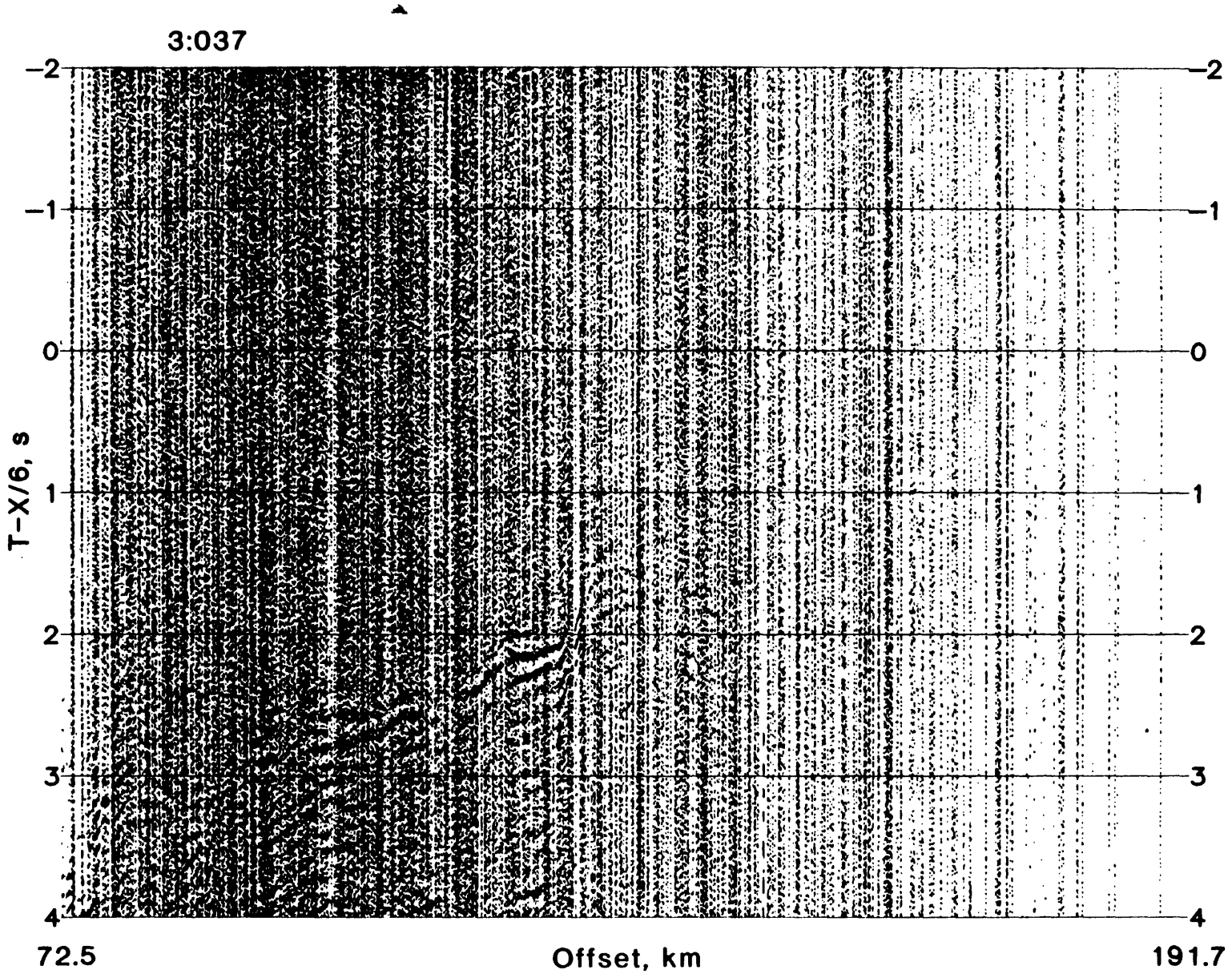

Figure 93. Stacked common receiver gather 037 for shots along LARSE air gun Line 3, reduced at 6 km/s.

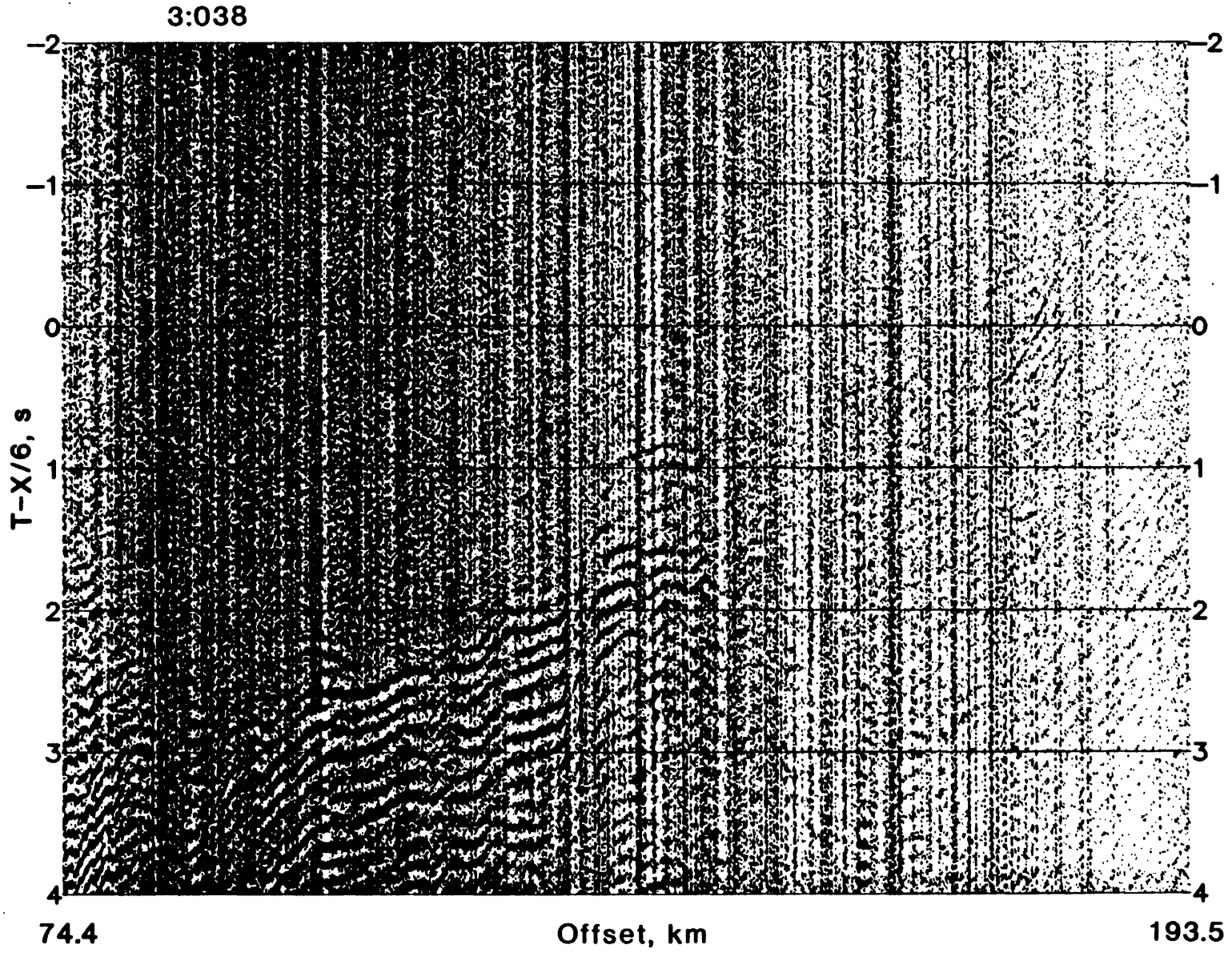

Figure 94. Stacked common receiver gather 038 for shots along LARSE air gun Line 3, reduced at 6 km/s.

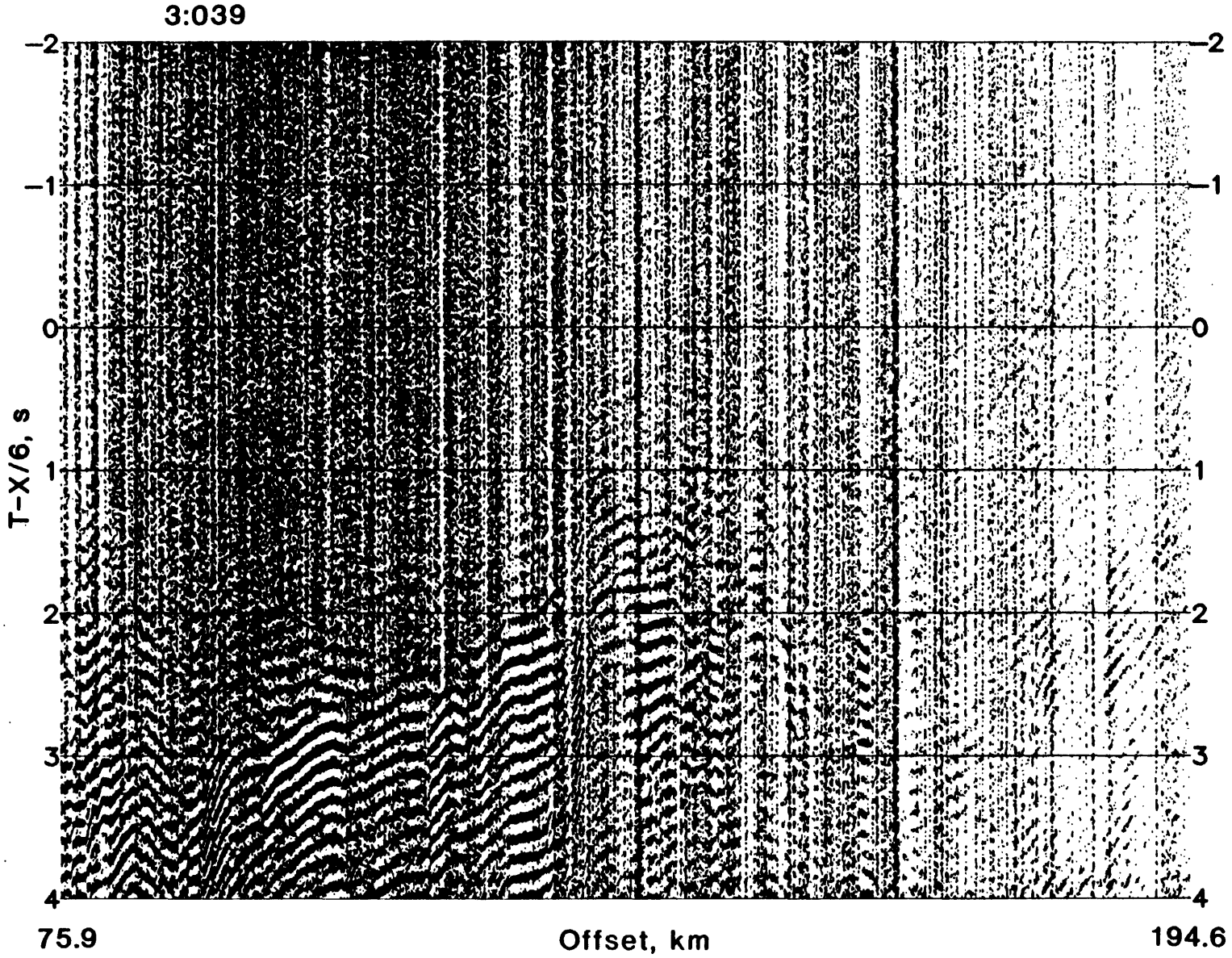

Figure 95. Stacked common receiver gather 039 for shots along LARSE air gun Line 3, reduced at 6 km/s.

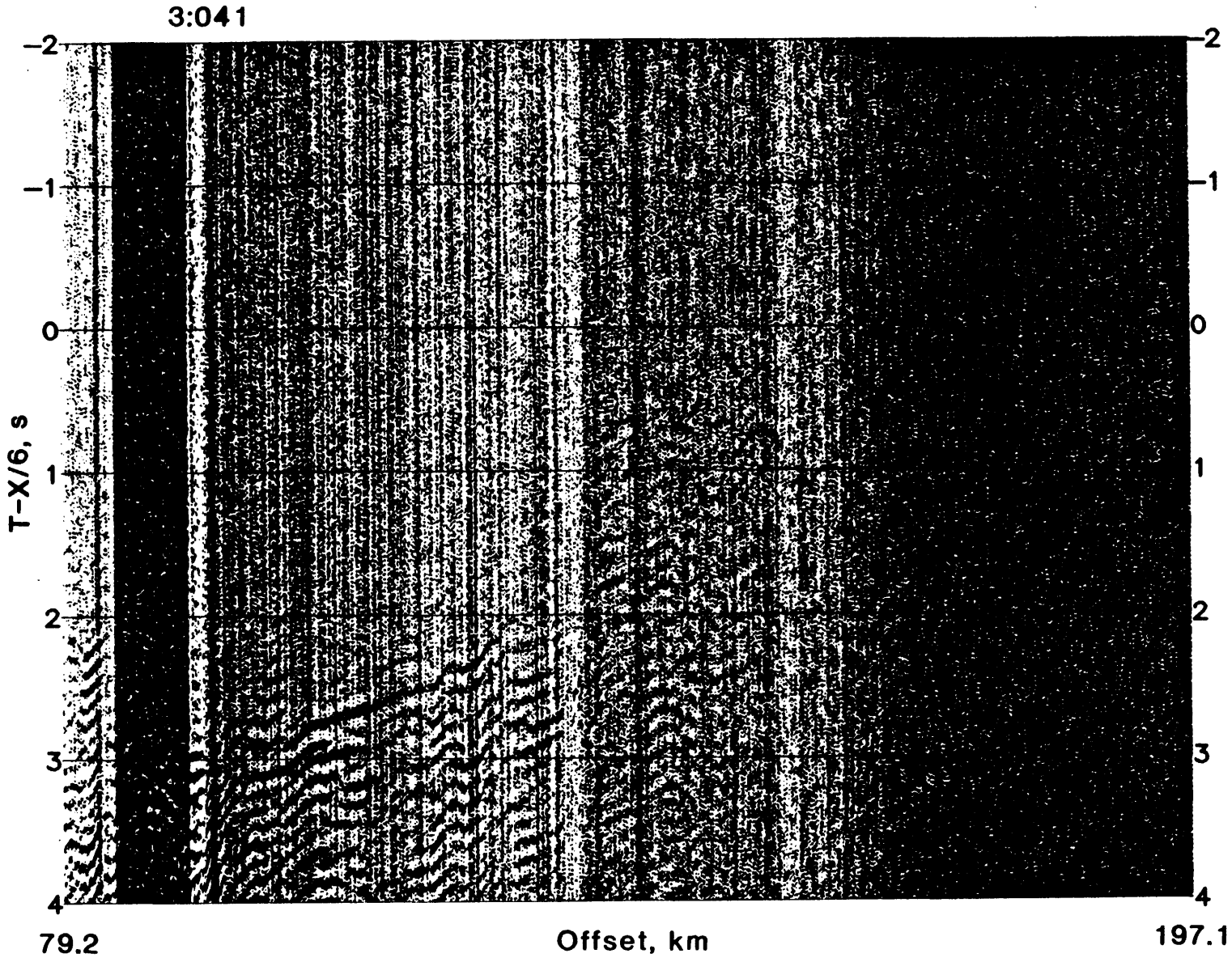

Figure 96. Stacked common receiver gather 041 for shots along LARSE air gun Line 3, reduced at 6 km/s.

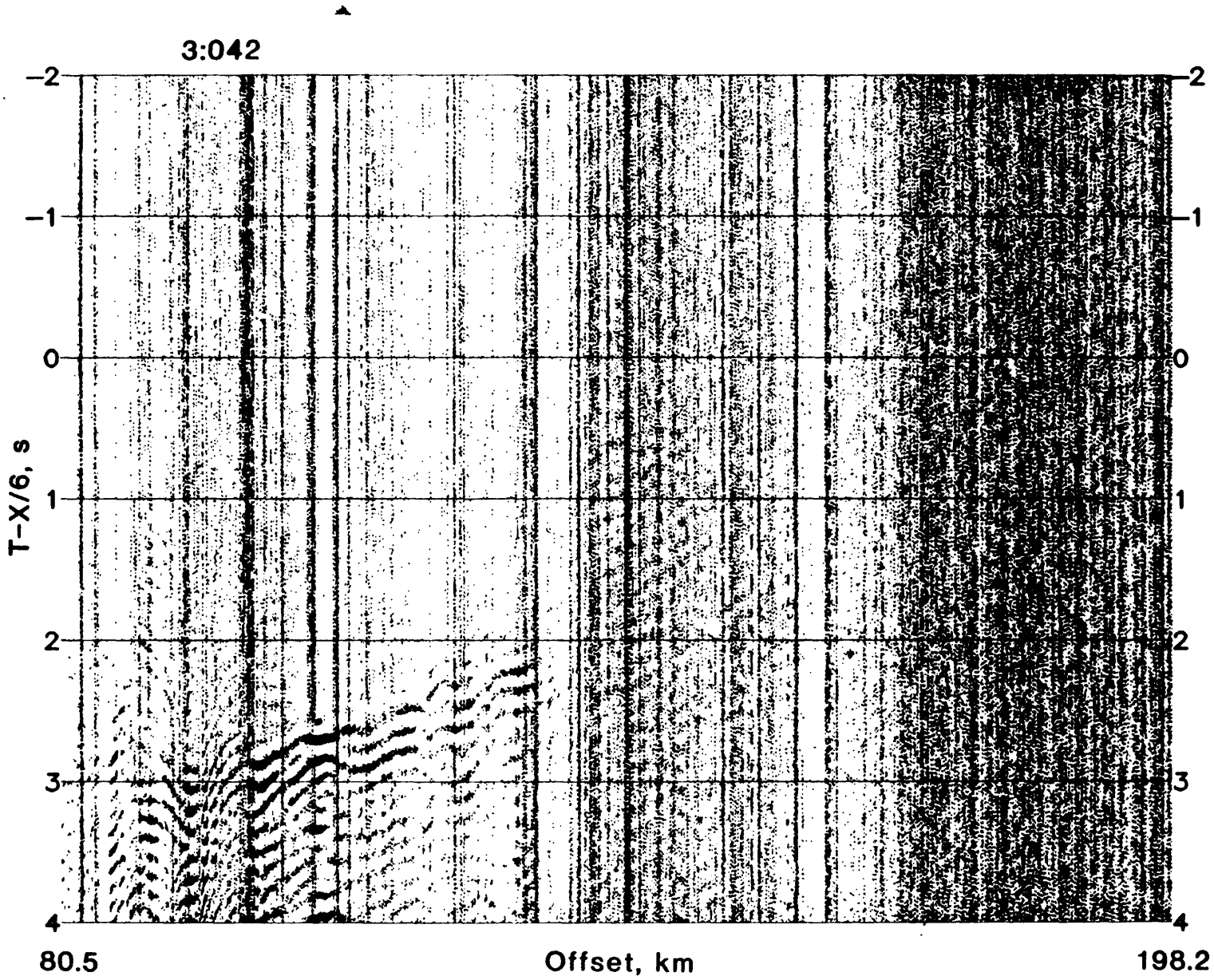

Figure 97. Stacked common receiver gather 042 for shots along LARSE air gun Line 3, reduced at 6 km/s.

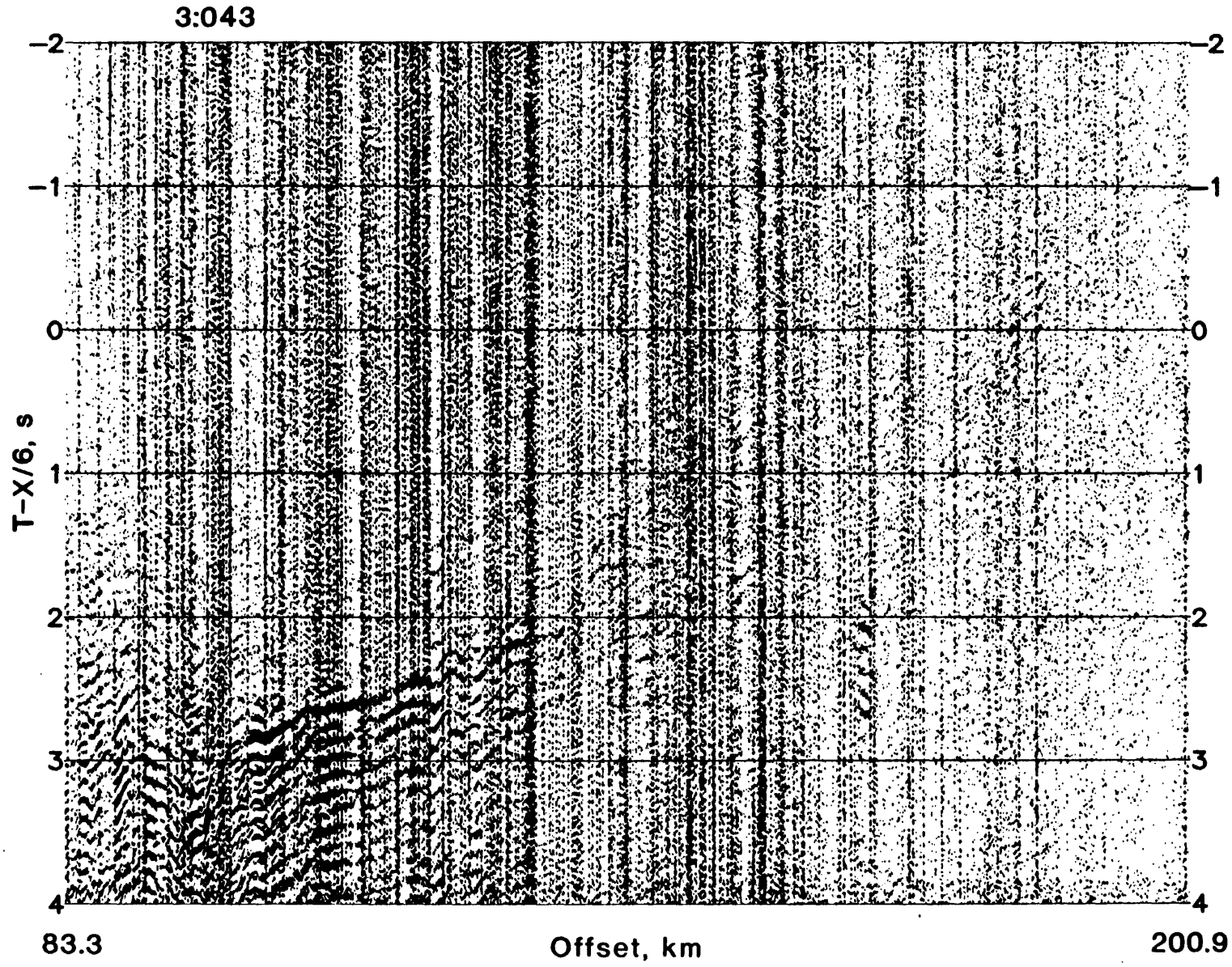

Figure 98. Stacked common receiver gather 043 for shots along LARSE air gun Line 3, reduced at 6 km/s.

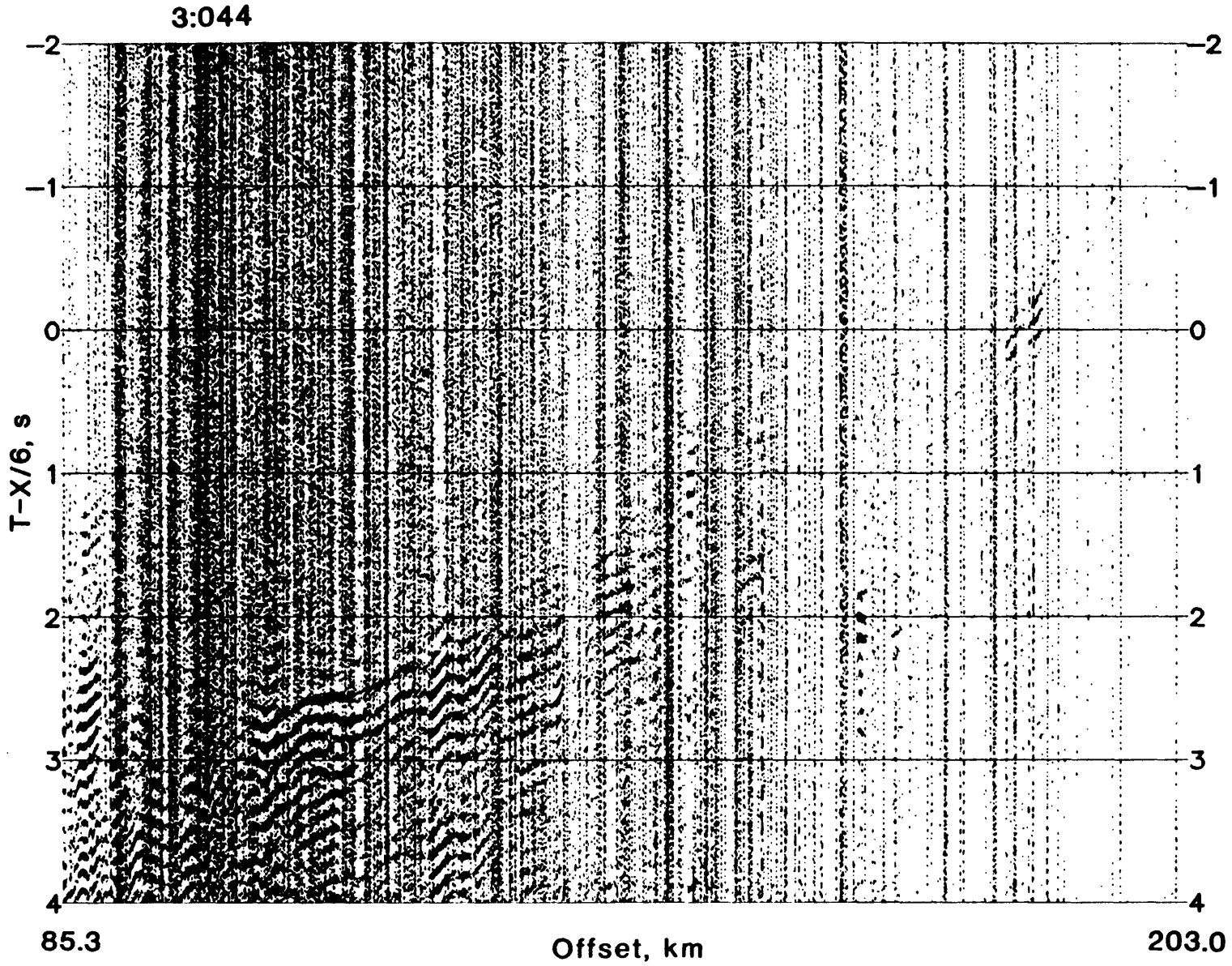

Figure 99. Stacked common receiver gather 044 for shots along LARSE air gun Line 3, reduced at 6 km/s.

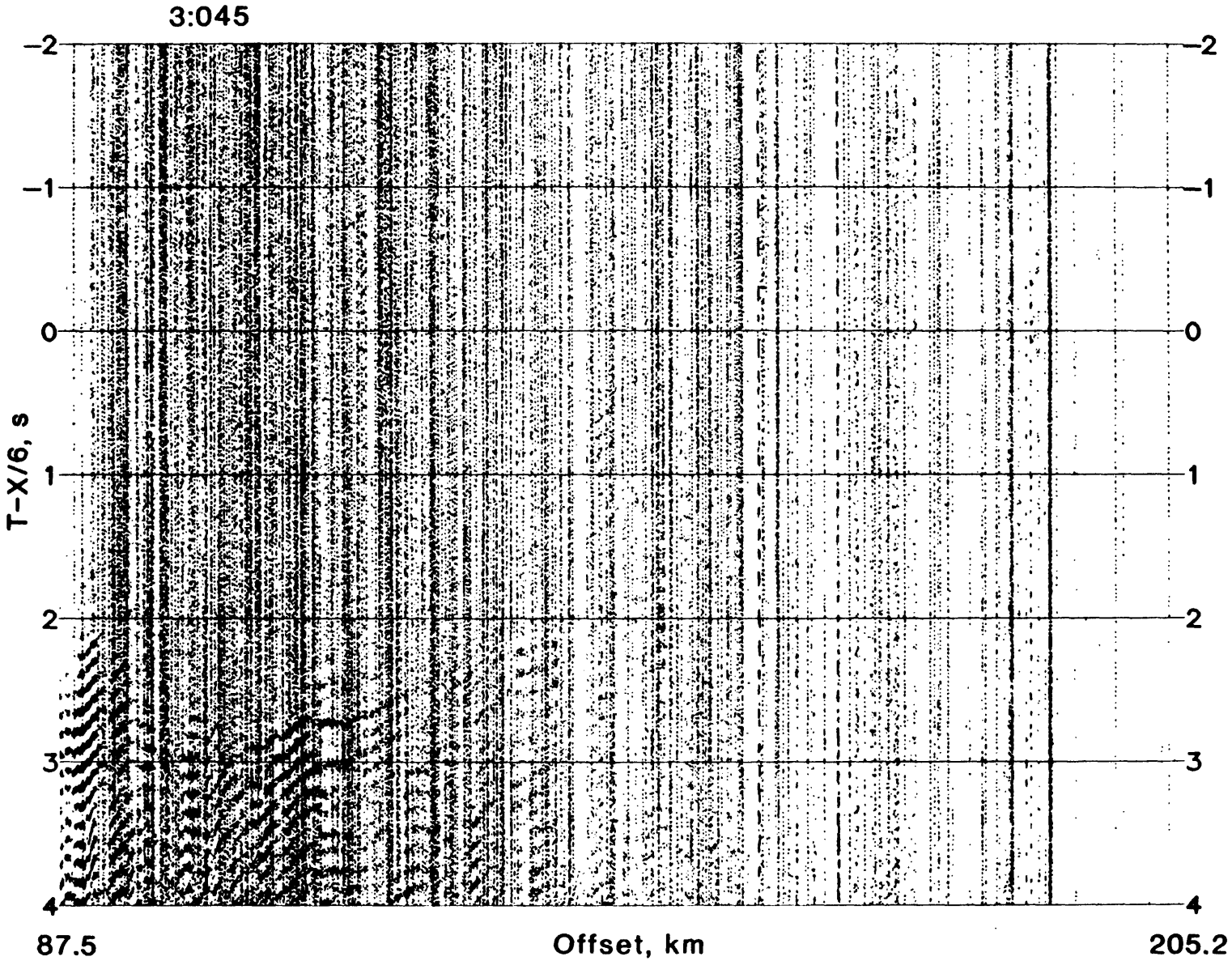

Figure 100. Stacked common receiver gather 045 for shots along LARSE air gun Line 3, reduced at 6 km/s.

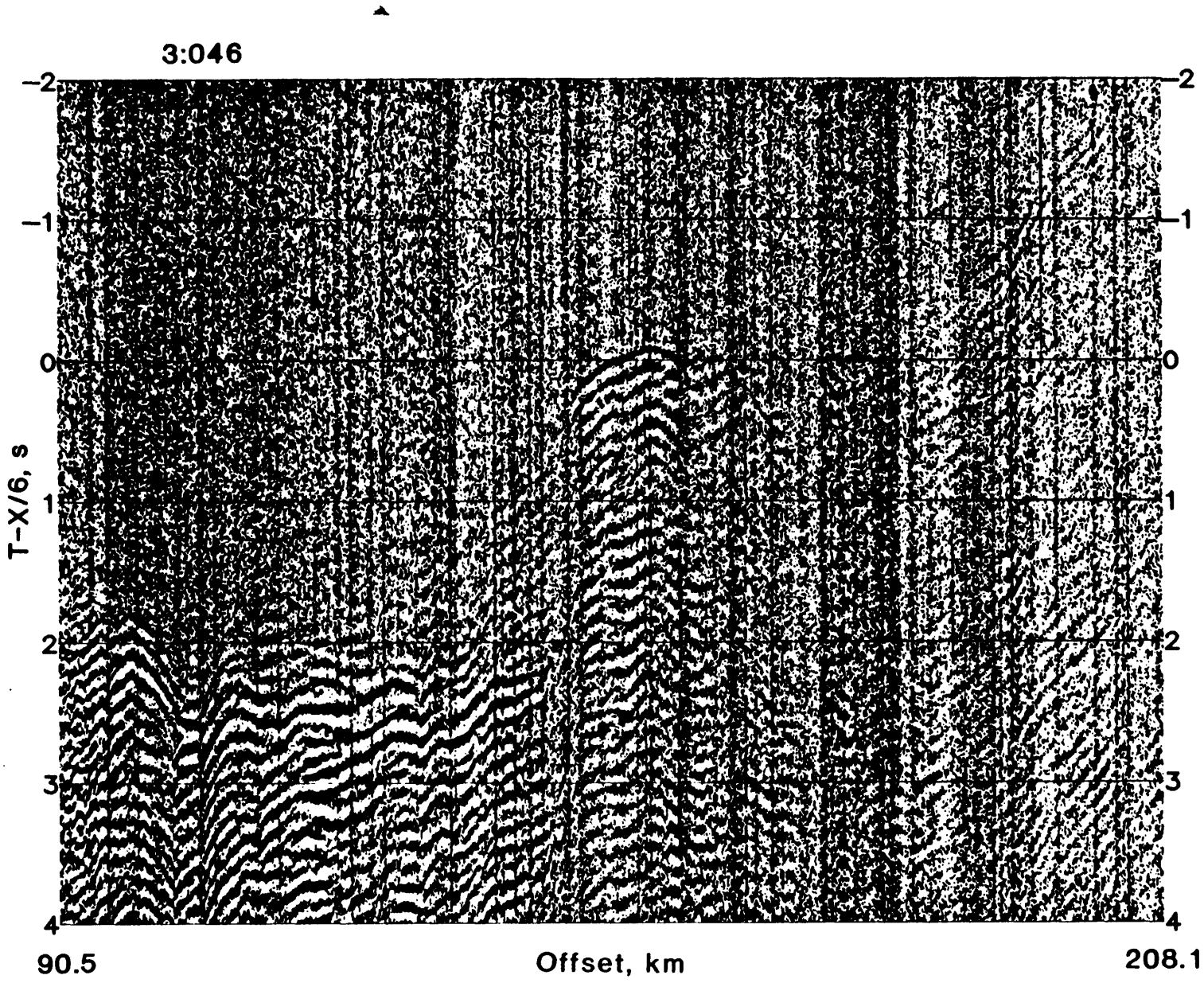

Figure 101. Stacked common receiver gather 046 for shots along LARSE air gun Line 3, reduced at 6 km/s.

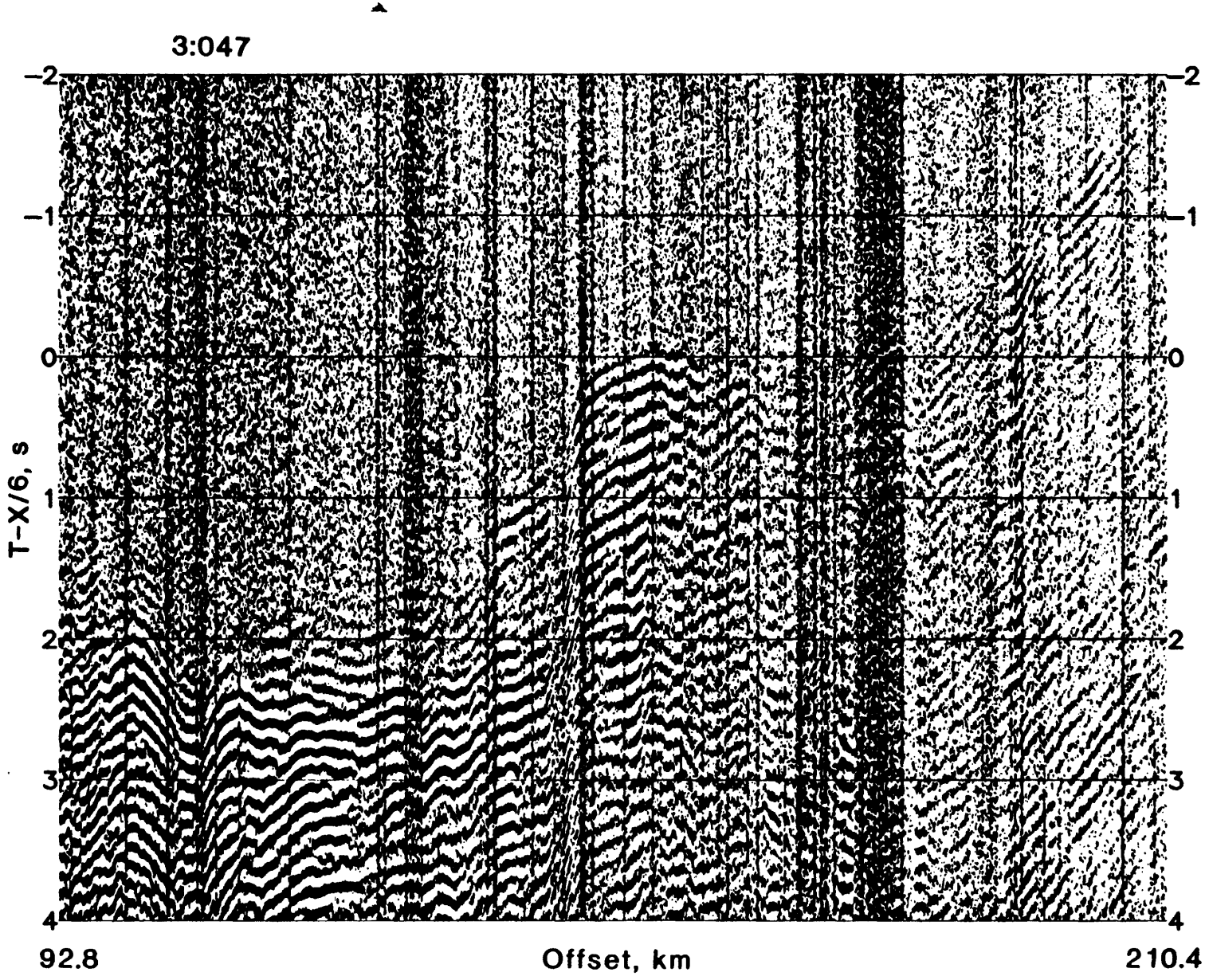

Figure 102. Stacked common receiver gather 047 for shots along LARSE air gun Line 3, reduced at 6 km/s.

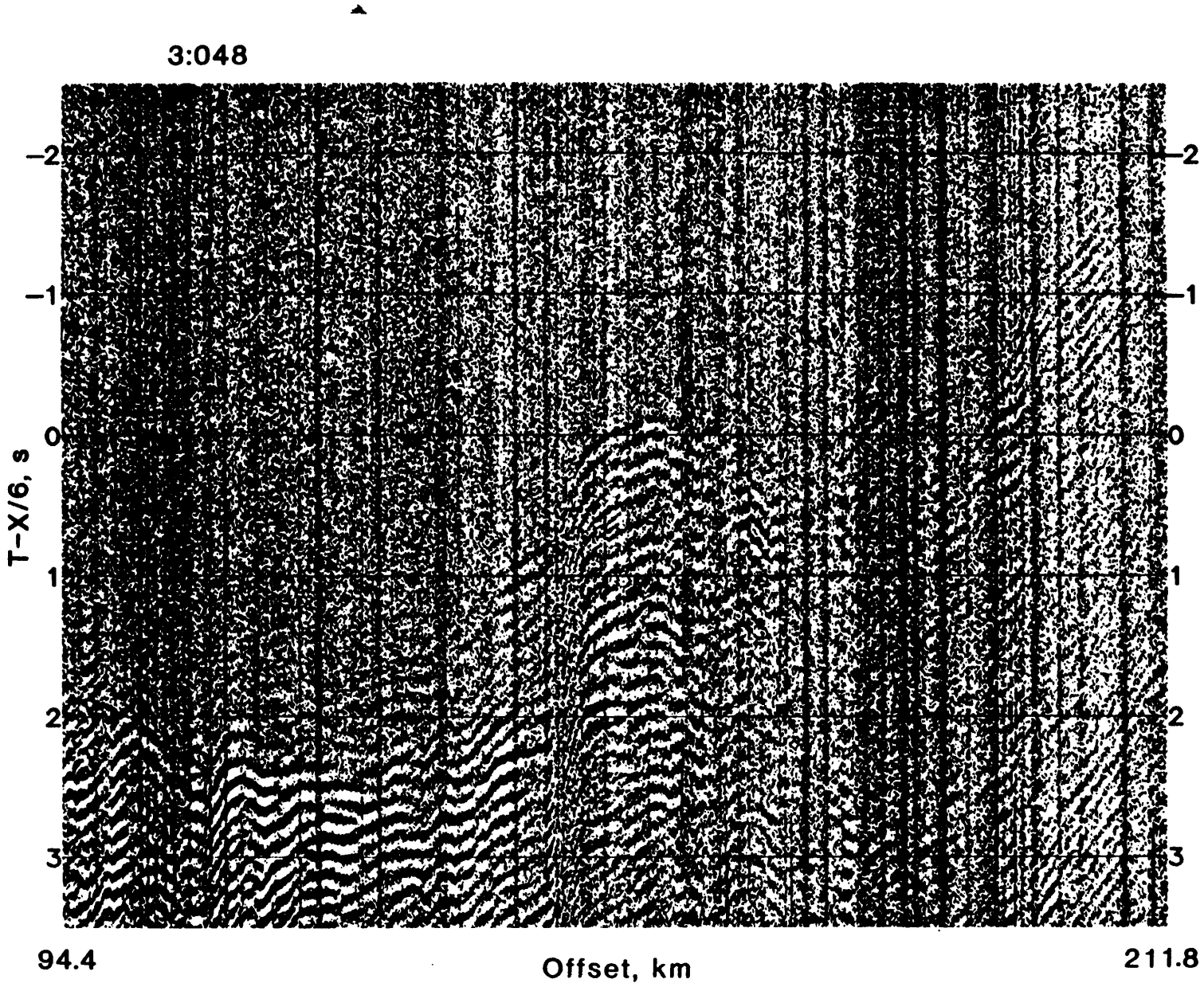

Figure 103. Stacked common receiver gather 048 for shots along LARSE air gun Line 3, reduced at 6 km/s.

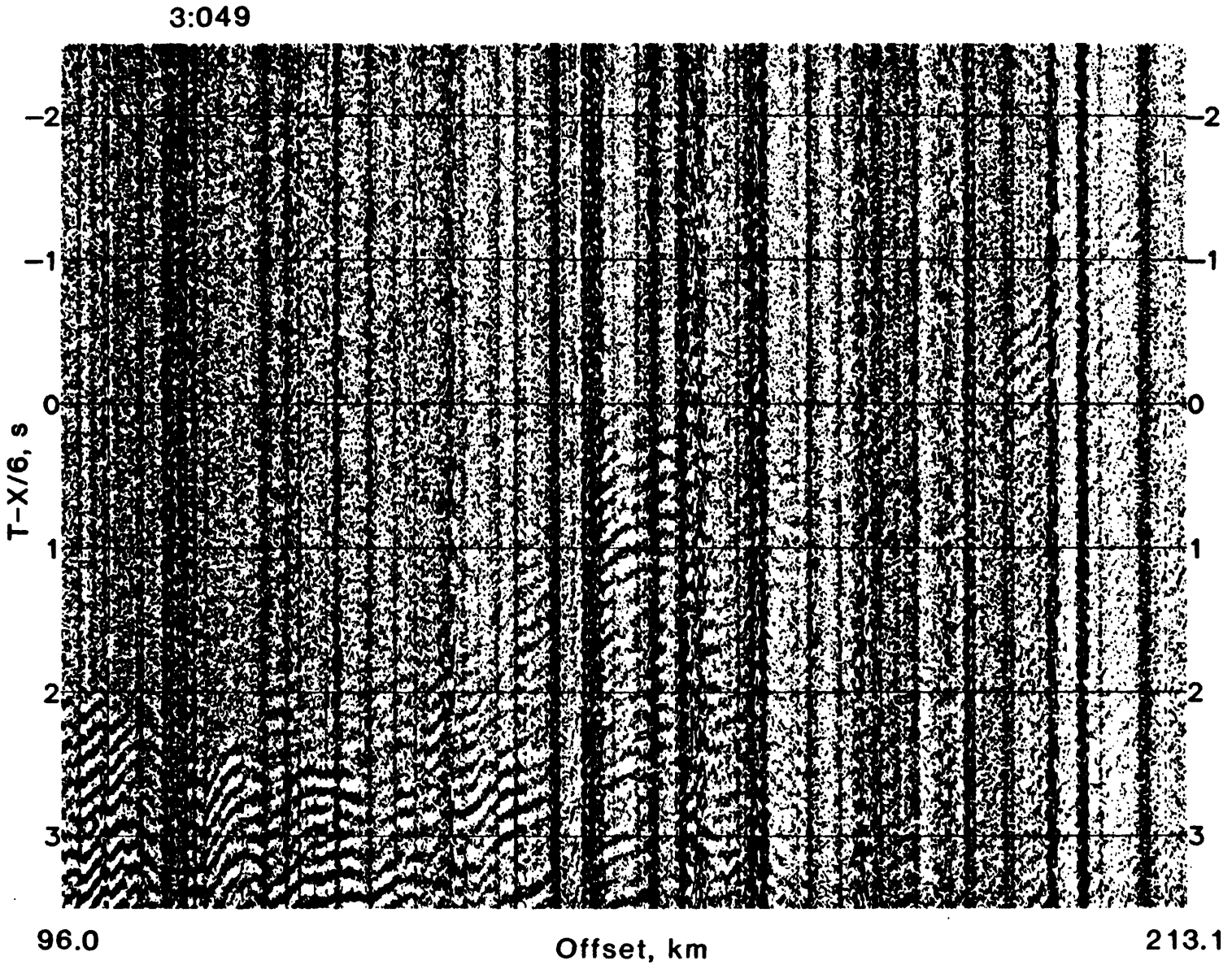

Figure 104. Stacked common receiver gather 049 for shots along LARSE air gun Line 3, reduced at 6 km/s.

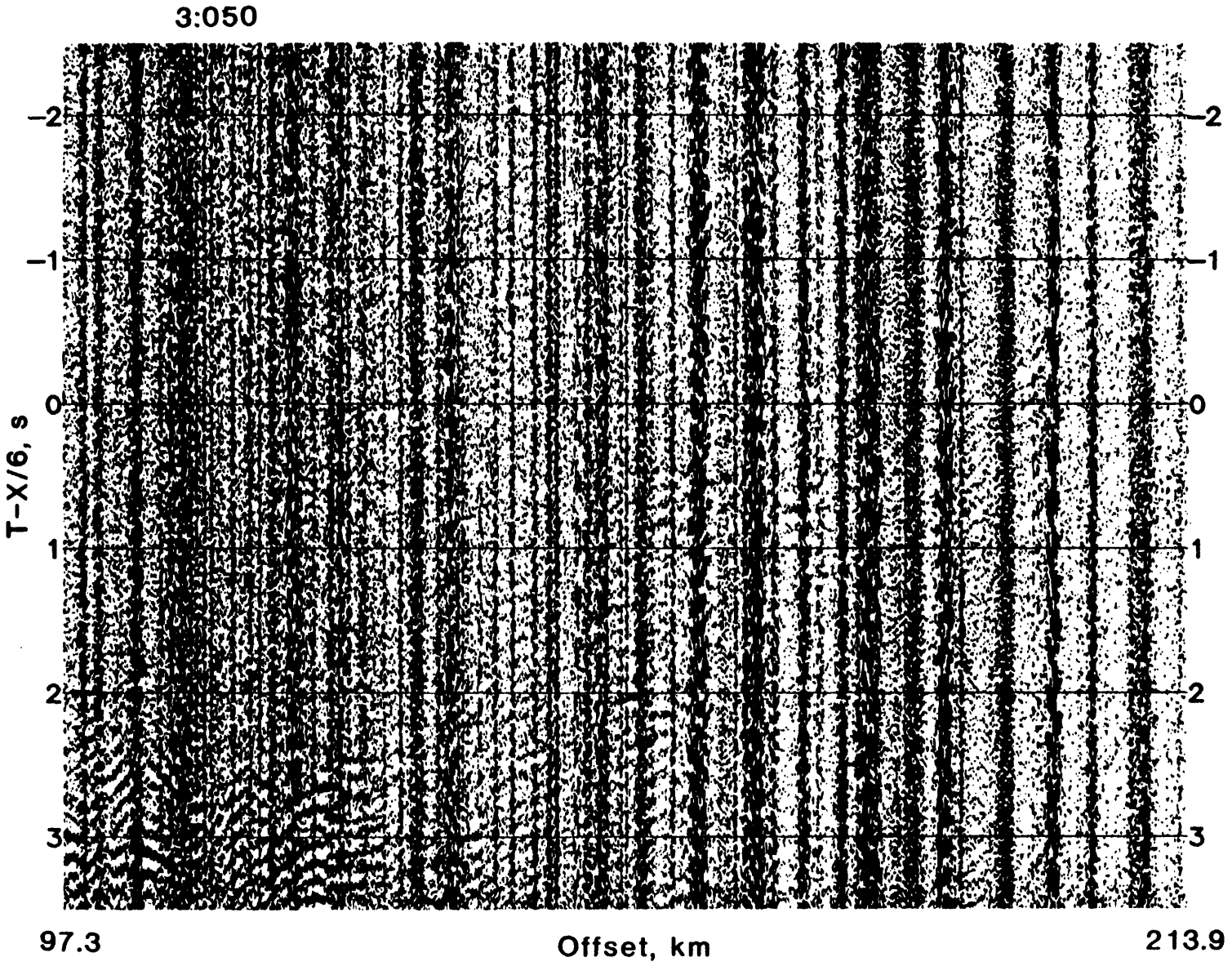

Figure 105. Stacked common receiver gather 050 for shots along LARSE air gun Line 3, reduced at 6 km/s.

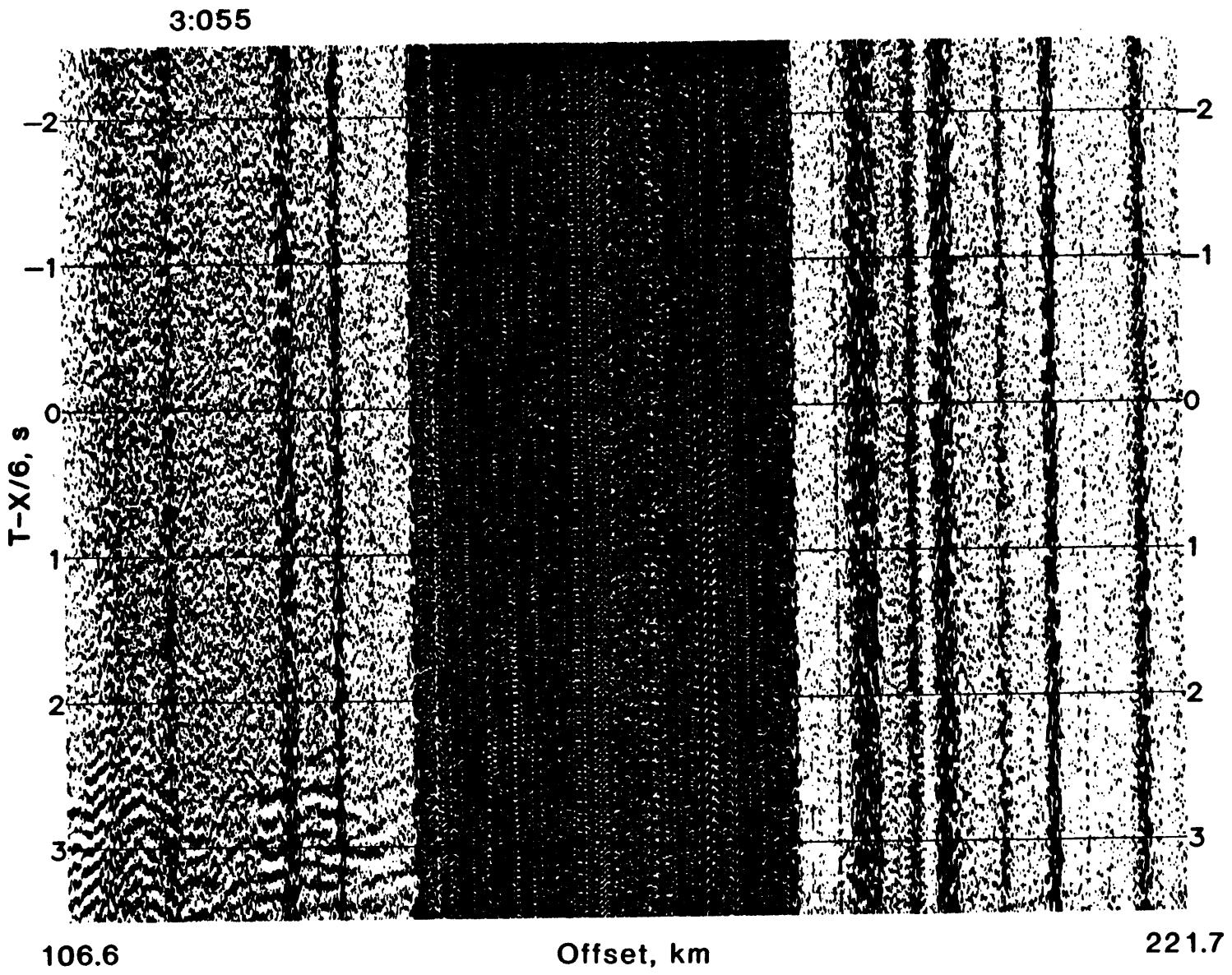

Figure 106. Stacked common receiver gather 055 for shots along LARSE air gun Line 3, reduced at 6 km/s.

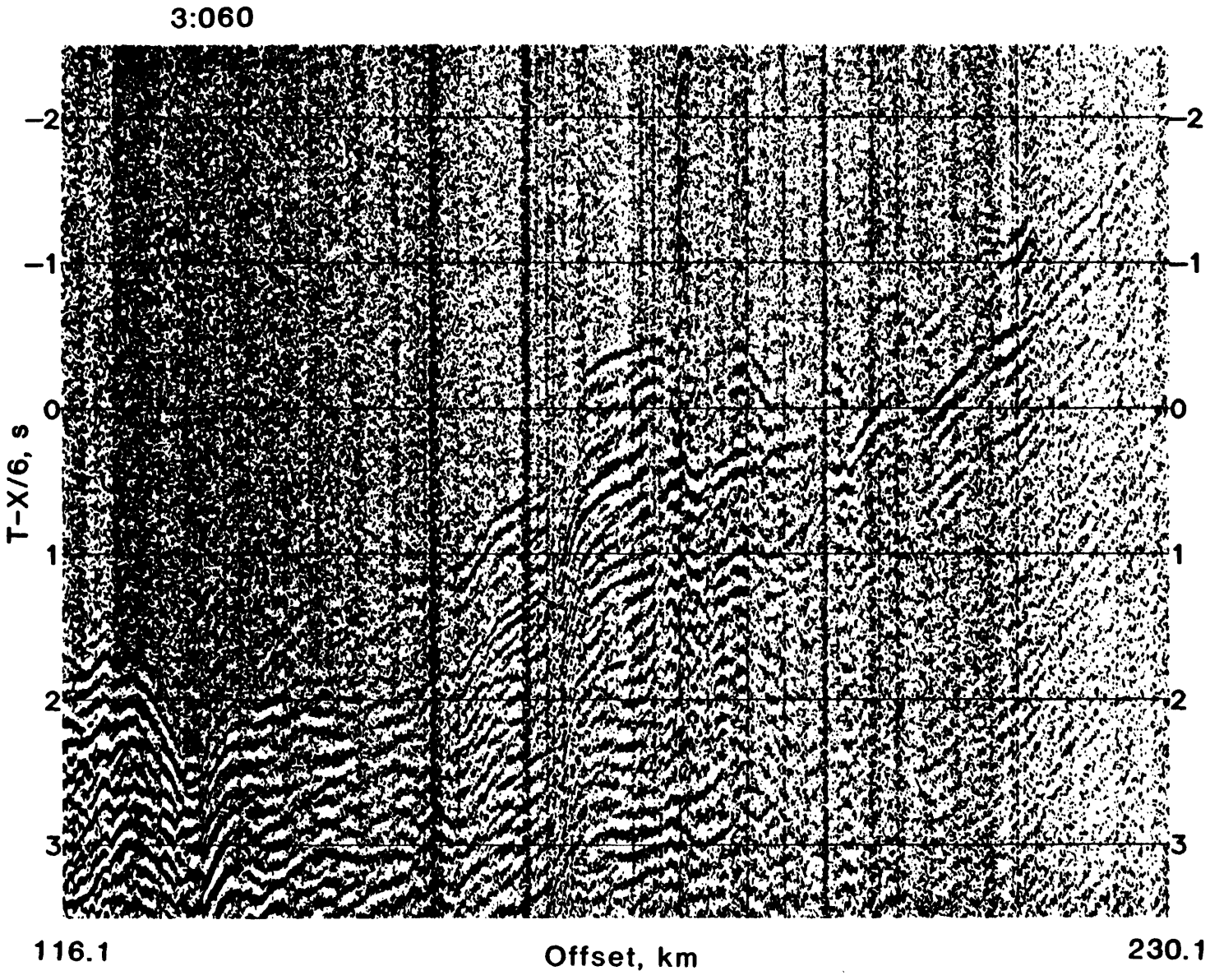

Figure 107. Stacked common receiver gather 060 for shots along LARSE air gun Line 3, reduced at 6 km/s.

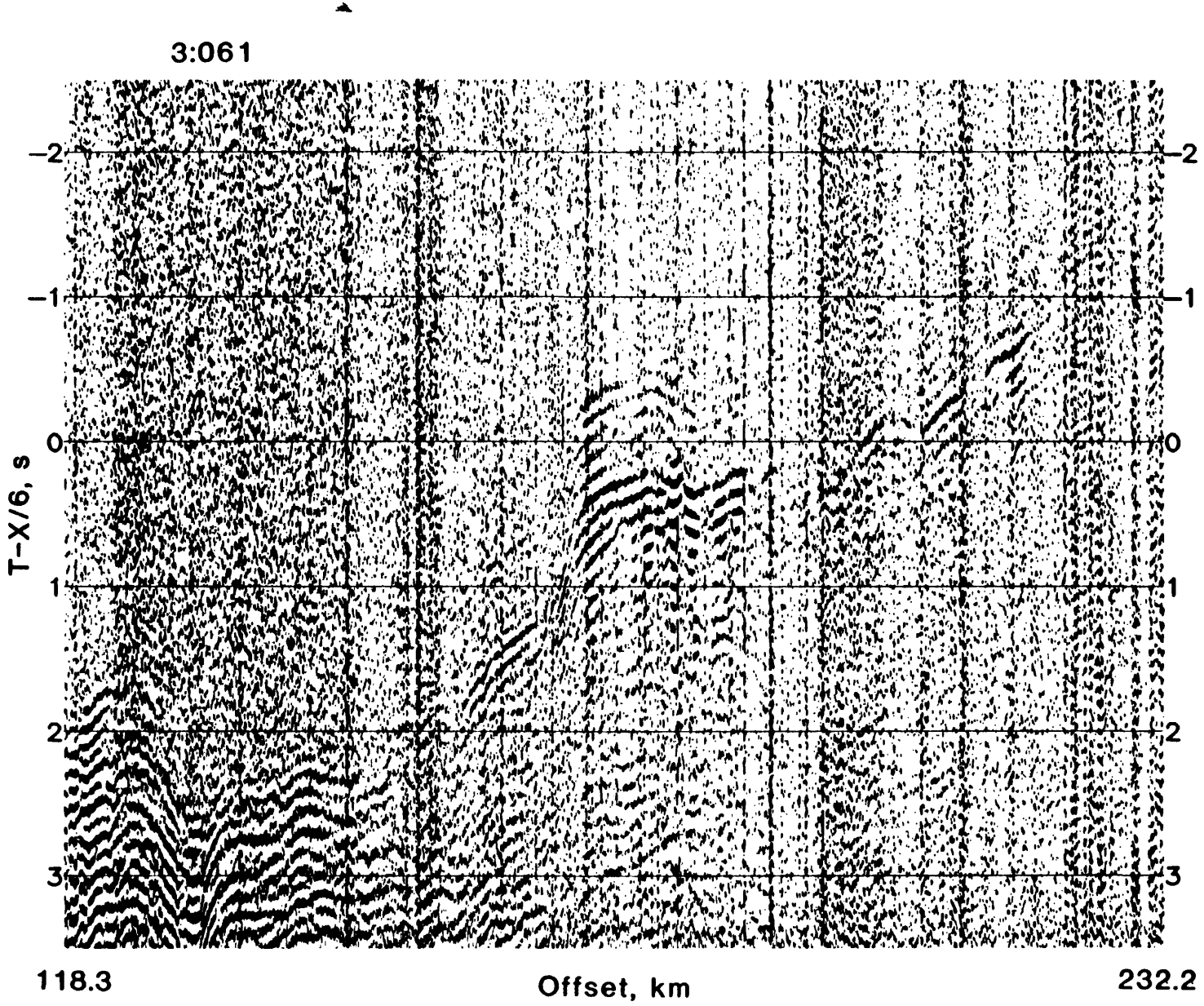

Figure 108. Stacked common receiver gather 061 for shots along LARSE air gun Line 3, reduced at 6 km/s.

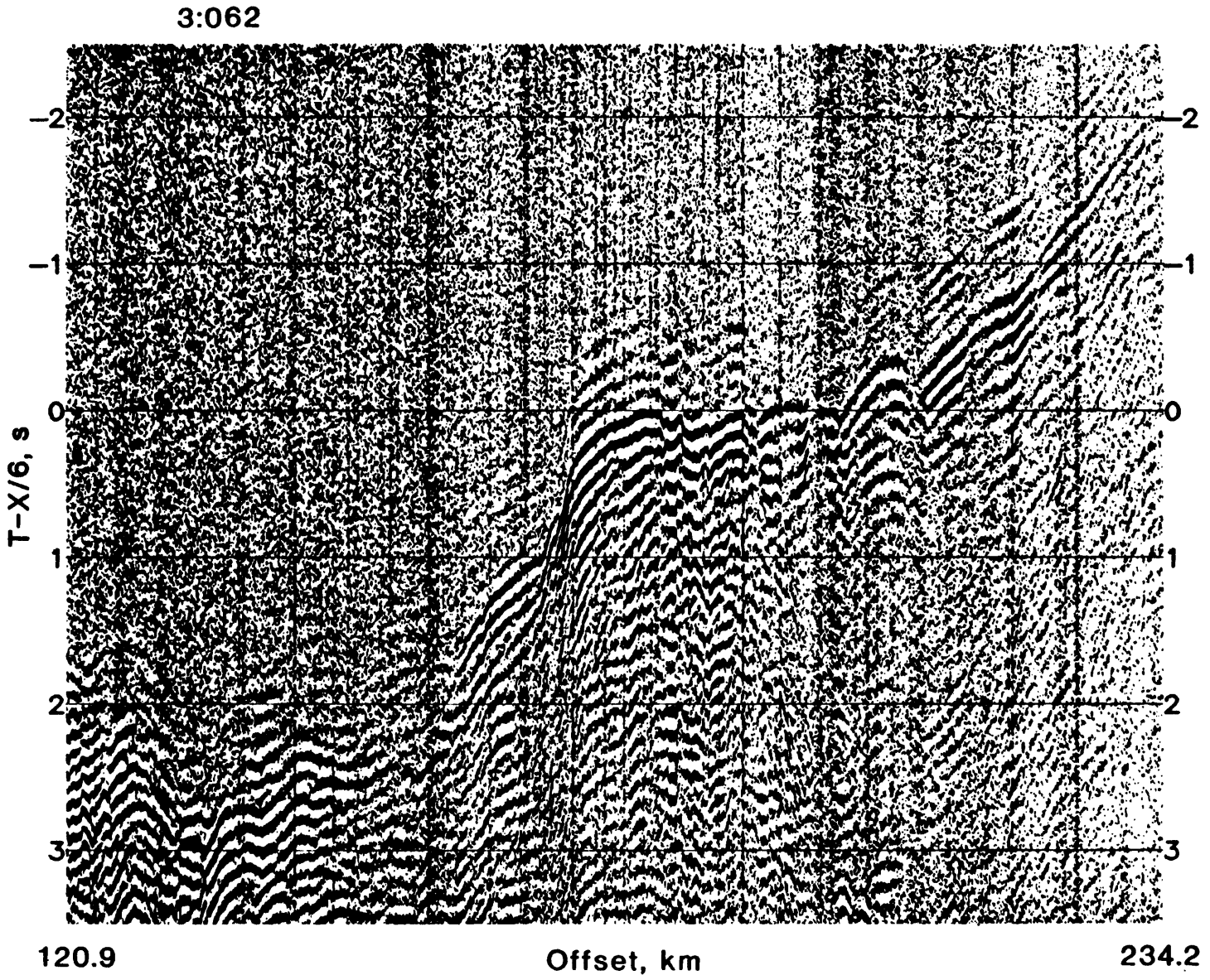

Figure 109. Stacked common receiver gather 062 for shots along LARSE air gun Line 3, reduced at 6 km/s.

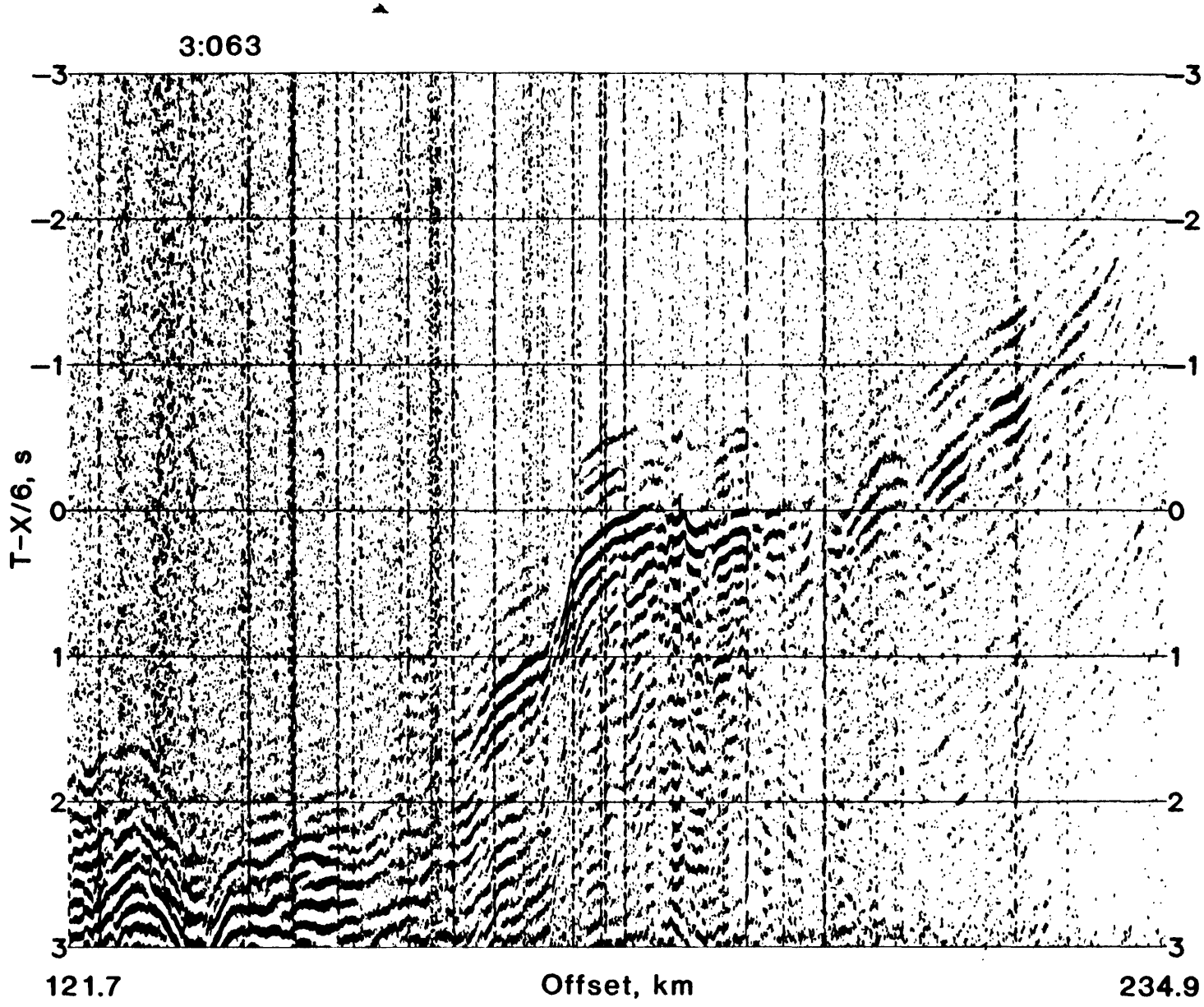

Figure 110. Stacked common receiver gather 063 for shots along LARSE air gun Line 3, reduced at 6 km/s.

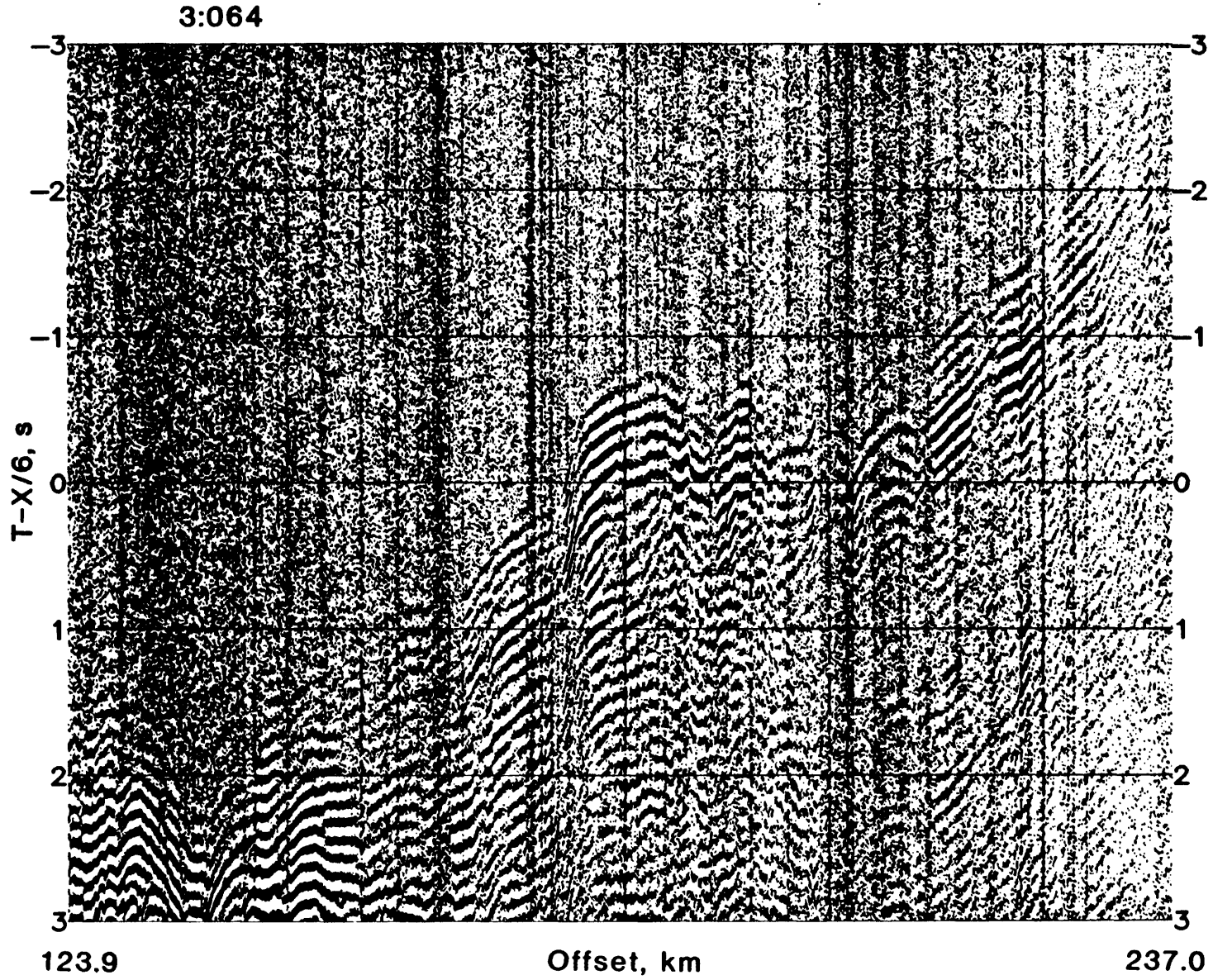

Figure 111. Stacked common receiver gather 064 for shots along LARSE air gun Line 3, reduced at 6 km/s.

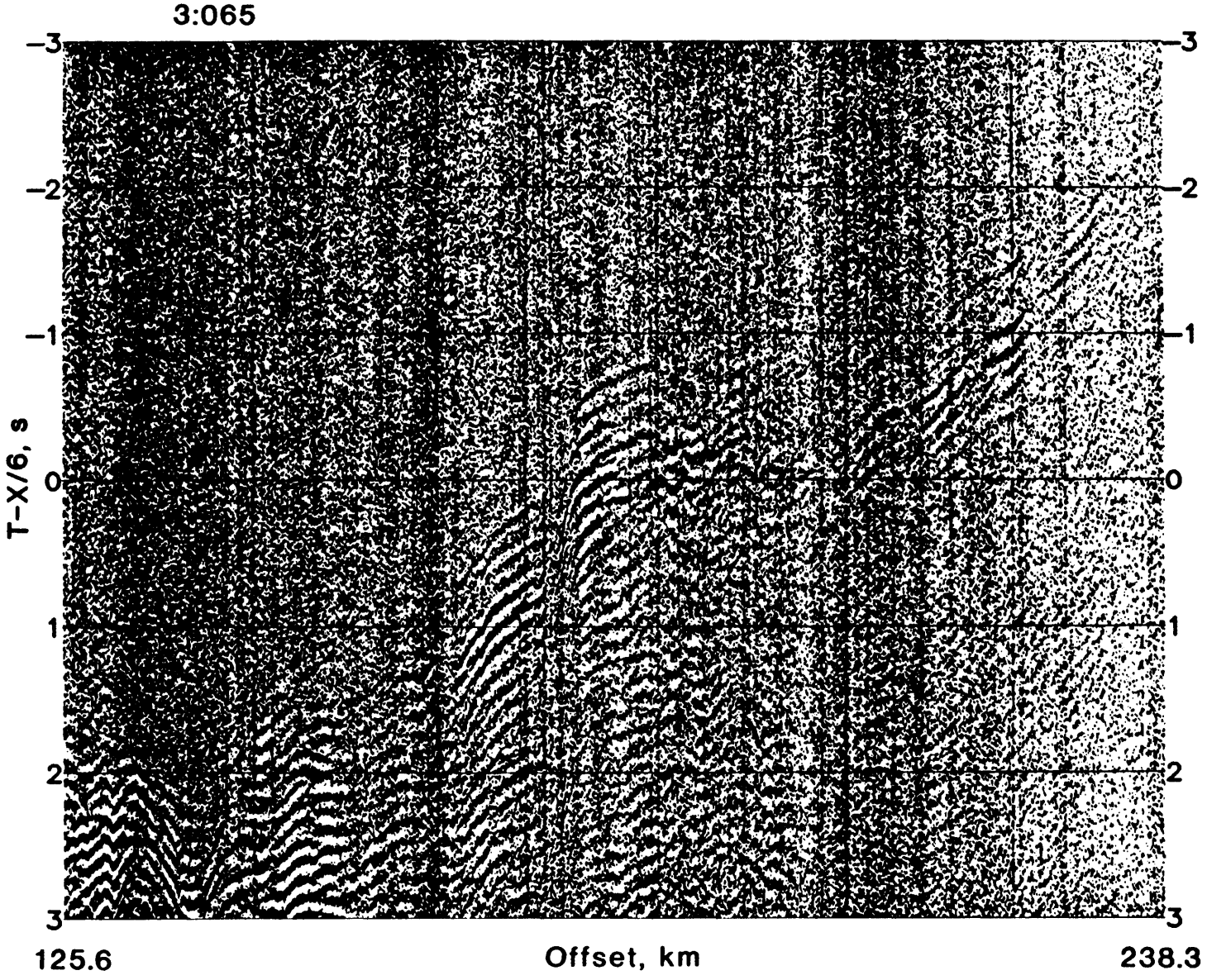

Figure 112. Stacked common receiver gather 065 for shots along LARSE air gun Line 3, reduced at 6 km/s.

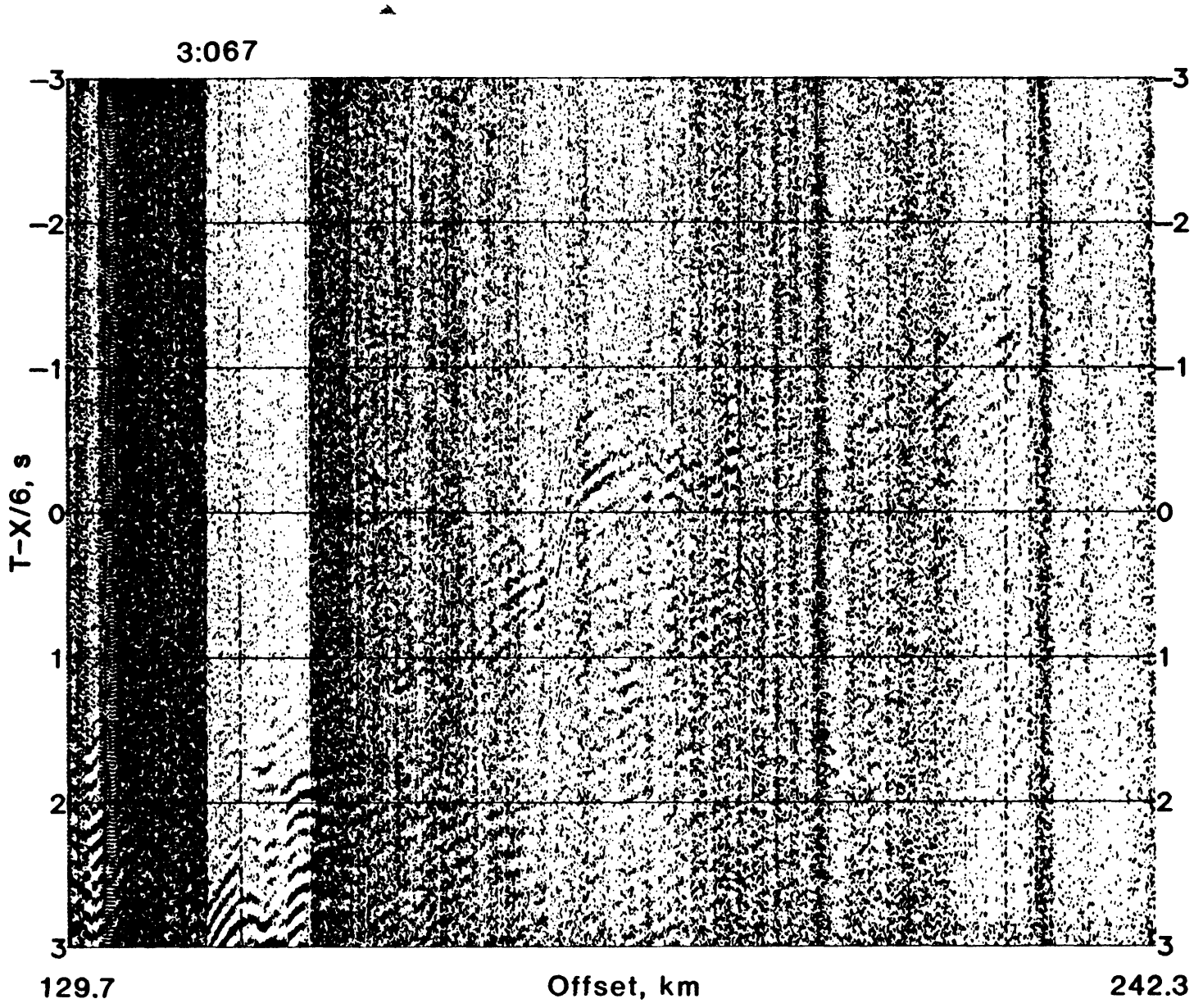

Figure 113. Stacked common receiver gather 067 for shots along LARSE air gun Line 3, reduced at 6 km/s.

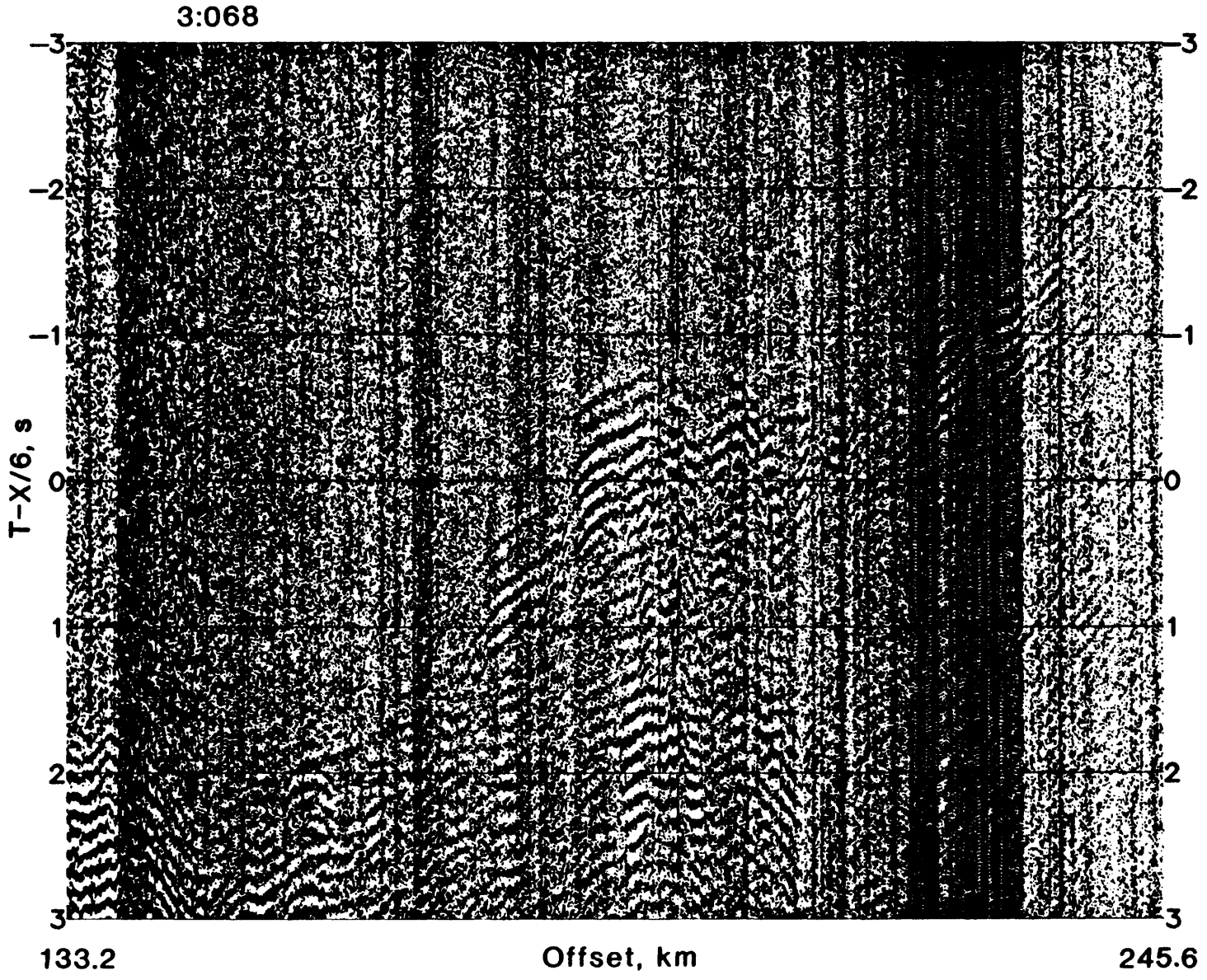

Figure 114. Stacked common receiver gather 068 for shots along LARSE air gun Line 3, reduced at 6 km/s.

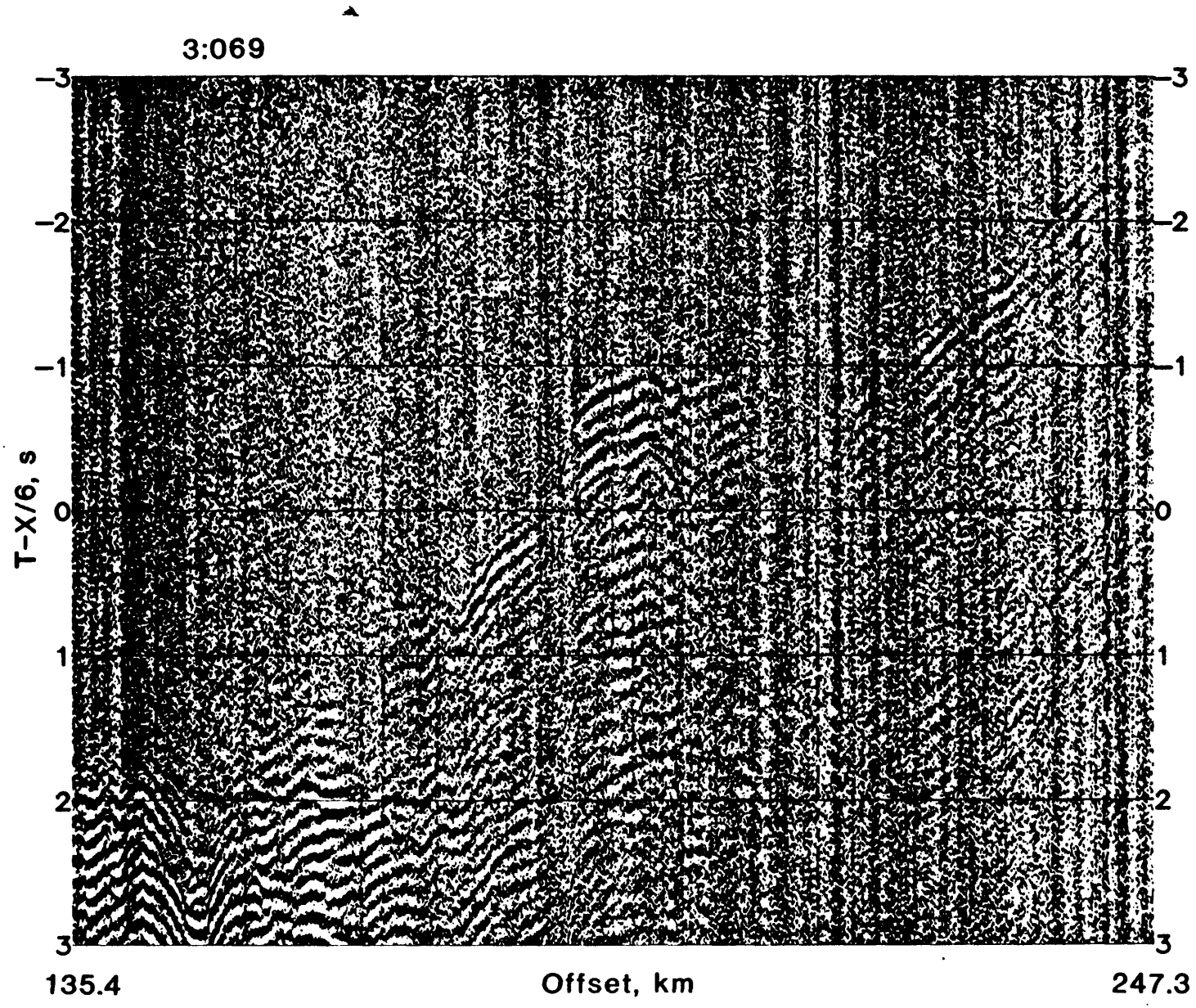

Figure 115. Stacked common receiver gather 069 for shots along LARSE air gun Line 3, reduced at 6 km/s.

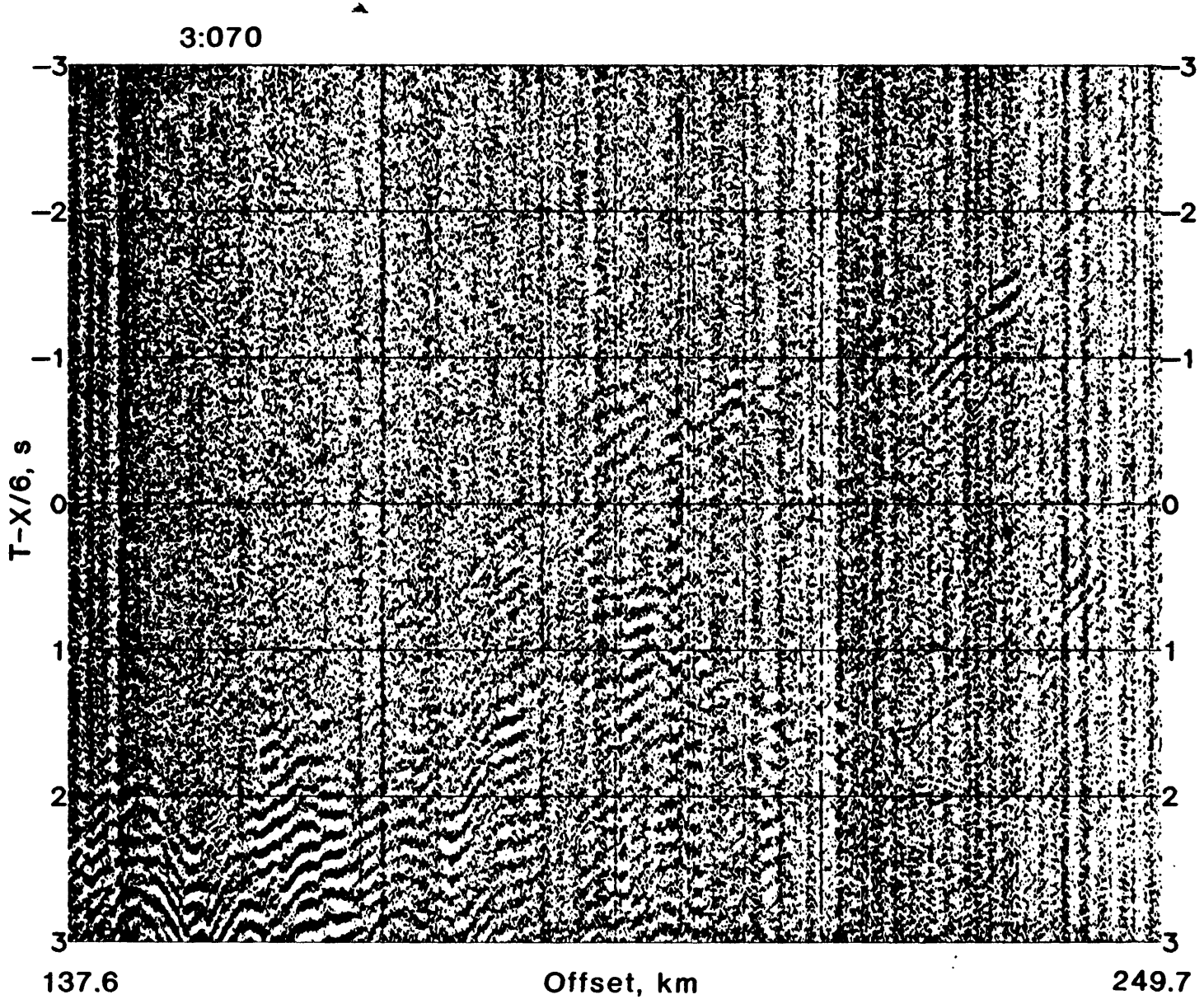

Figure 116. Stacked common receiver gather 070 for shots along LARSE air gun Line 3, reduced at 6 km/s.

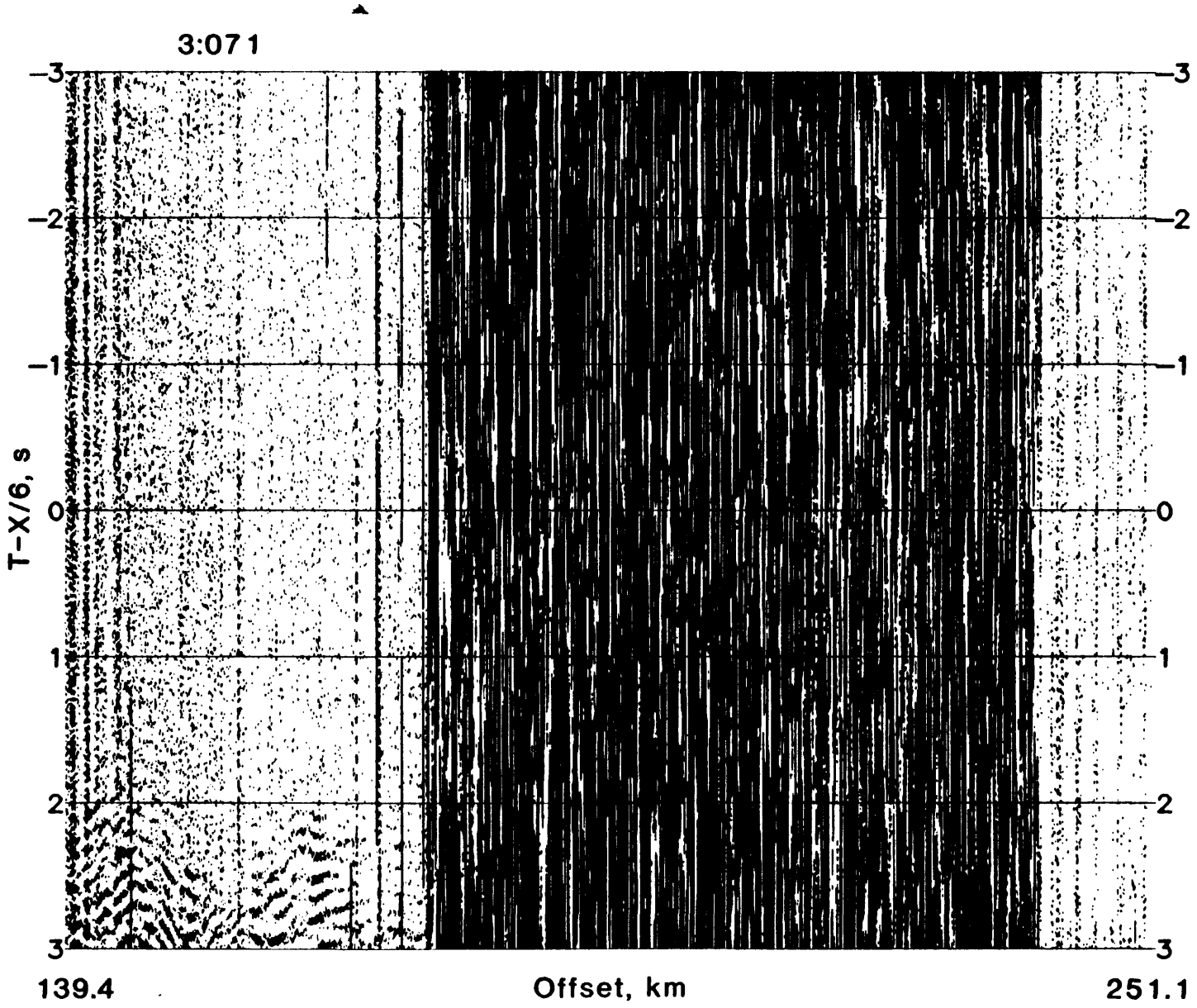

Figure 117. Stacked common receiver gather 071 for shots along LARSE air gun Line 3, reduced at 6 km/s.

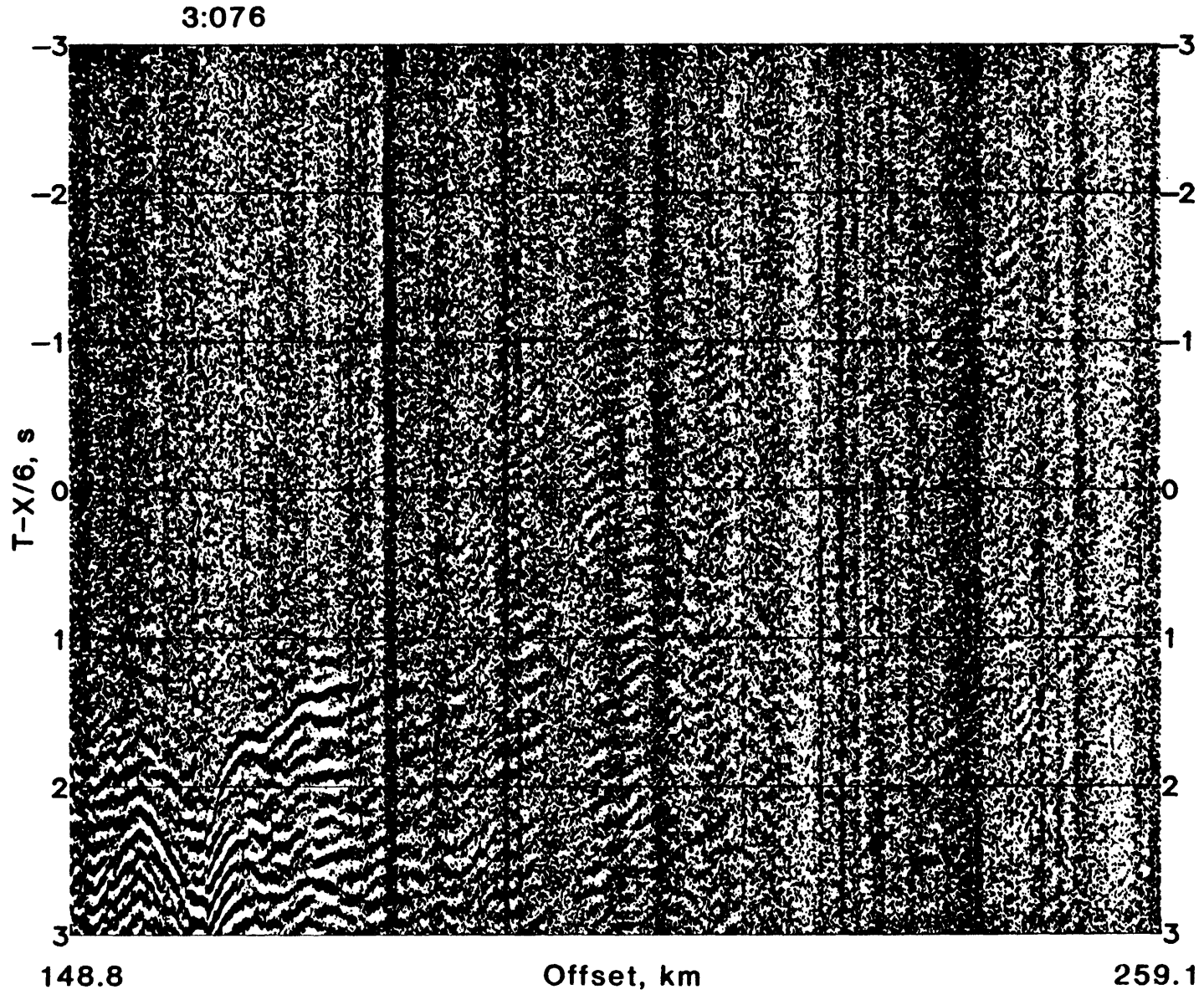

Figure 118. Stacked common receiver gather 076 for shots along LARSE air gun Line 3, reduced at 6 km/s.

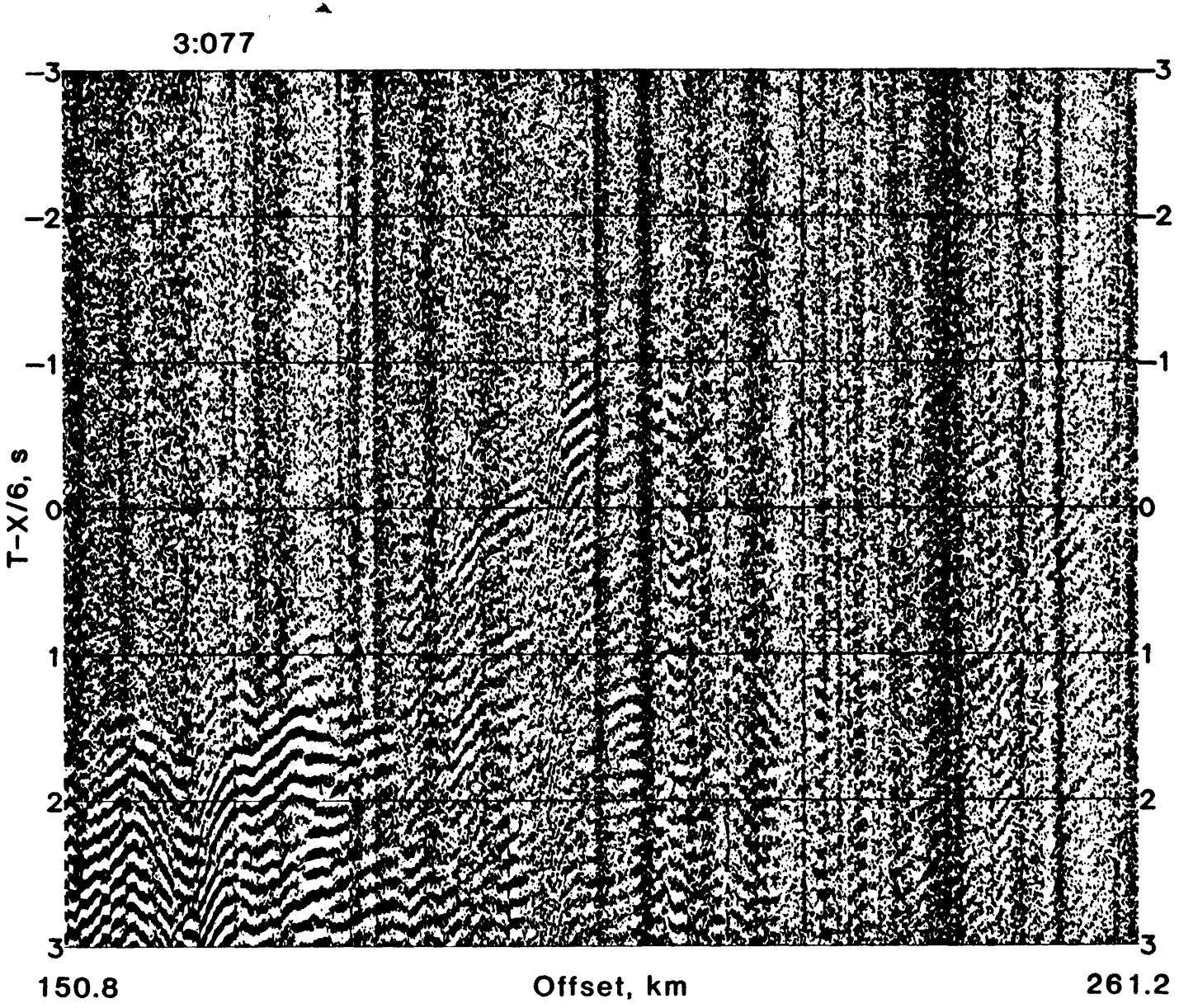

Figure 119. Stacked common receiver gather 077 for shots along LARSE air gun Line 3, reduced at 6 km/s.

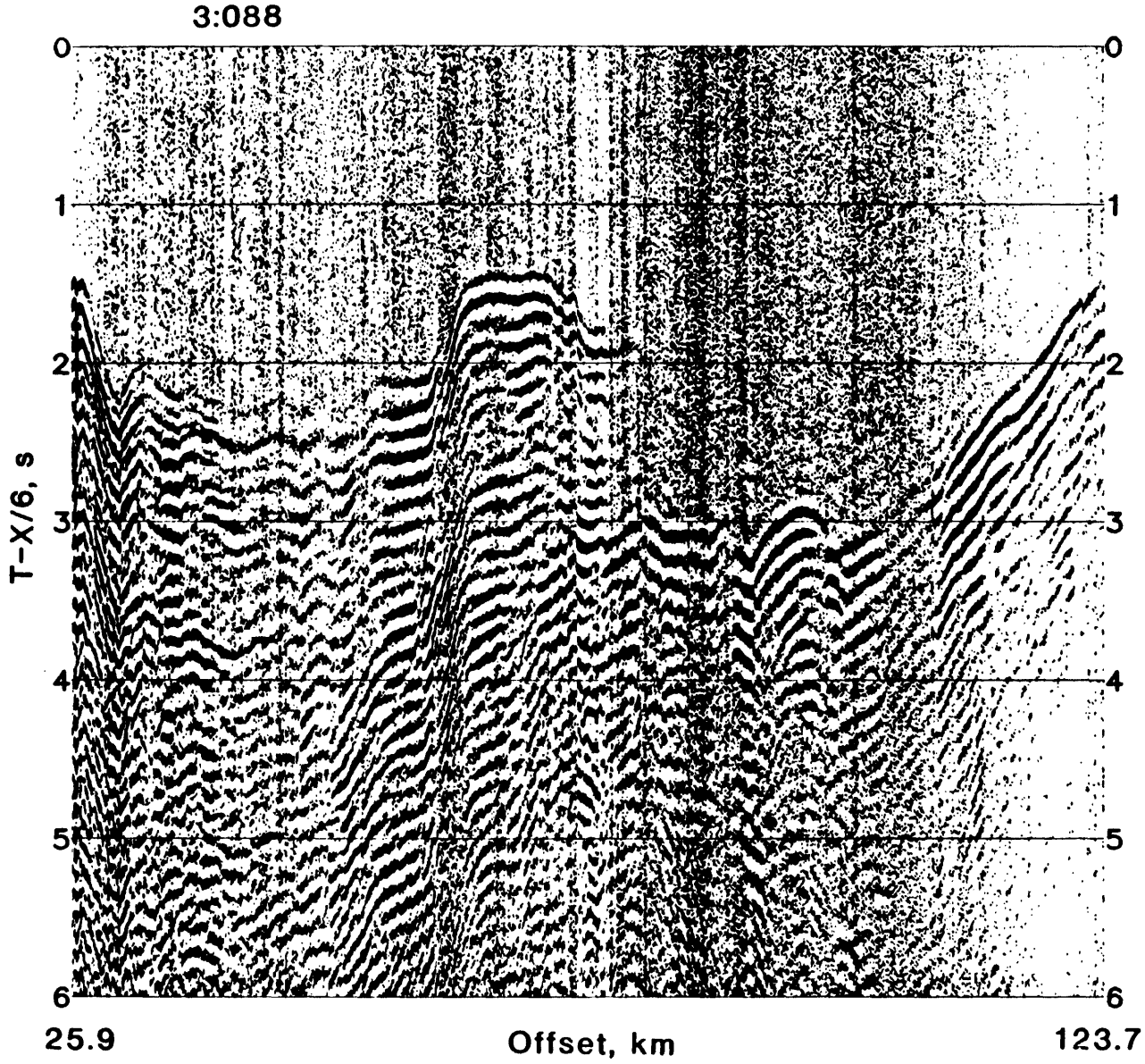

Figure 120. Stacked common receiver gather 088 for shots along LARSE air gun Line 3, reduced at 6 km/s.

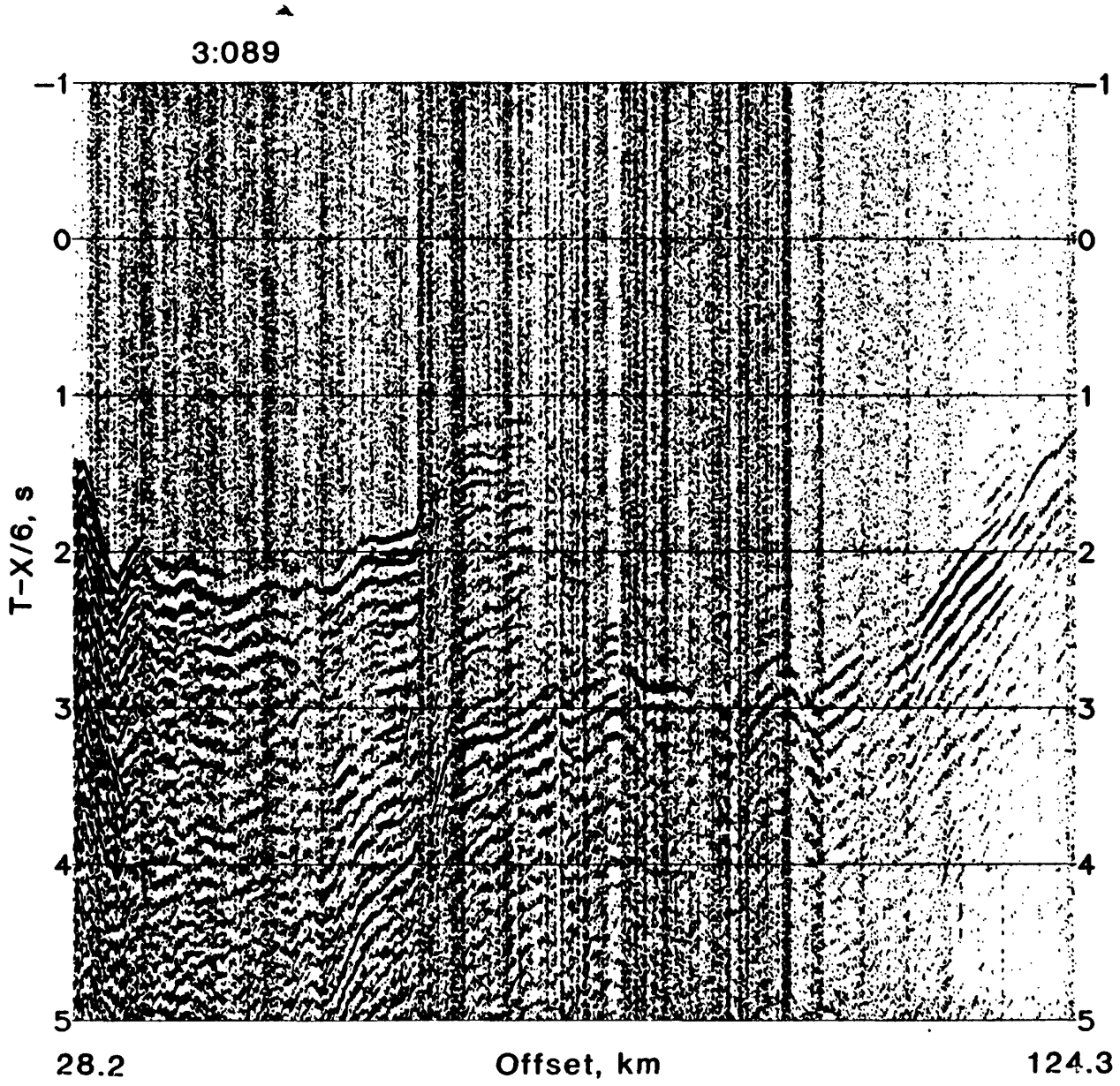

Figure 121. Stacked common receiver gather 089 for shots along LARSE air gun Line 3, reduced at 6 km/s.

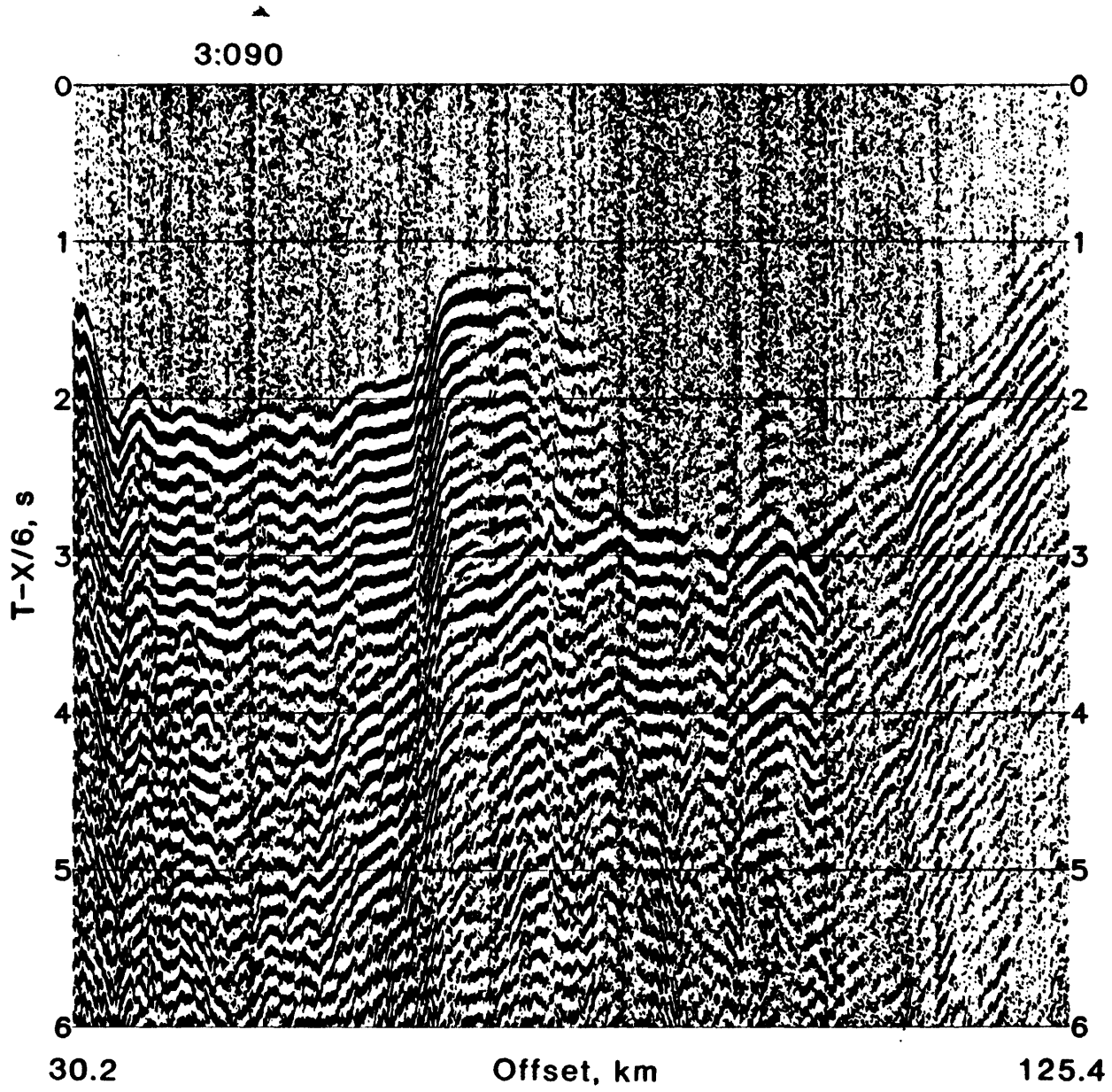

Figure 122. Stacked common receiver gather 090 for shots along LARSE air gun Line 3, reduced at 6 km/s.

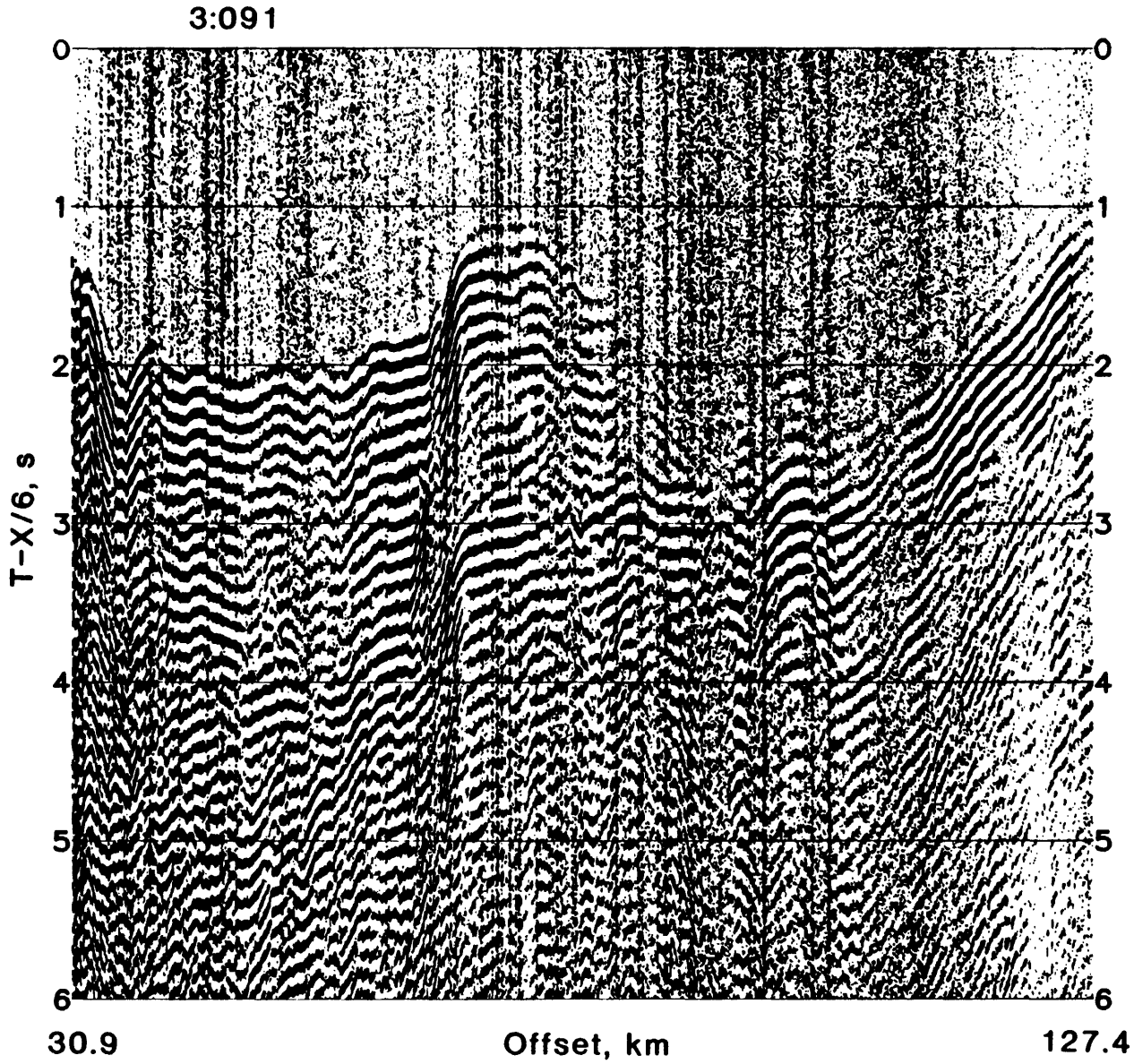

Figure 123. Stacked common receiver gather 091 for shots along LARSE air gun Line 3, reduced at 6 km/s.

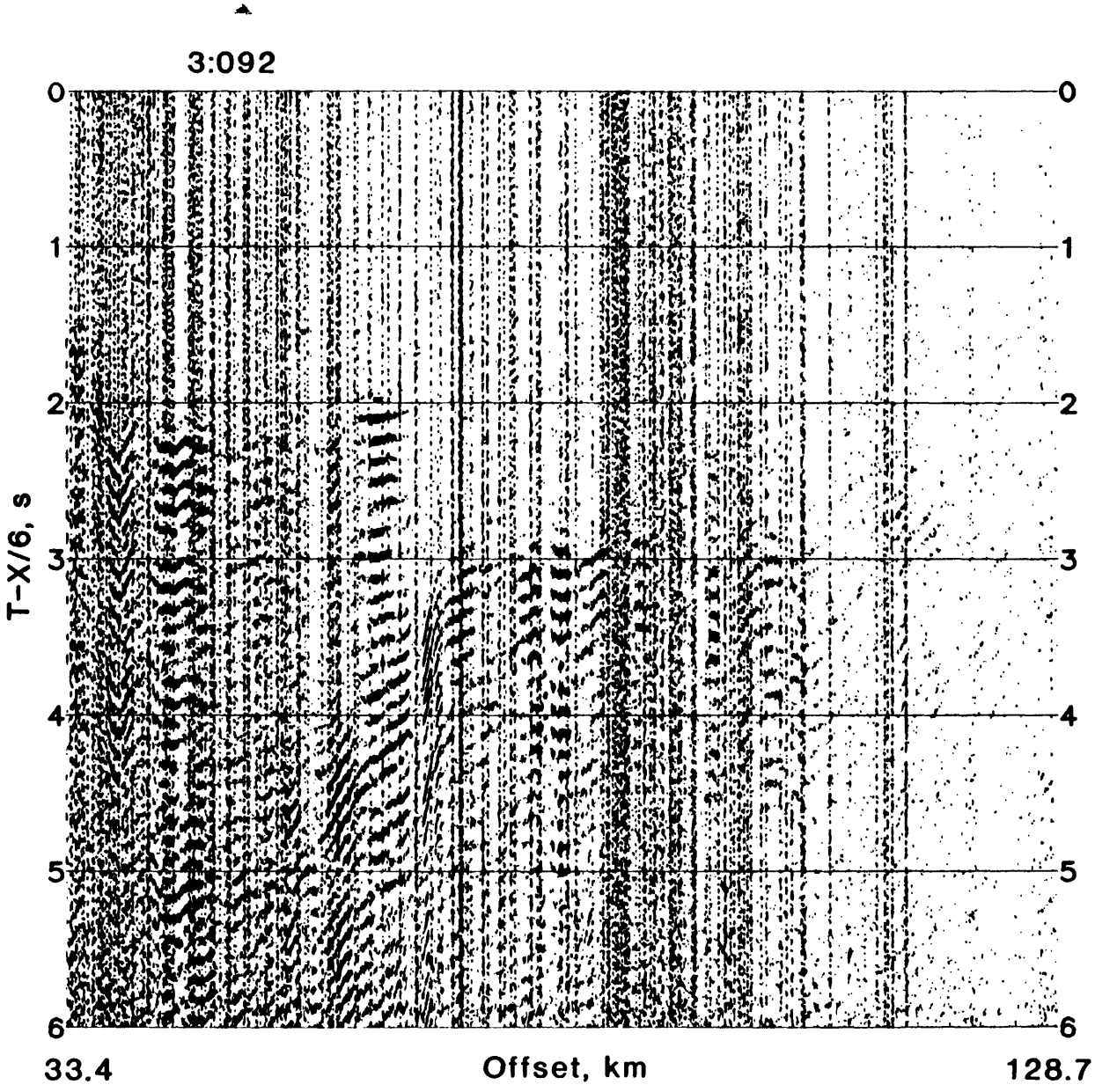

Figure 124. Stacked common receiver gather 092 for shots along LARSE air gun Line 3, reduced at 6 km/s.

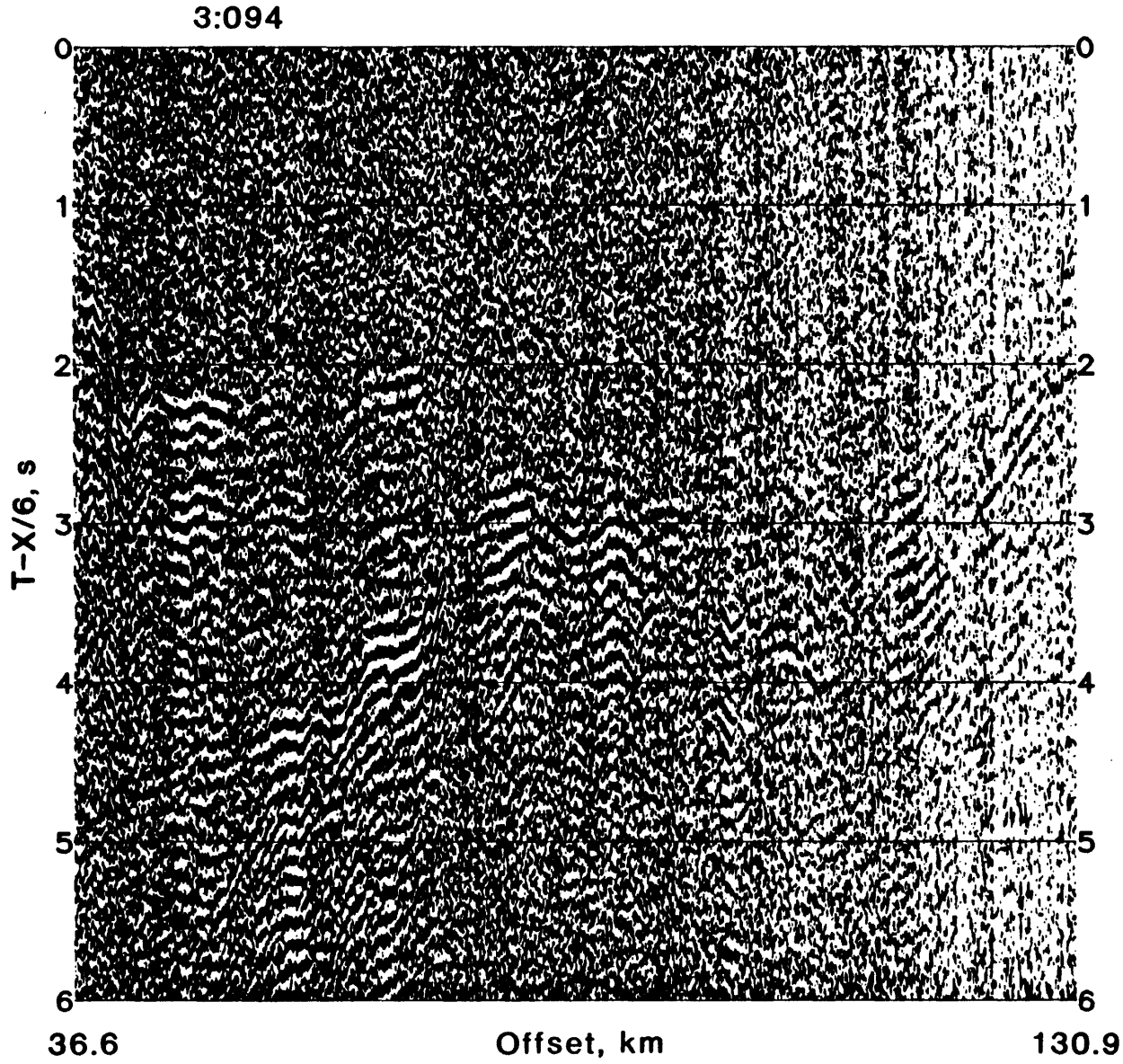

Figure 125. Stacked common receiver gather 094 for shots along LARSE air gun Line 3, reduced at 6 km/s.

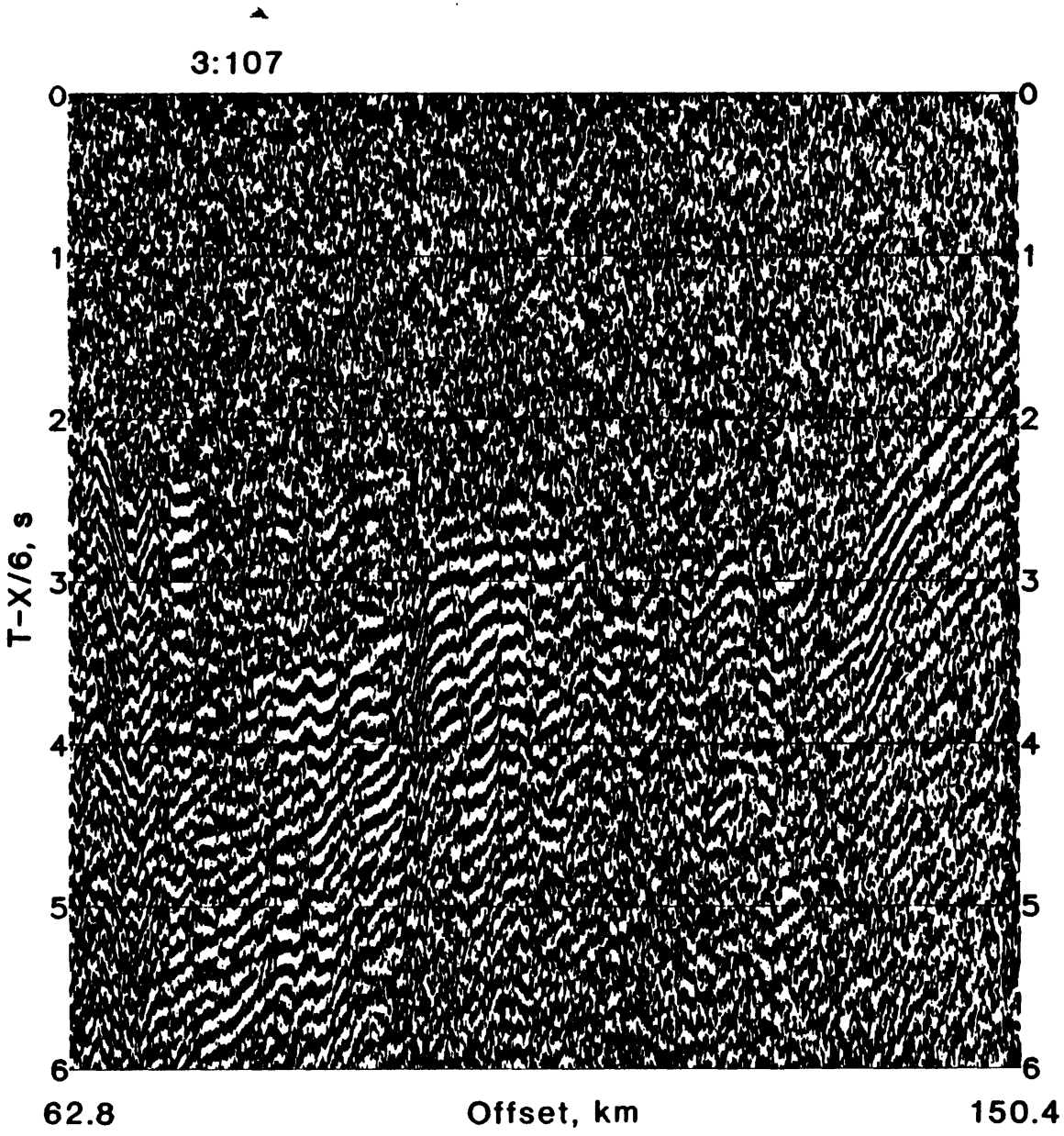

Figure 126. Stacked common receiver gather 107 for shots along LARSE air gun Line 3, reduced at 6 km/s.

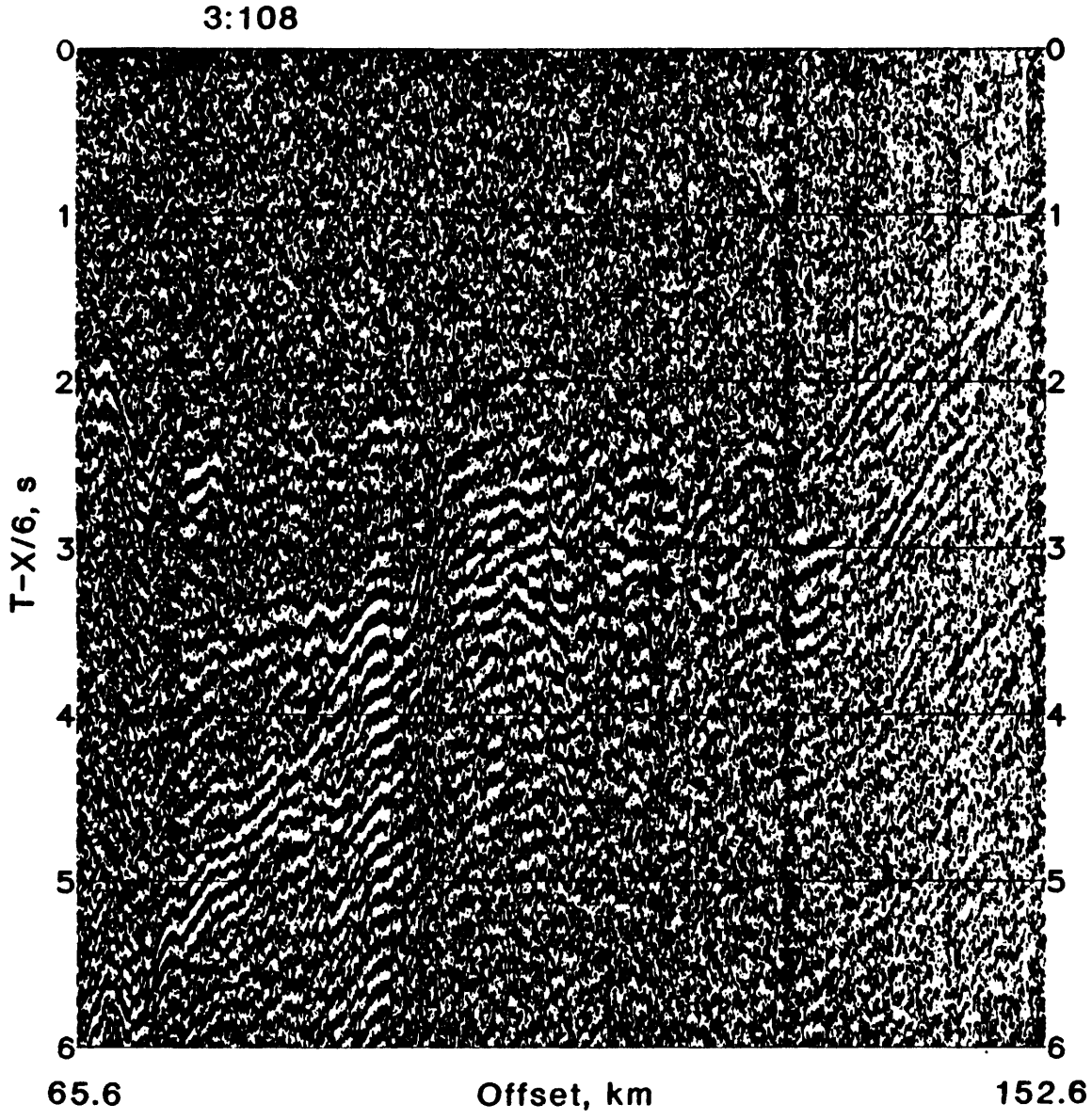

Figure 127. Stacked common receiver gather 108 for shots along LARSE air gun Line 3, reduced at 6 km/s.

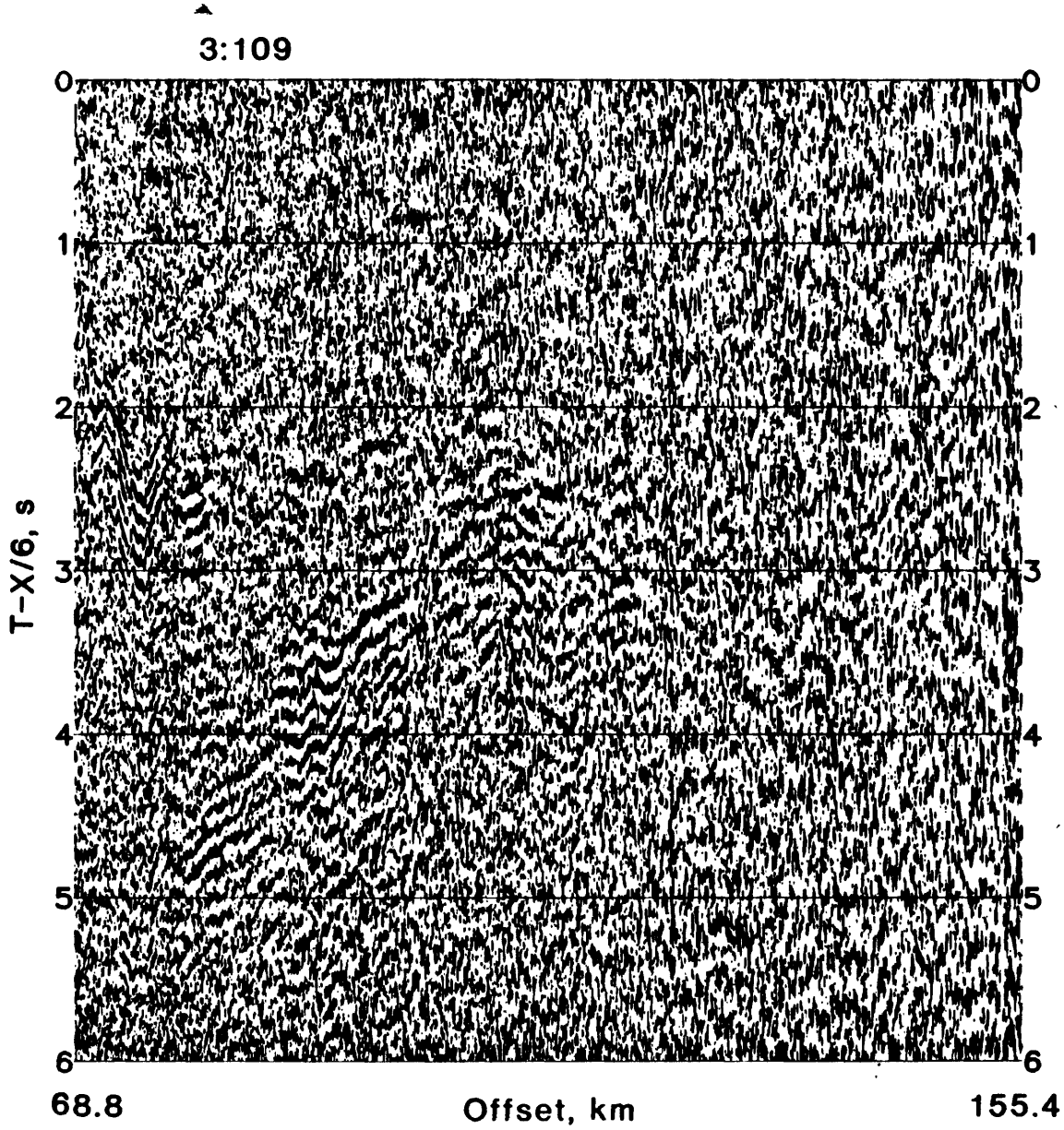

Figure 128. Stacked common receiver gather 109 for shots along LARSE air gun Line 3, reduced at 6 km/s.

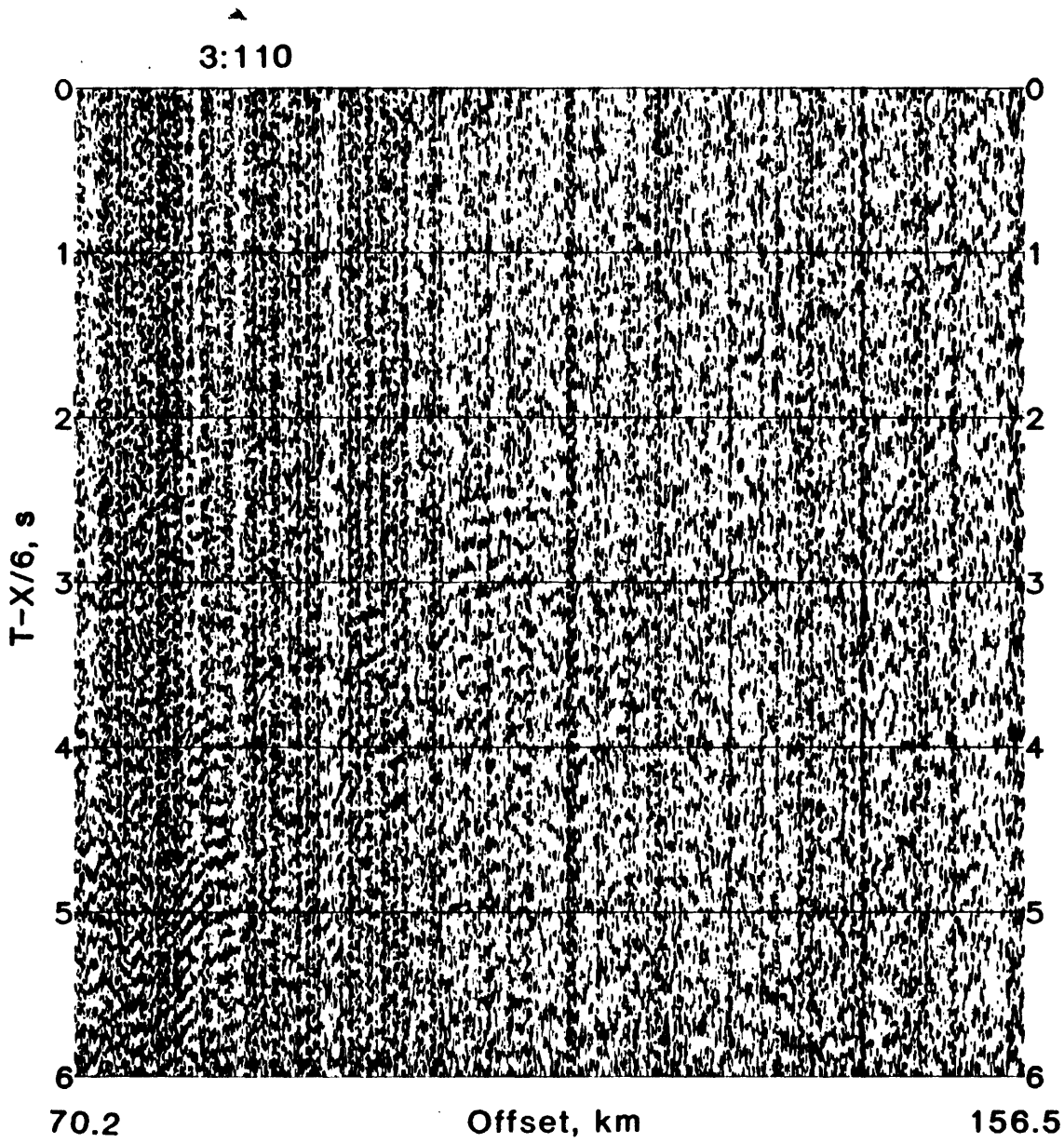

Figure 129. Stacked common receiver gather 110 for shots along LARSE air gun Line 3, reduced at 6 km/s.

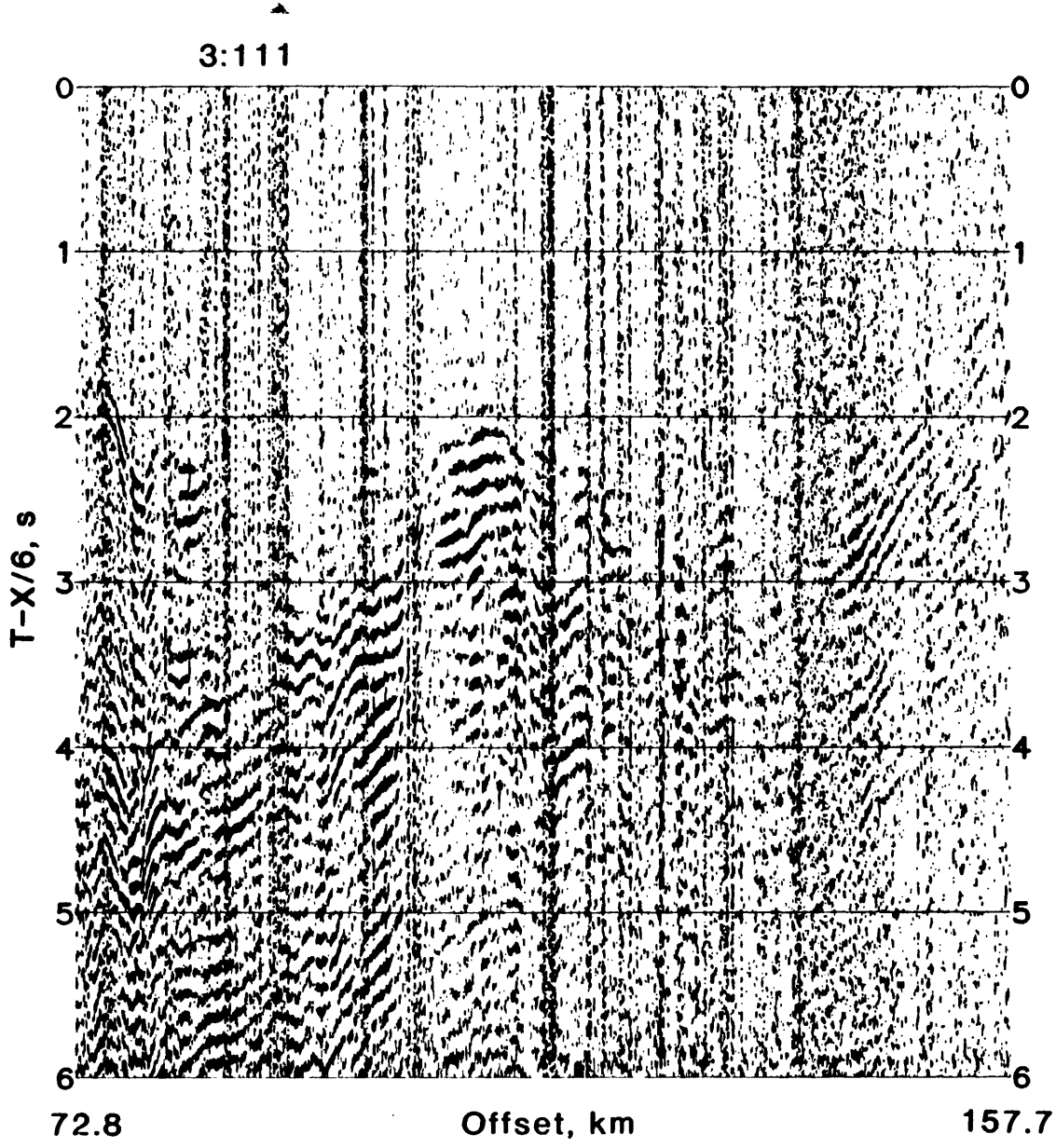

Figure 130. Stacked common receiver gather 111 for shots along LARSE air gun Line 3, reduced at 6 km/s.

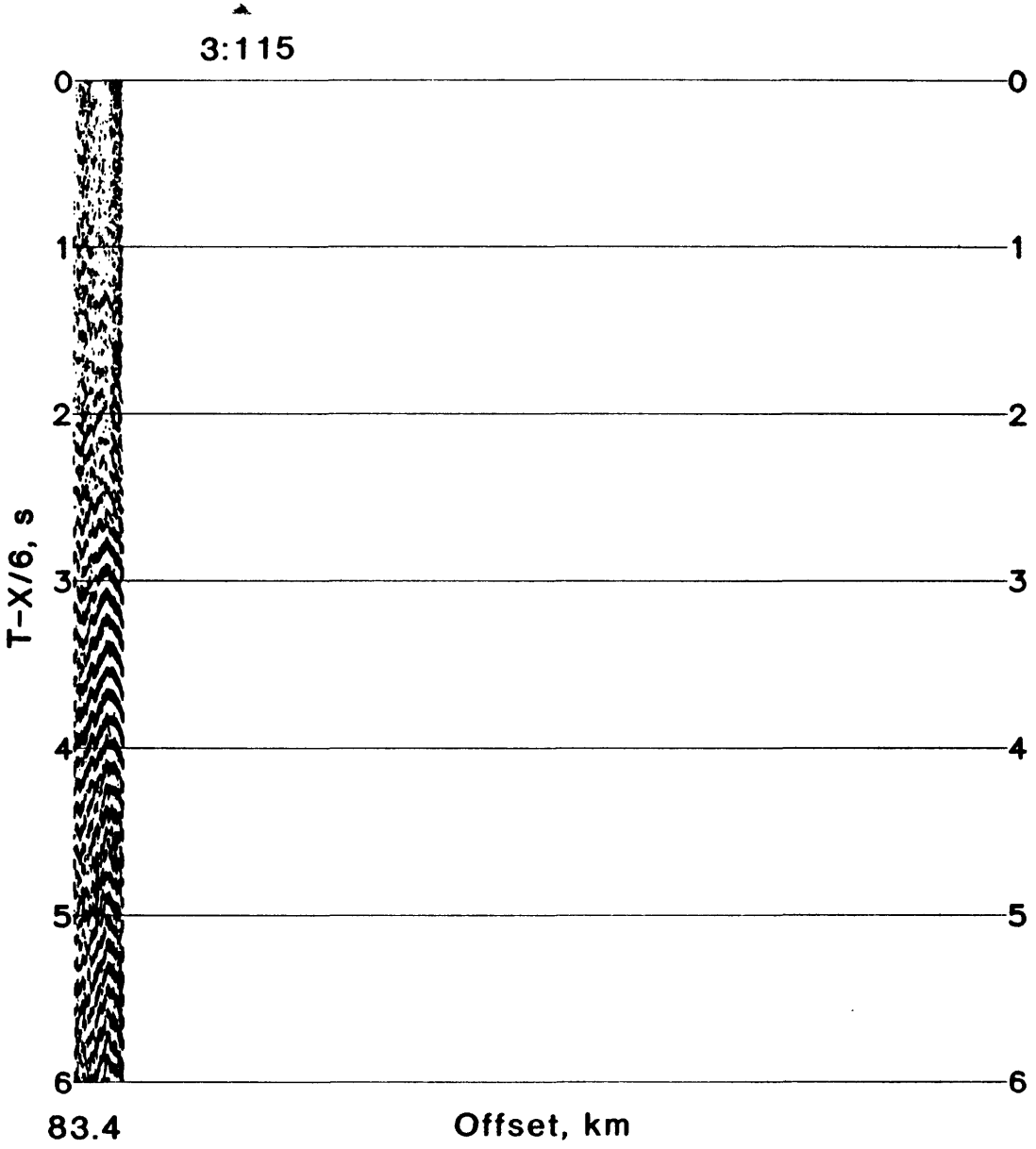

Figure 131. Stacked common receiver gather 115 for shots along LARSE air gun Line 3, reduced at 6 km/s.

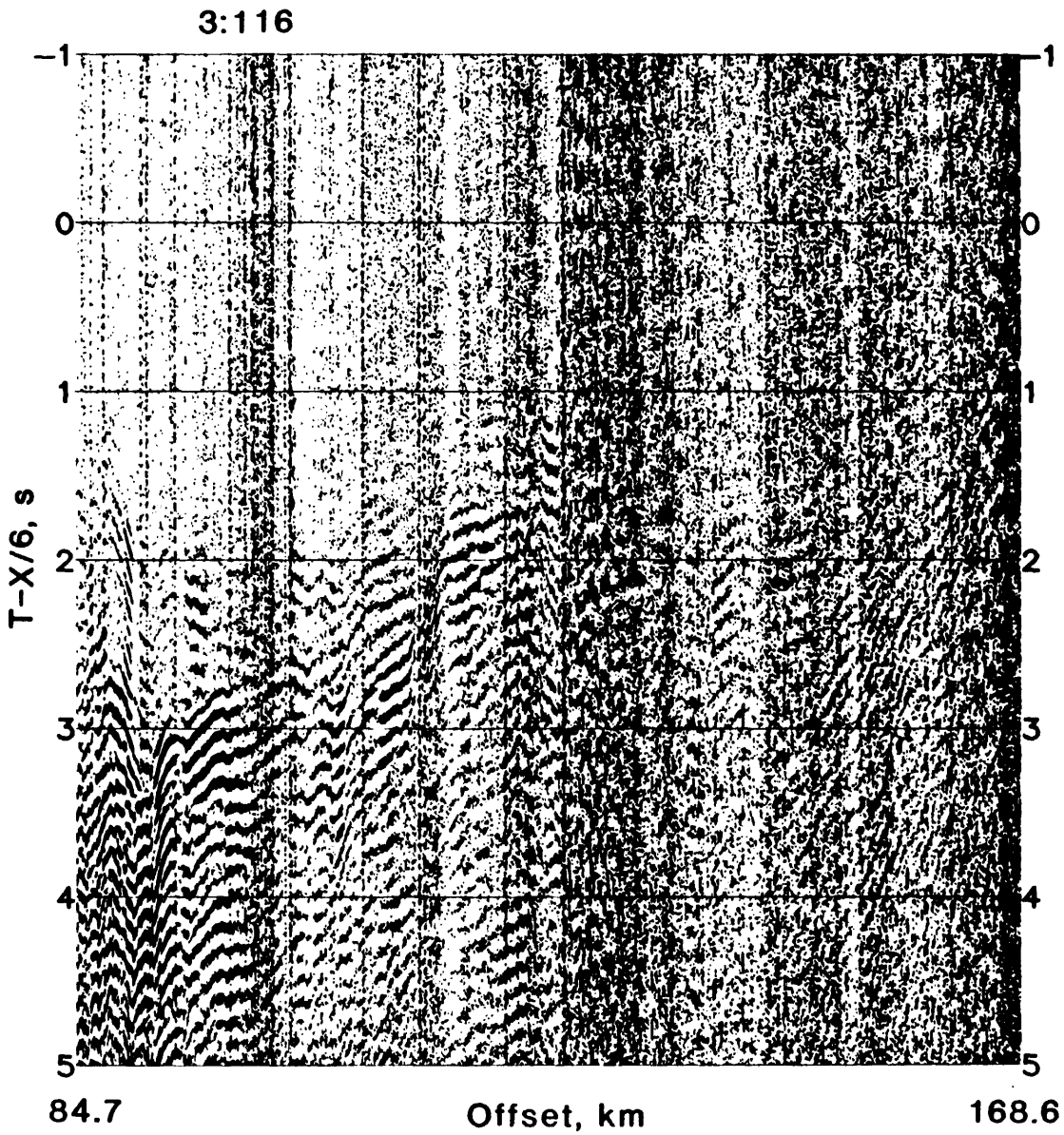

Figure 132. Stacked common receiver gather 116 for shots along LARSE air gun Line 3, reduced at 6 km/s.

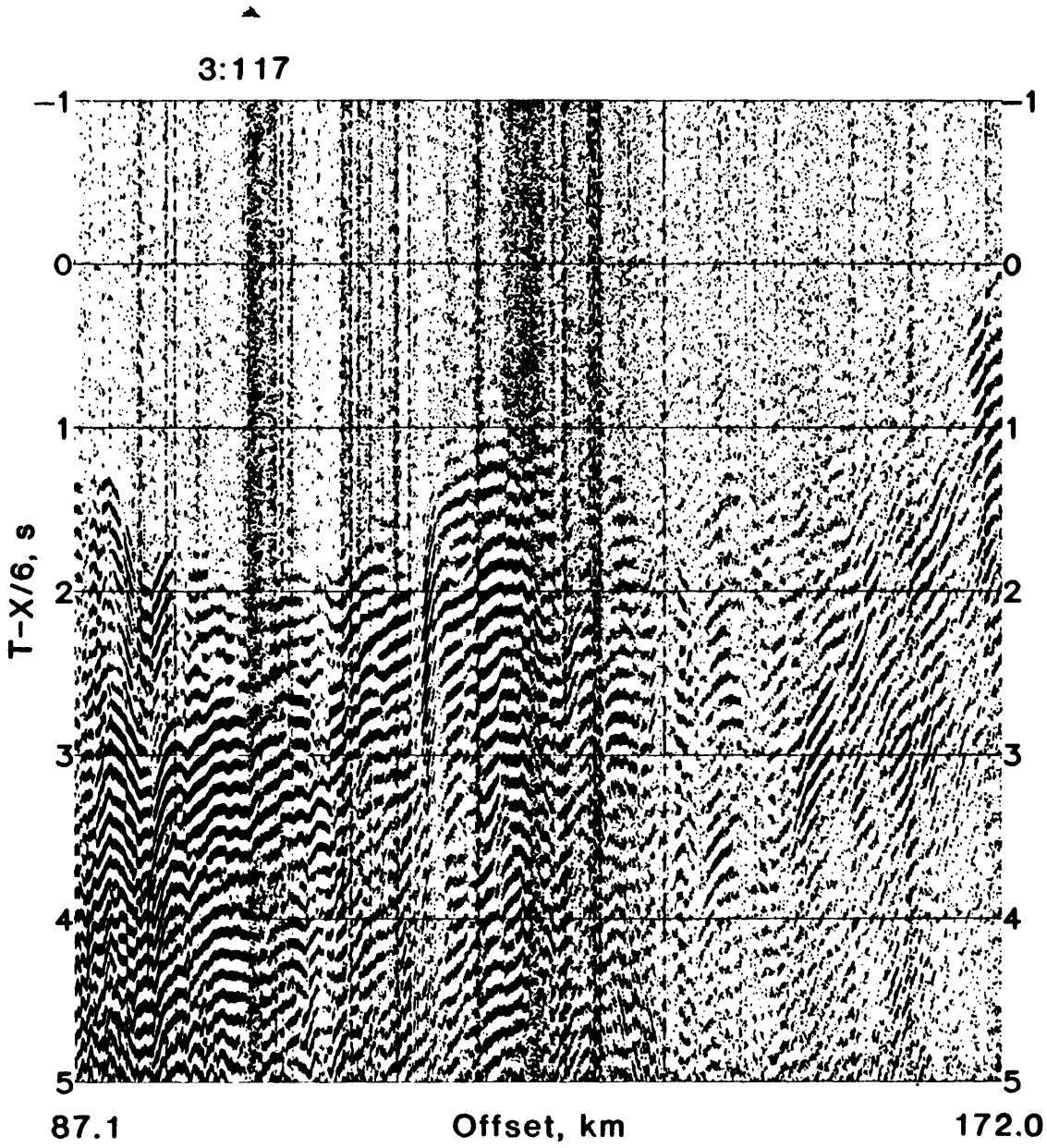

Figure 133. Stacked common receiver gather 117 for shots along LARSE air gun Line 3, reduced at 6 km/s.

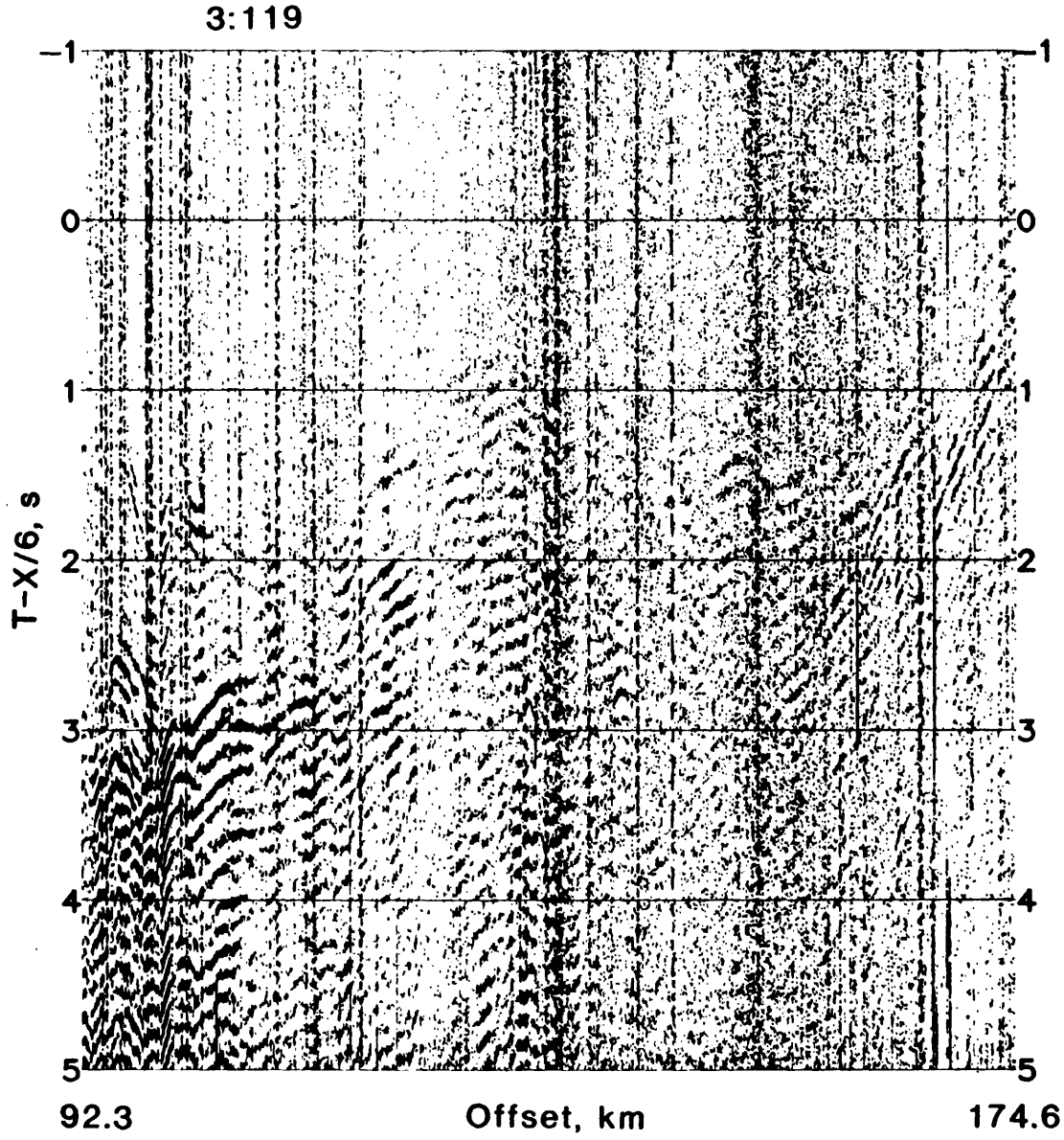

Figure 134. Stacked common receiver gather 119 for shots along LARSE air gun Line 3, reduced at 6 km/s.

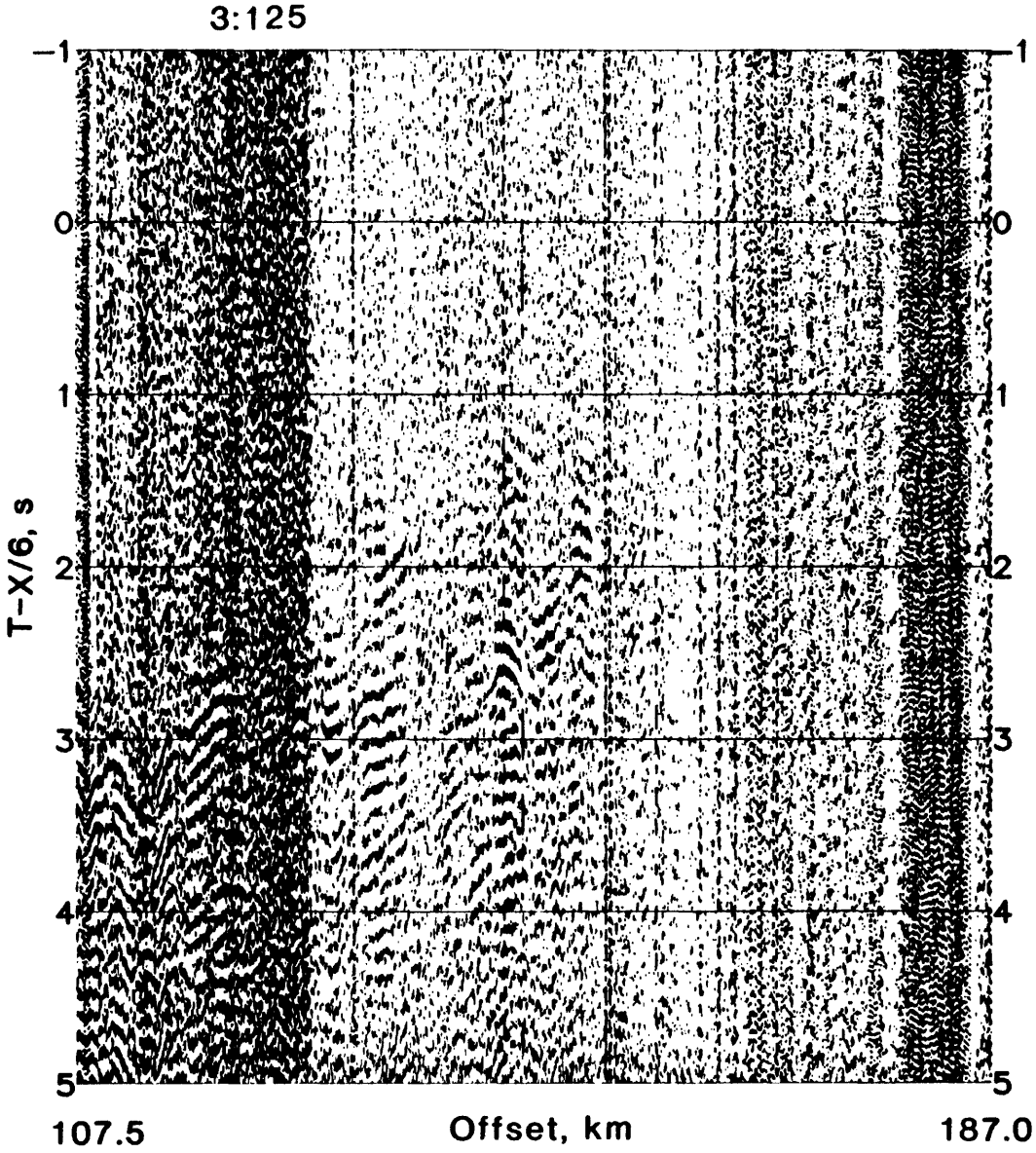

Figure 135. Stacked common receiver gather 125 for shots along LARSE air gun Line 3, reduced at 6 km/s.

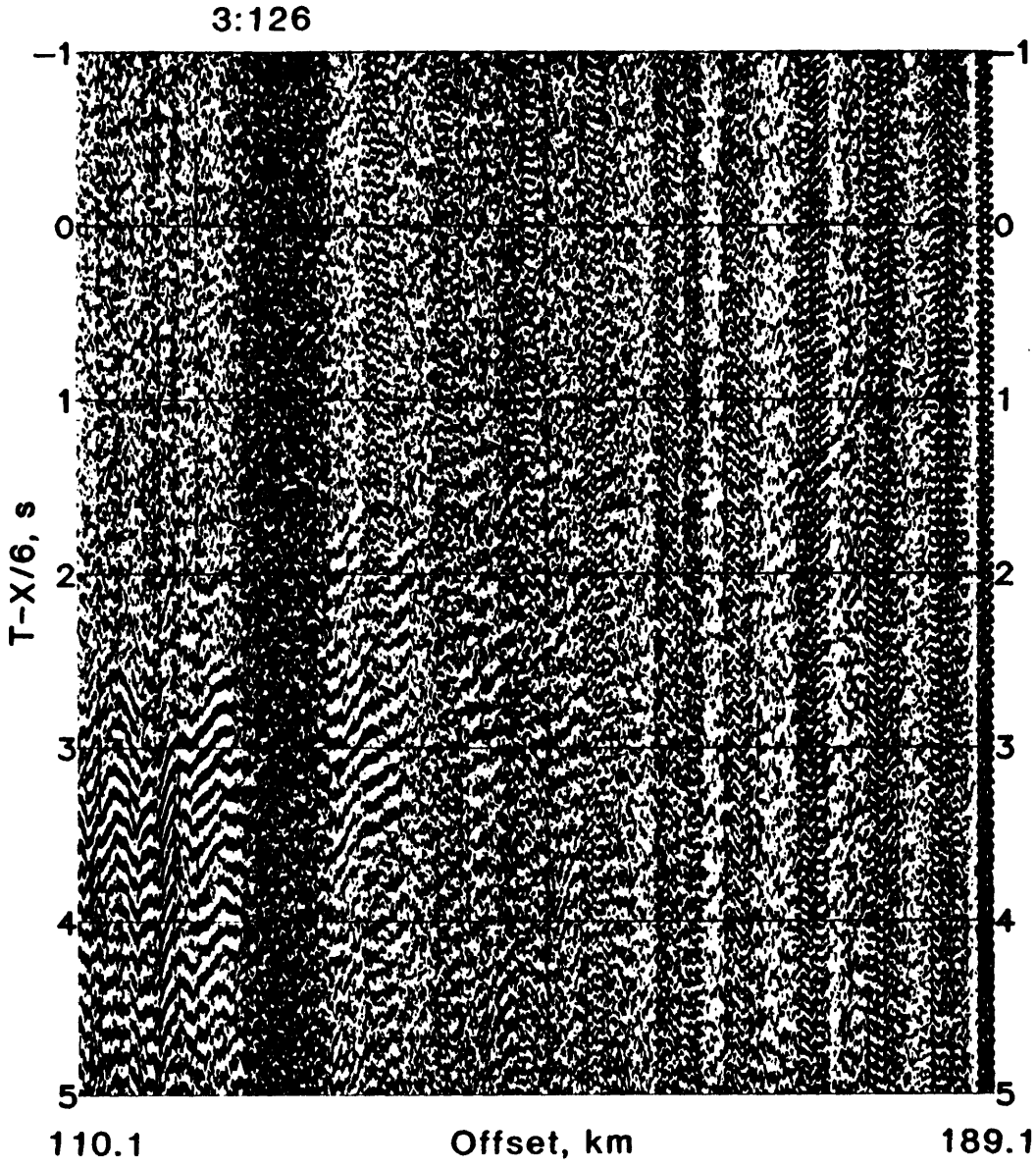

Figure 136. Stacked common receiver gather 126 for shots along LARSE air gun Line 3, reduced at 6 km/s.

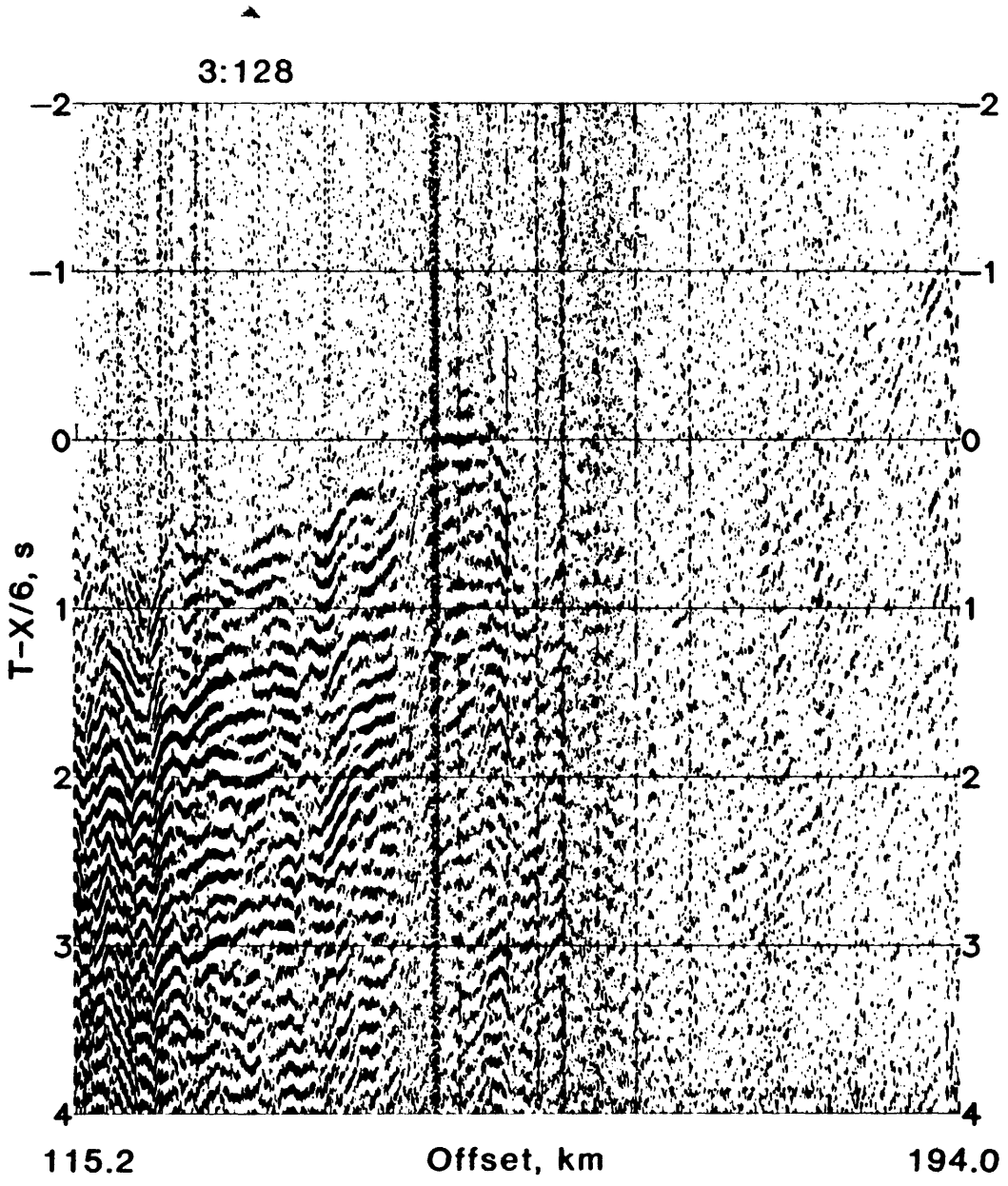

Figure 137. Stacked common receiver gather 128 for shots along LARSE air gun Line 3, reduced at 6 km/s.

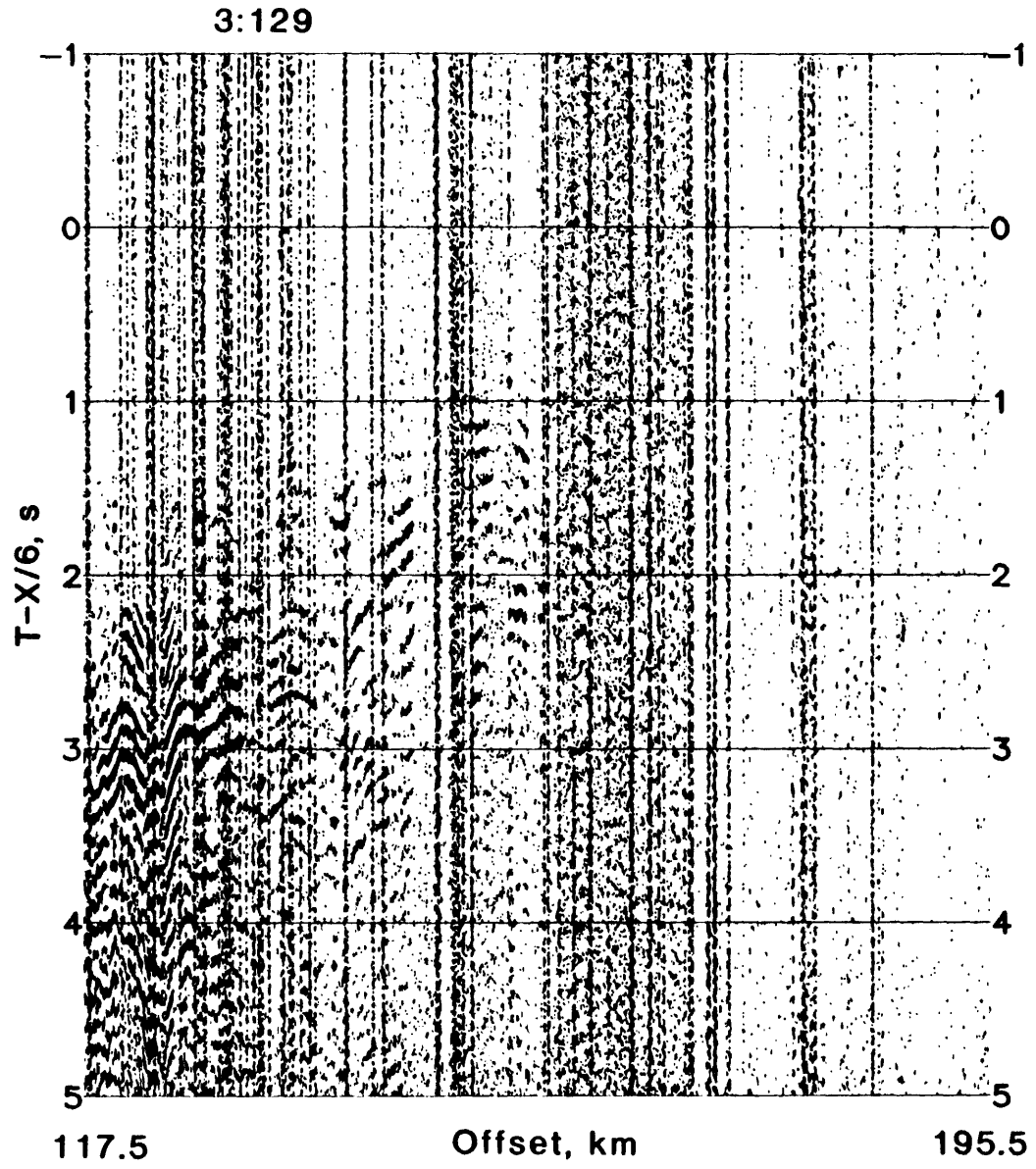

Figure 138. Stacked common receiver gather 129 for shots along LARSE air gun Line 3, reduced at 6 km/s.

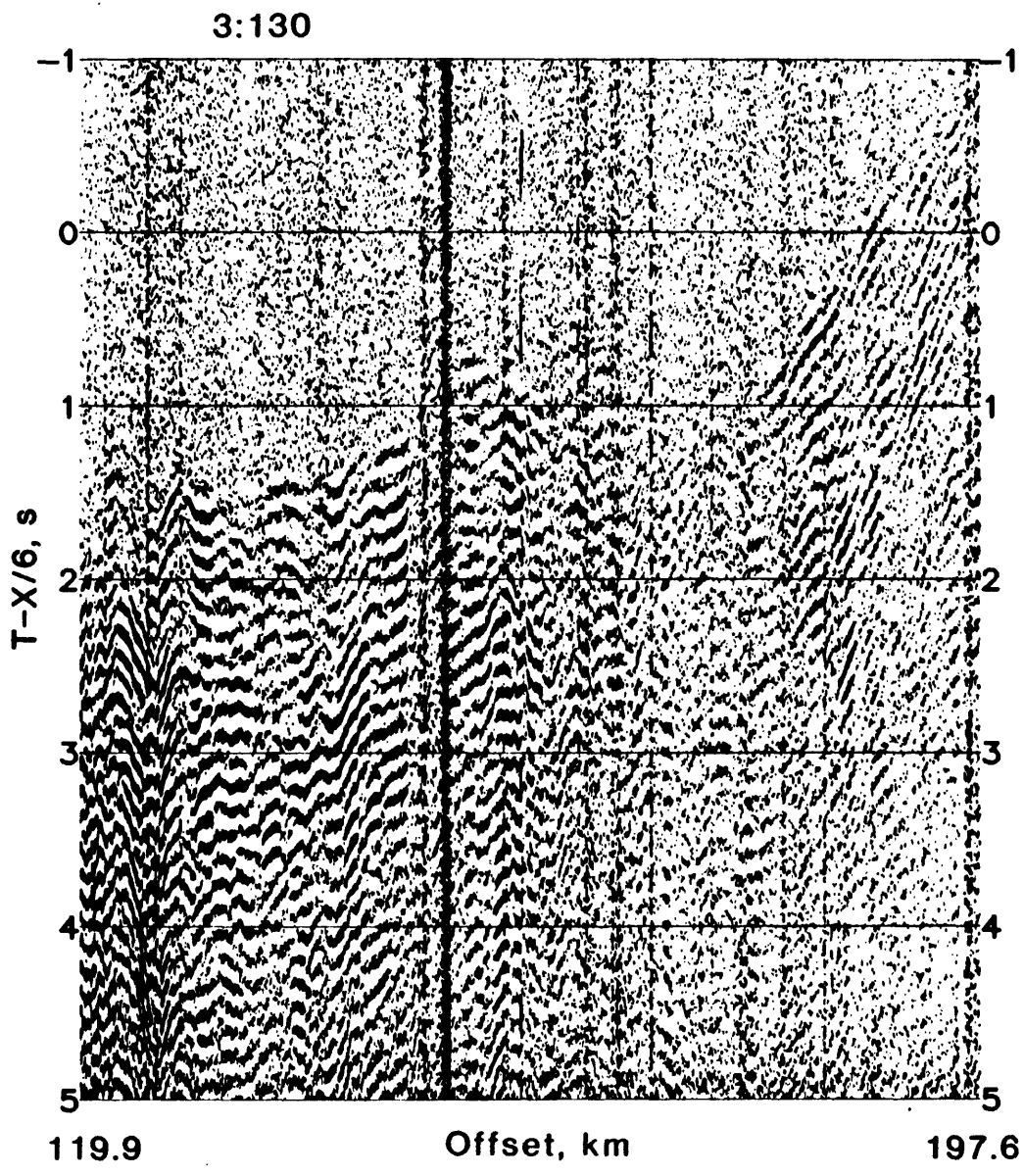

Figure 139. Stacked common receiver gather 130 for shots along LARSE air gun Line 3, reduced at 6 km/s.

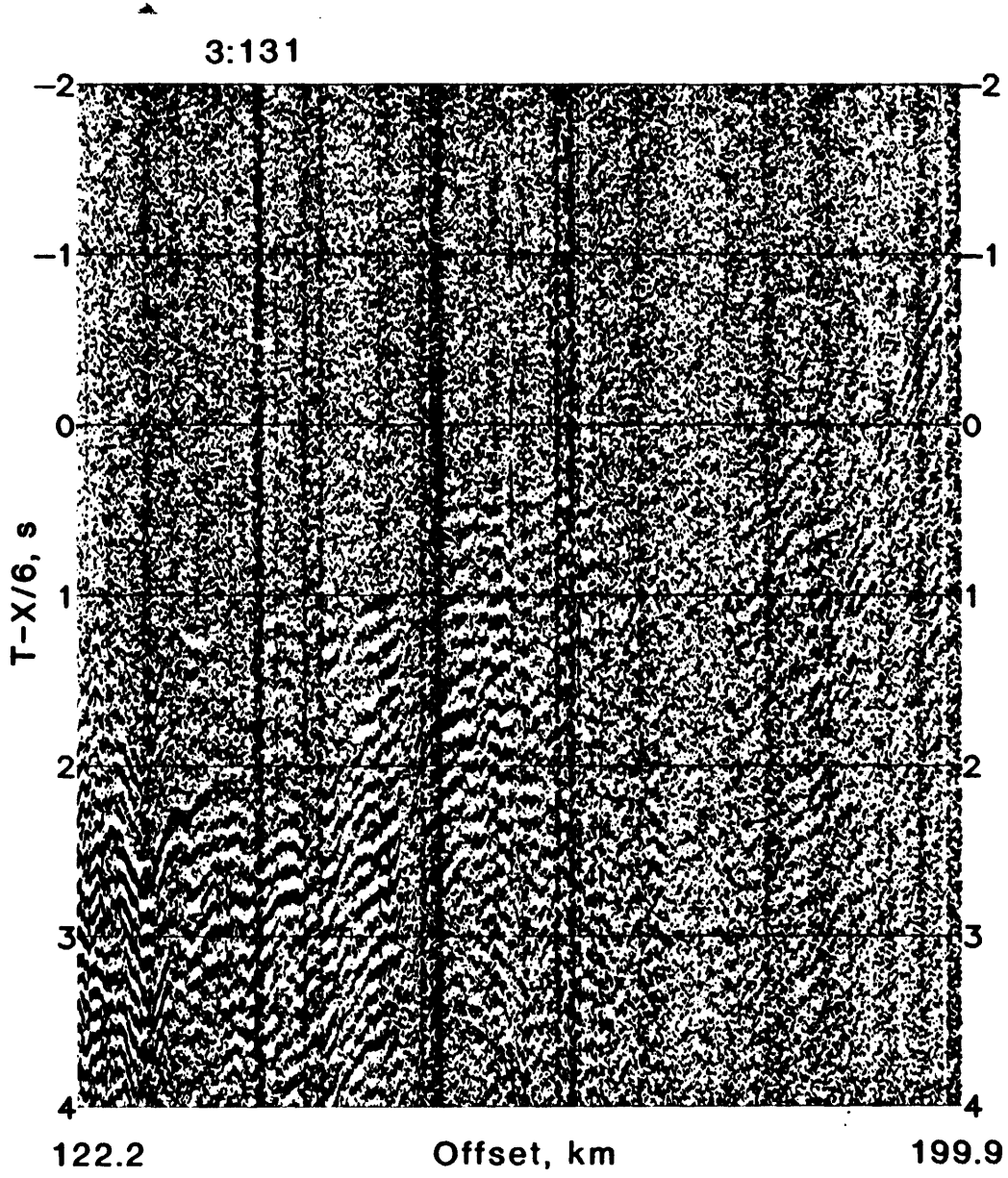

Figure 140. Stacked common receiver gather 131 for shots along LARSE air gun Line 3, reduced at 6 km/s.

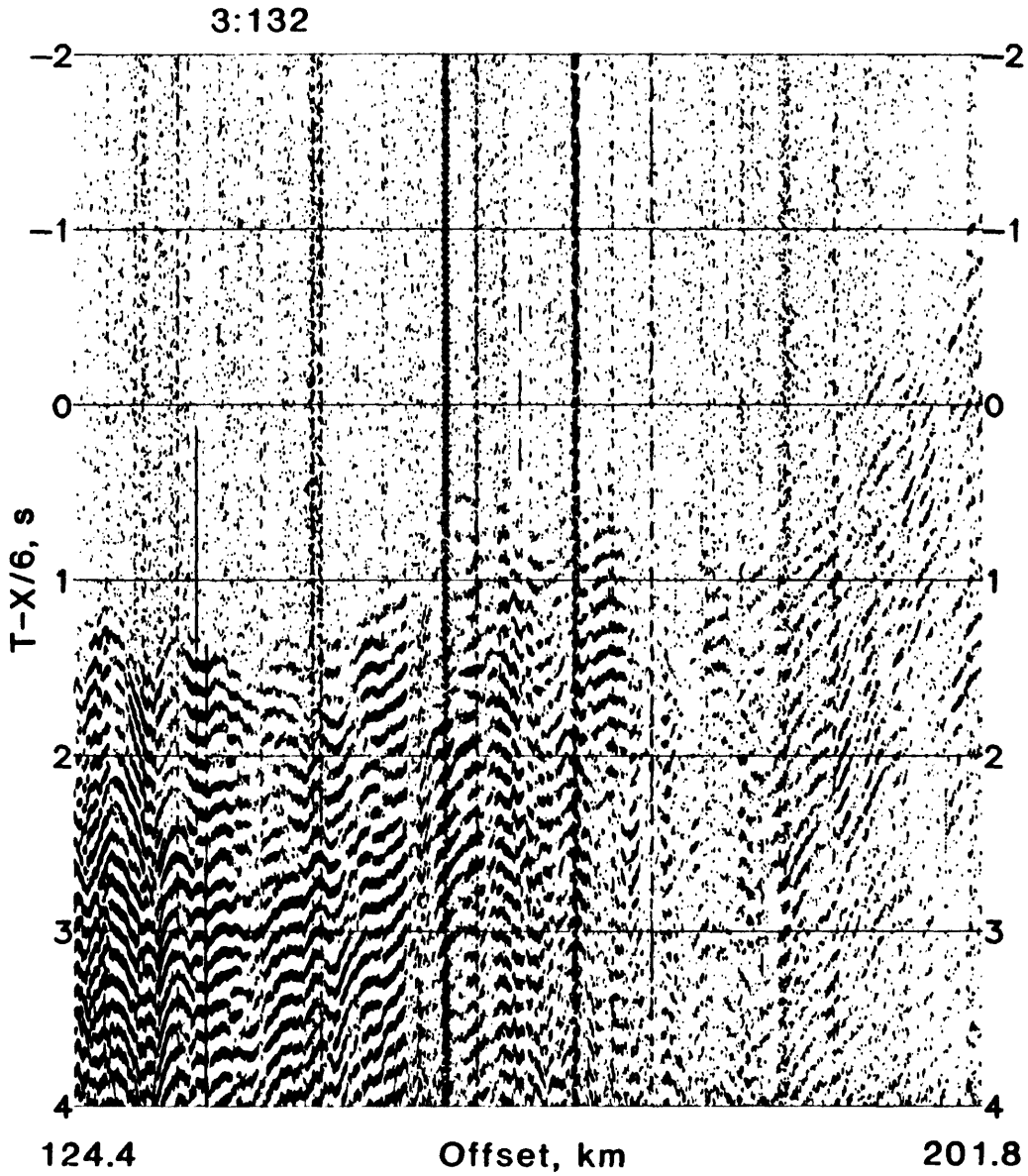

Figure 141. Stacked common receiver gather 132 for shots along LARSE air gun Line 3, reduced at 6 km/s.

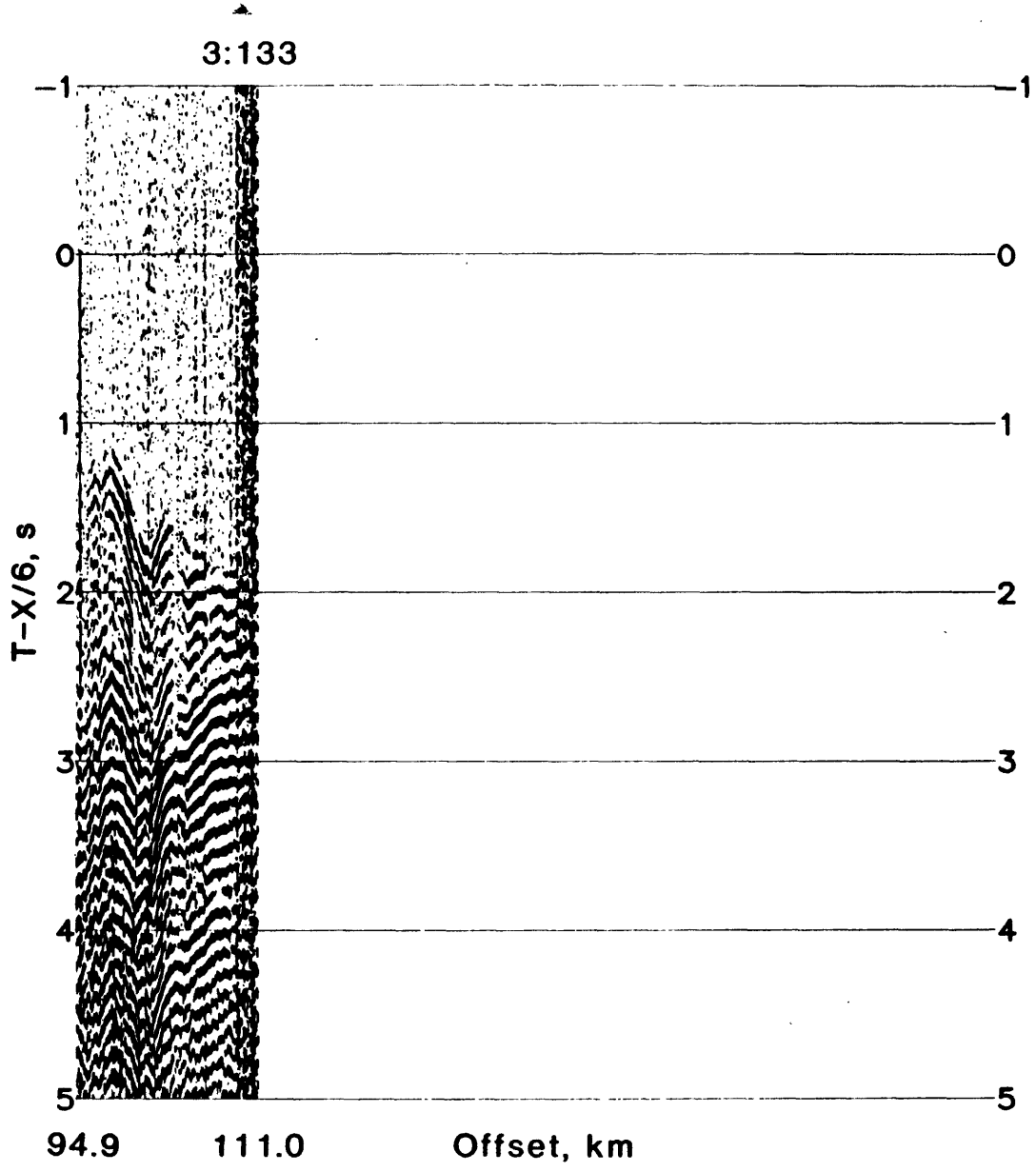

Figure 142. Stacked common receiver gather 133 for shots along LARSE air gun Line 3, reduced at 6 km/s.

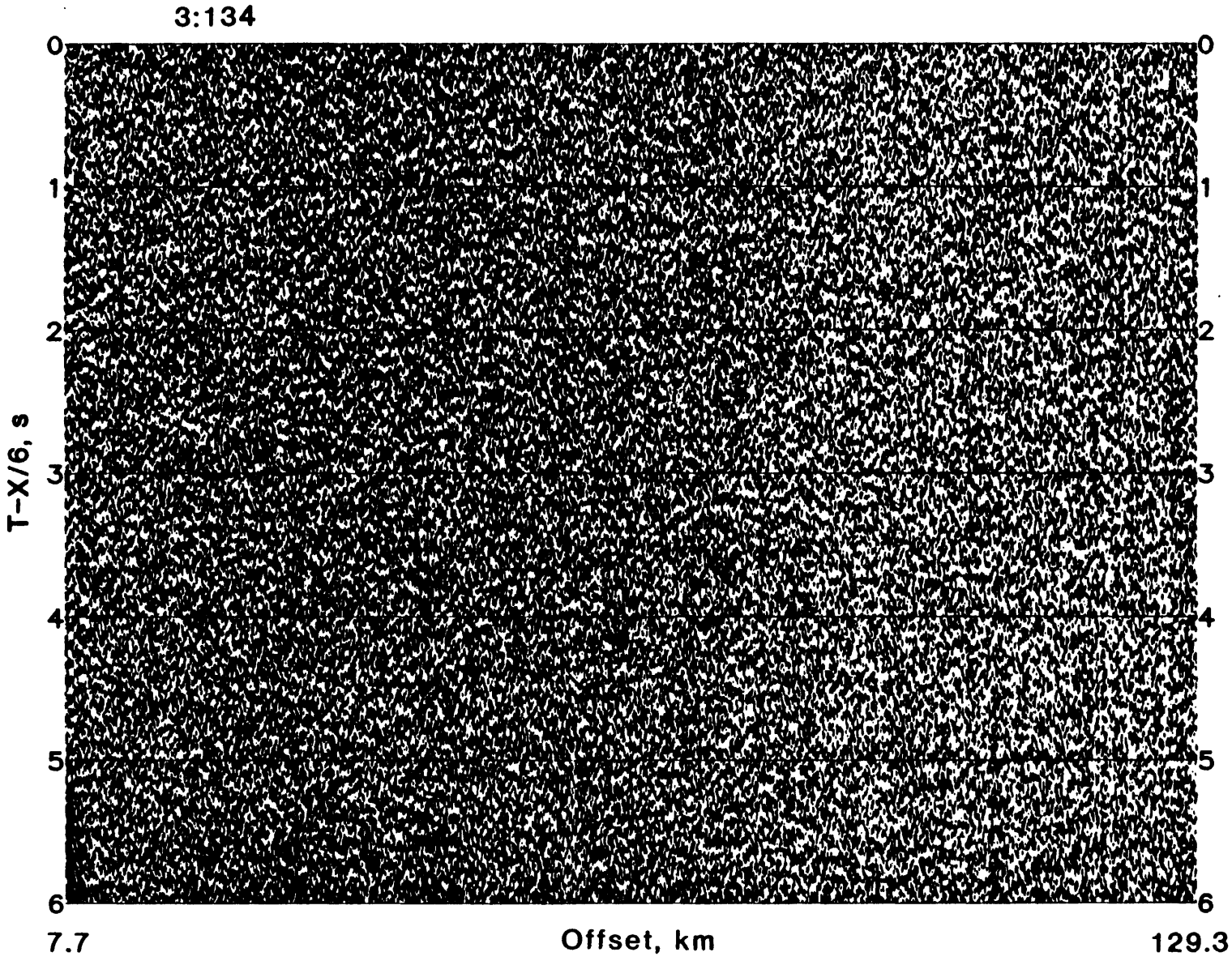

Figure 143. Stacked common receiver gather 134 for shots along LARSE air gun Line 3, reduced at 6 km/s.

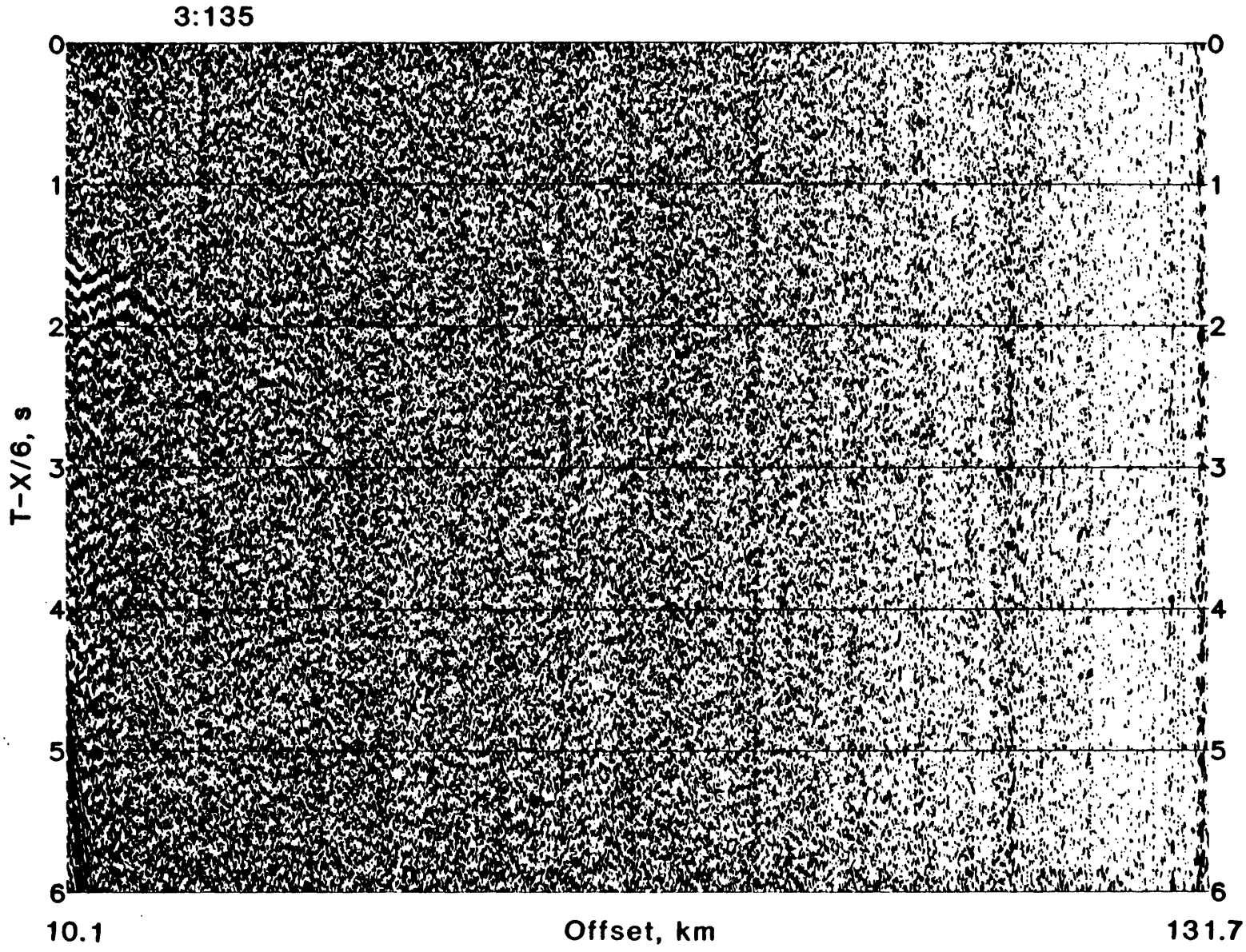

Figure 144. Stacked common receiver gather 135 for shots along LARSE air gun Line 3, reduced at 6 km/s.

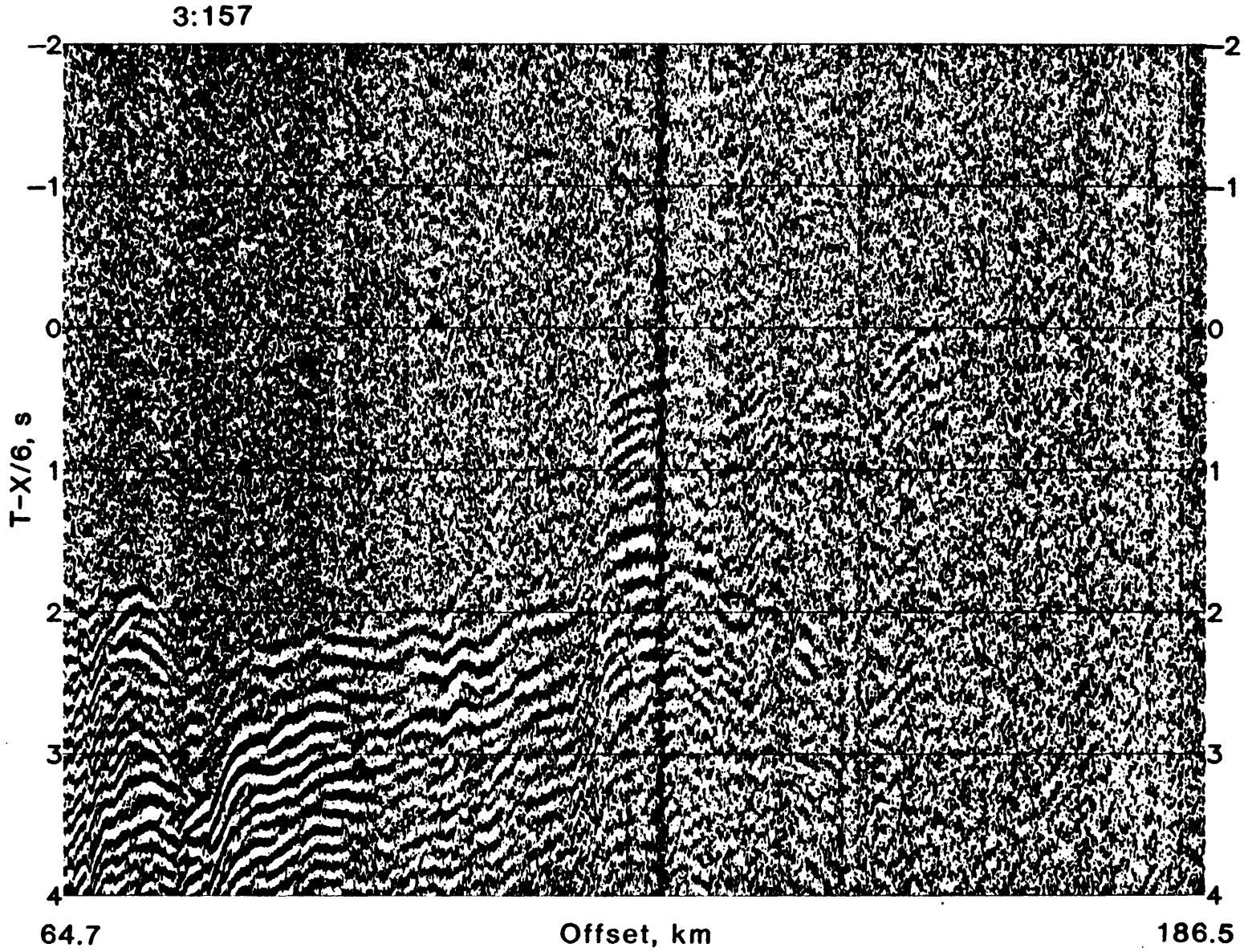

Figure 145. Stacked common receiver gather 157 for shots along LARSE air gun Line 3, reduced at 6 km/s.

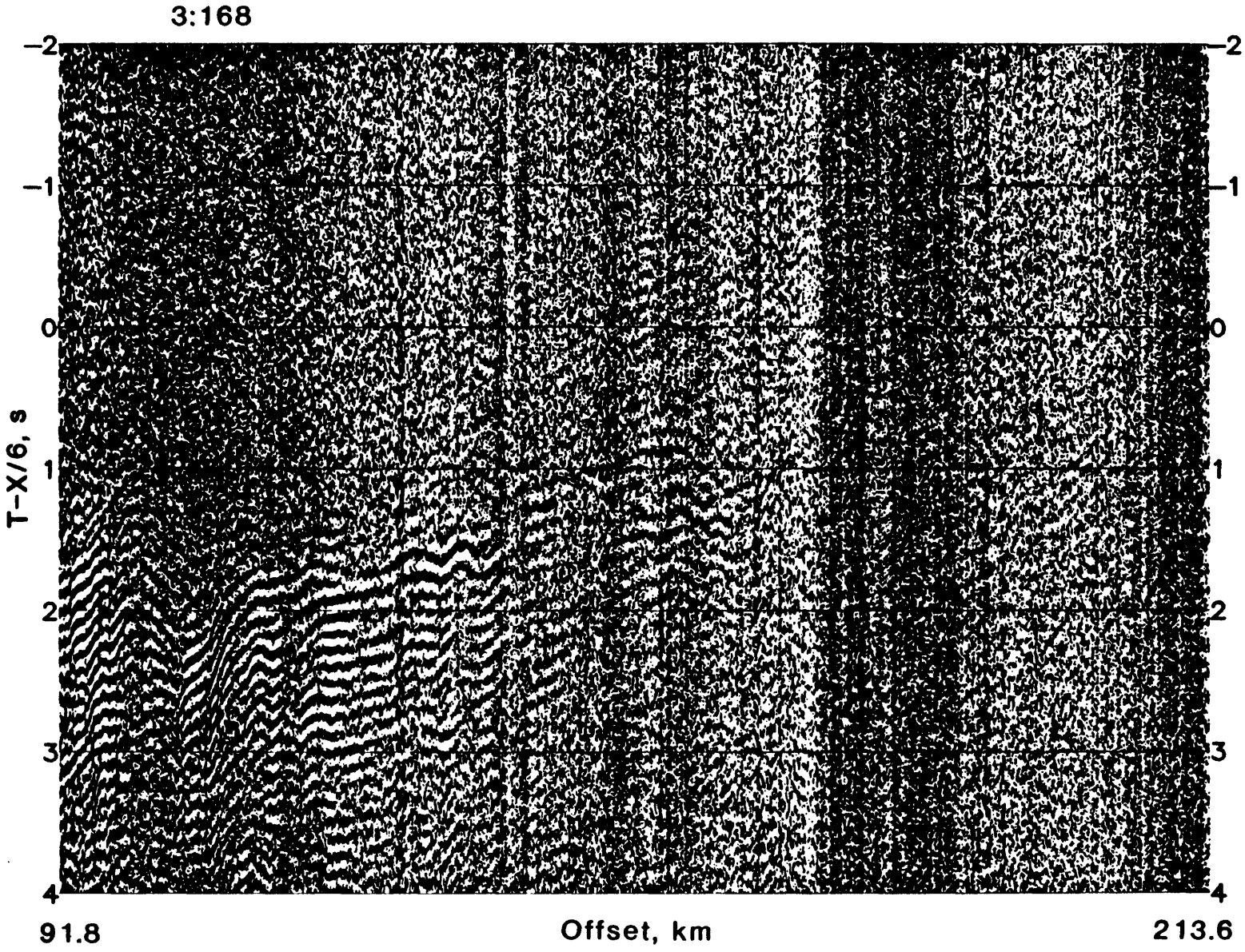

Figure 146. Stacked common receiver gather 168 for shots along LARSE air gun Line 3, reduced at 6 km/s.

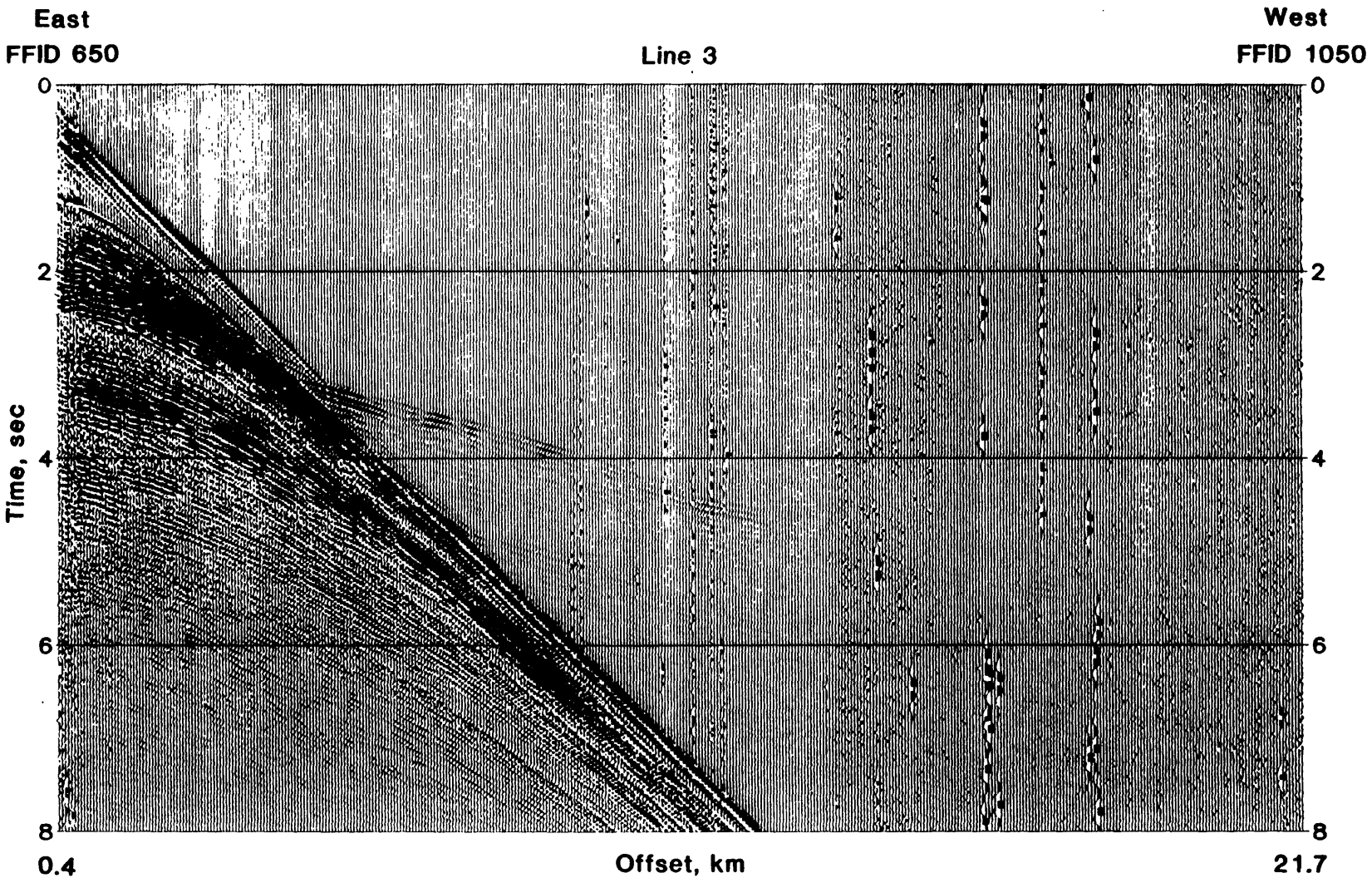

Figure 147. Record from Sonobuoy 1 for shots along LARSE air gun Line 3, bandpassed filtered between 5 and 15 Hz.

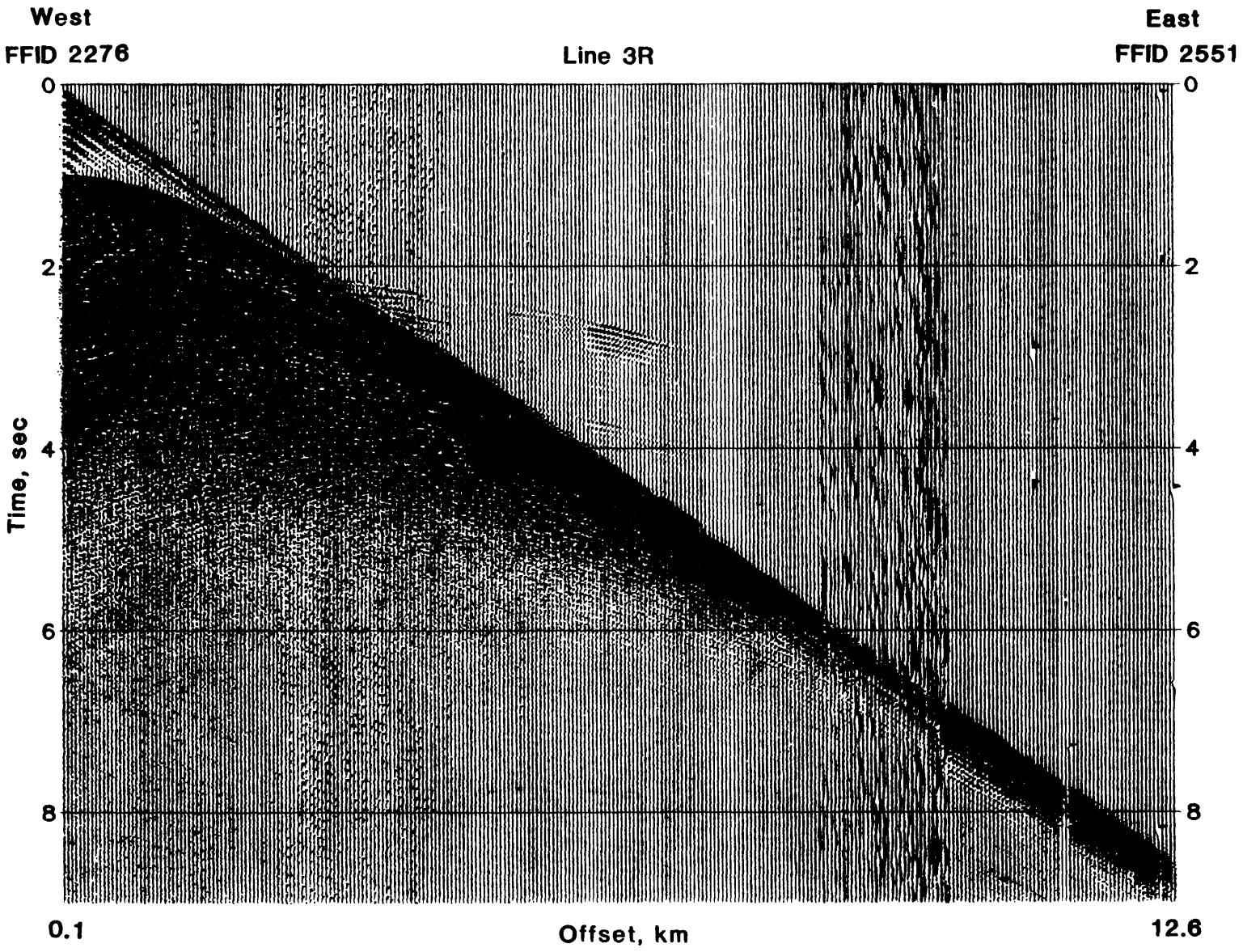

Figure 148. Record from Sonobuoy 2 for shots along LARSE air gun Line 3R.

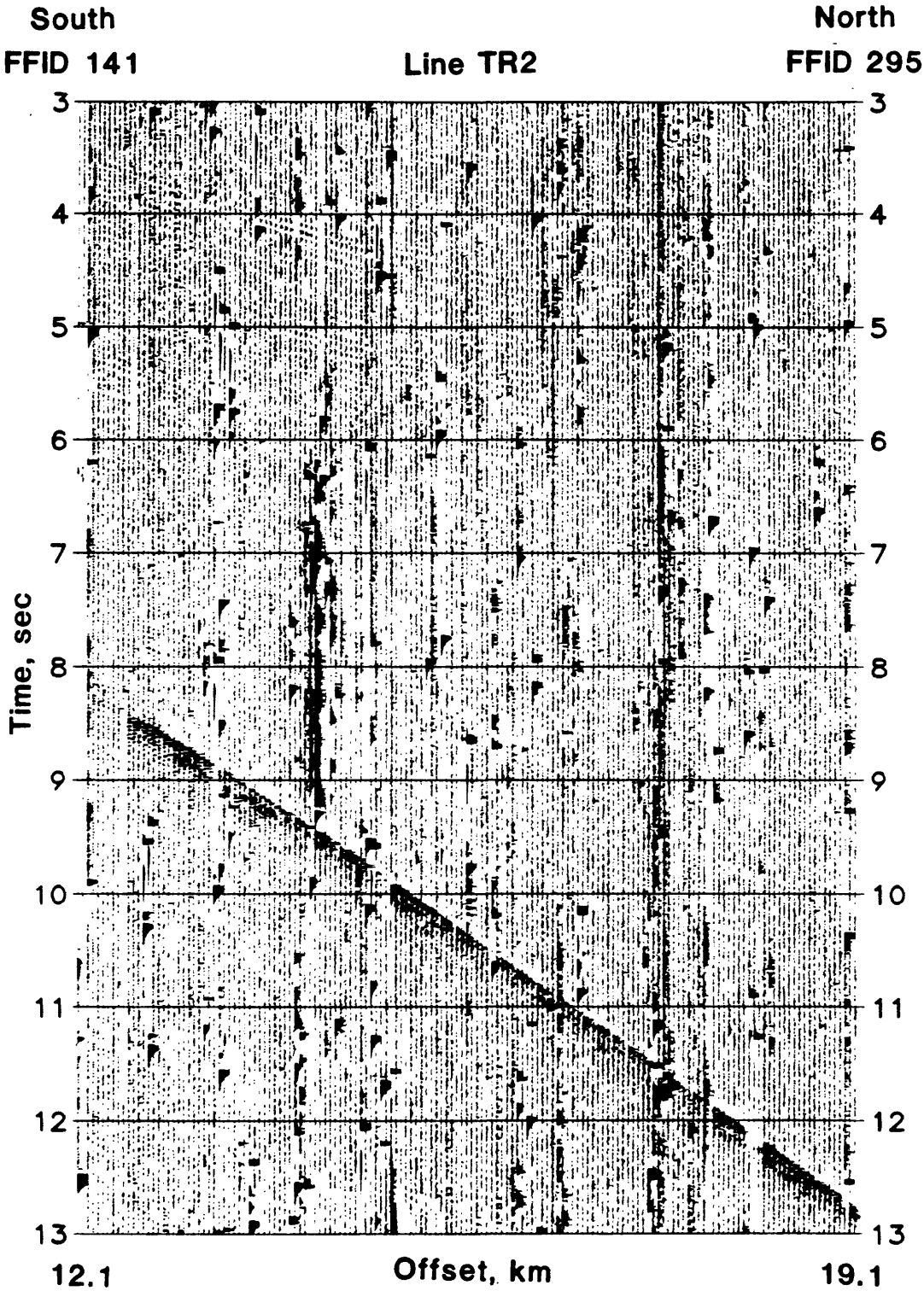

Figure 149. Record from Sonobuoy 2 for shots along LARSE air gun Line TR2.

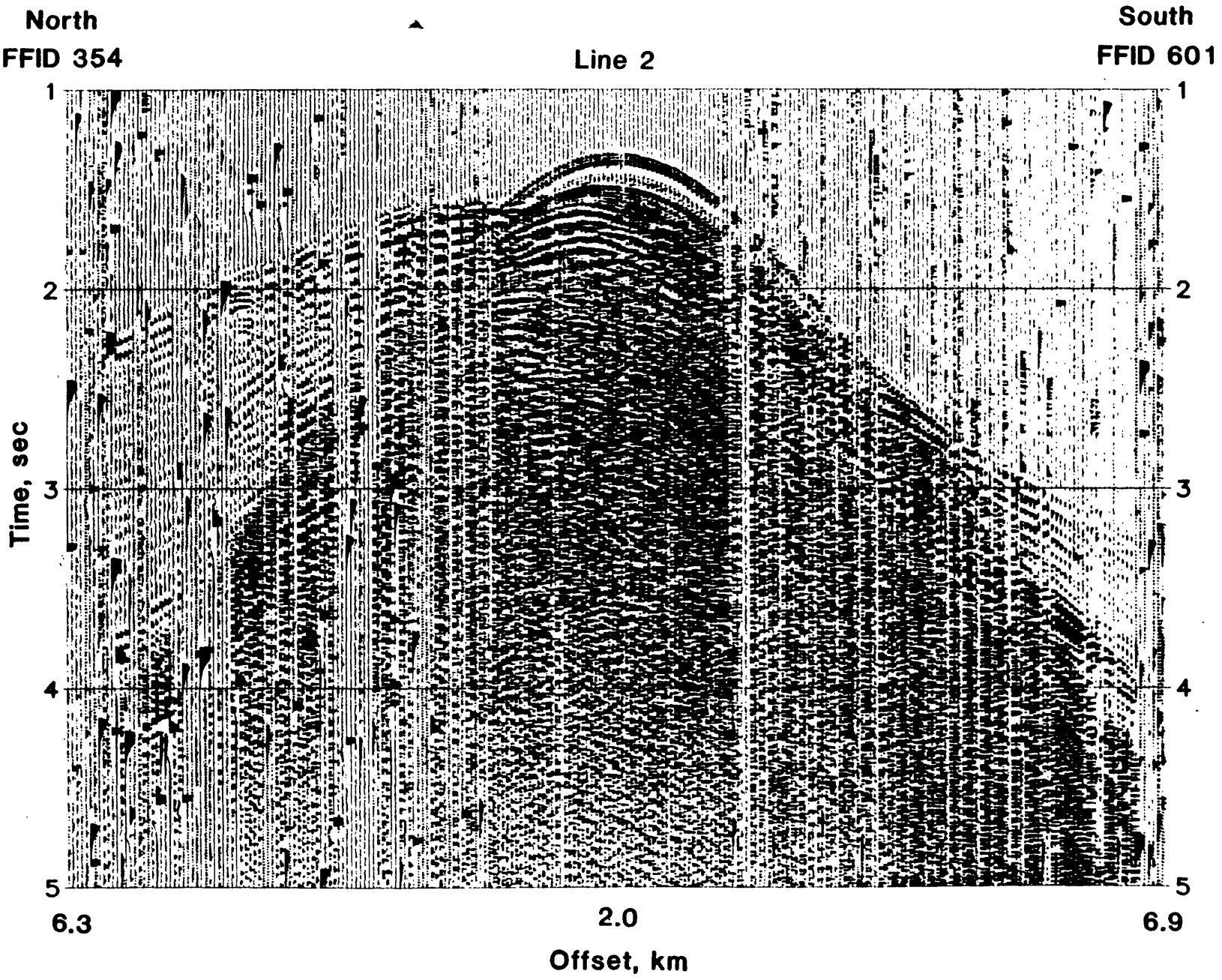

Figure 150. Record from Sonobuoy 2 for shots along LARSE air gun Line 2.

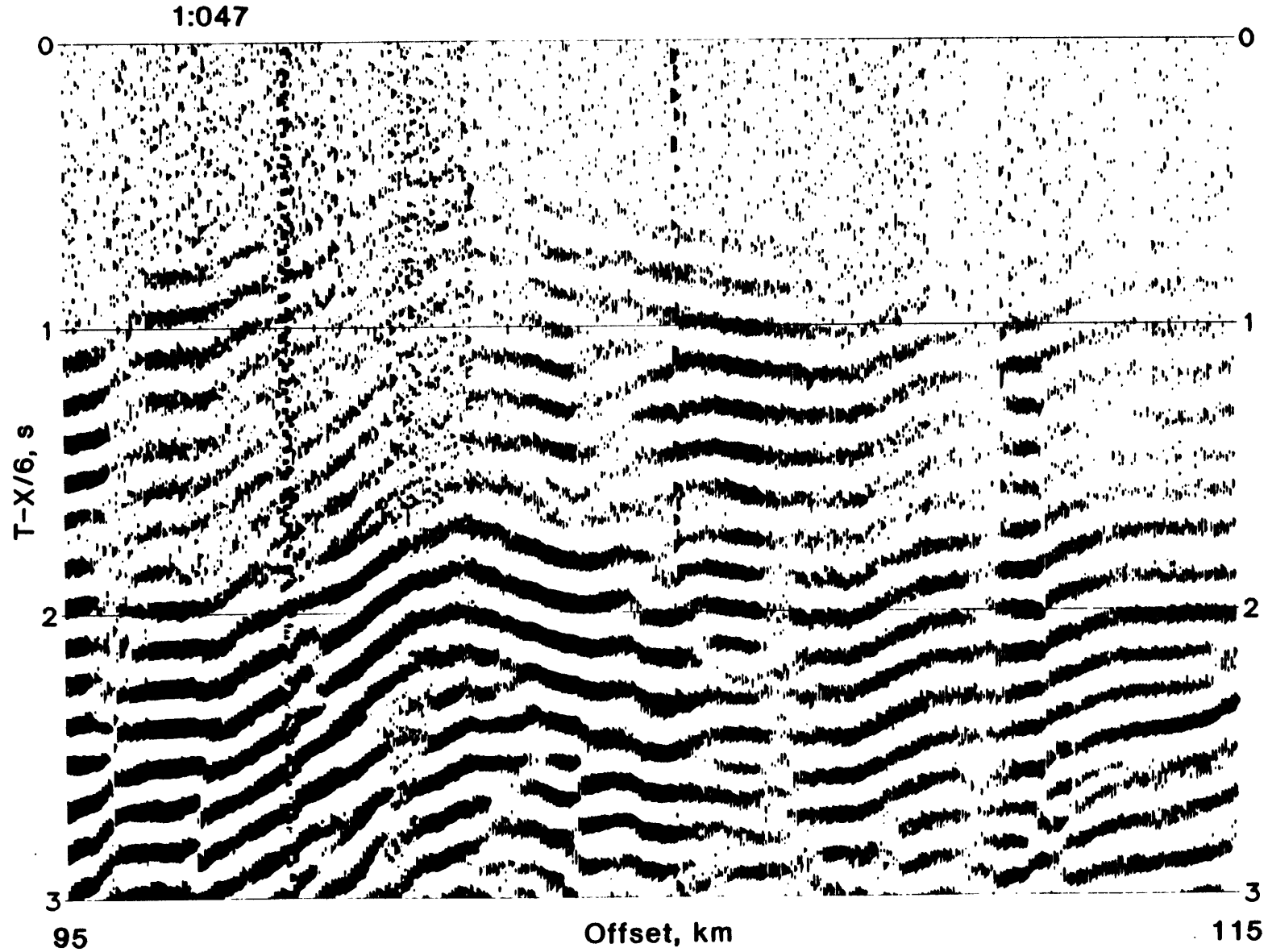

Figure 151. Expanded view of stacked common receiver gather 047 for shots along LARSE air gun Line 1.

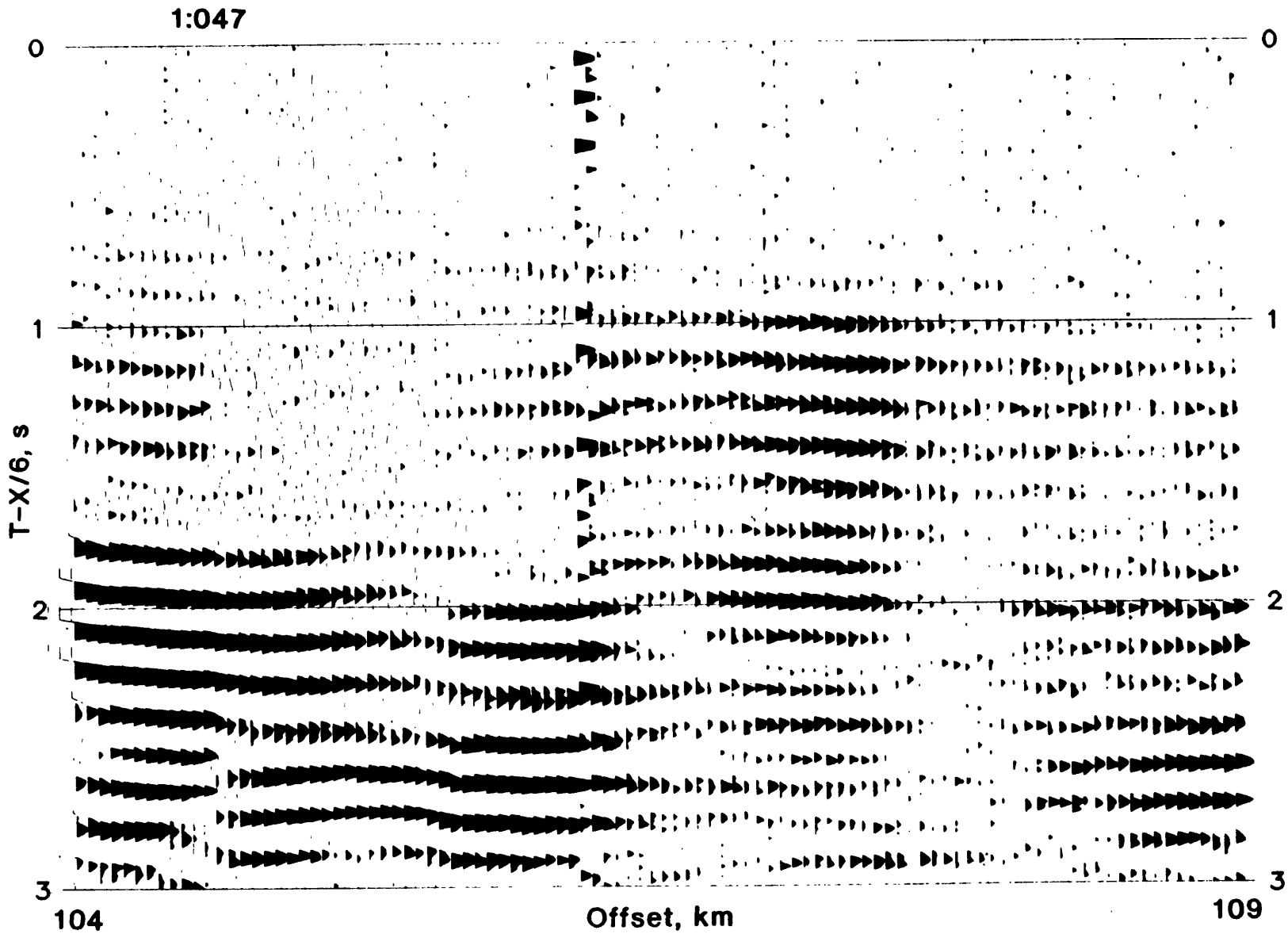

Figure 152. Expanded view of stacked common receiver gather 047 for shots along LARSE air gun Line 1.

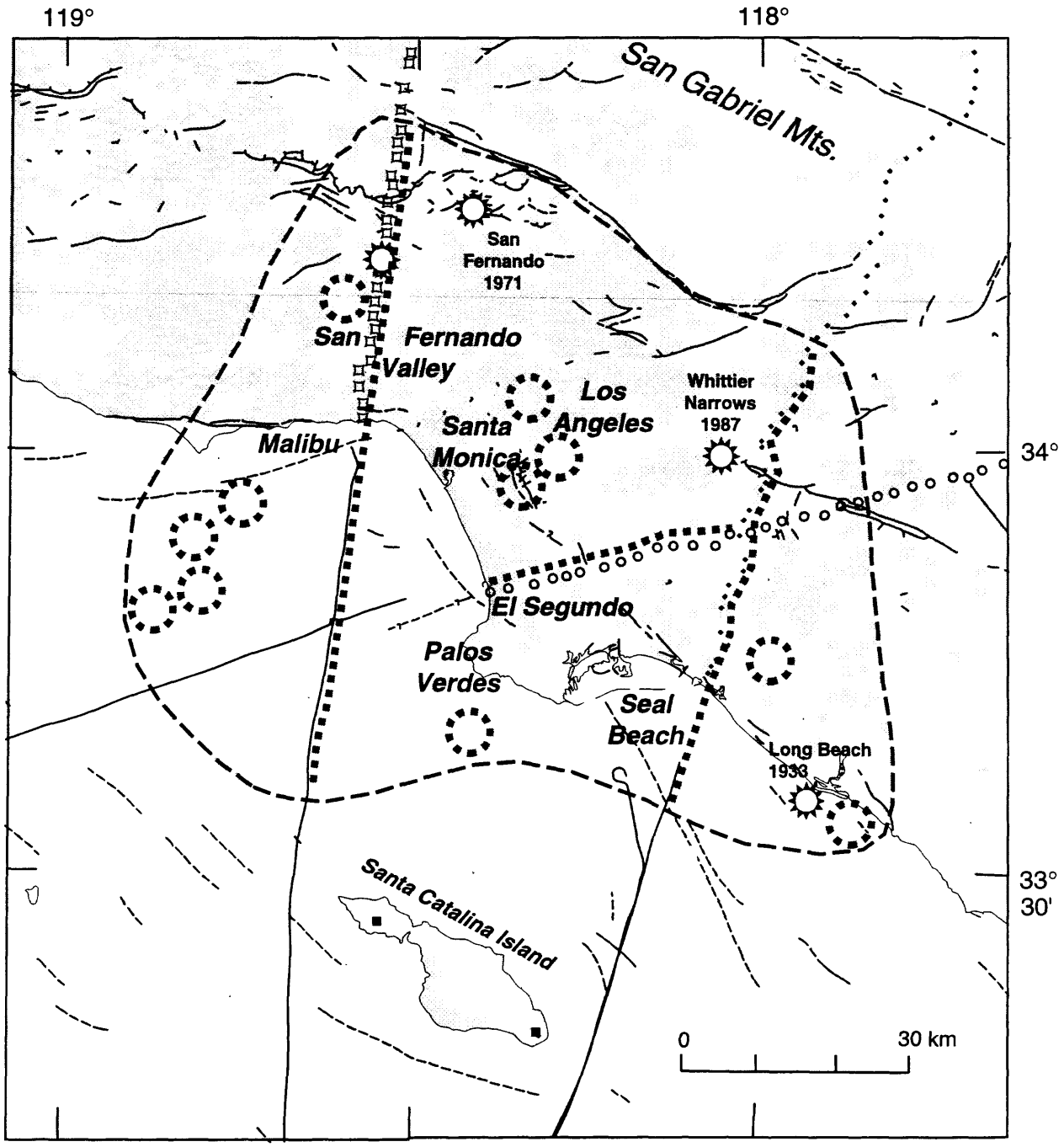

Fig. 153. Map showing location of post-critical Moho reflection (PmP) midpoints having amplitudes 2 to 5 times larger than the preceding Pg or Pn arrivals. Thick dashed gray lines show locations of observed midpoints and dashed line bounds region where strong PmP arrivals observed during the LARSE study were reflected.